STRATHCLYDE INSTITUTE OF PHARMACY & BIOMEDICAL SCIENCES

University of Strathclyde Science

STUDY ON THE EFFECTS OF BITTER TASTE RECEPTOR AGONISTS ON THE RAT PULMONARY ARTERY

A thesis presented by

Samiyah Mohammed A Alshehri

In a fulfilment of the degree of Doctor of Philosophy

Strathclyde Institute of Pharmacy and Biomedical Sciences

University of Strathclyde

Glasgow, United Kingdom

July-2019

Declaration

“This thesis is the result of the author’s original research. It has been composed by the author and had not been previously submitted for examination which has led to the award of a degree. The copyright of this thesis belongs to the author under the terms of the United Kingdom Copyright Acts as qualified by University of Strathclyde Regulation 3.50. Due acknowledgement must always be made of the use of any material contained in, or derived from, this thesis”.

Signed:

Date:

Table of Contents

Declaration ..... **I**

Table of Contents ..... **II**

List of Figures ..... **VIII**

List of Tables ..... **XII**

List of Abbreviations ..... **XIII**

Dedication ..... **XVI**

Acknowledgments ..... **XVII**

Abstract ..... **XIX**

Chapter 1 ..... **1**

General Introduction **1**

1.1 The Pulmonary Circulation **1**

1.1.1 The Function of the Pulmonary Circulation 1

1.1.2 Pulmonary Artery 3

1.1.3 Regulation of the Pulmonary Arterial Tone 5

1.1.3.1 Autonomic Nervous System *5*
1.1.3.2 Humoral Regulation *7*
1.1.3.3 Role of the Endothelium *8*
1.1.3.4 Respiratory Gases *9*

1.1.4 Pulmonary Vascular Disease 9

1.1.5 Vascular Smooth Muscle Contraction 10

1.1.6 Vascular Smooth Muscle Relaxation 11

1.2 Bitter Taste Receptors **13**

1.2.1 Signal Transduction by Bitter Taste Receptor in Gustatory Tissues 13

1.2.2 Pharmacological Characterization of the TAS2Rs 14

1.2.3 Bitter Taste Agonists 17

1.2.4 The Extra-Oral Function of the TAS2Rs 18

1.2.5 TAS2Rs in Smooth Muscles 24

1.2.5.1 TAS2Rs in the Gastrointestinal Tract *24*
1.2.5.2 TAS2Rs in the Central Nervous Systems *25*
1.2.5.3 TAS2Rs in the Male Reproductive System *26*
1.2.5.4 TAS2Rs in the Female Reproductive System and Uterus *26*
1.2.5.5 TAS2Rs in the kidney *26*
1.2.5.6 TAS2Rs in the Bladder *27*

1.2.5.7 TAS2Rs in the Thyroid *27*
1.2.5.8 TAS2Rs in the Lower Respiratory System *28*
1.2.5.9 TAS2Rs in Vasculatures *35*

1.3 Aims of the Present Study **38**

Chapter 2 ..... **39**

The Effect of Bitter Taste Agonists on the Rat Aorta and Pulmonary Artery **39**

2.1 Introduction **40**

2.2 Materials and Methods **42**

2.2.1 Animals and Tissue Preparation 42

2.2.2 Contractile Agents 46

2.2.3 Bitter Taste Agonists 46

2.2.4 Contractile Response to Phenylephrine, KCl, and U46619 46

2.2.5 The Effect of Bitter Taste Agonists on the Rat Aorta and Pulmonary Artery 47

2.2.6 The Effect of Bitter Taste Agonists on the Resting Tone of the Rat Pulmonary Artery 47

2.2.7 Removing the Endothelium from the Rat Pulmonary artery 47

2.2.8 Criteria for Including and Excluding the Tissues for Analysis 48

2.2.9 Data Analysis 48

2.3 Results **50**

2.3.1 Contractility of the Rat Aorta and Pulmonary Artery 50

2.3.1.1 Phenylephrine Induces a Concentration-Dependent Contraction of the Rat Aorta and Pulmonary Artery *50*
2.3.1.2 KCl Induces a Concentration-Dependent Contraction of the Rat Aorta and Pulmonary Artery *52*

2.3.2 The Effect of Bitter Taste Agonists on the Rat Aorta/Pulmonary Artery 54

2.3.2.1 The Effect of quinine on the Rat Aorta *56*
2.3.2.2 The Effect of Denatonium on the Rat Aorta *56*

2.3.3 The Effect of Bitter Taste Agonists on the Rat Pulmonary Artery 58

2.3.4 Endothelium Dependency of Bitter Taste Agonists Mediated Vasorelaxation in the Rat Pulmonary Artery. 62

2.3.4.1 Confirmation of the Removal of the Endothelium *62*
2.3.4.2 Phenylephrine Induces a Concentration-Dependent Contraction of the Denuded-Endothelial Pulmonary Artery *65*
2.3.4.3 The Effect of Bitter Taste Agonists on the Endothelium Denuded Rat Pulmonary Artery *66*

2.3.5 U46619 Induces a Concentration-Dependent Contraction of the Rat Pulmonary Artery 69

2.3.6 Quinine Evokes a Relaxation of the U46619 Pre-Contracted Rat Pulmonary Artery 70

2.4 Discussion **71**

2.4.1 Relaxant Effect of Bitter Taste Agonist 71

2.4.2 Influence of Contractile Agent on Quinine-Induced Relaxation 73

2.4.3 Endothelium Dependency of Bitter Taste Agonist Induced Relaxation of the Rat Pulmonary artery 73

2.4.4 Specificity of Bitter Taste Agonist and Their Pharmacological Actions 74

Chapter 3..... 76

Mechanisms of Bitter Taste Agonist-Mediated Vasorelaxant Effect on the Rat Pulmonary Artery 76

3.1 Introduction 77

3.1.1 Inhibition of L-type Voltage-Dependent Calcium Channels..... 77

3.1.2 Contribution of Potassium-Activated Calcium Channels in the Induced Vasorelaxation of Bitter Taste Agonists 79

3.2 Methods 81

3.2.1 Inhibitors..... 81

3.2.2 Effect of TEA on Bitter Taste Agonist-Mediated Relaxation 81

3.2.3 Effect of Iberiotoxin on the Bitter Taste Agonists Mediated Relaxation 82

3.2.4 Effect of the L-Type Voltage-Dependent Calcium Channels (VDCCs) Agonists on Bitter Taste Mediated Relaxation. 82

3.2.5 Effect of a G- Protein βγ-Subunit Inhibitor on Bitter Taste Agonist-Mediated Relaxation on the Rat Pulmonary Artery Tissue 83

3.2.6 Statistical Analysis 83

3.3 Results..... 84

3.3.1 The Effect of TEA on the Bitter Taste Agonists-Induced Relaxation of the Rat Aorta and Pulmonary Artery. 84

3.3.2 The Effect of Iberiotoxin on the Bitter Taste Agonist-Induced Relaxation of the Rat Pulmonary Artery 90

Figure 3.5 Representative Traces of the Effect of Iberiotoxin on the Bitter Taste Agonist-Induced Relaxation of the Rat Pulmonary Artery 91

3.3.3 Role of the L-type voltage-dependent calcium channels on the Bitter Taste Agonist-Mediated Relaxation. 94

3.3.3.1 Effect of Bay K8644 on Quinine Induced Relaxation of the Rat Pulmonary Artery. 94

3.3.3.2 The Effect of FPL64176 on the Quinine-Induced Relaxation of the Rat Pulmonary Artery 97

3.3.4 The Role of the G-Protein βγ-subunits in the Mechanism of action of Bitter Taste Agonists99

3.4 Discussion 102

3.4.1 Role of Potassium channels in Bitter Taste Agonists Mediated Relaxation of the Rat Aorta and Pulmonary Artery 103

3.4.2 Role of L-type Voltage-Dependent Calcium Channel in Bitter Taste Agonists induced Relaxation of the Rat Pulmonary Artery 104

3.4.3 Involvement of G-Protein Beta-Gamma ($G_{\beta\gamma}$) Subunits in Bitter Taste Agonists Induced Relaxation of the Rat Pulmonary Artery 105

Chapter 4..... 107

Influence of Bitter Taste Agonists on Ca^{2+} Signalling on Rat Pulmonary Artery Isolated Smooth Muscle Cells 107

4.1 Introduction 108

4.1.1 Vascular Smooth Muscle Cells 108
4.1.2 Effect of $[Ca^{2+}]_i$ in the VSMCs 108
4.1.3 $[Ca^{2+}]_i$ Indicators and Measurements 111
4.1.3.1 $[Ca^{2+}]_i$ Indicators Used in Bitter Taste Agonist Research 112
4.1.3.2 Effect of Bitter Taste Agonists on $[Ca^{2+}]_i$ 113
4.2 Methods 116
4.2.1 Rat Pulmonary Artery SMC Isolation 116
4.2.2 Measurement of $[Ca^{2+}]_i$ 118
4.2.3 Drugs and Inhibitors 120
4.2.4 The Effect of Bitter Taste Agonists on the $[Ca^{2+}]_i$ on Isolated Rat Pulmonary Artery SMCs 120
4.2.5 The Effect of ATP-Induced Changes in $[Ca^{2+}]_i$ of the Rat Pulmonary Artery SMCs. 121
4.2.6 Effects of Bitter Taste Agonists on ATP-Induced $[Ca^{2+}]_i$ Transients in Rat Pulmonary Artery SMCs 121
4.2.7 Effect of Dextromethorphan on KCl-Induced Increase in $[Ca^{2+}]_i$ 122
4.2.8 Effect of Dextromethorphan on Intracellular Ca^{2+} Stores 122
4.2.9 Role of Ca^{2+} Stores in the Dextromethorphan-Induced increase in $[Ca^{2+}]_i$ 122
4.2.10 Intracellular Signalling Pathway for Dextromethorphan Responses 123
4.2.11 Data Analysis 123
4.3 Results 125
4.3.1 The Effect of Quinine, Denatonium, and Dextromethorphan on Intracellular Ca^{2+} Stores in Rat Pulmonary Artery SMCs 125
4.3.2 ATP-Induced Changes in $[Ca^{2+}]_i$ of the Rat Pulmonary Artery Cells 127
4.3.3 Effects of Bitter Taste Agonists on ATP-Induced $[Ca^{2+}]_i$ Transient in Rat Pulmonary Artery SMCs 129
4.3.4 Effect of Dextromethorphan on ATP-Induced Ca^{2+} Oscillation 137
4.3.5 Effects of Dextromethorphan on the KCl-Induced Increase in $[Ca^{2+}]_i$ 140
4.3.6 Effect of Dextromethorphan on Intracellular Ca^{2+} Levels 143
4.3.7 Effects of Ca^{2+} Stores on the Dextromethorphan-Induced Increases in Ca^{2+} Fluorescence. 144
4.3.8 Intracellular Signalling Pathway for Dextromethorphan Response 145
4.4 Discussion 146
4.4.1 Ca^{2+} Responses to Quinine, Denatonium, and Dextromethorphan in the Rat Pulmonary Artery SMCs 146
4.4.2 Effects of Bitter Taste Agonists on ATP-Induced $[Ca^{2+}]_i$ Transient in Rat Pulmonary Artery SMCs 147
4.4.3 Possible Mechanisms Involved in the Dextromethorphan-Induced Increase in $[Ca^{2+}]_i$ 148
4.4.3.1 Role of VDCC in the Dextromethorphan-Induced Increase in $[Ca^{2+}]_i$ 148
4.4.3.2 Role of Intracellular Stores in the Dextromethorphan-Induced Increase in $[Ca^{2+}]_i$ 149
Chapter 5 151

Determination of the Types of Bitter Taste Receptors Expressed in the Rat Pulmonary Artery 151

5.1 Introduction 152

5.1.1 The Expression of Bitter Taste Receptors in the Vascular System 152

5.2 Methods 154

5.2.1 Animals and Tissue Sources 154

5.2.2 DNA Isolation for the Rat Genotyping (DNA Extraction) 154

5.2.3 PCR Primers for the *Tas2r* Genotyping and Gene Expression 156

5.2.3.1 PCR Primers for Tas2r Genotyping 156
5.2.3.2 DNA Agarose Gel Electrophoresis 158
5.2.3.3 Purification of the PCR Products 159

5.2.4 Rat Pulmonary Artery Whole Transcriptome RNA Sequencing Analysis 161

5.2.4.1 Tissue Harvest and Total RNA Isolation 161
5.2.4.2 RNA Concentration 161
5.2.4.3 RNA Integrity 162
5.2.4.4 Whole Transcriptome RNA-Seq 162
5.2.4.5 Gene Expression Analysis 163
5.2.4.6 Selecting the Reference Gene 163
5.2.4.7 Positive Controls 164

5.2.5 Real-Time Polymerase Chain Reaction (RT-PCR) 164

5.2.5.1 PCR Primers for Tas2r Real-Time Quantitative PCR 164
5.2.5.2 cDNA Synthesis 167
5.2.5.3 Quantitative Real-Time Polymerase Chain Reaction (RT-qPCR) 168
5.2.5.4 Delta Ct [ΔCt] Quantification Method 169

5.2.6 Data and Statistical Analysis 169

5.3 Results 170

5.3.1 The genotyping analysis of theTas2rs in the Rat Pulmonary Artery Using Endpoint RT-PCR 170

5.3.2 RNA Concentration 172

5.3.3 RNA Integrity Concentration 172

5.3.4 Detecting the Expression of the Tas2rs in the Rat Pulmonary Arteries by Using RNA Sequencing Analysis 178

5.3.4.1 Gene Expression Analysis 178

5.3.5 Validation of the RNA Sequencing Analysis for Expression of the TAS2Rs in the Rat Pulmonary Arteries by Using RT-qPCR 179

5.3.5.1 Real-Time Polymerase Chain Reaction (RT-PCR) 179

5.4 Discussion 184

5.4.1 TAS2R Expression in the Rat Pulmonary Arteries 184

Chapter 6 187

General Discussion and Conclusion 187

6.1 Role of Bitter Taste Agonist in Vasorelaxation 188

6.2 Mechanisms of Bitter Taste Agonist-Induced Vasorelaxation of Rat Pulmonary Arteries....191

6.3 Expression of TAS2Rs in the Rat Pulmonary Artery....197

6.4 Limitations....198

6.5 Future Directions....201

6.6 Conclusion....202

Chapter 7....204

Appendixes....204

Chapter 8....211

List of References....211

List of Figures

Figure 1.1 The Pulmonary Circulation..... 2

Figure 1.2 Structure of the Pulmonary Arteries. 4

Figure 1.3 Vascular Smooth Muscle Relaxation..... 12

Figure 1.4 Bitter Taste Agonist Relax Airway Smooth Muscle by Localized $[Ca^{2+}]_i$ and Activation of BKca. 32

Figure 1.5 Bitter Taste Agonist Relax Airway Smooth Muscle Cell by Inhibiting L-type VDCCs. 34

Figure 2.1 Images of the Dissected Rat Aorta 43

Figure 2.2 Images of the Rat Pulmonary Artery Dissection. 44

Figure 2.3 Diagram of the Myograph Apparatus. 45

Figure 2.4 Concentration-Response Curves to Phenylephrine in the Rat Aorta and Pulmonary Artery..... 51

Figure 2.5 Concentration-Response Curve to KCl in the Rat Aorta and Pulmonary Artery. 53

Figure 2.6 Representative Traces of Bitter Taste Agonist-Induced Relaxation of the Phenylephrine Pre-contracted Rat Aorta/Pulmonary Artery..... 55

Figure 2.7 Quinine- and Denatonium- Induced Relaxation of the Phenylephrine Pre-contracted Rat Aorta. 57

Figure 2.8 Quinine-and Denatonium-Induced Relaxation of the Phenylephrine Pre-contracted Rat Pulmonary Artery..... 59

Figure 2.9 Dextromethorphan-Induced Relaxation of the Phenylephrine Pre-contracted Rat Pulmonary Artery..... 60

Figure 2.10 Representative Traces of the effect of Bitter Taste Agonists on the Resting Tone of the Rat Pulmonary Artery..... 61

Figure 2.11 The Effect of Carbachol on the Endothelium Intact and Denuded Pulmonary Artery. 63

Figure 2.12 Carbachol-Induced Relaxation in the Rat Pulmonary Artery. 64

Figure 2.13 Concentration-Response Curve to Phenylephrine in the Endothelium Intact and Denuded Rat Pulmonary Artery. 65

Figure 2.14 Bitter Taste Agonists-Induced Relaxation of the Endothelium Intact and Denuded Rat Pulmonary Artery. 67

Figure 2.15 Dextromethorphan-Induced Relaxation of the Intact and Denuded Endothelial Rat Pulmonary Artery. 68

Figure 2.16 Concentration-Response Curve to U46619 of the Rat Pulmonary Artery. 69

Figure 2.17 Quinine-Induced Relaxation of the U46619 Pre-contracted Rat Pulmonary Artery. 70

Figure 3.1 Representative Traces of the Effect of TEA on Bitter Taste Agonists - Induced Relaxation of Pre-contracted Rat Aorta / Pulmonary Artery. 85

Figure 3.2 The Effect of TEA on the Denatonium-Induced Relaxation of the Pre-Contracted Rat Aorta 86

Figure 3.3 The Effect of TEA on the Quinine-Induced Relaxation of the Pre-Contracted Rat Pulmonary Artery. 88

Figure 3.4 The Effect of TEA on the Denatonium and Dextromethorphan Induced Relaxation of the Pre-Contracted Rat Pulmonary Artery. 89

Figure 3.5 Representative Traces of the Effect of Iberiotoxin on the Bitter Taste Agonist-Induced Relaxation of the Rat Pulmonary Artery 91

Figure 3.6 The effect of Iberiotoxin on the Quinine and Denatonium Induced Relaxation of the Pre-Contracted Rat Pulmonary Artery. 92

Figure 3.7 The effect of Iberiotoxin on the Dextromethorphan-Induced Relaxation of the Pre-Contracted Rat Pulmonary Artery. 93

Figure 3.8 Representative traces of the Effect of the Bay K8644 and FPL64176 on Quinine Induced Relaxation of the Rat Pulmonary Artery 95

Figure 3.9 The Effect of Bay K8644 on the Quinine-Induced Relaxation of the Pre-Contracted Rat Pulmonary Artery. 96

Figure 3.10 The effect of FPL64176 on the Quinine-Induced Relaxation of the Pre-Contracted Rat Pulmonary Artery. 98

Figure 3.11 The Effect of Gallein on the Quinine and Denatonium-Induced Inhibition of the Pre-Contracted Rat Pulmonary Artery. 100

Figure 3.12 The Effect of Gallein on the Dextromethorphan-Induced Relaxation of the Pre-Contracted Rat Pulmonary Artery. 101

Figure 3.13 Diagrammatic Overview of the Proposed Pathways of Bitter Taste Agonist-Induced Relaxation..... 102

Figure 4.1 Schematic Showing Increased levels of $[Ca^{2+}]_i$ in Pulmonary Artery SMCs Are Required for Pulmonary Vasoconstriction. 110

Figure 4.2 Rat Pulmonary Artery SMCs Isolation. 117

Figure 4.3 Schematic Diagram Representing the Intracellular Calcium Measurement in the Isolated Rat Pulmonary Artery Smooth Muscle Cells. 119

Figure 4.4 Representative Traces of the Effect of Bitter Taste Agonists on Cal-520 AM Fluorescence in the Rat Isolated Pulmonary Artery SMCs. 126

Figure 4.5 A Representative Trace Shows the Effects of ATP on $[Ca^{2+}]_i$ of the Rat Isolated Pulmonary Artery SMCs. 128

Figure 4.6 Representative Raw Control Traces show the effect of ATP and Quinine of the Rat Isolated Pulmonary Artery SMCs. 130

Figure 4.7 Effect of Quinine on the ATP-Induced Increase in Cal-520 AM fluorescence in Rat Isolated Pulmonary Artery SMCs. 131

Figure 4.8 Representative Raw Control Traces show the effect of ATP and Denatonium of the Rat Isolated Pulmonary Artery SMCs..... 134

Figure 4.9 Effect of Denatonium on the ATP-Induced Increase in Cal-520 AM fluorescence in Rat Isolated Pulmonary Artery SMCs. 135

Figure 4.10 The Effects of Dextromethorphan on the ATP-Induced Increase in Ca^{2+} fluorescence in the Rat Isolated Pulmonary Artery SMCs. 138

Figure 4.11 The Effects of KCl on the Dextromethorphan-Induced Increase in Ca^{2+} fluorescence of the Rat Isolated Pulmonary Artery SMCs. 141

Figure 4.12 The Effects of Ca^{2+}-Free Solution on the Dextromethorphan-Induced Increases in Ca^{2+} fluorescence of the Rat Isolated Pulmonary Artery SMCs. 143

Figure 4.13 The Effect of Thapsigargin on the Response of Rat Isolated Pulmonary Artery SMCs to Dextromethorphan. 144

Figure 4.14 The Effect of U73122 on the Response of Isolated Pulmonary Artery SMCs to Dextromethorphan. 145

Figure 5.1 Diagram Representing the Basic Protocol of the Total DNA Isolation from the Rat Liver Tissue. 155

Figure 5.2 Diagram for the Basic Protocol of the DNA Band Gel Purifications. 160

Figure 5.3 . The PCR Screening of the TAS2Rs in the Rat Pulmonary Artery. 171

Figure 5.4 RNA Integrity Report for the Rat Pulmonary Artery Incubated in RNA-later. 174

Figure 5.5 RNA Integrity Report for the Rat Pulmonary Artery Incubated in Qiazol. 175

Figure 5.6 RNA Integrity Report for the Rat Bronchi Incubated in the RNA-later. 176

Figure 5.7 RNA Integrity Report for the Rat Tongue Incubated in the RNA- later. 177

Figure 5.8 Histogram Showing the Expression of the Tas2r108 and Tas2r139, ß2M, P2X1, Gnat1, and Gnat2 in the Rat Pulmonary Artery. 181

Figure 6.1 Overview of Possible Signalling Mechanisms Involved in Bitter Taste Agonists-Induced Relaxation in The Rat Pulmonary Artery. 200

List of Tables

Table 1.1 Pharmacology Profiles of 25 Human TAS2Rs Stimulated with 104 Natural and Synthetics Bitter Taste Agonists* 15

Table 1.2 List of Bitter Taste Agonists used in this Study..... 17

Table 1.3 The Distribution and Expression of the Known TAS2R in the Various Tissues and Species. 18

Table 5.1 PCR Primer Sequences for the Tas2r Genotyping of Rat Pulmonary Artery. 157

Table 5.2 Real-Time Quantitative PCR Primer Sequences for Rat *Tas2rs* Gene Expression Analysis 165

Table 5.3 Procedure for Synthesis of cDNA from RNA Samples 168

Table 5.4 RNA Concentrations for the Rat pulmonary Artery Tissues. 172

Table 5.5 Different Tissues that were Used for the RNA Integrity Concentrations. 173

Table 5.6 Summary of the Gene Expression of the Rat Pulmonary Artery Sample. 178

Table 5.7 Expressed Gene Lists of Interest in the Rat Pulmonary Artery. 179

Table 5.8 Expression Levels of the Tas2r108, Tas2r139, β2M, P2X1, Gnat1 and Gnat2 in the Rat Pulmonary Artery. 182

Table 5.9 Ct values for the Tas2r108, Tas2r139, Reference Gene and Positive Controls for All the Three Samples and Representative Sample. 183

List of Abbreviations

$[Ca^{2+}]_i$	Intracellular calcium concentration
ACh	Acetylcholine
AII	Angiotensin II
ATP	Adenosine 5'-triphosphate
BK_{Ca}	Large conductance Ca^{2+}-activated K^+ channels
bp	Base pair
Ca^{2+}	Calcium
Ca^{2+}orange-AM	Ca^{2+}orange-acetoxymethyl ester
cAMP	Cyclic adenosine monophosphate
CCK	Cholecystokinin
CGABA	γ-aminobutyric acid
cGMP	Guanosine monophosphate
CO_2	Carbon dioxide
Ctrl	Control
CYX	Cyclohexamide
DAG	Diacylglycerol
DMSO	Dimethyl sulphoxide
EDRF	Endothelium-derived relaxing factor
eNOS	Endothelial nitric oxide synthase
Fluo-4 AM	Fluo-4-acetoxymethyl ester
FPKM	Fragments per kilobase of exon model per million mapped reads
FPS	Frames per second
Fura-2 AM	Fura-2-acetoxymethyl ester
GC	Guanylyl cyclase
GLP-1	Glucagon-like peptide-1
Gnat1	Guanine nucleotide-binding protein G (t) subunit alpha-1 isoform X1
Gnat2	Guanine nucleotide-binding protein G (t) subunit alpha-2
GNAT3	G protein subunit alpha transducin 3

GPCRs	G-protein coupled receptors
IbTX	Iberiotoxin
IP_3	Inositol 1,4,5-triphosphate
Mch	Methacholine
MLC	Myosin light chain
MLCK	Myosin light-chain kinase
NANC	Non-adrenergic non-cholinergic
NMDA	N-methyl-D-aspartate
NO	Nitric oxide
O_2	Oxygen
PA	Pulmonary artery
PAEC	Pulmonary artery endothelial cells
PAFB	Pulmonary artery fibroblasts
PASMC	Pulmonary artery smooth muscle cells
PDE	Phosphodiesterase
PDE-5	Phosphodiesterase type 5
$PGF_{2\alpha}$	Prostaglandin $F_{2\alpha}$
PIP_2	Phosphatidylinositol 4,5-bisphosphate
PKA	Protein kinase A
PKC	Protein kinase C
PKG	Protein kinase G
PLCβ	Phospholipase-Cβ
$PLC\beta_2$	Phospholipase C-beta-2
PSS	Physiological salt solution
PTC	Phenylthiocarbamide
PTX	Pertussis toxin
ROCC	Receptor operated calcium channel
ROCE	Receptor-operated Ca^{2+} entry
ROI	Region of interest
RQI	RNA quality indicator
RT-PCR	Reverse-transcription polymerase chain reaction

RT-qPCR	Real-time quantitative reverse-transcription PCR
SERCA	Sarcoplasmic/endoplasmic reticulum Ca^{2+}- ATPase
SMCs	Smooth muscle cells
SOCC	Store-operated Ca^{2+} channel
SOCE	Store-operated Ca^{2+} entry
TAS2R	Bitter taste receptor type 2
TEA	Tetraethylammonium chloride
U46619	9,11-dideoxy-11α, 9α-epoxy methanoprostaglandin
VDCC	Voltage-dependent calcium channel
VSMCs	Vascular smooth muscle cells

Dedication

To my beloved late father, Mohammed Abdullah Alshehri, whose prayers, support and love were instrumental in achieving my goals; it is my deepest regret that he was unable to see my dream become a reality. May his soul rest in peace.

Acknowledgments

In the Name of Allah, the Most Beneficent, the Most Merciful

Firstly, my deep thanks and gratitude are offered to ALLAH, the Almighty for the perseverance, health and support provided to me, which were instrumental in the completion of this thesis. This thesis is just the beginning of a journey of lifelong learning, and I am greatly thankful for the opportunities I have had to learn new skills and acquire knowledge, while studying for my PhD. This invaluable learning will be a huge support in the future, for both my personal and professional lives.

I wish to extend my great thanks to the people who have supported me and made such an effort to help me achieve my goals. Without them, this journey would not have been possible.

In particular, I would like to pass on my gratitude to Dr. Rothwelle Tate for his guidance and advice, which steered me successfully along the road leading to the completion of my PhD. He showed great kindness and patience, being always prepared to answer my questions. I consider it an honour to have worked with someone with such high levels of knowledge and expertise, and this had undoubtedly helped me to achieve the best possible outcomes from my research.

I must also express my love and gratitude for my soulmate Abdullah and my beautiful son, Mohammed. It is difficult to put into words how much your love and support have given me the strength and perseverance I needed; not only that, but you made my life in Glasgow so much brighter by your presence. I truly am grateful, for your support was an essential element of my success.

My deepest thanks must go to my mother, Fatema, who is the kindest person I know, along with sisters, Nadia, Sara, Noura, Nouf, Manal and Amal and my brothers, Abdullah and Turki. Their love and encouragement have been a great source of support and comfort, and I cannot express enough my enduring love for them.

Last, but certainly not least, I must thank the King Saud University and Royal Embassy of Saudi Arabia Cultural Bureau for the doctoral scholarship that they granted to me. This has helped me to overcome any obstacles I encountered during my PhD journey and give me vital financial support.

Abstract

Bitter taste receptors (TAS2Rs) have been implicated in roles other than taste perception. TAS2R agonists exert vasorelaxant effects in vascular smooth muscle from guinea pig, mouse and humans. We hypothesis that bitter taste agonists could modulate the pulmonary artery vascular tone. The mechanisms of action of bitter taste agonists, which are used to investigate the functions of TAS2Rs, are unclear. The purpose of this study was to pharmacologically characterise the effects of three common bitter taste agonists in the rat pulmonary artery *in vitro* to elucidate their mechanisms of action. In addition, this study sought to investigate which TAS2R subunits are expressed in the rat pulmonary artery. Myographic studies were conducted in rat pulmonary artery rings pre-contracted with phenylephrine or U46619 to study the pharmacological effect of bitter taste agonists as well as to investigate the possible mechanisms involved in their effects. The calcium fluorescence dye Cal-520 AM was used to measure the intracellular calcium levels in freshly isolated pulmonary artery SMCs. RNA sequencing analysis was conducted to determine the mRNA expression of the *Tas2r* subunits in the rat pulmonary artery. In addition, RT-qPCR was conducted using *Tas2r*-specific primers to validate the results from the RNA sequencing analysis. PCR-based genotyping was also carried out to examine the presence of any potential variations on rat TAS2R genes. Quinine, denatonium, and dextromethorphan caused a concentration-dependent relaxation of the pulmonary artery pre-contracted with phenylephrine. Removal of endothelium had no effect in the concentration-response curves for quinine, denatonium, and dextromethorphan, indicating that the effect of these agonists appears to be endothelium-independent in the rat pulmonary artery. Moreover, BK_{Ca} channels and the βγ subunit did not appear to be involved in the mechanism of action of bitter taste agonists on the rat pulmonary artery, as blocking these did not result in an overall significant change in the vasorelaxation. In summary, the results from this *in vitro* study shows that quinine, denatonium, and dextromethorphan have vasorelaxant activities in the rat pulmonary artery. The vasorelaxant action of quinine and denatonium appears to be through inhibition of extracellular calcium influx, most likely through inhibition of ROCC in pulmonary artery SMCs. Dextromethorphan-induced increases in $[Ca^{2+}]_i$ in the rat pulmonary

artery isolated SMCs. Dextromethorphan seems to has dual actions; involving the extracellular in nature in addition to inhibition of ROCC, partially via VDCC, and mostly from intracellular Ca^{2+} stores via the PLC–IP_3 pathway in pulmonary artery SMCs. The molecular biology studies have showed that Tas2r108 and Tas2r139 were expressed in the rat pulmonary artery. These findings suggest that these bitter taste agonists are effective vasorelaxant that might be used in pulmonary hypertension.

Chapter 1

General Introduction

1.1 The Pulmonary Circulation

1.1.1 The Function of the Pulmonary Circulation

The pulmonary vascular bed consists of all the blood vessels inside the lungs and also those connecting the lungs with the heart, including pulmonary arteries, pulmonary veins, and bronchial arteries. The pulmonary circulation is responsible for carrying and transporting the deoxygenated blood from the right side of the heart to the alveoli in the lungs to absorb the oxygen (O_2) and release the carbon dioxide (CO_2). Subsequently, the resultant oxygenated blood flows back to left side of the heart before being distributed to the rest of the body (Hussain *et al.*, 2017; Lee, 1971). The deoxygenated blood is then pumped from the right ventricle of the heart to the pulmonary trunk, which branches in to the left and right pulmonary arteries. These arteries supply the left and right lungs, respectively. Within the lungs, the pulmonary arteries follow the airways closely and have a similar branching pattern, until they form a network of capillaries surrounding the alveoli where the gas exchange takes place. The CO_2 from the blood diffuses into the alveoli for exhalation, and the inhaled O_2 then enters the blood through the alveoli. The oxygenated blood flows into the pulmonary venules and then to the small and large pulmonary veins. These large veins exit the lungs to transport the oxygenated blood into the left atrium of the heart for the systemic circulation (Comroe, 1966; Lee, 1971) (Figure 1.1).

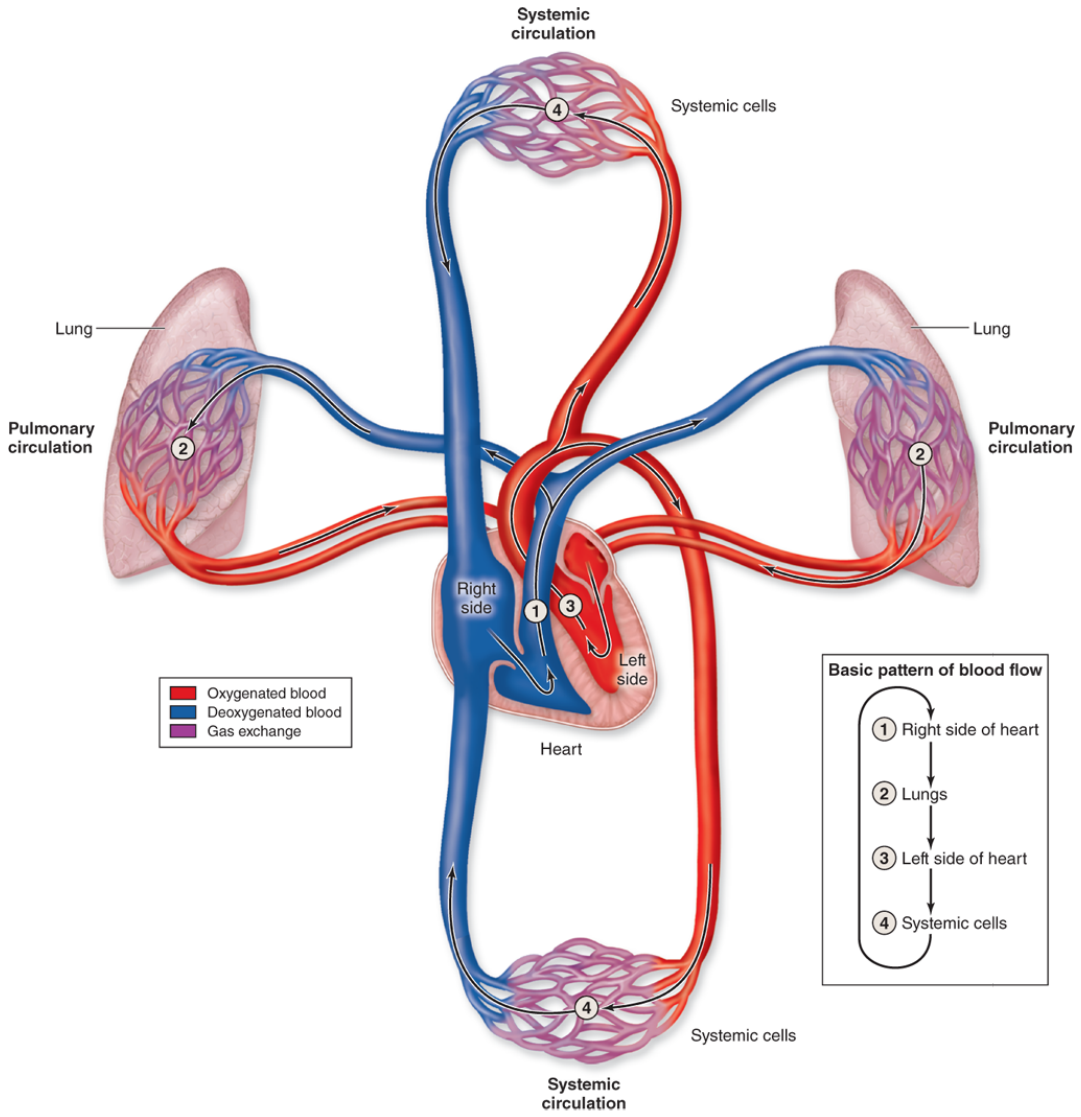

Figure 1.1 The Pulmonary Circulation.

A diagram which depicts the pulmonary circulation **1)** Deoxygenated blood from the body comes back to the heart in large veins and the veins take the blood into the right side of the heart then it pumps blood to the lungs by right ventricle **2)** Inside lungs, the blood picks up O_2 and CO_2 is removed and blood coming back from the lungs goes to the **3)** Left side of the heart **4)** The left side of the heart is pumps blood high in O_2 to the rest of the body for systemic circulation. This figure was adopted from Mescher (2018).

1.1.2 Pulmonary Artery

The walls of the pulmonary artery like other contractile vasculatures, consists of three layers; the internal layer is called the tunica intima which contain endothelial cells, the middle layer is called the tunica media which contain smooth muscle cells and the outer layer is called the tunica externa or adventitia which contain connective tissues, fibroblast and nerve endings (Brij and Peacock, 1998; Hislop and Reid, 1978; Levick, 2013; Townsley, 2011; Welsh and Peacock, 2013) (Figure 1.2). The pulmonary arteries have a thinner layer of smooth muscle and less elastic tissue in comparison to the systematic circulation arteries (Barnes and Liu, 1995). These essential features of the pulmonary arteries are very important in order to maintain the low-pressure and low-vascular resistance of the pulmonary circulation (Barnes and Liu, 1995; Iyinikkel and Murray, 2018; Revermann *et al.*, 2014; Townsley, 2011). The normal mean pulmonary artery pressure is about 15 mmHg at rest. The low-pressure and low vascular resistance structures of pulmonary circulation, along with the large surface area at gas exchanging sites created by the unique alveolar structure, in turn provide a favourable condition for an efficient CO_2 and O_2 exchange between the blood and the air within the alveoli. Unlike the systemic arteries, the pulmonary arteries carry deoxygenated blood and the gas exchange occurs at a capillary level whereas the lungs exchange the CO_2 (Gutierrez *et al.*, 2007; Redfield, Bock and Meakins, 1922).

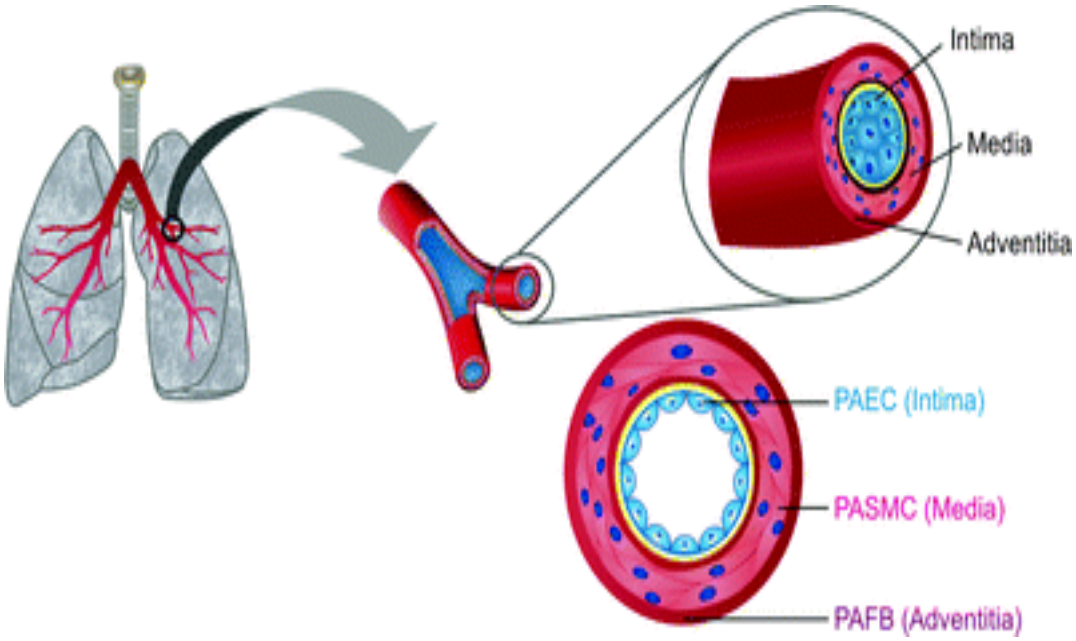

Figure 1.2 Structure of the Pulmonary Arteries.

Diagram shows the pulmonary vasculature starting from the lung and at following magnifications; The close-up structure displays the three main layers of the pulmonary artery: the intima, including pulmonary artery endothelial cells (PAEC), the media, including pulmonary artery smooth muscle cells (PASMC), and the adventitia, contain of mainly of pulmonary artery fibroblasts (PAFB) and fibres such as elastin and collagen. The figure was adopted from Remillard, Makino and Yuan (2011).

1.1.3 Regulation of the Pulmonary Arterial Tone

Unlike the systemic circulation, which is controlled mainly through the sympathetic nervous system, the pulmonary circulation is affected by both active and passive factors (Daly and Hebb, 1966). The passive factors, such as a change in the gravitational force, cardiac output, airway pressure, and left ventricular pressure can lead to a change in the pulmonary vascular resistance and the blood flow. However, active factors which include the autonomic nervous system, hormones, respiratory gases, and the endothelium effects, have a considerable effect on the pulmonary vascular resistance and the tone by causing either vasocontraction or vasodilation of the pulmonary arterial smooth muscle (Barer, 1980). The pulmonary circulation is mainly regulated by the active control factors, and such factors may be particularly relevant in a disease.

1.1.3.1 Autonomic Nervous System

The pulmonary arteries within the lungs are innervated by the vagus nerve and sympathetic fibers, which together form the pulmonary plexuses. These pulmonary plexuses are located within the anterior and posterior sides of the bronchial and vascular structures at the hila of the lungs (Hughes, 2001). The pulmonary plexus receives parasympathetic fibers originating from the dorsal root nucleus in the brainstem and sympathetic fibers which are derived from the cervical sympathetic chain and the upper thoracic sympathetic ganglia. Inside the lungs, these pulmonary plexuses further branch into the periarterial plexuses which innervates the pulmonary blood vessels, and the peribronchial plexuses, which innervate the bronchial airway trees (Richardson, 1979). The sympathetic nerves predominate, and they are located within the adventitia layer of the arteries. The two traditional autonomic control mechanisms, the adrenergic and cholinergic controls have been expanded with the discovery of the non-adrenergic non-cholinergic (NANC) nerves (Barnes and Liu, 1995; PARK *et al.*, 2000)

i. Adrenergic control

The sympathetic fibres have been shown to innervate the pulmonary vascular beds of different species (Barnes and Liu, 1995). For example, in humans, both α and β adrenoceptors have been identified in the pulmonary vasculatures, showing the important role of sympathetic innervation in the regulation of the pulmonary vascular tone (Boe and Simonsson, 1980). The functional role of the adrenergic receptors in the pulmonary artery has been demonstrated as a sympathetic nerve stimulation which leads to vasoconstriction through the α_1 adrenoceptors (Hussain and Marshall, 1997) and vasodilation through activation of the β_2 adrenoceptors (Hyman *et al.*, 1981). In accordance with these findings, the α_1 –adrenoceptor antagonist prazosin, was able to produce a decrease in the raised pulmonary vascular tone which was induced by noradrenaline (Segarra *et al.*, 1999). Indeed, there is an adrenergic innervation of the pulmonary circulation, however, its effect may not be as important as in the systematic circulation where it has a dominant effect on the basal vascular tone (Barnes and Liu, 1995).

ii. Cholinergic control

The pulmonary arteries are also innervated by cholinergic nerves, but they are not as substantial as seen in the respiratory airways (Barnes, 1986; Belmonte, 2005). The functional significance of the cholinergic innervation in the pulmonary circulation is less clear in comparison with the adrenergic control (Barnes and Liu, 1995). Acetylcholine (ACh) is released by the cholinergic nerves and acts on the muscarinic receptors to induce both vasoconstriction (Catravas, Buccafusco and El Kashef, 1984; McLean, 1986) and vasodilation (Fritts et al., 1958). The level of pre-existing tone could explain these conflict findings. Therefore, ACh induces vasoconstriction under rest, whereas it causes vasodilation under conditions of elevated tone (Hyman and Kadowitz, 1988, 1989). ACh response is also seems to be species-variation depending responses. For example, in human, Ach-mediated vasodilation effect under resting tension as well as during hypoxic pulmonary vasoconstriction (Fritts et al., 1958). Moreover, intravenous administration of ACh to the intact-chest cat induced an increase in the lobar arterial pressure at low tonic state of the pulmonary artery, while

intravenous administration of ACh to the intact-chest rabbit induced decrease in the lobar arterial pressure at high tonic state of the pulmonary artery (Hyman and Kadowitz, 1988, 1989).

iii. Non-Adrenergic Non-Cholinergic control

The non-adrenergic non-cholinergic (NANC) neuronal mechanisms of control are not sensitive to either adrenergic or cholinergic blockage (Barnes, Baraniuk and Belvisi, 1991). The NANC control of the pulmonary arteries can be either excitatory (e-NANC) or inhibitory (i-NANC) causing vasoconstriction or vasorelaxation, respectively (Inoue and Kannan, 1988). Adenosine 5'-triphosphate (ATP), which is released from the sympathetic nerves, is an example of the e-NANC transmitter in the rat pulmonary artery (Inoue and Kannan, 1988). The amplitude of the excitatory junction potential was inhibited by the α, β methylene ATP, but was not inhibited by the adrenergic and cholinergic, serotonergic and histaminergic antagonists (Inoue and Kannan, 1988). On the other hand, nitric oxide (NO) has been shown to act as an i-NANC transmitter in guinea-pig pulmonary artery rings, as its synthase inhibitors such as NG-nitro-L-arginine methyl ester (L-NAME), inhibit NO production and subsequently prevents the NO-induced vasodilation (Liu et al., 1992).

1.1.3.2 Humoral Regulation

The low-tone of the pulmonary circulation is also regulated by a variety of hormones and chemical mediators. Many of the circulating hormones and mediators have an influence on the pulmonary arterial tone through their actions at receptors on the smooth muscle. These actions mediate a vasoconstriction or vasodilation depending on which of the receptors are involved. Some of these mediate a pulmonary vasoconstriction, such as angiotensin II (AII), which constricts the isolated pulmonary arterial rings through the activation of the G-protein coupled receptors (GPCRs) (Boe and Simonsson, 1981). Moreover, AII has been proposed as a mediator of hypoxic pulmonary vasoconstriction (Berkov, 1974). But this was disproved later by two studies (Mcmurtry, 1984; Sylvester *et al.*, 2012).

Some hormones and mediators have a dual action, they are able to induce both a vasoconstriction and vasodilation depending on the pulmonary arterial tone (Liu *et al.*, 1989a;b; McCormack, Clarke and Barnes, 1989; Wiklund, Cederqvist and Gustafsson, 1989); they are able to cause a vasoconstriction when the pulmonary artery tone is low, whereas they are able to induce a vasodilation when the pulmonary arterial tone is high. Adenosine 5'-triphosphate (ATP) is an example of this type of dual effect mediator. It is able to produce a concentration-dependent contraction in the isolated pulmonary vessels at a resting tension, and is also able to induce a relaxation of the pre-contracted pulmonary artery (McCormack, Clarke and Barnes, 1989). The vasoconstriction is mediated through A_1 or P_{2X} receptors located on the smooth muscle whereas the vasorelaxation is mediated through A_2 or P_{2y} receptors on the smooth muscle cells or endothelium (McCormack, Clarke and Barnes, 1989; Qasabian *et al.*, 1997).

1.1.3.3 Role of the Endothelium

Some mediators can induce pulmonary arterial vasodilation through their actions on the endothelium (Barnes and Liu, 1995). The endothelium is also able to regulate the vascular tone and this was first discovered accidentally when rubbing the internal layer of the rabbit thoracic aorta, which caused the abolishment of the vasodilatory effect of ACh. That is, the intact vascular endothelium layer was essential for the ACh to mediate its effects (Furchgott and Zawadzki, 1980). This endothelium-dependent relaxation which was subsequently observed in a variety of other vascular tissues including arteries and veins, in response to a diverse range of pharmacological substances (Furchgott, 1984). Acetylcholine as well as other mediators such as noradrenaline (Liu *et al.*, 1991), 5-HT (Glusa and Richter, 1993), bradykinin (Ignarro *et al.*, 1987) and ATP (Liu *et al.*, 1992) were shown to induce a vasorelaxation through the endothelium. This vasorelaxation by was due to the binding to their specific receptors in the endothelial cells which subsequently induced the release of the relaxing factors, named by endothelium-derived relaxing factors (EDRF) (Cherry *et al.*, 1982). It was suggested that these EDRF identified as NO, based on the observations that noticed that the pharmacological similarities in the relaxation induced by EDRF to the relaxation induced by NO (Fuchgott, 1988).

1.1.3.4 Respiratory Gases

Unlike the systematic circulation, the pulmonary arteries displayed a vasoconstrictor response to hypoxia, low O_2 partial pressure, and to high CO_2 partial pressure (Farhi and Sheehan, 1990; Fishman, 1961). Hypoxic pulmonary vasoconstriction is a distinctive compensatory mechanism which occurs in the small pulmonary arteries (Euler and Liljestrand, 1946). Vasoconstriction of the pulmonary artery will occur in response to hypoxia in order to redirect the blood flow away from the oxygen-deficient alveoli in to the oxygen-rich alveoli, in order to maximize the arterial oxygenation (Fishman, 1961). The mechanism underlying hypoxic pulmonary vasoconstriction remains unclear and several hypotheses have been proposed to combat this (Voelkel, 1986). The two main hypotheses for the hypoxic pulmonary vasoconstriction have been proposed. The release of endogenous vasoconstrictors or the suppression of the endogenous vasodilators and a direct effect of the hypoxia on the pulmonary smooth muscle cells (Barnes and Liu, 1995).

It was previously thought a number of mediators, including catecholamine (Fishman, 1961), histamine (Houge, 1968), 5-HT (Fishman, 1961), AII (Berkov, 1974) and ATP (McCormack, Clarke and Barnes, 1989) could be candidates for endogenous vasoconstrictor induced hypoxia. However, none of these have been established as an essential for the hypoxic pulmonary vasoconstriction. Interestingly, endothelin-I was shown to have a crucial role in mediating the chronic hypoxic pulmonary vasoconstriction in rat (DiCarlo *et al.*, 1995). Weir (1978) was the first to propose the hypothesis that the suppression of the vasodilators production such as bradykinin could mediate a hypoxic pulmonary vasoconstriction. It was also proposed that hypoxia induces the inhibition of the voltage gated K^+ channels and subsequently induces a membrane depolarization, which in turn allows Ca^{2+} to enter the cell through voltage-dependent L-type channels in order to induce a contraction (Mcmurtry *et al.*, 1976).

1.1.4 Pulmonary Vascular Disease

Pulmonary hypertension is a condition associated with high pulmonary arterial pressure. The vascular remodelling and abnormal regulation of the pulmonary vascular

tone contribute to the development of pulmonary hypertension (MacLean *et al.*, 2000; Morrell *et al.*, 2009; Reeves and Rubin, 1998). Other conditions are also associated with an altered pulmonary vascular tone, as seen in pulmonary vasculitis and pulmonary thromboembolic disease (Reeves and Rubin, 1998). A clear understanding of the mechanisms responsible for the regulation of the pulmonary vascular tone is essential to understand the pathology of the pulmonary-associated disorders, which can then be used to identify novel therapeutic strategies.

1.1.5 Vascular Smooth Muscle Contraction

The vascular tone is a balance between the vasoconstrictive and vasodilating mediators. The contraction of the vascular smooth muscle is mainly dependent on the intracellular calcium concentration, $[Ca^{2+}]_i$. These levels can increase due to an influx of extracellular Ca^{2+} due to the opening of receptor-operated calcium channels (ROCCs), which are activated by the interaction of agonists with their receptors, and through voltage-dependent calcium channels (VDCCs), which are opened in response to a membrane depolarization (Horowitz *et al.*, 1996).

An increase in $[Ca^{2+}]_i$ is also through release in free cytosolic calcium from the intracellular stores. When an agonist such as phenylephrine, α-adrenoceptor agonist, bind to the GPCR on the smooth muscle cell membrane, the protein complex is started and the GPCR signalling pathway is initated. This results in a conformational change of the receptor which causes the dissociation of the Gαq and Gβγ subunits. The Gαq subunit then activates phospholipase-Cβ (PLCβ) which promotes the hydrolysis of phosphatidylinositol 4,5-bisphosphate (PIP_2) into diacylglycerol (DAG) and inositol 1,4,5-triphosphate (IP_3). DAG is able to activate the protein kinase C (PKC), whereas IP_3 induces the release of Ca^{2+} release from the sarcoplasmic reticulum (SR) through its interaction with the IP_3 receptor (Berridge, 1984b;a).

Together, both the extracellular and intracellular sources increase the $[Ca^{2+}]_i$. As a result of the increased $[Ca^{2+}]_i$, the Ca^{2+} then binds to calmodulin, which undergoes a conformational change. After which, the Ca^{2+} - calmodulin complex activates the myosin light chain kinase (MLCK) (Dillon *et al.*, 1981). The 20 kDa subunit of the

myosin light chain (MLC) is the target for the phosphorylation by MLCK. This phosphorylation enables the actin filament to interact with the myosin and then activate the myosin's magnesium-dependent ATPase activity. This ATPase then splits the high-energy phosphate bonds in ATP and thus provides the energy needed for the actin-myosin cross-bridge cycling which promotes smooth muscle contraction (Bárány, 1967; Hai and Murphy, 1989). Upon contraction, the vascular smooth muscle cells shorten, thus decreasing the diameter of the blood vessels in order to regulate the blood flow and pressure.

1.1.6 Vascular Smooth Muscle Relaxation

Lowering $[Ca^{2+}]_i$ is the main role to induce vascular smooth muscle relaxation. NO is an important mediator in vascular smooth muscle relaxation (Vallance, Collier and Moncada, 1989). Release of NO from endothelial cells has been seen after stimulation with a variety of substances including ACh (Moncada, Palmer and Higgs, 1991). Vascular smooth muscle relaxation initiated in the endothelial cells with stimulation of the endothelial NO synthase (eNOS) (Moncada, Palmer and Higgs, 1989; Palmer and Moncada, 1989). eNOS is able to catalyse the conversion of L-arginine into L-citrulline and NO (Pollock *et al.*, 1991). NO diffuses into smooth muscle cells and then activate soluble guanylyl cyclase (GC). This activation leads to the conversion of guanosine triphosphate (GTP) to cyclic guanosine monophosphate (cGMP) (Furchgott and Vanhoutte, 1989). cGMP activates protein kinase G (PKG) which phosphorylates several muscle proteins to induce vascular smooth muscle relaxation (Carvajal *et al.*, 2000) (Figure 1.3).

NO can affect vascular smooth muscle cells also through GC-independent pathways. For examples, via activating K^+ channels, including opening of ATP-sensitive K^+ channels (Wolin *et al.*, 1998), or through activation of large-conductance Ca^{2+}-activated K^+ channels can in turn lead to the opening of this channel and cause a membrane hyperpolarization and subsequently vasodilation (Bolotina *et al.*, 1994), or through activation of voltage-gated K^+ channels (Yuan *et al.*, 1996), or via acceleration of Ca^{2+} sequestration into intracellular stores through stimulation of the sarcoplasmic-endoplasmic reticulum Ca^{2+}-ATPase (SERCA) (Adachi *et al.*, 2004;

Cohen *et al.*, 1999). sGC-dependent and independent pathways can be implicated simultaneously (Zhao *et al.*, 1997).

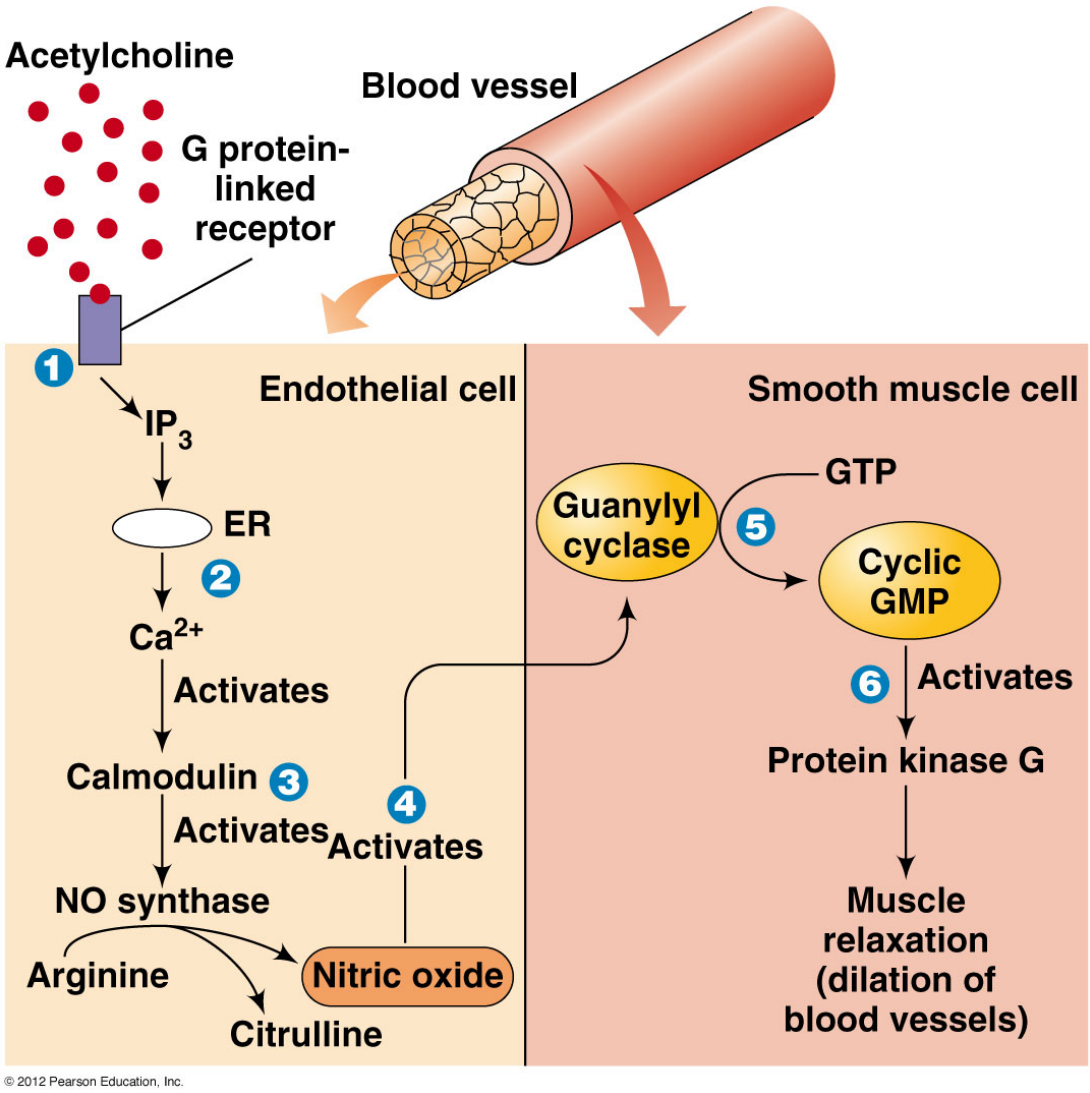

Figure 1.3 Vascular Smooth Muscle Relaxation.

This figure displays the vascular smooth muscle GC-dependent pathway **1)** acetylcholine binds to GPCR and causes IP_3 production **2)** IP_3 releases Ca^{2+} ions from SR **3)** Ca^{2+} and calmodulin form complex which stimulates eNOS to produce NO **4)** NO synthase converts L-arginine to L-citrulline and NO **5)** NO leaves endothelial cell into smooth muscle cells **6)** In smooth muscle cell, NO activates GC to induce cGMP **7)** cGMP activates PKG which subsequently produce vascular muscle relaxation. This figure was adopted from Bullock and Hales (2012).

1.2 Bitter Taste Receptors

Taste perception plays a vital role in evaluating the nutritional value and quality of food after ingestion. Humans can sense a variety of foods, but can only distinguish five basic tastes, which are: sweet, salty, umami, sour and bitter (Finger and Kinnamon, 2011). The bitter taste is detected in the taste bud regions of the tongue through the taste sensing type 2 receptors, which belong to a family of GPCRs (Adler *et al.*, 2000; Chandrashekar *et al.*, 2000; Matsunami, Montmayeur and Buck, 2000; Mueller *et al.*, 2005). The standard gene symbol assigned by HUGO Gene Nomenclature Committee (HGNC) for bitter taste receptor coding genes is *TAS2R*. As their name implies, TAS2Rs are involved in the sensation of either natural or artificial bitter substances. The molecular basis of bitter taste perception is thought to have evolved for functional reasons. Although a clear relation between toxicity and bitterness has not been established (Glendinning, 1994), the bitter taste perception is thought to be able to detect toxins as a wide range of chemical substances have a bitter taste. The ability to sense a bitter taste has proved to be advantageous to avoid the ingestion of many bitter tasting substances that could be toxic (Meyerhof *et al.*, 2010). Chandrashekar *et al*., (2000) were the first to study and provide evidence of the molecular components involved in the perception of bitter taste. They hypothesised that a large family of genes whose products were able to detect bitter substances must exist.

1.2.1 Signal Transduction by Bitter Taste Receptor in Gustatory Tissues

The signalling pathway in the taste bud cells which expresses the TAS2Rs, starts once a bitter tasting agonist binds to one or more of the TAS2Rs. This then induces a conformational change in the receptor and subsequently activates the intracellular heterotrimeric G-protein complex (Chaudhari and Roper, 2010). The heterotrimeric G-protein which is involved in taste transduction is composed predominantly of Gα gustducin or G protein subunit alpha transducin 3 (GNAT3), along with the Gβ3 and Gγ13 subunits (Huang *et al.*, 1999). The bitter taste agonist mediated activation of the heterotrimeric G-protein in turn leads to the dissociation of a Gα gustducin and the Gβ3γ13 subunits (Wong, Gannon and Margolskee, 1996; Caicedo *et al.*, 2003). Once

this complex has been activated, the Gβ3γ13 subunits activates phospholipase C-beta 2 (PLCβ2), which in turn hydrolyses the phosphatidylinositol-4,5-bisphosphate (PIP_2) into inositol-1,4,5-triphosphate (IP_3) and diacyl glycerol (DAG). The IP_3 then stimulates the release of the Ca^{2+} from the intracellular calcium stores by acting on the IP_3 receptors (IP_3R) on the endoplasmic reticulum (Zhang *et al.*, 2003). The Gα gustducin subunit can activate phosphodiesterase (PDE) in order to reduce the cAMP levels (Clapp *et al.*, 2008). This activation then leads to a reduction in protein kinase A (PKA) activity. The PKA acts as an inhibitor of the IP_3R mediated Ca^{2+} release by phosphorylating the receptor and making it unresponsive to the activation by a secondary messengers such as IP_3 (Clapp *et al.*, 2008). The overall elevated Ca^{2+} level results in the opening of the transient receptor potential cation channel member 5 (TRPM5) (Pérez *et al.*, 2002). This then leads to the depolarization of the cell membrane and the activation of the sodium channels. Consequently, this results in an action potential being generated that in turn causes the release of ATP. The ATP then activates the purinergic receptors on the afferent nerve fibers, which transmits the chemosensory signals to the central nervous system CNS (Kinnamon, 2012).

1.2.2 Pharmacological Characterization of the TAS2Rs

Pharmacologically, the TAS2Rs are characterized by two important features. Firstly, the TAS2Rs have a relatively low affinity and thus require high concentrations of the bitter taste agonists, ranging from μM to mM, to activate them (Clark, Liggett and Munger, 2012; Meyerhof *et al.*, 2010). Secondly, they are broadly tuning, allowing them to have the ability to respond to a number of different bitter taste agonists. This can be explained through two mechanisms; the TAS2Rs may have more than a single agonist-binding pocket, and each of these pockets are designed to accommodate subgroups of agonists with common structural details. However, they may only possess a single binding pocket which accommodates a number of agonists through its ability to adapt and overlap sets of amino acids residues (Meyerhof *et al.*, 2010). A screening study was conducted on 104 bitter taste agonists for human TAS2Rs, including natural and synthetic bitter compounds (Meyerhof *et al.*, 2010). They showed that three TAS2Rs were very broadly tuned, which consist of TAS2R10, TAS2R14 and TAS2R46. Each responded to around 30 structurally different

compounds, and together detected about half of all bitter compounds applied. Another group of TAS2Rs responded to a narrow range of compounds, which are TAS2R3, TAS2R5, TAS2R8, TAS2R13, TAS2R49 and TAS2R50. They respond to fewer bitter compounds (about 3 of the 104). The majority of the TAS2Rs show an intermediate degree of tonicity, including TAS2R1, TAS2R4, TAS2R7, TAS2R16, TAS2R38, TAS2R39, TAS2R40, TAS2R43, TAS2R44, and TAS2R47. They responded to 6-20% of the bitter compounds studied. The last group comprise TAS2R16 and TAS2R38, which are considered specifically tuned receptors and they were sensitive to a single bitter compound (Meyerhof *et al.*, 2010). Therefore, this might indicate that humans detect numerous bitter compounds with a very small number of generalist receptors and a small number of compounds with specialist receptors, while the majority of TAS2Rs appear to be of intermediate tonicity (Table 1.1).

Table 1.1 Pharmacology Profiles of 25 Human TAS2Rs Stimulated with 104 Natural and Synthetics Bitter Taste Agonists*

TAS2R subtype	Pharmacological Action	Natural Bitter compound/s Responded	Synthetic Bitter compound/s Responded
TAS2R1	Intermediate tuned	Amarogentin, arborescin, cascarillin, chloramphenicol, humulone isomers, parthenolide, picrotoxinin, thiamine, and yohimbine	Dextromethorphan, diphenidol, diphenylthiourea, sodium cyclamate, and sodium thiocyanate
TAS2R3	Narrow tuned	None	Chloroquine
TAS2R4	Intermediate tuned	Amarogentin, arborescin, artemorin, campher, colchicine, parthenolide, picrotoxinin, thiamine, and yohimbin	Azathioprine, chlorpheniramine, dapsone, denatonium benzoate, and diphenidol.
TAS2R5	Narrow tuned	None	1,10-Phenanthroline
TAS2R7	Intermediate tuned	Caffeine, papaverine, and quinine	Chlorpheniramine, dapsone, and diphenidol
TAS2R8	Narrow tuned	Chloramphenicol, and parthenolide	Denatonium benzoate
TAS2R10	broadly tuned	Absinthin, arborescin, arglabin, artemorin, brucine, campher, caffeine, cascarillin, chloramphenicol, coumarin, cucurbitacin B, cucurbitacin E, erythromycin, papaverine, parthenolide, picrotoxinin, quassin, quinine, strychnine, thujon , and yohimbine	Azathioprine, benzoin, chloroquine, chlorpheniramine, cycloheximide, denatonium benzoate, dextromethorphan, diphenidol, famotidine, and haloperidol

TAS2R13	Narrow tuned	None	Denatonium benzoate, and diphenidol
TAS2R14	broadly tuned	Absinthin, arborescin, arglabin, aristolochic acid, artemorin, campher, caffeine, cascarillin, coumarin, cucurbitacin B, falcarindiol, humulone isomers, noscapine, papaverine, parthenolide, picrotoxinin, quassin, and thujon	azathioprine, benzamide, benzoin, carisoprodol, chlorhexidine, chlorpheniramine, diphenhydramine, diphenidol, diphenylthiourea, divinylsulfoxid, flufenamic acid, haloperidol, 4-hydroxyanisol, and sodium benzoate
TAS2R16	Intermediate tuned	Amygdalin D, arbutin, helicin, D-salicin, sinigrin	Diphenidol, and sodium benzoate
TAS2R38	Intermediate tuned	Allylisothiocyanyte, ethylpyrazine, Limonin, phenylethyl isothiocyanate, sinigrin, and Yohimbine	Acetylthiourea, caprolactam, chlorpheniramine, dimethyl thioformamide, diphenidol, diphenylthiourea, N-ethylthiourea, N,N-ethylene thiourea, methimazole, 4(6)-methyl-2-thiouracil, methylthiourea , phenylthiocarbamide, propylthiouracil, sodium cyclamate, and sodium thiocyanate
TAS2R39	Intermediate tuned	Amarogentin, chloramphenicol, colchicine, quinine, and thiamine	Acetaminophen, azathioprine, chloroquine, chlorpheniramine, denatonium benzoate, and diphenidol
TAS2R40	Intermediate tuned	Humulone isomers, and quinine	chlorpheniramine, dapsone, diphenhydramine, and diphenidol
TAS2R43	Intermediate tuned	Aloin, amarogentin, arborescin, arglabin, aristolochic acid, caffeine, chloramphenicol, falcarindiol, grossheimin, helicin, and quinine	Acesulfame K, cromolyn, denatonium benzoate, diphenidol, and saccharin
TAS2R44	Intermediate tuned	Aristolochic acid, parthenolide, quinine	Acesulfame K, diphenidol, famotidine, and saccharin
TAS2R46	Broadly tuned	Absinthin, amarogentin, andrographolide, arborescin, arglabin, artemorin, brucine, caffeine, cascarillin, chloramphenicol, cnicin, colchicine, crispolide, grossheimin, parthenolide, picrotoxinin, quassin, quinine, strychnine, tatridin B, and yohimbine	Azathioprine, carisoprodol, chlorpheniramine, denatonium benzoate, diphenidol, hydrocortisone, and orphenadrine
TAS2R49	Narrow tuned	None	Cromolyn, and diphenidol
TAS2R50	Narrow tuned	Amarogentin, and andrographolide	None

* (Meyerhof *et al.*, 2010).

1.2.3 Bitter Taste Agonists

In humans, 25 TAS2Rs have been identified and the genes which encode for them are located on the chromosome 5p15, 7q31 and 12p13 (Reichling, Meyerhof and Behrens, 2008). There are thousands of substances which are consider to be bitter by humans (Wiener *et al.*, 2011). Meyerhof *et al.* (2010) conducted a study on a collection of 104 bitter tasting compounds, of which 58 were natural and 46 were synthetic compounds. The study looked at investigating the ability of these compounds to activate the subtypes of TAS2Rs (Meyerhof *et al.*, 2010). The TAS2Rs responded to an enormous number of bitter tasting compounds, some of them were naturally occurring such as caffeine, quinine and noscapine, while others were synthetic compounds such as denatonium, dextromethorphan and propylthiouracil. Lists of bitter taste agonists relevant in this study are shown in Table 1.2.

Table 1.2 List of Bitter Taste Agonists used in this Study

TAS2R Agonist	Action	TAS2R Activated in Human	References
Quinine	Antimalarial	TAS2R4, TAS2R7, TAS2R14, TAS2R31, TAS2R39, TAS2R40, TAS2R43 and TAS2R44	(Meyerhof *et al.*, 2010)
Denatonium	Synthetic compound for laboratory work + Aversive agent	TAS2R4, TAS2R8, TAS2R46 and TAS2R47	(Brockhoff *et al.*, 2007; Klein-Schwartz, 1991)
Dextromethorphan	Antitussive	TAS2R1 and TAS2R10	(Meyerhof *et al.*, 2010)

1.2.4 The Extra-Oral Function of the TAS2Rs

The distribution of the gene expression of TAS2Rs in mammals has gained interest in recent years due to a growing appreciation that their function is not limited to taste perception as they could also functions as receptors for endogenous chemical mediators. The expression of TAS2R mRNAs has been identified in a number of organs and tissues the human, rat and mouse and these are listed in Table 1.3. The extra-oral expression support the concept that there is more than taste function to the TAS2Rs and they are able to exert non-gustatory functions outside of the mouth (Finger and Kinnamon, 2011).

Table 1.3 The Distribution and Expression of the Known TAS2R in the Various Tissues and Species.

This table shows the distribution and expression of different TAS2R subunits expressed in different systems and species.

Tissue /organs/ systems source	Species	TAS2R subunit	Cell or tissue types	References
Tongue	Rat	TAS2R2, TAS2R3, TAS2R4, TAS2R7 and TAS2R8	Taste receptor cells	(Adler *et al.*, 2000)
		TAS2R40, TAS2R105, TAS2R107, TAS2R118, TAS2R121, TAS2R136 and TAS2R140	Tongue circumvallate papilla	(Sekine *et al.*, 2012)
	Mouse	TAS2R108	Tongue	(Sakai *et al.*, 2016)
		TAS2R5, TAS2R8	Taste receptor cells	(Chandrashekar *et al.*, 2000)
		TAS2R131	Tongue	(Voigt *et al.*, 2012)
Brain	Human	TAS2R4, TAS2R5, TAS2R10, TAS2R13, TAS2R14 and TAS2R50	Frontal cortex	(Garcia-Esparcia *et al.*, 2013)
	Rat	TAS2R1	Brain stem, cerebellum	(Dehkordi *et al.*, 2012)
		TAS2R4, TAS2R10 (except brain stem) and TAS2R38	Brain stem, cortex cerebellum,	(Singh *et al.*, 2011)

			nucleus accumbens (NAc) and C6 glial cells.	
		TAS2R144	Cultured cells from choroid plexus epithelium cells	(Tomás *et al.*, 2016)
Airway	Human	TAS2R4, TAS2R38, TAS2R43 and TAS2R46	Ciliated airway epithelium cell	(Shah *et al.*, 2009)
		TAS2R1, TAS2R3, TAS2R4, TAS2R5, TAS2R8, TAS2R9, TAS2R10, TAS2R13 TAS2R14, TAS2R19, TAS2R20, TAS2R30, TAS2R31, TAS2R42, TAS2R45, TAS2R46 and TAS2R50	Isolated airway smooth muscle cells	(Deshpande *et al.*, 2010)
		TAS2R38	Upper respiratory epithelial cells	(Lee *et al.*, 2012)
		TAS2R3, TAS2R4, TAS2R5, TAS2R7, TAS2R8, TAS2R9, TAS2R10, TAS2R14, TAS2R19, TAS2R20, TAS2R31, TAS2R38, TAS2R39, TAS2R43, TAS2R45 and TAS2R46	Bronchi	(Grassin-Delyle *et al.*, 2013)
		TAS2R31	Airway smooth muscle	(Camoretti-Mercado *et al.*, 2015)
	Rat	TAS2R119, TAS2R121, TAS2R107, TAS2R123, TAS2R105, TAS2R134, TAS2R126	Nasal respiratory epithelium, Larynx, trachea	(Tizzano *et al.*, 2010)
	Mouse	TAS2R107	Airway smooth muscle cells	(Zhang *et al.*, 2013)
		TAS2R105 and TAS2R108	Trachea	(Krasteva *et al.*, 2011)
		TAS2R108	Bronchi	(Sakai *et al.*, 2016)
		TAS2R107	Airway smooth muscle cells	(Tan and Sanderson, 2014)

	Guinea pig	TAS2R3, TAS2R4 and TAS2R10	Trachea	(Pulkkinen *et al.*, 2012)
Gastro-intestinal tract	Human	TAS2R1, TAS2R4 and TAS2R38	Large intestine	(Kaji *et al.*, 2009)
		TAS2R1, TAS2R3, TAS2R4, TAS2R5, TAS2R38, TAS2R39, TAS2R40, TAS2R41 and TAS2R60	Large intestine (colon, cecum)	(Dotson *et al.*, 2008)
	Rat	TAS2R1, TAS2R2, TAS2R3, TAS2R4, TAS2R5, TAS2R6, TAS2R7, TAS2R8, TAS2R9, TAS2R10, TAS2R11 and TAS2R12	Duodenum	(Wu *et al.*, 2002)
		TAS2R1, TAS2R2, TAS2R3, TAS2R5, TAS2R6, TAS2R7, TAS2R8, TAS2R9, TAS2R10, TAS2R11 and TAS2R12	Antrum	(Wu *et al.*, 2002)
		TAS2R1, TAS2R2, TAS2R3, TAS2R6, TAS2R7, TAS2R8, TAS2R9, TAS2R10, TAS2R11 and TAS2R12	Fundus	(Wu *et al.*, 2002)
		TAS2R2, TAS2R3, TAS2R5, TAS2R6, TAS2R8, TAS2R10 and TAS2R12.	gastric endocrine cells.	(Wu *et al.*, 2002)
		TAS2R10	Enteric nervous system and smooth muscle cells of the rat ileum	(Jing *et al.*, 2013)
		TAS2R1, TAS2R2, TAS2R3, TAS2R4, TAS2R6, TAS2R7, TAS2R8, TAS2R9 and TAS2R12	Intestinal entereoendocrine cells STC-1	(Wu *et al.*, 2002)
		TAS2R1, TAS2R16 and TAS2R26	Large intestine	(Kaji *et al.*, 2009)
	Mouse	TAS2R108	Ileum	(Sakai *et al.*, 2016)
		TAS2R138	Small intestine (duodenum, jejunum)	(Jeon et al., 2008)
		TAS2R5 and TAS2R19	Stomach (antrum, fundus) and duodenum	(Wu *et al.*, 2002)
	Mouse	TAS2R108 and TAS2R138	Stomach (antrum, fundus) and duodenum	(Wu, Chen and Rozengurt, 2005)

		TAS2R2, TAS2R5, TAS2R7, TAS2R18, TAS2R19, TAS2R23, TAS2R26, and TAS2R30	Intestinal entereoendocrine cells STC-1	(Wu *et al.*, 2002)
		TAS2R108, TAS2R137, TAS2R138, TAS2R144 and TAS2R135	STC-1 cells	(Chen *et al.*, 2006)
		TAS2R108 and TAS2R138	Stomach, colon and small intestine	(Vegezzi *et al.*, 2014)
	Pig	TAS2R1, TAS2R3, TAS2R7, TAS2R9, TAS2R10, TAS2R16, and TAS2R38	Gastrointestinal tract	(Colombo *et al.*, 2012)
Thymus	Mouse	TAS2R131		(Voigt *et al.*, 2012)
Endocrine system: Thyroid gland	Human	TAS2R4, TAS2R10, TAS2R38, TAS2R42, and TAS2R43	Human thyroid and human thyrocyte line Nthy Ori 3-1	(Clark *et al.*, 2014)
	Mouse	TAS2R38	Mouse thyrocytes	(Clark *et al.*, 2014)
Kidney	Mouse	TAS2R108, TAS2R119, TAS2R135, TAS2R137, TAS2R138, TAS2R140 and TAS2R143	Kidney tissue	(Rajkumar *et al.*, 2014)
		TAS2R105, TAS2R106, TAS2R110, TAS2R113, TAS2R114, TAS2R134 and TAS2R143	Kidney tissue	(Liu *et al.*, 2015)
Bladder	Human	TAS2R1, TAS2R4, TAS2R5, TAS2R7, TAS2R8, TAS2R9, TAS2R10, TAS2R13 TAS2R14, TAS2R20, TAS2R30, TAS2R31, TAS2R38, TAS2R39, TAS2R40, TAS2R45 and TAS2R50	Human detrusor smooth muscle	(Zhai *et al.*, 2016)
	Mouse	TAS2R108	Isolated mouse urethral brush cells	(Deckmann *et al.*, 2014)
		TAS2R102, TAS2R103, TAS2R108, TAS2R109, TAS2R114, TAS2R116, TAS2R117, TAS2R120, TAS2R122, TAS2R126, TAS2R130, TAS2R131, TAS2R135, TAS2R137, TAS2R138, TAS2R139, TAS2R140, TAS2R143 and TAS2R144	Mouse detrusor smooth muscle	(Zhai *et al.*, 2016)
Endocrine systems	Human	TAS2R9	Human enteroendocrine NC1-H716 cells	(Dotson *et al.*, 2008)

Reproductive systems	Human	TAS2R38	Amniotic epithelium, syncytiotrophoblast and decidua cells in human placenta and placenta cell line	(Wölfle *et al.*, 2016)
		TAS2R4, TAS2R5, TAS2R10, TAS2R10 and TAS2R13	Freshly isolated human myometrial tissues	(Zheng *et al.*, 2017)
		TAS2R4, TAS2R5, TAS2R7, TAS2R8, TAS2R10, TAS2R13, TAS2R14, TAS2R31, TAS2R39, TAS2R42, TAS2R43, TAS2R45 and TAS2R50	Cultured hTERT-infected human myomerial cells	(Zheng *et al.*, 2017)
	Mouse	TAS2R126, TAS2R135, TAS2R137 and TAS2R143	Myometrium cells from pregnant mice.	(Zheng *et al.*, 2017)
		TAS2R5	Testis	(Li and Zhou, 2012)
		All 35 TAS2R genes were expressed in mouse testis	Testis	(Xu *et al.*, 2012)
Cardiovascular system	Human	TAS2R3, TAS2R4, TAS2R5, TAS2R9, TAS2R10, TAS2R13, TAS2R14, TAS2R19, TAS2R20, TAS2R30, TAS2R31, TAS2R43, TAS2R45, TAS2R46 and TAS2R50	Heart	(Foster *et al.*, 2013)
		TAS2R46	Human aortic smooth muscle cells and bone marrow stromal cells	(Lund *et al.*, 2013)
		TAS2R1, TAS2R3, TAS2R4, TAS2R5, TAS2R7, TAS2R8, TAS2R9, TAS2R10, TAS2R13, TAS2R14, TAS2R39, TAS2R42, TAS2R43, TAS2R44, TAS2R45, TAS2R46, TAS2R47, TAS2R48, TAS2R49, TAS2R50 and TAS2R60	Pulmonary artery smooth muscle cells	(Upadhyaya *et al.*, 2014)

		TAS2R3, TAS2R4, TAS2R10 and TAS2R14	Pulmonary artery	(Manson *et al.*, 2014)
		TAS2R3, TAS2R4, TAS2R7, TAS2R10, TAS2R14, TAS2R39 and TAS2R40	Human omental artery	(Chen *et al.*, 2017)
	Rat	TAS2R107	Aorta	(Xin and Chen, 2017)
		TAS2R108, TAS2R120, TAS2R121, TAS2R126, TAS2R135, TAS2R137 and TAS2R143	Heart	(Foster *et al.*, 2013)
		TAS2R39, TAS2R40, TAS2R108, TAS2R114, TAS2R130, TAS2R137 and TAS2R140	Rat mesenteric and cerebral arteries	(Chen *et al.*, 2017)
	Mouse	TAS2R108	Aorta	(Sakai *et al.*, 2016)
		TAS2R108, TAS2R120, TAS2R121, TAS2R126, TAS2R135, TAS2R137 and TAS2R143	Heart	(Foster *et al.*, 2013)
		TAS2R108, TAS2R137 and TAS2R143	Heart	(Foster *et al.*, 2014)

1.2.5 TAS2Rs in Smooth Muscles

1.2.5.1 TAS2Rs in the Gastrointestinal Tract

The expression of the TAS2Rs are not restricted solely to the oral cavity. The TAS2Rs have also been reported to be expressed in regions of the gastrointestinal tract of rats (Jing *et al.*, 2013; Kaji *et al.*, 2009; Wu *et al.*, 2002), mouse (Chen *et al.*, 2006; Jeon *et al.*, 2008; Sakai *et al.*, 2016; Vegezzi *et al.*, 2014; Wu *et al.*, 2002), pigs (Colombo *et al.*, 2012) and humans (Dotson *et al.*, 2008; Kaji *et al.*, 2009) (Table 1.2). TAS2Rs have been found on the enteroendocrine cell lines (STC-1), and play an important role in several functions of the gastrointestinal tract (Wu *et al.*, 2002). Bitter taste agonists have been reported to play a crucial role in releasing gastrointestinal hormones including cholecystokinin (CCK) and glucagon-like peptide-1 (GLP-1) and hunger hormone ghrelin. For example, Denatonium (a TAS2R108 agonist) and phenylthiocarbamide (PTC) (a TAS2R138 agonist) both stimulate the mouse STC-1 cells to release peptide hormone cholecystokinin (CCK) in the duodenum. CCK responsible for stimulating the digestion of fat and proteins. This was seen to occur in concentration-dependent manner with both denatonium and PTC (Chen *et al.*, 2006). Another example for the role of TAS2Rs in regulating CCK hormone was reported by Jeon *et al.* (2008) who showed that a low-cholesterol diet or store depletion culture cause an increase in TAS2R expression in the mouse STC-1 cell line, which in turn stimulate the release of CCK. These results suggest that this regulation is a protective mechanism during herbal diet that contains low cholesterol and is potentially rich in plant toxins (Jeon *et al.*, 2008). Bitter taste agonists have been also reported to regulate gastrointestinal hormone GLP-1, Dotson *et al.* (2008) showed that TAS2R9 ligands (ofluxacin, pirenzepine, and procainamide) induced a concentration response rise in the glucagon-like peptide-1 (GLP-1), which is a hormone that regulates the glucose homeostasis by stimulating insulin release from the pancreatic β-cells and inhibiting glucagon secretion from the pancreatic α–cells (Baggio and Drucker, 2007). Bitter taste agonists have also impact on the hunger hormone ghrelin, intra-gastric administration of the bitter taste agonists (denatonum, PTC, salicin, and propylthiouracil) in mice stimulated the secretion of the hunger hormone ghrelin,

which resulted in a short term increase in food intake followed by a prolonged decrease in food intake (Janssen *et al.*, 2011).

Bitter taste receptors can modulate gastrointestinal motility, the effect of the denatonium on the mouse gastrointestinal smooth muscle was shown to have a concentration-dependent action. In mouse fundic muscle strips, at lower concentrations, denatonium was able to induce a smooth muscle contraction, whereas at higher concentrations it produced a relaxation (Avau *et al.*, 2015). In regards to the gastric emptying, the intra-gastric administration of denatonium was able to induce a TAS2R-dependent delay in the gastric emptying (Avau *et al.*, 2015; Glendinning *et al.*, 2008; Janssen *et al.*, 2011). In humans, healthy volunteers showed an impaired fundic relaxation in response to the intra-gastric nutrient infusion and a decreased nutrient volume tolerance and subsequently an increased satiation through the oral challenge test after the intra-gastric administration of denatonium when compared to those given the placebo (Andrews *et al.*, 2013; Avau *et al.*, 2015).

From a drug development prospective, the bitter taste agonists may contribute to possesing a protective role upon the ingestion of a bitter compounds and could be considered as a novel targets to treat gastrointestinal motility disorders (Avau *et al.*, 2015). Additionally, propylthiouracil induces anion efflux from both human and rat colonic mucosa. Therefore, bitter taste agonists may be used to decrease the absorption of a toxic substance by inducing anion secretion (Kaji *et al.*, 2009).

1.2.5.2 TAS2Rs in the Central Nervous Systems

Several studies have been able to demonstrate the presence of TAS2Rs in different regions of the central nervous systems in human (Garcia-Esparcia *et al.*, 2013) and rat (Dehkordi *et al.*, 2012; Singh *et al.*, 2011; Tomás *et al.*, 2016) (Table 1.2). The administration of quinine and denatonium was able to induce a concentration-dependent increase in $[Ca^{2+}]_i$ both in the rat primary neuronal cells and C6 glial cells. These findings indicate that the TAS2Rs are functional in the CNS (Singh *et al.*, 2011). Garcia-Esparcia *et al.* (2013) showed that in Parkinson's disease patients, the TAS2R4 and TAS2R50 were decreased, whereas, TAS2R10 and TAS2R13 were both increased in both the pre-motor and parkinsonian stages in the frontal cortex area (Garcia-

Esparcia *et al.*, 2013). Additionally, Ansoleaga *et al.* (2013) demonstrated that the TAS2R4, TAS2R5, TAS2R14 and TAS2R50 were all dowenregulated in the dorsolateral prefrontal cortex of Schizophrenia patients (Ansoleaga *et al.*, 2013). These results may indicate that the expression of the TAS2Rs in Parkinson's disease and Schizophrenia patients seems to be dysregulated and this might be due to the side effects induced by antipsychotic medications which are mostly bitter tasting (Ansoleaga *et al.*, 2013; Garcia-Esparcia *et al.*, 2013).

1.2.5.3 TAS2Rs in the Male Reproductive System

The expression of all 35 of the TAS2R genes were detected in the mouse male reproduction system (Li and Zhou, 2012; Xu *et al.*, 2012) (Table 1.2). Xu *et al.* (2012) showed that a mixture of bitter taste agonists were able to induce a rise in $[Ca^{2+}]_i$ in spermatids. This indicates that the TAS2Rs may have an important role in spermatogenesis (Xu *et al.*, 2012). Moreover, the ablation of the TAS2R105 in mice led to the loss of spermatids and smaller testes which subsequently induced male infertility (Li and Zhou, 2012). These findings indicate that the TAS2Rs have an important role in spermatogenesis as well as a possible function in sensing and avoiding toxic substances that may present during fertilization (Lu *et al.*, 2017).

1.2.5.4 TAS2Rs in the Female Reproductive System and Uterus

In the female reproductive system, TAS2R38 was expressed in human placental cell line. Diphenidol (a TAS2R38 agonists) was found to induce Ca^{2+} influx. However, the functional of TAS2R38 has not been characterised in placenta (Wölfle *et al.*, 2016). In the uterus, a broad range of bitter taste agonists were able to activate the bitter taste receptor signalling pathway, which in turn induced a relaxation of the pre-contracted myometrial cells in a pre-term birth. Thus, the bitter taste receptors agonists could be used as a possible target for tocolytics drug development therapy (Zheng *et al.*, 2017).

1.2.5.5 TAS2Rs in the kidney

The TAS2Rs were also shown to be expressed in the kidney of mice (Rajkumar *et al.*, 2014; Liu *et al.*, 2015) (Table 1.2). The ablation of TAS2R105 resulted in an increase

in the glomerulus size and renal tubules. These findings indicate that the TAS2R105 has an important role in maintaining the structure of the kidney glomerulus and tubules (Liu *et al.*, 2015).

1.2.5.6 TAS2Rs in the Bladder

Several TAS2Rs have been reported to be expressed in the human and mouse bladder tissues (Deckmann *et al.*, 2014; Zhai *et al.*, 2016) (Table 1.2). The activation of the TAS2R108 in the mouse urethral chemosensory cells resulted in the contraction of the bladder (Deckmann *et al.*, 2014). Zhai *et al.* (2016) showed that the bitter taste agonists (quinine and denatonium) were able to induce a concentration-dependent relaxation of the carbachol pre-contracted mouse detrusor muscle. Moreover, oral gavage of chloroquine was able to significantly supress the overactive bladder symptoms in mice with partial bladder outlet obstruction (Zhai *et al.*, 2016). Therefore, the TAS2Rs may provide a new target to develop a drug for the treatment of overactive bladder (Zhai *et al.*, 2016).

1.2.5.7 TAS2Rs in the Thyroid

Clark *et al.* (2014) showed that TAS2Rs are expressed in human and mouse thyrocytes, and the human thyrocyte cell line Nthy-Ori3-1 (Table 1.2). The stimulation of the thyrocytes by the bitter taste agonists lead to a dose-dependent decrease in thyroid stimulating hormone which subsequently induced iodine efflux in thyrocytes and decreased the secretion of the thyroid hormones. These findings indicating that the TAS2Rs may have a protective role in the ingestion of potentially toxic substances. Moreover, a polymorphism in the human TAS2R42 was shown to be associated with a low level of the thyroid hormones in the circulation (Clark *et al.*, 2014). These findings indicate that TAS2Rs may be a novel target for the treatment of hypo-or hyperthyroidism.

1.2.5.8 TAS2Rs in the Lower Respiratory System

i. The Role of the TAS2Rs in Asthma

Asthma is defined as a chronic obstructive airway disease which is characterised by abnormal smooth muscle contractility, inflammation of the respiratory tract and an increase in airway secretion (Cockcroft and Davis, 2006). The TAS2R13, TAS2R14 and TAS2R19 were found to be up-regulated in leukocytes in patients with severe asthma. Treatment of patients with asthma with bitter taste agonists resulted in the inhibition of the pro-inflammatory cytokines and eicosanoid release from the blood leukocytes (Orsmark-Pietras et al., 2013). These findings suggest that the bitter taste agonists have an anti-inflammatory role and can therefore act as a potential target for the management of asthma.

ii. The Expression of TAS2Rs in the Airways

In the airways, expression of the TAS2Rs was first reported in the respiratory epithelial cells (Shah *et al.*, 2009). They found that *TAS2R4, TAS2R38, TAS2R43* and *TAS2R46* mRNAs were expressed on the ciliated airway epithelial cells from human trachea and bronchi. The direct stimulation of these receptors with bitter taste agonists were found to enhance the frequency of cilia beat and facilitating clearance of bacterial and chemical irritants (Shah *et al.*, 2009). Deshpande *et al.* (2010) conducted a quantitative reverse transcription polymerase chain reaction (RT-qPCR) to study the 25 known TAS2R subtypes in order to determine their expression in human airway smooth muscle. The majority of these receptors were expressed with the following subtypes being the most highly expressed; TAS2R10, TAS2R14 and TAS2R31 (Deshpande *et al.*, 2010). A separate study in 2013 looked at the intact human bronchi and found that the TAS2R5, TAS2R10 and TAS2R14 were the receptors that were involved in bitter taste agonist induced airway smooth muscle relaxation (Grassin-Delyle *et al.*, 2013) (Table1.2).

iii. Proposed Mechanisms Underpinning the Bitter Taste Agonist-Mediated Airway Smooth Relaxation

The process of contraction and relaxation are the main features of the airway smooth muscle cells, and provide these cells with the ability to regulate the airway tone and to control the air flow resistance (Pelaia *et al.*, 2008). The first study to display the relaxant ability of the bitter taste agonists in the airway smooth muscle cells was carried out in a mouse (Deshpande *et al.*, 2010). They found that the bitter taste receptor agonists induced a relaxation of the airway smooth muscle cell in a concentration-dependent manner. It was shown in mouse-isolated airway that bitter taste agonists were able to induce a concentration–dependent relaxation. Moreover, in an asthmatic mouse model, the bitter taste agonists induced a more potent bronchodilatory effect when compared to the traditional β-adrenoceptor agonists (Deshpande *et al.*, 2010). This bronchodilatory effect was further confirmed by other research groups who were able to find a similar effect on the human bronchi and mouse airway smooth muscle cells (Grassin-Delyle *et al.*, 2013; Zhang *et al.*, 2013). Once the bitter taste agonist binds to the TAS2Rs, a receptor conformational changes occurs, which is then followed by the activation of the conical signalling cascade that in turn causes the airway smooth muscle to relax (Deshpande *et al.*, 2010; Zhang *et al.*, 2013). The signalling cascade and the mechanism by which the bitter taste agonists are able to mediate a bronchodilation are still not fully established. However, there have been several different pathways which have been proposed.

A. Bitter Taste Agonists-Mediate their Bronchodilation by Increasing $[Ca^{2+}]_i$

Two research groups have shown that the TAS2Rs induced bronchodilation was due to an increase in $[Ca^{2+}]_i$. Deshpande *et al.* (2010) proposed that the increase in $[Ca^{2+}]_i$ was due to a localized $[Ca^{2+}]_i$ signal. They showed that in cultured human airway smooth muscle, bitter taste agonists (such as saccharine, denatonium, and chloroquine) evoked an increase in $[Ca^{2+}]_i$. The study showed this increase was to a similar level to which normally causes bronchoconstriction, with agonists such as histamine and bradykinin. The increase in $[Ca^{2+}]_i$ evoked by bitter taste agonists was inhibited by Gβγ inhibitor (gallein), a PLCβ inhibitor (U73122) or partially inhibited by an IP_3 receptor antagonist (2-APB). The results suggested that bitter taste agonists mediated

their effect through releasing Ca^{2+} from this intracellular store (Figure 1.2) (Deshpande *et al.*, 2010).

Zhang *et al.* (2013) proposed that the increase in $[Ca^{2+}]_i$ was the result of a slight increase in the global $[Ca^{2+}]_i$. They examined the Ca^{2+} response in freshly isolated airway smooth muscle cells from mice using fluorescence imaging (fluo-3, as a calcium fluorescent indicator) to assess the effect of the bitter taste agonists on the global $[Ca^{2+}]_i$ under resting conditions. They observed that chloroquine was only able to modestly raise the global $[Ca^{2+}]_i$, and the level of increase was much lower than that seen when the cells were treated with methacholine (Mch). In addition, chloroquine was able to increase the fluo-3 fluorescence in the presence and in absence of extracellular Ca^{2+}, which indicates that chloroquine is able to release Ca^{2+} from internal stores (Zhang *et al.*, 2013).

B. Bitter Taste Agonists-Mediate their Relaxation Through the BK_{Ca} Channel.

The first hypothesis to explain the mechanism underlying the bitter taste agonist mediated airway relaxation was suggested by Deshpande *et al.* (2010) where they proposed that an increase in the localized Ca^{2+} signal results in the opening of (BK_{Ca}) channels. This opening then lead to the hyperpolarization of the cell membrane and ultimately produces a relaxation of the airway smooth muscle (Figure 1.4 A) (Deshpande *et al.*, 2010).

Magnetic twisting cytometry was used on a single cell from human isolated airway smooth muscle to measure the dynamic changes in cell stiffness after applying different compounds. A baseline measurement was made using isoproterenol (a β-adrenergic agonist) and histamine to produce a relaxation and contraction, respectively. The application of saccharine or chloroquine resulted in a relaxation of the airway smooth muscle. This relaxation was not blocked by pre-treatment of these airway smooth mucle cells with H89 (a PKA inhibitor), but was blocked when pre-treated with U73122. Moreover, a cAMP radioimmunoassay was performed to measure the cAMP level in cells which were treated with either chloroquine or isoproterenol. The findings showed an in increase in the level of cAMP with

isoproterenol but not with chloroquine. These results indicate that the bitter taste agonist-mediated relaxation was not a result of an increase in cAMP. However, when the human airway smooth muscle cells were pre-treated with charybdoxin (a Ca^{2+}-dependent K^+ antagonist) and iberiotoxin (a selective BK_{Ca} channel antagonist) there was an ablation of the bitter taste agonists (saccharine and chloroquine) -mediated airway smooth muscle relaxation. These results suggest that these channels were involved in the signalling pathway of the bitter taste agonists (Figure 1.4 B) (Deshpande *et al.*, 2010).

Camoretti-Mercado *et al.* (2015) showed that the bitter taste agonist-mediated relaxation of the airway smooth muscle was through a heterogenity of mechanisms. One of these mechanisms supported above hypothesis. They showed saccharine to be able to stimulate the TAS2R through a $[Ca^{2+}]_i$-dependent cell surface transducer (BK_{Ca} channel) that would then cause a hyperpolarization of the airway smooth muscle cells and in turn cause a relaxation in the absence of a contractile stimulus.

Zhang *et al.* (2013) did not support this mechanism of action as they found that iberiotoxin was not able to block the bitter taste agonist-mediated airway smooth muscle relaxation. They used freshly isolated mouse airways to examine the effect of iberiotoxin on the relaxation of the chloroquine pre-contracted with Mch. There results showed that chloroquine was still able to produce a full relaxation in the presence of iberiotoxin (Zhang *et al.*, 2012). Moreover, they examined the direct effect of the bitter taste agonists on the BK_{Ca} channels using a patch clamp technique and were able to show that chloroqine did not activate the BK_{Ca} channels (Grassin-Delyle *et al.*, 2013; Zhang *et al.*, 2012).

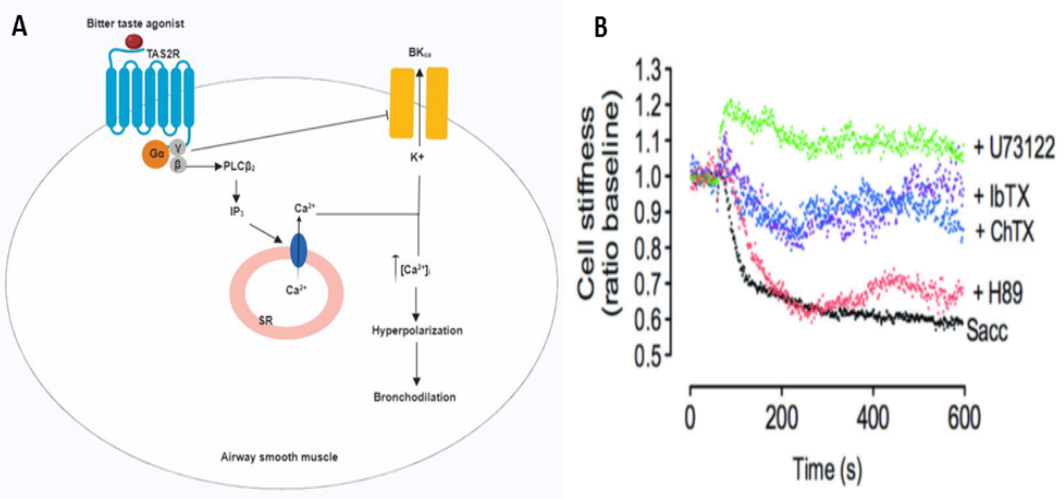

Figure 1.4 Bitter Taste Agonist Relax Airway Smooth Muscle by Localized $[Ca^{2+}]_i$ and Activation of BKca.

A) This model depicts the signalling cascade activated by bitter taste agonists. After bitter taste agonist binding to the receptor. G protein dissociated to Gα and βγ subunits. The βγ subunit then activates PLCβ$_2$ which then generate IP$_3$. The IP$_3$ lead to release Ca^{2+} from the sarcoplasmic reticulum. This will induce a localized Ca^{2+} signal that will activates BKca channel and then result in a hyperpolarization of the membrane and therefore causes bronchodilation of the airway smooth muscle. **B)** The relaxation responses in isolated airway smooth muscle cells to 1 mM saccharin are inhibited by the PLCβ inhibitor U73122 (1 μM), 10 nM of the BKCa antagonists iberiotoxin and charybdotoxin, but are unaffected by 100 nM of the PKA inhibitor H89. (B was adopted from Deshpande *et al.* (2010).

C. Bitter Taste Agonists-Mediated their Relaxation Through the Inhibition of the L-type Voltage-Dependent Calcium Channels

A further study conducted by Zhang *et al.* (2013) proposed that in addition to the slight increase in the global $[Ca^{2+}]_i$, the bitter taste agonists were able to reverse this increase in $[Ca^{2+}]_i$ evoked by bronchoconstriction and lead to bronchodilation. This reversal is mediated by a suppression of the L-type VDCC (Zhang *et al.*, 2013). The airway smooth muscle cells were pre-contracted with Mch and were then treated with chloroquine. The airway smooth muscle cell shortening and Ca^{2+} response were measured. The rapid increase in $[Ca^{2+}]_i$ and concurrently shortening of the cells were showed after the pre-contracted cells with Mch. Chloroquine was able to completely reverse the $[Ca^{2+}]_i$ increase and relaxed the cells. In order to understand the mechanism involved in the reduction of the $[Ca^{2+}]_i$, they used patch clamp technique to record the L-type VDCC current. They found that chloroquine blocked the L-type VDCC current (Figure 1.5 A) (Zhang *et al.*, 2013).

To further investigate at which level in the bitter taste agonists signalling pathway are L-type VDCC inhibited, airway smooth muscle cells were pre-treated with different inhibitors and then pre-contracted with KCl and further relaxed using chloroquine. The changes in $[Ca^{2+}]_i$, were recorded while several inhibitors were applied. Pertussis toxin (PTX), G-protein blocker, gallein, anti-βγ, Gβγ blocker, U73122, and 2-APB were used as the inhibitors. The pre-treatment with PTX, gallein, and anti-βγ prevented the chloroquine-induced reversal of the KCl induced increase in $[Ca^{2+}]_i$. However, pre-treatment with U73122 or 2-APB failed to alter chloroquine's ability to reverse a KCl-induced increase in $[Ca^{2+}]_i$. These results indicate that chloroquine inhibited the L-type VDCC via a Gβγ subunit but not through PLCβ and IP_3, to reverse the increase in $[Ca^{2+}]_i$. Therefore, this study showed two mechanisms of action by which the TAS2Rs induce bronchodilation; under resting conditions, chloroquine induces a moderate increase in the $[Ca^{2+}]_i$ and when pre-contracted, TAS2Rs of the tissues block the activation of L-type VDCC (Figure 1.5 (B)) (Zhang *et al.*, 2013).

This was further supported by Camoretti-Mercado *et al.* (2015) who reported that aristolochic acid (a TAS2R31 agonist) would inhibit the $[Ca^{2+}]_i$ elevation by

endothelin-1 and reverse the depolarization and subsequently result in the bronchodilation and a reduction in the stiffness (Camoretti-Mercado *et al.*, 2015).

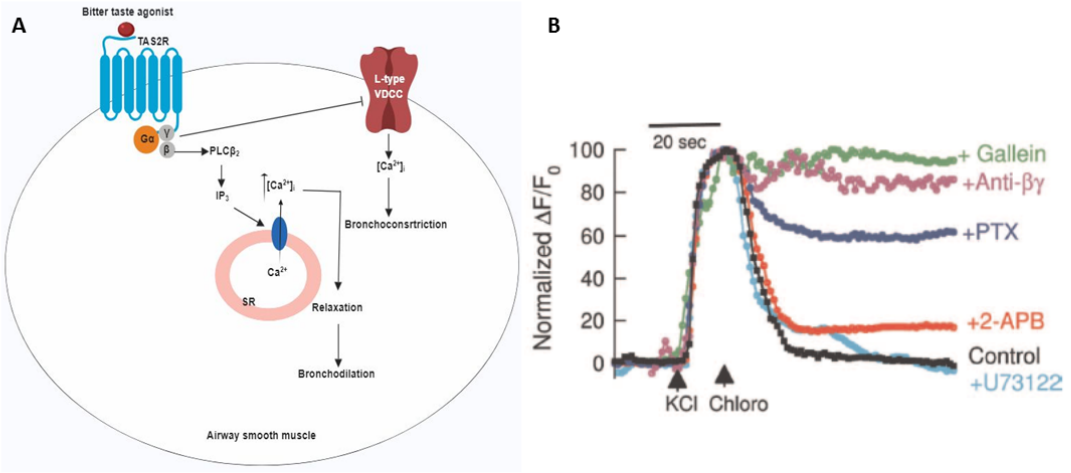

Figure 1.5 Bitter Taste Agonist Relax Airway Smooth Muscle Cell by Inhibiting L-type VDCCs.

A) This model showing the signalling cascade activated by bitter taste agonist of airway smooth muscle cell. After bitter taste agonist binding to the receptor. G protein dissociated to Gα and βγ subunits. The βγ subunit then activates PLCβ_2 which then generate IP_3. The IP_3 lead to release Ca^{2+} from the sarcoplasmic reticulum. This will increase the global $[Ca^{2+}]_i$ signal but not sufficient to induce contraction. The βγ subunit will supress L-type VDCC to reverse the increase in $[Ca^{2+}]_i$ evoked by bronchoconstrictors which results in bronchodilation and relaxation of airway smooth muscle. **B)** Representative recordings of changes in $[Ca^{2+}]_i$ in response to KCl followed by chlororoquine with and without pretreatment with gallein, PTX , anti- βγ and 2-APB and U73122 (B was adopted from Zhang *et al.* (2013).

1.2.5.9 TAS2Rs in Vasculatures

i. TAS2Rs and Vascular Smooth Muscle Contractility

Airway smooth muscle is not the only type of smooth muscle in which bitter taste agonists induce contractility changes. Some studies showed that bitter taste agonists might have role in regulating vascular smooth muscle as well. Manson *et al.* (2014) reported that different bitter taste agonists including chloroquine, quinine, denatonium, noscapine and dextromethorphan-induced relaxation of pre-contracted human pulmonary artery, mouse aorta and guinea pig aorta. This was supported by Sai *et al*. (2014) who showed that chloroquine-induced vasorelaxant effects of pre-contracted rat thoracic aortic rings. Furthermore, Denatonium has been reported to inhibit the phenylephrine-induced contractions of mouse aortic tissues (Sakai *et al.*, 2016). On the other hand, Upadhyaya *et al.* (2014) reported that dextromethorphan-induced vasoconstriction in human pulmonary artery smooth muscle. They reported that dextromethorphan-mediated increase in Ca^{2+} and this lead to activates MLCK and subsequently increases the phosphorylated MLC and leading to vasoconstriction (Upadhyaya *et al.*, 2014). From above studies, we can report that bitter taste agonists have a role in regulating the vascular smooth muscle contractility.

ii. Expression of TAS2Rs in the Vasculature

In the vasculatures, expression of the TAS2Rs was first reported in human bone marrow derived mesenchymal (hMSC) and vascular smooth muscle cells (VSMCs) (Lund et al., 2013). Manson et al. (2014) reported that mRNA for TAS2R3, TAS2R4, TAS2R10 and TAS2R14 was detected in human pulmonary artery. These TAS2Rs mRNAs along with those of TAS2R7, TAS2R34, and TAS2R40 were also identified in human pulmonary artery in a subsequent study (Wu et al., 2017). In mice, Sakai et al. (2016) found that mRNA for TAS2R108 was detected in aorta using RT-qPCR. In rat, mRNA of rat TAS2Rs, including TAS2R39, TAS2R40, TAS2R108, TAS2R114, TAS2R130, TAS2R137, and TAS2R140, was expressed in rat mesenteric and cerebral arteries, but TAS2R114 was not expressed in the cerebral arteries (Chen et al., 2017). Discovery and identification of TAS2Rs expression across a variety of tissues and

organs along with TAS2Rs subtype groupings opens up opportunities the use of bitter taste agonists in therapeutic applications.

iii. Possible Mechanisms Underlining the Bitter Taste Agonist-Mediated Vasorelaxation

Multiple mechanisms have been proposed in bitter taste agonists-induced vasorelaxation, including blocking of BKca and/ or L- type VDCC. Vasorelaxation effect of bitter taste agonists was reported to be independent on of BK_{Ca} (Manson *et al.*, 2014; Wu *et al.*, 2017) or VDCCs. Manson *et al.* (2014) reported that the vasorelaxation effect was dependent on the caveolae, which is a type of membrane invagination that is important in signal transduction, since relaxation in response to bitter taste agonists was decreased in caveolin-1 knock-out mice. Sai *et al*. (2014) reported that the vasorelaxation effect of chloroquine on the rat thoracic aorta was through blockage of VDCC. Wu *et al.* (2017) supported these findings and showed that in addition to block VDCC, chloroquine may block store-operated Ca^{2+} channels (SOCC) and receptor-operated Ca^{2+} channels (ROCC) in the rat pulmonary artery smooth muscle cells. Therefore, the vasorelaxant effects of bitter taste agonists in vasculature are complex, and perhaps different mechanisms are involved in the overall effects observed. Until now, the definite mechanism by which this occurs remains uncertain.

iv. Bitter Taste Agonists and their Effect on Blood Pressure

A variety of herbal extracts and other plant-derived substances such as polyphenols have bitter taste sensory properties (Olivier and van Wyk, 2013; Schulz, Hänsel and Tyler, 2001). The potential of these plant-derived bitter compounds to interact with TAS2Rs could have physiological implications on those animals that ingest them. For example, bitter tasting isoflavones from Soy have been found to activate human TAS2R14 and TAS2R39 (Roland *et al.*, 2013; Roland *et al.*, 2011).

It has been reported that there is an inverse relationship between bitter polyphenols and blood pressure (Roura *et al.*, 2016). For example, in elderly hypertensive populations, urinary total polyphenol excretion was positively associated with plasma

NO levels and negatively associated with blood pressure and prevalence of hypertension (Medina-Remón *et al.*, 2015; Medina-Remón *et al.*, 2011). Caffeine is bitter compound known to have an effect on blood pressure, specifically in hypertensive individuals; in a short-term (1-2h) test, ingesting caffeine-increased blood pressure into the hypertension range in 19% of normotensive and 89% of the hypertensive subjects studied (Hartley *et al.*, 2000). Chloroquine one of the bitter compound has been reported to reduced blood pressure in humans (Anigbogu *et al.*, 1993; Looareesuwan *et al.*, 1986). Denatonium also one of bitter taste compound that has antihypertensive properties; in rats, Lund *et al*. (2013) reported that intravenous injection of dentonium induced a transient drop in blood pressure. Moreover, in mice, intraperitoneal injection of denatonium was able to reduce systolic, diastolic, and mean blood pressures (Sakai *et al.*, 2016).

In summary, current studies suggest these bitter dietary compounds reduce blood pressure via endothelium-dependent NO relaxation mechanisms (Medina-Remón *et al.*, 2011; Lorenz *et al.*, 2004; Chiva-Blanch *et al.*, 2012). As TAS2Rs are involved in NO synthesis in the vascular endothelium, together, this suggests TAS2Rs might play a key role in the regulation of blood pressure by bitter tasting compounds and warrants further investigation.

Bitter taste receptors appear to be an effective relaxant of the vascular smooth muscles and their action through TAS2Rs would make this a novel target for drug development in pulmonary hypertension. The mechanism of action of these bitter taste agonists is still unclear, but it could be that different bitter taste agonists act through one or more of these mechanisms to produce relaxation of the pulmonary blood vessels. There are still unanswered questions and key research that needs to be conducted for this class of bitter taste agonists to be further developed in pulmonary hypertension. Could bitter taste agonists reduce vascular remodelling by inhibiting cell proliferation of pulmonary artery smooth muscle cells and/or endothelial cells? Could these bitter taste agonists help to decrease vasoconstriction of the pulmonary artery wall? These answers would be expected to provide enough knowledge for these bitter taste agonists to be used in the treatment of pulmonary hypertension and specifically where the current medications are inadequate in producing a therapeutic response.

1.3 Aims of the Present Study

The aim of this research was to build on the current pool of knowledge around bitter taste receptor agonists as potential treatments for pulmonary hypertension. To investigate this, the relaxation of pre-contractions of the rat pulmonary artery was used as a model system to demonstrate this effect. Moreover, this research also intended to understand whether the vascular endothelium has a role in bitter taste agonist-mediated vasorelaxation and to test this, we utilized and compared endothelium-intact and endothelium-denuded pulmonary artery rings in a series of organ bath experiments with bitter taste agonists. Furthermore, the study looked at the potential involvement of BK_{Ca} channels, VDCC and the G-protein βγ subunits in vasorelaxation with bitter taste agonists to better understand the mechanism of action and signalling pathway of these agonists. As the regulation of $[Ca^{2+}]_i$ in the pulmonary artery plays a key role in modulation of vascular tone, this study aimed to investigate the effect of bitter taste agonists (quinine, denatonium and dextromethorphan) on the $[Ca^{2+}]_i$ of the isolated pulmonary artery SMCs and to elucidate if the increase in $[Ca^{2+}]_i$ is due to extracellular Ca^{2+} influx and/or Ca^{2+} release from intracellular stores, as well the intracellular mechanism involved in the bitter taste agonists-induced increase in $[Ca^{2+}]_i$ of the rat pulmonary artery SMCs, such as the activation of phospholipase C. Additionally, this project aimed to investigate the mRNA expression of the Tas2r subunits in the rat pulmonary artery using RNA-Seq. RT-qPCR was also be carried out using *Tas2r*-specific primers to conduct further gene expression analysis.

Chapter 2

The Effect of Bitter Taste Agonists on the Rat Aorta and Pulmonary Artery

2.1 Introduction

The tone of the pulmonary artery is regulated by several factors, some of which cause constriction while others result in the dilation of the pulmonary artery (Barnes and Liu, 1995). Bitter taste receptor agonists have been reported to play a role in the regulation of the pulmonary vascular tone through their interaction with TAS2Rs on the pulmonary artery (Manson *et al.*, 2014; Upadhyaya *et al.*, 2014). Manson *et al.* (2014) showed that chloroquine mediates a relaxation of phenylephrine pre-contracted human pulmonary arteries. On the other hand, Upadhyaya *et al.* (2014) observed dextromethorphan to induce vasoconstriction in the newborn piglet's pulmonary artery tissues.

Chloroquine and quinine are used in the treatment of malaria (White, 1996), and are both considered to be bitter tasting drugs (Manson *et al.*, 2014; Wu *et al.*, 2017). Additionally, chloroquine has been shown to produce vasodilation of pulmonary artery, and in turn, lowering of blood pressure (Wu *et al.*, 2017). These studies showed that these bitter tasting anti-malarial drugs have antihypertensive properties.

Similarly, the bitter tasting drugs dextromethorphan and denatonium were also seen to reduce blood pressure and cause vasorelaxation in several species. A study by Wu *et al.* (2012) showed that treatment with dextromethorphan led to a significant reduction in blood pressure in hypertensive rats. Moreover, a study by Manson *et al.* (2014) showed that dextromethorphan caused a relaxation of phenylephrine pre-contracted human pulmonary arteries. Intravenous injections of denatonium into rats resulted in a significant transient drop in blood pressure within 1 minute which returned to baseline over the next 5 minutes (Lund *et al.*, 2013). Additionally, a study conducted by Sakai *et al.* (2016) showed that intraperitoneal denatonium injection (30 mg/kg) lowered the systolic, diastolic, and mean blood pressure in mice. Denatonium was found to induce relaxation of phenylephrine pre-contracted mice thoracic aorta (Sakai *et al.*, 2016). Furthermore, denatonium has also been reported to relax KCl or phenylephrine pre-contracted rat aorta in a concentration-dependent manner (Xin and Chen, 2017). The findings of these research groups provide

evidence which suggests that bitter taste agonists can modulate vascular tone through their engagement with their respective bitter taste receptors.

The vascular endothelium has also shown to play a crucial role in the regulating of the pulmonary vascular tone through the release of vasoactive mediators (Barnes and Liu, 1995; Furchgott, 1983). Carbachol, a muscarinic receptor agonists, has shown to trigger the release of endothelium-derived relaxing factor (EDRF) such as NO (Bolton, Lang and Takewaki, 1984). This is through the activation of the muscarinic receptors found on the endothelial cells, which in turn induce the relaxation of the vascular smooth muscles (Bolton, Lang and Takewaki, 1984). The endothelium-derived relaxation of pre-contracted pulmonary arteries by carbachol has been demonstrated in some studies (Bolton, Lang and Takewaki, 1984; Furchgott, 1981; Furchgott and Zawadzki, 1980). A study done by Furchgott (1981), who showed carbachol to accidentally relax NE pre-contracted rat aortic rings only in the presence of the endothelium. Therefore carbachol could be used as an experimental tool to assess the presence or absence of endothelium in the pulmonary vasculature. The role of endothelium in bitter taste receptor mediated vasorelaxation was investigated in several studies (Manson *et al.*, 2014; Sai *et al.*, 2014; Upadhyaya *et al.*, 2014; Wu *et al.*, 2017).

The main aim of this chapter will be to utilise the rat vasculature as an *in vitro* model system to examine the potential role of bitter taste agonists as antihypertensive agents. To achieve this, this study will initially examine the effect of a range of bitter taste agonists on the rat aorta in the contracted states. Moreover, to investigate the effect of different bitter taste agonists on the pulmonary artery in the contracted states and on their normal resting tone. In addition, to understand whether the vascular endothelium has a role in bitter taste agonist-mediated vasorelaxation, the endothelium dependency of the denuded endothelium rat pulmonary artery will be investigated.

2.2 Materials and Methods

2.2.1 Animals and Tissue Preparation

The animals used were male Sprague Dawley rats, weighing 250 - 350 g and were obtained from the Biological Procedures Unit (BPU), University of Strathclyde. The rats were housed in a temperature and humidity-controlled room and had free access to food and water. The rats were sacrificed by either cervical dislocation according to the UK Home Office Schedule 1 guidelines on animal experimentation, or by an overdose (100 mg/kg) of the anaesthetic pentobarbitone (Pentoject), which was administrated by an intraperitoneal injection.

The thoracic cavity of the rat was cut open and the heart and lungs were removed *en bloc*. The thoracic aorta was carefully dissected and placed in ice-cold physiological salt solution. The physiological salt solution (PSS) had the following composition (in mM); NaCl 150, HEPES 10, KCl 5.4, glucose 10, $CaCl_2$ 1.8 and $MgCl_2$ 1.2. The PSS was prepared using Milli-Q water and NaOH was used to adjust the pH to 7.4. The aorta (0.5 mm in diameter) and the pulmonary arteries (main extra pulmonary arteries with an internal diameter 0.4 mm and the intrapulmonary arteries with an internal diameter 0.3 mm) were cleared of any surrounding adipose tissue and lung parenchyma under a dissecting microscope (Nikon SMZ645). They were then cut into 4-5 mm long rings (Figure 2.1 and 2.2).

Each tissue was mounted in a 1 ml organ bath, with 4 tissues obtained from each animal. The tissue was mounted on two parallel stainless-steel wires, passing through the lumen of the ring. One of the stainless steel wires was fixed to a supporting structure for aortic rings, while the other was attached to triangle shaped stainless steel wire that was mounted by a thread, and connected to a Grass force displacement transducer (FT03C) (for the pulmonary artery rings, the stainless steel wire was connected to a rectangular tube that was attached to a fixed supportive structure). The transducers were connected to a PowerLab 4/30 bridge amplifier (ADInstruments), and the contractile force was recorded with Chart 5 software v.5.5.6 (2008) (ADInstruments) (Figure 2.3).

The organ bath was maintained at 37˚C, and the bath solution was bubbled with air through a crimped syringe needle, to ensure adequate mixing after the addition of each drug. The aortic tissue was placed under a resting tension of 1 g, while the pulmonary artery issue was at 0.5 g. The tissue was allowed to equilibrate for one hour before any experimental protocol was commenced. During this period, the tissue was washed frequently with fresh PSS. The viability of the tissue was then tested by the addition of KCl (50 mM) into 1 ml PSS. KCl was added and left inside for 5 minutes before washing out, and the tissue was then left to recover for a period of 20 minutes. This cycle was repeated 3 to 4 times until the contractile responses were consistent.

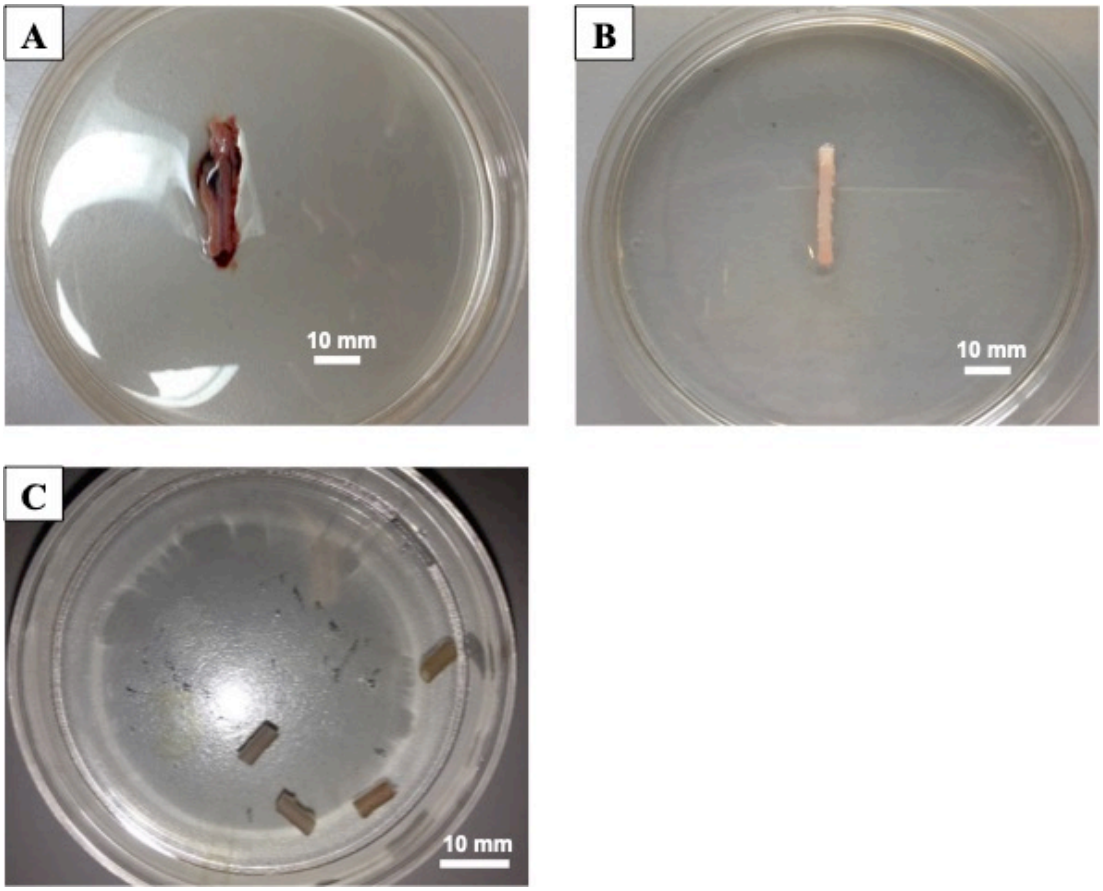

Figure 2.1 Images of the Dissected Rat Aorta

Images of the aorta before (A) and after (B) clearing the surrounding adipose tissue (C) The tissue was then cut into 4-5 mm rings with a 0.5 mm diameter.

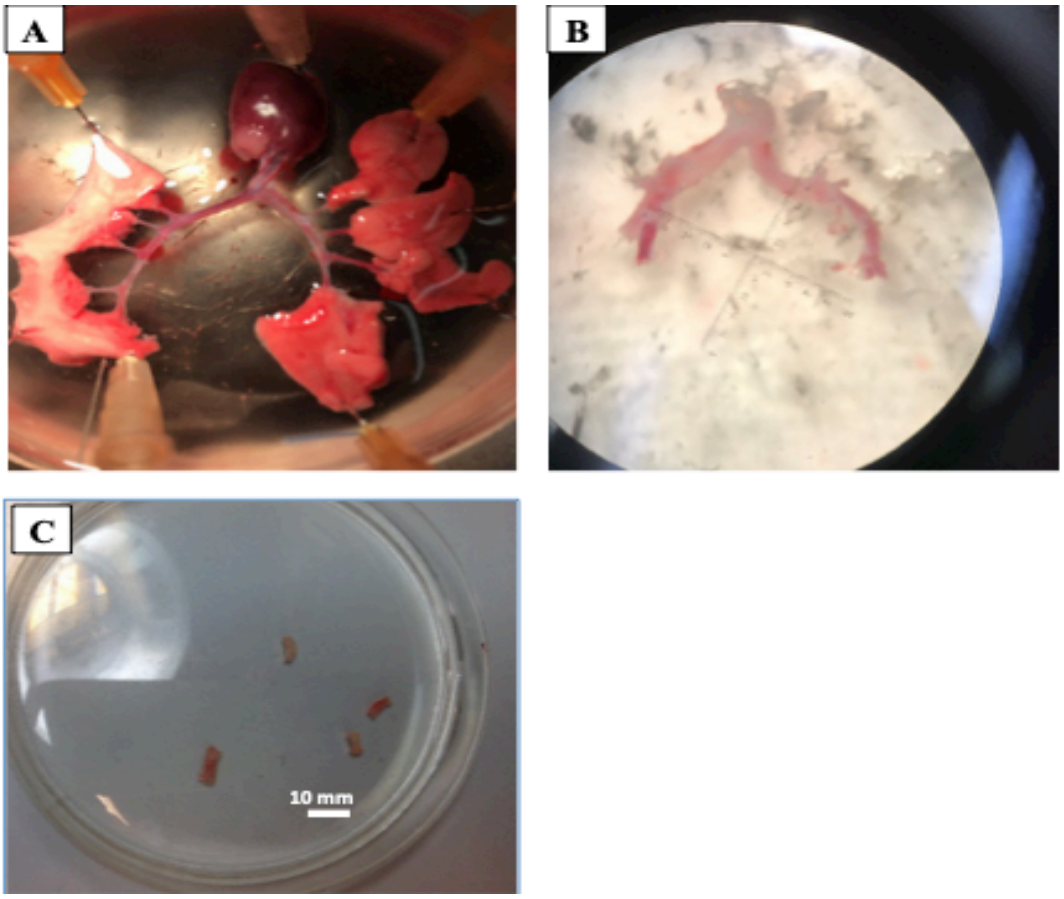

Figure 2.2 Images of the Rat Pulmonary Artery Dissection.

(**A**) The right and left extra-pulmonary arteries were dissected first (internal diameter 0.4 mm), then the intrapulmonary arteries* (internal diameter 0.3 mm) (**B**) The rat pulmonary artery was cleared of any surrounding lung parenchyma. (**C**) The rat pulmonary arteries were cut into 4-5 mm long rings. *Extra-pulmonary arteries (large pulmonary arteries), Intrapulmonary artery (small pulmonary arteries).

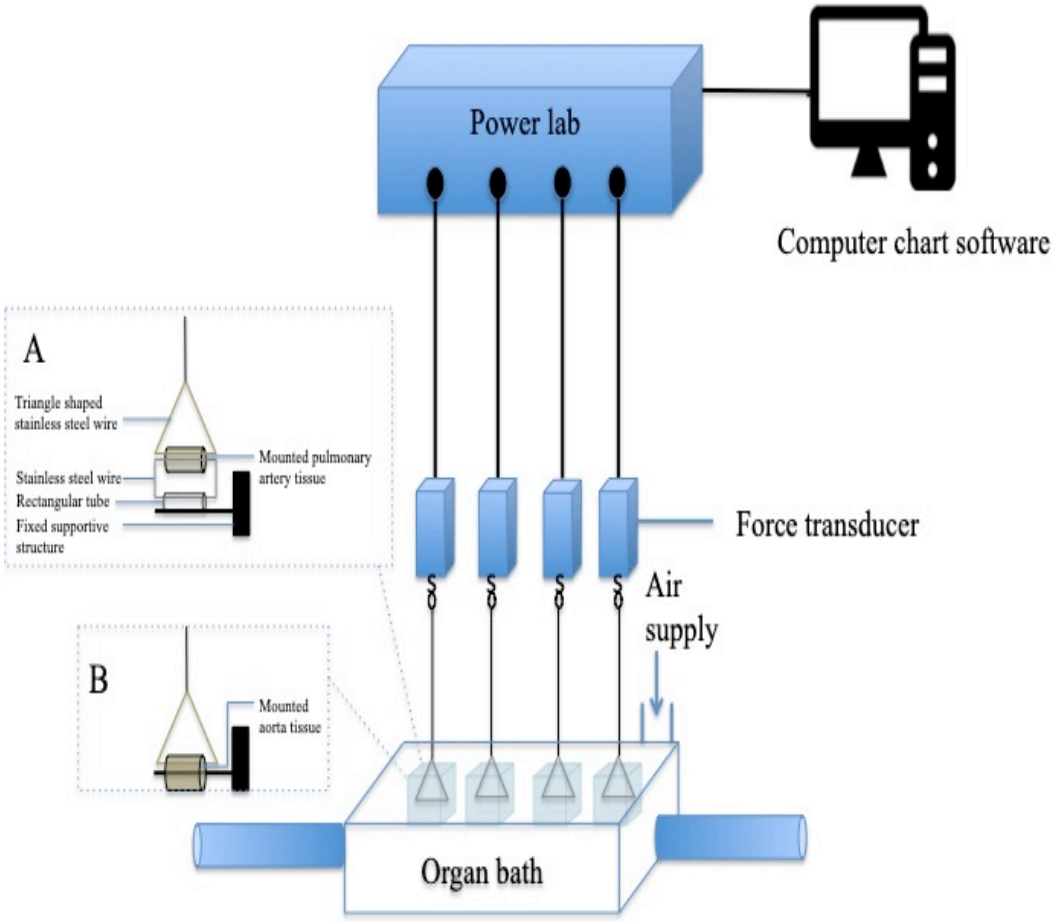

Figure 2.3 Diagram of the Myograph Apparatus.

The experimental set-up was used to record contractions of (A) isolated rat pulmonary artery and (B) rat aorta preparations.

2.2.2 Contractile Agents

KCl (AnaLaR Grade, BDH laboratory supplies, Poole, UK) was prepared as a 2 M stock solution. Phenylephrine (Sigma-Aldrich, Poole, UK) was prepared as a 0.1 M stock in deionised water and subsequently diluted in PSS for further use. The thromboxane A_2 analogue U46619 9,11-dideoxy-11α, 9α-epoxy methanoprostaglandin (Tocris Bioscience, Bristol, UK) was obtained as a 0.01 M stock in methyl acetate. This was evaporated under a gentle stream of nitrogen, and then immediately dissolved in DMSO and subsequently diluted in PSS for further use.

2.2.3 Bitter Taste Agonists

The bitter taste agonists used were quinine hydrochloride dihydrate, denatonium benzoate, and dextromethorphan hydrobromide (all from Sigma-Aldrich). Each was prepared as a 0.01 M stock solution in Milli-Q water, and then serial dilutions were made in PSS for later use. In this study, the bitter taste receptor agonists; quinine (TAS2R4, 7, 10, 14, 31, 39, 40, 43 and 44) (Meyerhof *et al.*, 2010), denatonium (TAS2R4, 8, 46 and 47) (Brockhoff *et al.*, 2007), and dextromethorphan (TAS2R 1 and 10) (Meyerhof *et al.*, 2010) were selected to be further investigated on the basis of the observations in previous studies.

2.2.4 Contractile Response to Phenylephrine, KCl, and U46619

To obtain a concentration-response curve for KCl and to determine its IC_{50} on the rat aorta and pulmonary artery, KCl was added cumulatively in concentrations ranging from 5 mM to 80 mM. A similar protocol was followed for phenylephrine using concentrations ranging from 1×10^{-9} M to 3×10^{-5} M for the aorta, and 1×10^{-9} M to 3×10^{-6} M for the pulmonary artery. To investigate the reversibility of the phenylephrine contractions, the tissue was washed out with fresh PSS every 10 minutes for approximately one hour. Furthermore, to test the effect of the pre-contractile on the pulmonary artery U46619 was used in concentrations ranging from 1×10^{-10} M to 3×10^{-6} M.

2.2.5 The Effect of Bitter Taste Agonists on the Rat Aorta and Pulmonary Artery

To examine the effects of the TAS2R agonists, the blood vessel (either aorta or pulmonary artery) was pre-contracted with 1 x 10^{-6} M phenylephrine until the contraction stabilized. The bitter taste agonist was then added cumulatively in a concentration range from 1 x 10^{-6} to 3 x 10^{-4} M (1 x 10^{-6} to 3 x 10^{-3} for dextromethorphan). This project is primary focused on the rat pulmonary artery; therefore, U46619 was used only with the pulmonary artery. For each of the tissue studies, one tissue that was pre-contracted always served as a time control.

2.2.6 The Effect of Bitter Taste Agonists on the Resting Tone of the Rat Pulmonary Artery

To investigate the effect of the bitter taste agonists on the resting tone, the bitter taste agonist was cumulatively added in a concentration range from 1 x 10^{-6} to 3 x 10^{-4} M. One of the tissues was used as a vehicle control.

2.2.7 Removing the Endothelium from the Rat Pulmonary artery

Endothelium-derived mediators are often involved in the mechanism of relaxation of the vascular system (Furchgott, 1983). In order to investigate whether the bitter taste agonist effect is dependent on the presence of the endothelium, the relaxant response was measured in the absence of the endothelium. The endothelium was denuded by gently rubbing the luminal surface of the rat pulmonary artery ring with a modified wooden cocktail stick. The removal of the endothelium was confirmed by the abolition of the relaxation of pre-contracted pulmonary artery rings with carbachol, as previously described by Furchgott (1981). The tissue was considered as being endothelium-intact if carbachol produced more than 50% relaxation. If the relaxation was less than 10%, then it was considered as being endothelium-denuded.

2.2.8 Criteria for Including and Excluding the Tissues for Analysis

In order for the tissue to be included for analysis, the response to phenylephrine had to be 0.4 gram (g) or greater for the aorta and 0.1 g or greater for the pulmonary arterial tissue. The vehicle control would be excluded from the experiment if it produced a relaxation greater than 30% over the course of the experiment**.**

2.2.9 Data Analysis

Calculations and statistical analysis were performed using GraphPad Prism (version 5). Relaxation of the aorta and pulmonary artery were expressed as a percentage of the initial contraction obtained i.e. the measured tension following the addition of bitter taste agonists divided by the maximum steady state tension produced by the contractile stimulus being used (phenylephrine or U46619), x100. Non-linear regression analysis (GraphPad Prism, version 5) was used for fitting of the log concentration-response curves and determination of the IC_{50} (concentration required to produce 50% of the maximum relaxation effect). The IC_{50} was calculated as an average of IC_{50} values of the number of experimental repeats. The I_{max} is the maximum relaxation achieved by the tissue under examination. One tissue that was pre-contracted always served as a time control. All data are presented as mean ± standard error of the mean (s.e.m). The experiments were repeated several times and the number of observations were expressed in the format of n = number of tissues used/number of animals. $P < 0.05$ was considered to be statistically significant. Unless otherwise specified, the curves were fitted as sigmoidal concentration-response curves to the Hill equation as detailed below.

$$Y = Bottom + \frac{Top - Bottom}{1 + 10^{(Log\ IC50 - X) * Hill\ Slop}}$$

Y is the response in (g)

X is the logarithm of agonist concentration (M)

Bottom is the Y value at the bottom Plateau (g)

Top is the Y value at the top plateau (g)

Hill Slope is slope factor

2.3 Results

2.3.1 Contractility of the Rat Aorta and Pulmonary Artery

2.3.1.1 Phenylephrine Induces a Concentration-Dependent Contraction of the Rat Aorta and Pulmonary Artery

Phenylephrine, which acts on α-adrenoceptor and mediates vasoconstriction via Ca^{2+} release, was used to investigate the contractile response of the rat aorta and pulmonary artery (Hussain and Marshall, 1997). Phenylephrine produced a concentration-dependent contraction in the aorta and the maximum contraction produced was 0.5 ± 0.1 g when using 3 x 10^{-5} M phenylephrine (Figure 2.4 A). The EC_{50} was 1.2 ± 0.3 x 10^{-6} M (n = 11/4). Furthermore, phenylephrine produced a concentration-dependent contraction in the pulmonary artery with an EC_{50} of 3.7 ± 0.8 x 10^{-8} M (Figure 2.4 B), and a maximum contraction of 0.2 ± 0.1 g was observed at 1 x 10^{-6} M phenylephrine (n = 6/4). The contractions induced by phenylephrine were reversible upon its washout and the tissues returned back to their resting tension within 60 minutes. These results indicate that the phenylephrine is more potent as a contractile agent in the aorta than in the pulmonary artery ($P < 0.05$).

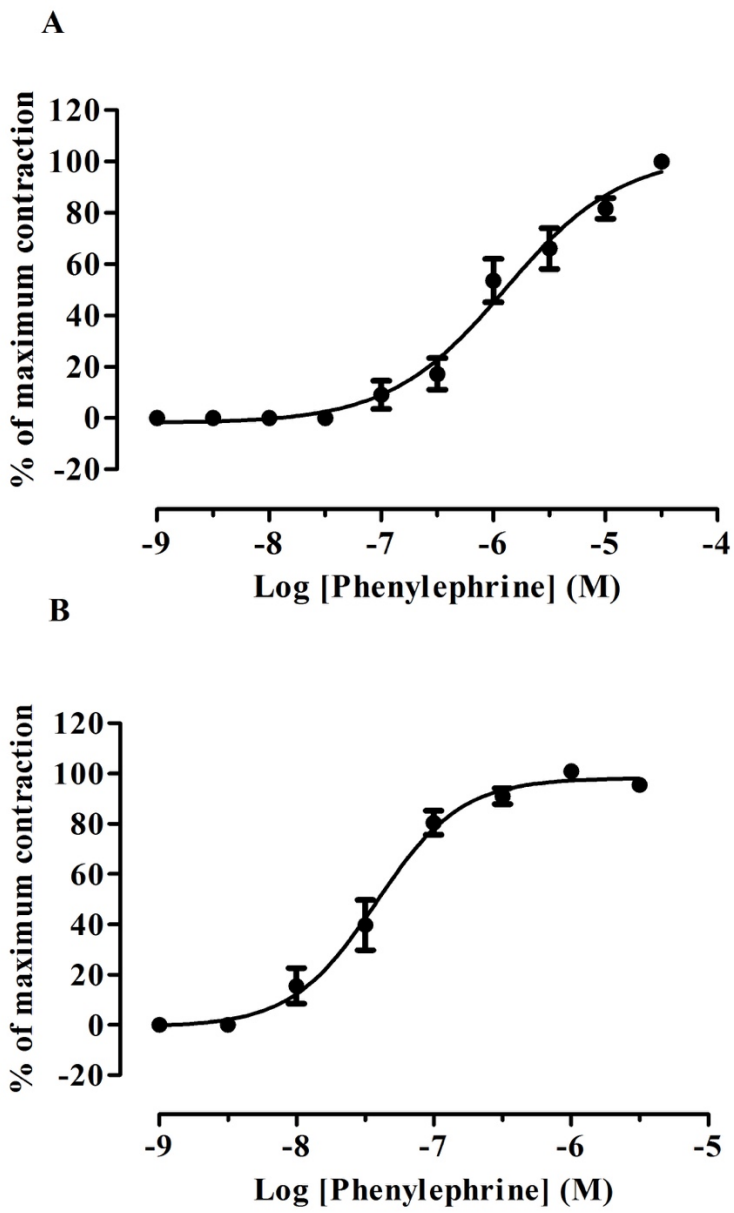

Figure 2.4 Concentration-Response Curves to Phenylephrine in the Rat Aorta and Pulmonary Artery

Phenylephrine was cumulatively added to the (**A**) rat aorta ($1 \times 10^{-9} - 3 \times 10^{-5}$ M), and (**B**) pulmonary artery in concentration ($1 \times 10^{-9} - 3 \times 10^{-6}$ M). The magnitude of the maximum contraction of the aorta was 0.5 ± 0.07 g (n = 11/4) and 0.24 ± 0.06 g for the pulmonary artery (n = 6/4). The contractile response is expressed as a percentage of the maximum contraction to phenylephrine, and is depicted as mean ± s.e.m.

2.3.1.2 KCl Induces a Concentration-Dependent Contraction of the Rat Aorta and Pulmonary Artery

Smooth muscle contractions also occur due to the influx of Ca^{2+} from the extracellular medium in response to KCl and other stimuli (Ratz *et al.*, 2005). KCl produced a concentration-dependent contraction of both the aorta (Figure 2.5 A) and the pulmonary artery (Figure 2.5 B). The magnitude of the maximum contraction produced in the aorta was 1.1 ± 0.1g (with 80 mM KCl) and the EC_{50} was 28 ± 2.0 mM (n = 8/4). Whereas, in the pulmonary artery, the maximum contraction was approximately half of that of the aorta at 0.6 ± 0.1 g (with 80 mM KCl) and a resulting EC_{50} of 12.3 ± 1.2 mM (n = 6/3). These results indicate that KCl was shown to be more potent in the rat pulmonary artery than aorta ($P < 0.05$).

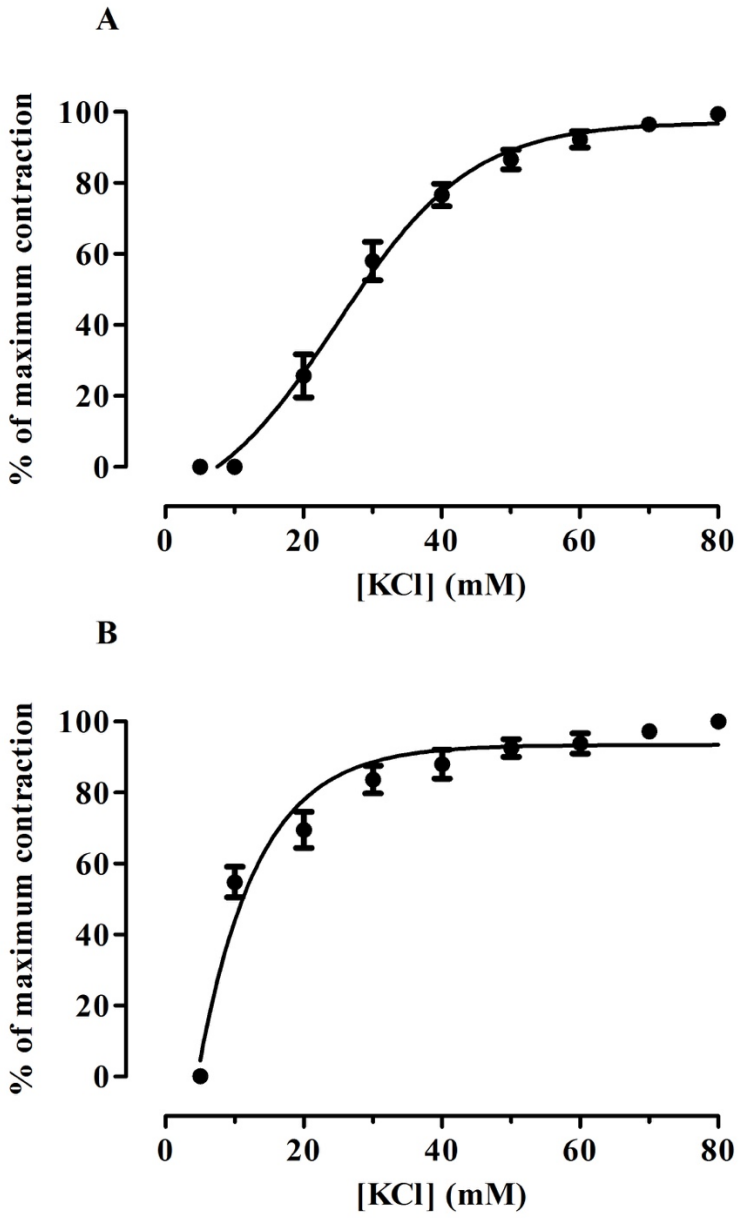

Figure 2.5 Concentration-Response Curve to KCl in the Rat Aorta and Pulmonary Artery.

KCl was cumulatively added to the (**A**) rat aorta, and (**B**) pulmonary artery (5- 80 mM). The data were fitted to a sigmoidal curve (Hill equation). The magnitude of the maximum contraction of the aorta was 1.12 ± 0.1 g (n = 8/4) and 0.56 ± 0.12 g for the pulmonary artery (n = 6/3). The data is presented as a percentage of the maximum contraction of KCl, and is depicted as mean ± s.e.m.

2.3.2 The Effect of Bitter Taste Agonists on the Rat Aorta/Pulmonary Artery

Rat aorta/pulmonary artery was pre-contracted with 1 x 10^{-6} M phenylephrine. Then, bitter taste agonist was added cumulatively in a concentration range from 1 x 10^{-6} to 3 x 10^{-4} M (1 x 10^{-6} to 3 x 10^{-3} for dextromethorphan). For each of the tissue studies, one tissue that was pre-contracted always served as a time control. The representative traces are shown in (Figure 2.6 A and B).

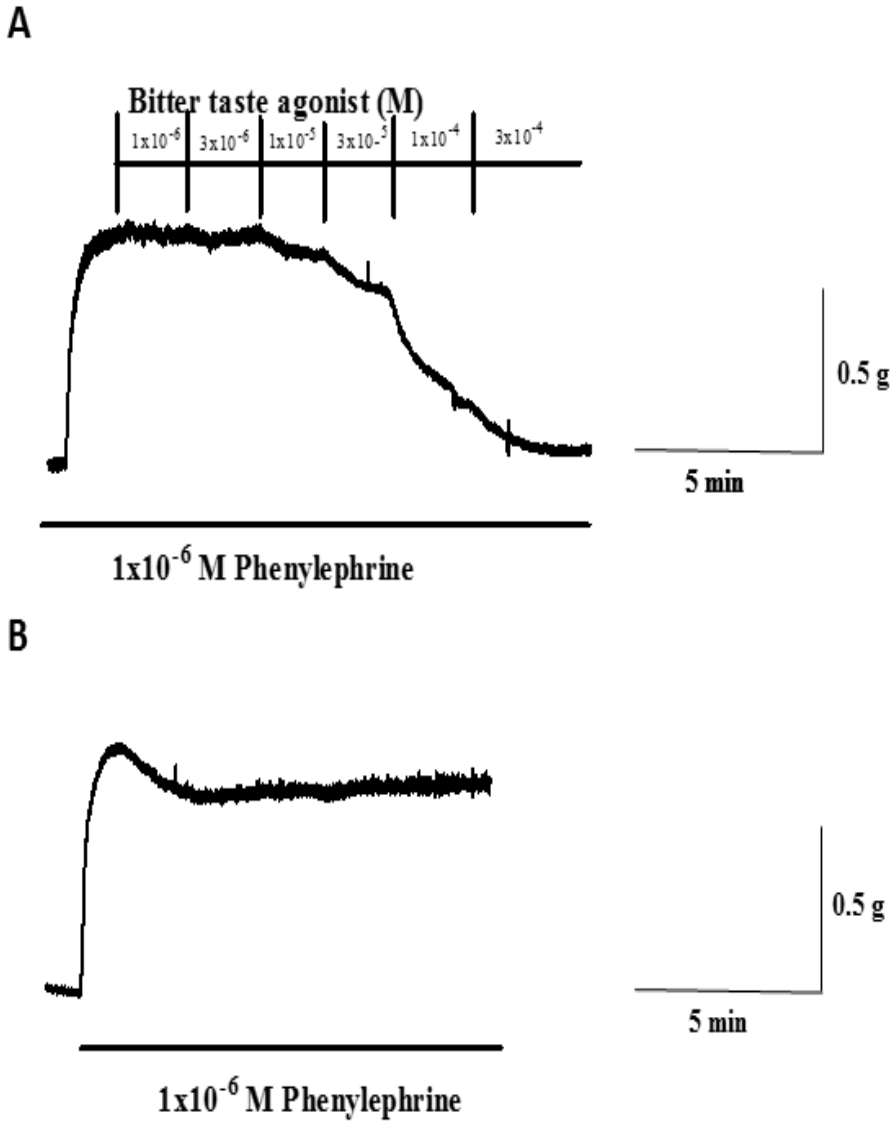

Figure 2.6 Representative Traces of Bitter Taste Agonist-Induced Relaxation of the Phenylephrine Pre-contracted Rat Aorta/Pulmonary Artery.

Rat aorta/pulmonary artery was pre-contracted with 1 x 10^{-6} M phenylephrine and then the bitter taste agonist was cumulatively added (1 x 10^{-6} – 3 x 10^{-4} M) (1 x 10^{-6} to 3 x 10^{-3} for dextromethorphan). (**A**) Representative trace of the relaxant effect of the bitter taste agonist. (**B**) In the absence of the bitter taste agonist, a vehicle control was used as a time control.

2.3.2.1 The Effect of quinine on the Rat Aorta

The ability of the bitter taste agonists to relax phenylephrine (1 x 10^{-6} M) pre-contracted aorta was studied following cumulative additions of quinine (1 x 10^{-7} – 3 x 10^{-4} M). Quinine produced a concentration-dependent relaxation, and the IC_{50} was determined to be 5.3 ± 2.4 x 10^{-5} M (n = 4/4). The lowest concentration at which quinine produced a measurable effect on the aorta was 1 x 10^{-5} M, which relaxed the tissue by 20 ± 7%. The highest concentration of quinine used (3 x 10^{-4} M) was found to relax the aorta by 97 ± 3%. The vehicle control was used over the course of the experiment showed a 9.0 ± 9.0 % relaxation; indicating quinine's relaxation was not due to a spontaneous decline in the contractile state of the tissue (n = 3/4) (Figure 2.7 A). Once quinine was washed out, the tissue was pre-contracted and allowed to reach a reproducible magnitude of contraction that occurred within 60 minutes, and then quinine was cumulatively added, indicating the reversibility of quinine.

2.3.2.2 The Effect of Denatonium on the Rat Aorta

Bitter taste agonists act through different bitter taste receptors to produce their response (Meyerhof *et al.*, 2011), and the relaxant effects of denatonium (TAS2R10) was further studied to investigate whether different receptors produce varying responses. Denatonium was also capable of producing a concentration-dependent relaxation of the pre-contracted aorta with an IC_{50} of 3.0 ± 0.5 x 10^{-5} M (n = 3/3). The first addition of denatonium to have a noticeable effect was 1 x 10^{-5} M and produced 28 ± 6.0% relaxation. At the highest concentration (3 x 10^{-4} M), denatonium produced a relaxation of 93 ± 3%. The vehicle control tissue relaxed by 5.0 ± 6.0 % over the course of the experiments, thus indicating that denatonium has a vasorelaxant effect on the rat aorta (n = 3/3) (Figure 2.7 B). The potencies and efficacies of these two bitter taste agonists were not statistically different in the rat aorta ($P > 0.05$).

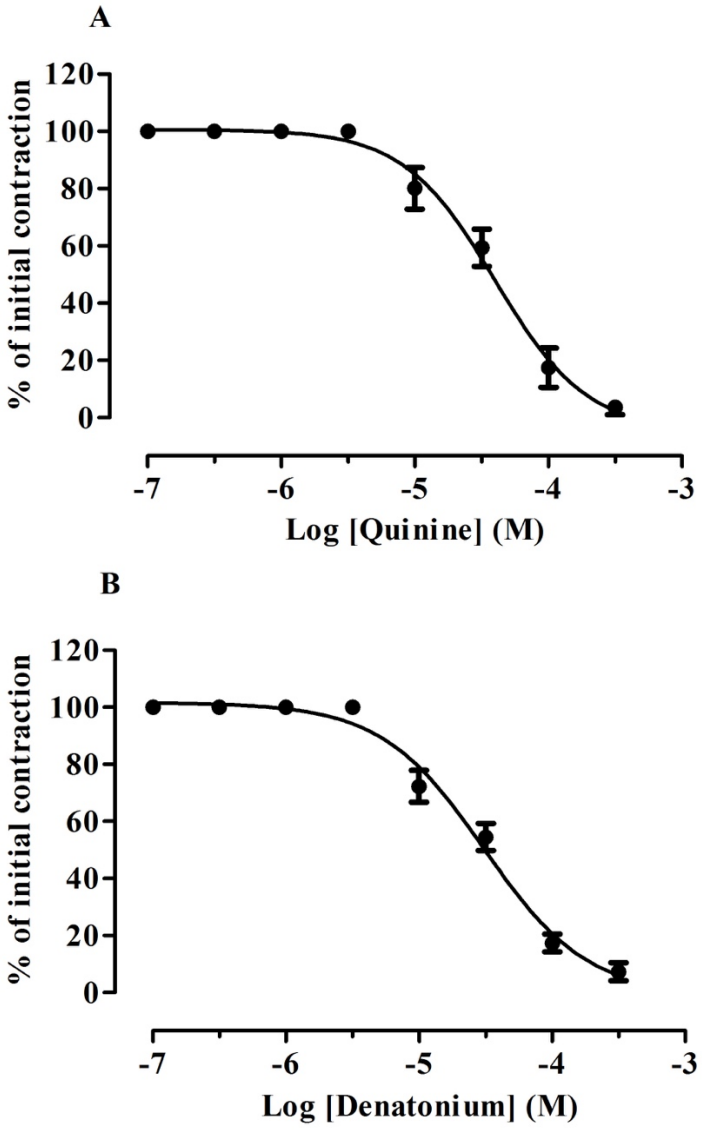

Figure 2.7 Quinine- and Denatonium- Induced Relaxation of the Phenylephrine Pre-contracted Rat Aorta.

Rat aorta was pre-contracted with phenylephrine (1 x 10^{-6} M) and then relaxed with cumulative additions of the bitter taste agonists (1 x 10^{-7} M - 3 x 10^{-4} M). (**A**) Concentration-response curve for quinine with a magnitude of the initial contraction equal to 0.6 ± 0.1g (n = 4/4). (**B**) Concentration-response curve for denatonium with a magnitude of the initial contraction equal to 0.6 ± 0.03g (n = 3/3). The data is expressed as a percentage of the initial contraction to phenylephrine and is depicted as the mean ± s.e.m.

2.3.3 The Effect of Bitter Taste Agonists on the Rat Pulmonary Artery

To examine the relaxant effect of the bitter taste agonists on other vascular tissue, endothelium-intact rat pulmonary arteries were pre-contracted with phenylephrine before cumulative additions of the agonist. Quinine produced a concentration-dependent relaxation and the IC_{50} was 1.6 ± 1.7 x 10^{-4} M with an I_{max} of 111 ± 5.7% (*n* = 6/6) (Figure 2.8 A). Additionally, denatonium produced a concentration-dependent relaxation with an IC_{50} of 6.5 ± 1.0 x 10^{-4} M, and an I_{max} of 97 ± 4% (*n* = 6/6) (Figure 2.8 B). In a similar manner, dextromethorphan (TAS2R1 and 10) produced a relaxation with an IC_{50} of 2.6 ± 0.2 x 10^{-5} M and an I_{max} of 109 ± 13% (*n* = 5/5) (Figure 2.9). The potencies and efficacies of these bitter taste agonists were not statistically different ($P > 0.05$). Over the course of these experiments, the vehicle control showed a relaxation of 1.3 ± 0.8% (*n* = 10/17). The effect of the bitter taste agonists was further evaluated on the resting tone, where quinine, denatonium and dextromethorphan had no effect on the resting tone (*n* = 4/3, 4/3 and 5/4, respectively) (Figure 2.10).

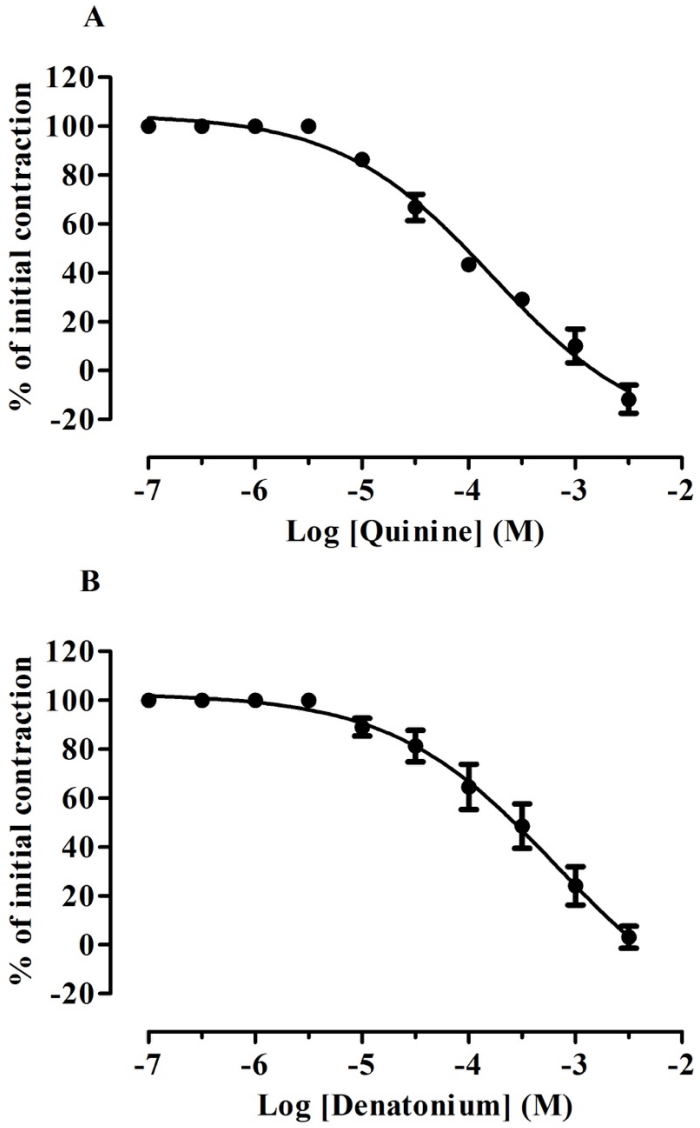

Figure 2.8 Quinine-and Denatonium-Induced Relaxation of the Phenylephrine Pre-contracted Rat Pulmonary Artery.

Rat pulmonary artery was pre-contracted with phenylephrine (1 x 10^{-6} M) and then relaxed with cumulative additions of the bitter taste agonists (1 x 10^{-7} M to 3 x 10^{-4} M). (**A**) Concentration-response curve for quinine with a magnitude of the initial contraction equal to 0.2 ± 0.02g (*n* = 6/6). (**B**) Concentration-response curve for denatonium with a magnitude of the initial contraction equal to 0.25 ± 0.04g (*n* = 6/6). The data is expressed as a percentage of the initial contraction to phenylephrine and is depicted as the mean ± s.e.m.

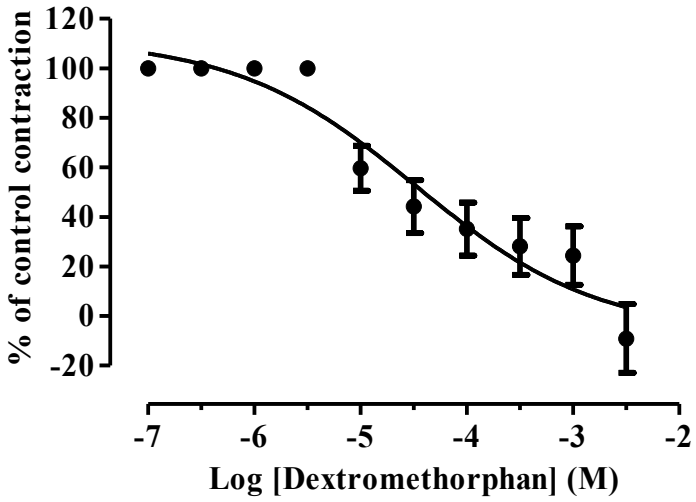

Figure 2.9 Dextromethorphan-Induced Relaxation of the Phenylephrine Pre-contracted Rat Pulmonary Artery.

Rat pulmonary artery was pre-contracted with phenylephrine (1 x 10^{-6} M) and then relaxed with cumulative additions of dextromethorphan (1 x 10^{-7} M - 3 x 10^{-4} M). Concentration-response curve for dextromethorphan with a magnitude of the initial contraction equal to 0.28 ± 0.07g (n = 5/5). The data is expressed as a percentage of the initial contraction to phenylephrine and is depicted as the mean ± s.e.m.

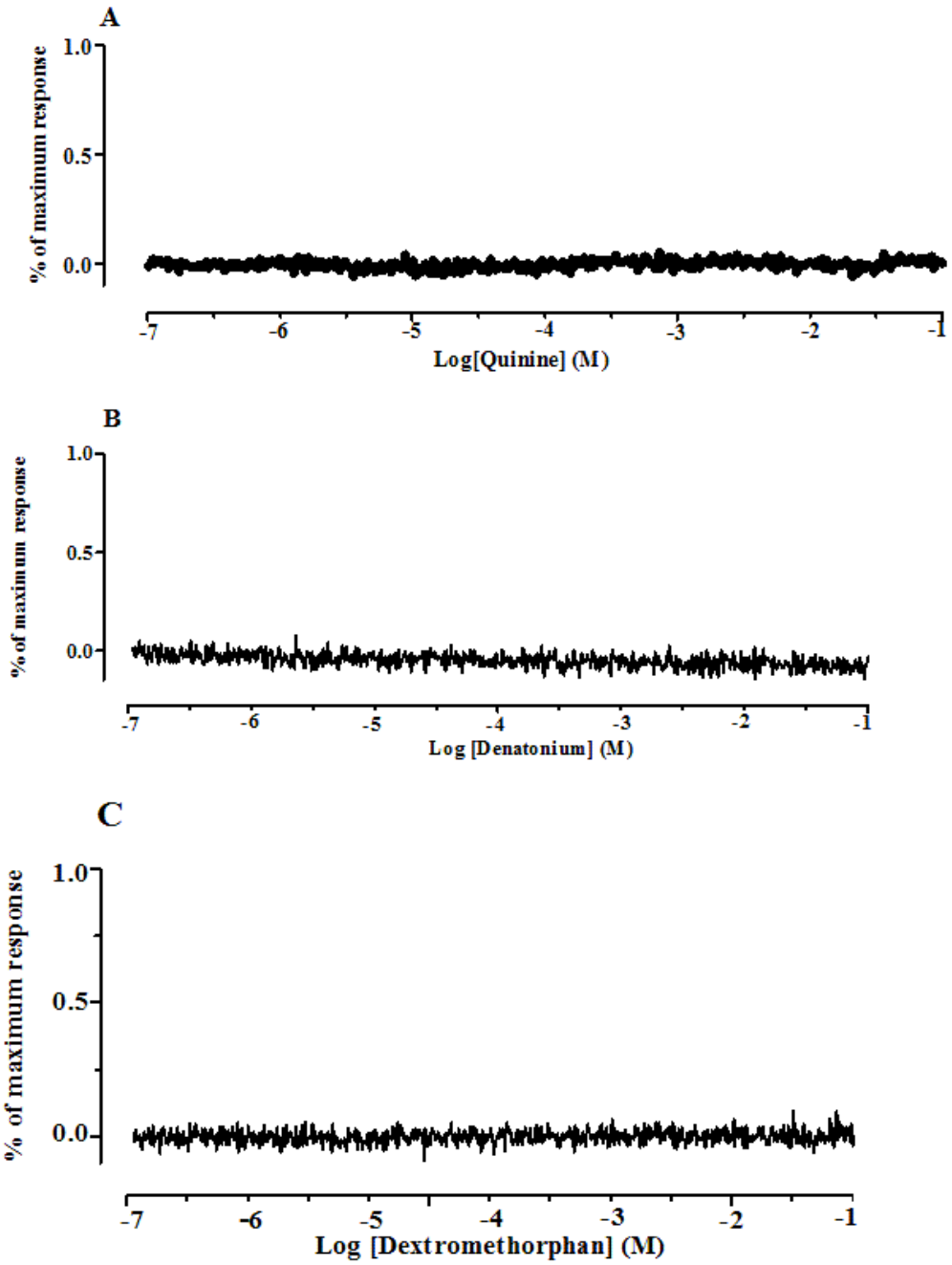

Figure 2.10 Representative Traces of the effect of Bitter Taste Agonists on the Resting Tone of the Rat Pulmonary Artery.

Bitter taste agonists were cumulatively added (1 x 10^{-7} – 1 M) **(A)** Representative trace of quinine (*n* = 4/3), **(B)** Denatonium (*n* = 4/3), and (**C**) Dextromethorphan (n = 5/4).

2.3.4 Endothelium Dependency of Bitter Taste Agonists Mediated Vasorelaxation in the Rat Pulmonary Artery.

2.3.4.1 Confirmation of the Removal of the Endothelium

The addition of carbachol to pre-contracted endothelium-intact pulmonary arteries produced a relaxation of 92 ± 8 %, indicating that the endothelium is intact (n = 16/4). Whereas in the endothelium denuded, carbachol produced a significantly lower relaxation equal to 4.5 ± 1.0% (P <0.0001) (n = 11/4). This relaxation response indicates that this method effectively removed the endothelium from the pulmonary artery (Figure 2.11) and (Figure 2.12).

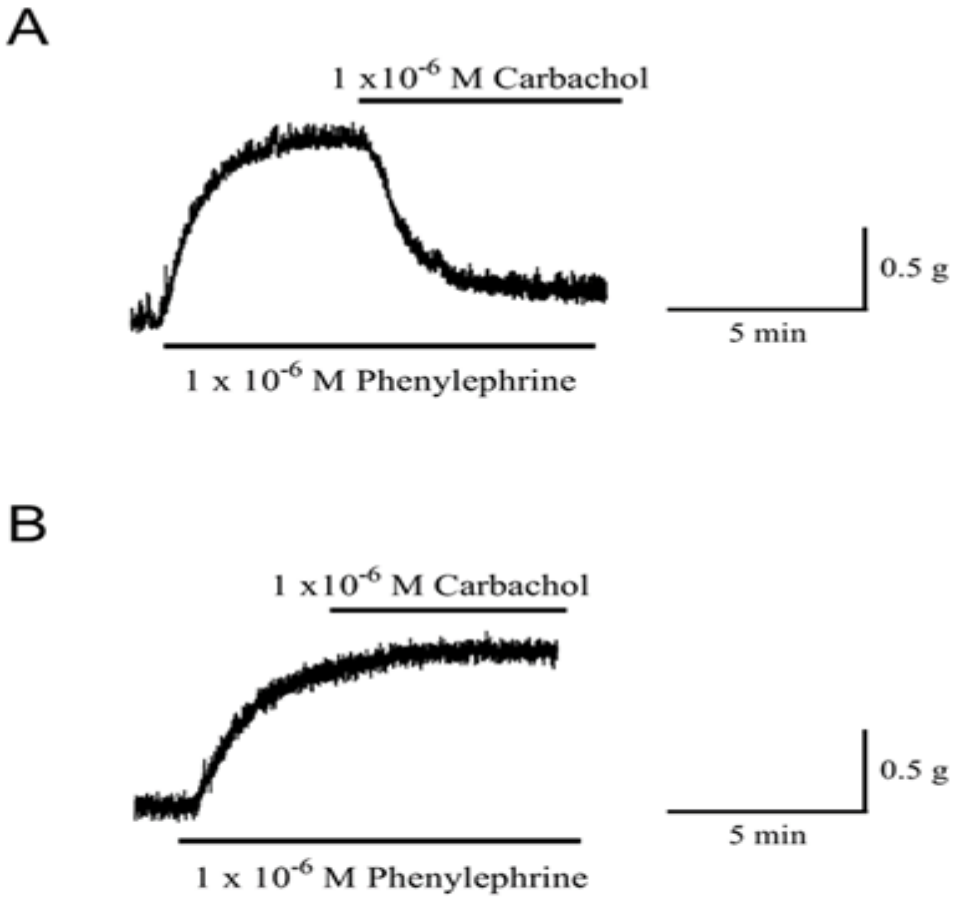

Figure 2.11 The Effect of Carbachol on the Endothelium Intact and Denuded Pulmonary Artery.

Rat pulmonary artery was pre-contracted with (1 x 10^{-6} M) phenylephrine and then 1 x 10^{-6} carbachol was added. (**A**) Represenative recording of the carbachol incuded relaxation on the intact pulmonary artery endothelium (*n* = 16/4). (**B**) Representative recording of carbachol on the denuded pulmonary artery endothelium (*n* = 11/4).

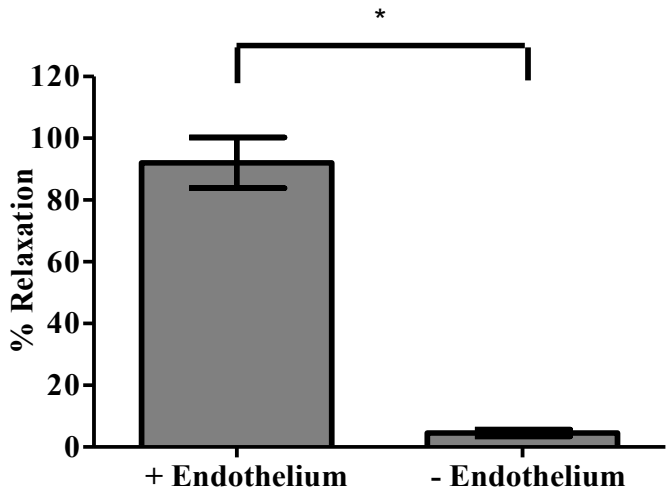

Figure 2.12 Carbachol-Induced Relaxation in the Rat Pulmonary Artery.

Rat pulmonary artery was pre-contracted with (1 x 10^{-6} M) phenylephrine and then 1 x 10^{-6} carbachol was added. The relaxation was significantly higher when the endothelium was intact (n = 16/4) in comparasion with the denuded endothelium (n = 11/4). The data is expressed as a percentage relaxation to phenylephrine contraction and is depicted as the mean ± s.e.m. (*P < 0.0001).

2.3.4.2 Phenylephrine Induces a Concentration-Dependent Contraction of the Denuded-Endothelial Pulmonary Artery

The endothelium-dependency on phenylephrine-induced contractions was initially examined. Removal of the endothelium from the rat pulmonary artery tissue had no significant effect on the contractile response to phenylephrine (1 x 10^{-6} M). Phenylephrine was able to produce a concentration-dependent contraction with an EC_{50} of 3.7 ± 0.8 x 10^{-8} M in the absence of the endothelium (Control $P > 0.05$). Similarly, the maximum contraction for the endothelium denuded was 0.20 ± 0.02 g, which was statistically not significantly different from the endothelium intact (Control 0.24 ± 0.02 g) (Figure 2.13). This indicates that the contractile viability of the tissues was not compromised by removing the endothelium (n = 16).

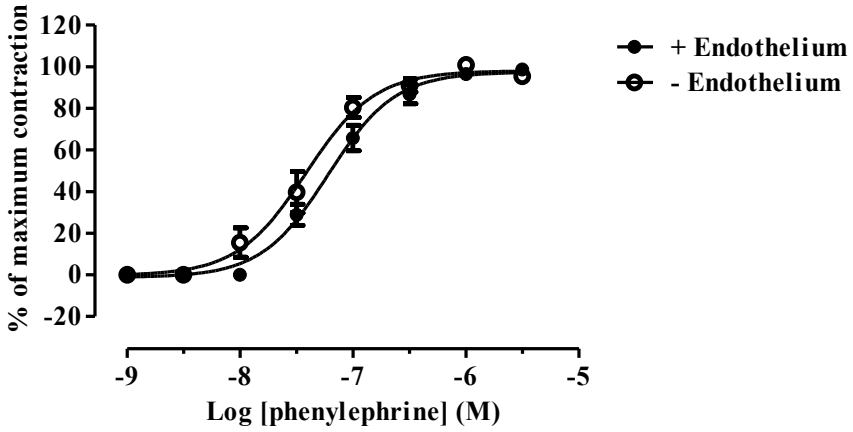

Figure 2.13 Concentration-Response Curve to Phenylephrine in the Endothelium Intact and Denuded Rat Pulmonary Artery.

Phenylephrine was cumulatively added to the pulmonary artery (1 x 10^{-9} – 3 x 10^{-6} M) and a concentration-response curve was fitted for the endothelium intact and denuded. The data were fitted to a sigmoidal curve (Hill equation), and the magnitude of the maximum contraction of the intact endothelium was 0.24 ± 0.02g (n = 4) and 0.20 ± 0.02g for the denuded endothelium (n = 6/4). The contractile response is expressed as a percentage of the maximum contraction to phenylephrine, and is depicted as mean ± s.e.m.

2.3.4.3 The Effect of Bitter Taste Agonists on the Endothelium Denuded Rat Pulmonary Artery

The relaxant effect mediated by the bitter taste agonists was investigated on endothelium denuded pulmonary artery tissues. Each of the bitter taste agonists used was capable of producing a concentration-dependent relaxation of the phenylephrine pre-contracted endothelium denuded tissue. The IC_{50} for quinine in the absence of the endothelium was 9.2 ± 3.0 x 10^{-5} M which was not statistically significant when compared with its respective control in the presence of the endothelium ($P > 0.05$). Additionally, the maximum relaxation was not significantly different at 108 ± 16% for the denuded tissue (n = 6/ 4) (Figure 2.14 A). This indicates that the endothelium is not required for the quinine-induced relaxation.

Furthermore, denatonium induced a concentration-dependent relaxation with an IC_{50} 2.3 ± 0.6 x 10^{-4} M which was observed to be statistically not significant when compared with its control in the presence of endothelium ($P > 0.05$). Moreover, the I_{max} was also not significantly changed at 120 ± 6% for denuded endothelium denuded (n = 6/4) (Figure 2.14 B). Similarly, dextromethorphan induced a relaxation with an IC_{50} of 5.0 ± 2.1 x 10^{-5} M which was not statistically significant when compared with its control in the presence of endothelium ($P > 0.05$) (n = 5/5) (Figure 2.15). Therefore, these results further indicate that endothelium is not essential for the denatonium and dextromethorphan induced relaxations.

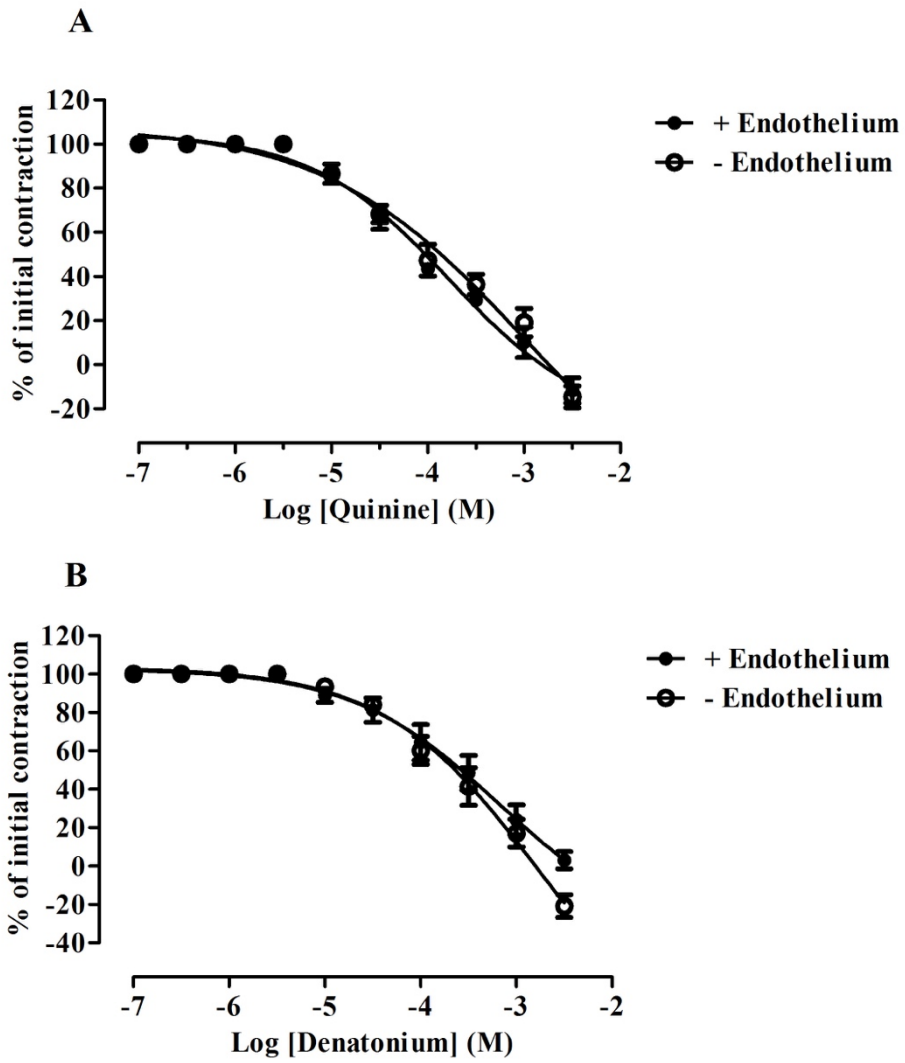

Figure 2.14 Bitter Taste Agonists-Induced Relaxation of the Endothelium Intact and Denuded Rat Pulmonary Artery.

The endothelial intact and denuded rat pulmonary arteries were pre-contracted with phenylephrine (1 x 10^{-6} M) and then relaxed with cumulative additions of the bitter taste agonists (1 x 10^{-7} M to 3 x 10^{-3} M). (**A**) Concentration-response curve for quinine in the presence (n = 6/6) and absence (n = 6/4) of the endothelium. (**B**) Concentration-response curve for denatonium in the presence (n = 6/6) and absence (n = 6/4) of the endothelium. The data is expressed as a percentage of the initial contraction to phenylephrine and is depicted as the mean ± s.e.m. (+ endothelium curve has already been shown in Figure 2.8 (A and B).

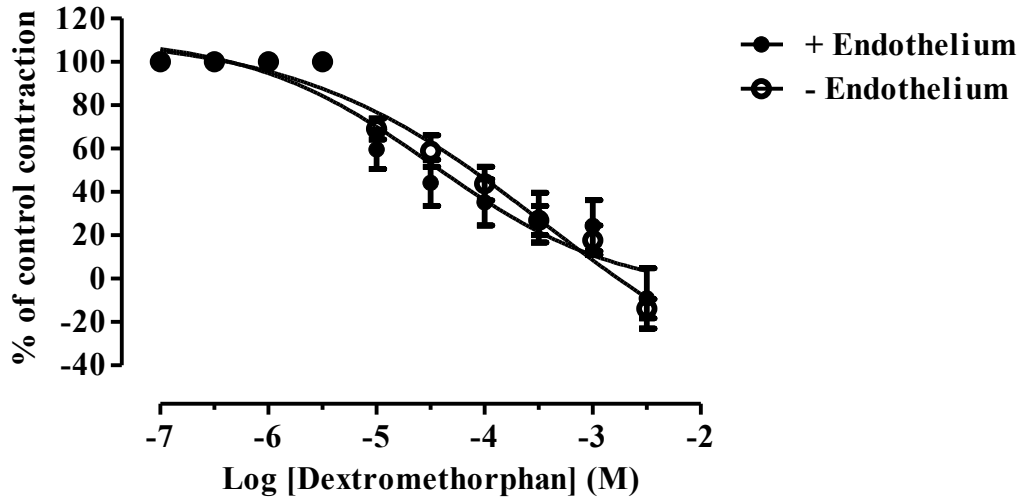

Figure 2.15 Dextromethorphan-Induced Relaxation of the Intact and Denuded Endothelial Rat Pulmonary Artery.

Intact and denuded endothelial rat pulmonary arteries were pre-contracted with phenylephrine (1 x 10^{-6} M) and then relaxed with cumulative additions of dextromethorphan (1 x 10^{-7} M to 3 x 10^{-3} M). Concentration-response curve for dextromethorphan in the presence (n = 5/5) and absence (n = 5/5) of the endothelium. The data is expressed as a percentage of the initial contraction to phenylephrine and is depicted as the mean ± s.e.m. (+ endothelium curve has already been shown in Figure 2.9).

2.3.5 U46619 Induces a Concentration-Dependent Contraction of the Rat Pulmonary Artery

U46619, a thromboxane A2 mimetic (Jiang, Chan and Chang, 1994), was used to investigate the contractile response of the rat pulmonary artery. A concentration-dependent contraction was observed with cumulative additions of U46619 with an IC_{50} of 5.6 ± 2.7 x 10^{-8} M (Figure 2.16). The arterial rings reached a maximal contraction of 0.34 ± 0.12 g at 3.5 x 10^{-6} M (*n* = 9/4).

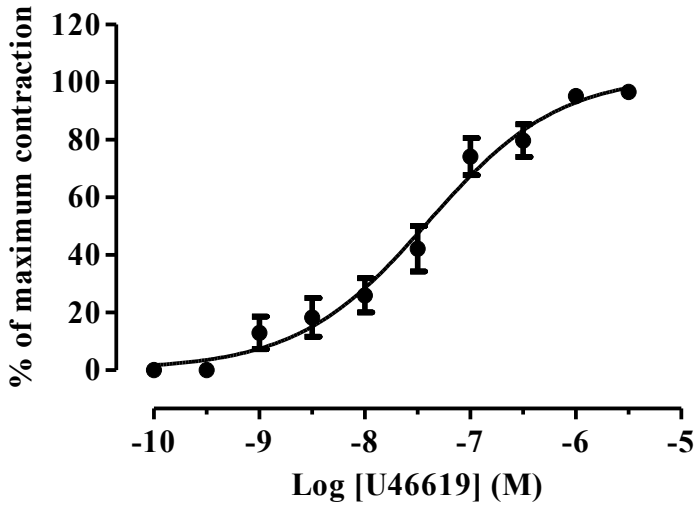

Figure 2.16 Concentration-Response Curve to U46619 of the Rat Pulmonary Artery.

U46619 was cumulatively added to the rat pulmonary artery (1 x 10^{-10} – 3 x 10^{-6} M, and the magnitude of the maximum contraction of the pulmonary artery was 0.34 ± 0.12 g (*n* = 9/4). The data is presented as a percentage of the maximum contraction to U46619 and is depicted as mean ± s.e.m.

2.3.6 Quinine Evokes a Relaxation of the U46619 Pre-Contracted Rat Pulmonary Artery

The relaxant effect of quinine was further investigated on the U46619 (1 x 10^{-6} M) pre-contracted endothelium-intact pulmonary artery tissue. Quinine produced a concentration-dependent relaxation, and the IC_{50} was 1.8 ± 0.2 x 10^{-3} M (Figure 2.17). Following the addition of 3 x 10^{-3} M quinine, a 106 ± 4.1% relaxation was observed (*n* = 4/4). The efficacy of quinine was similar with the phenylephrine and U46619 pre-contracted tissue.

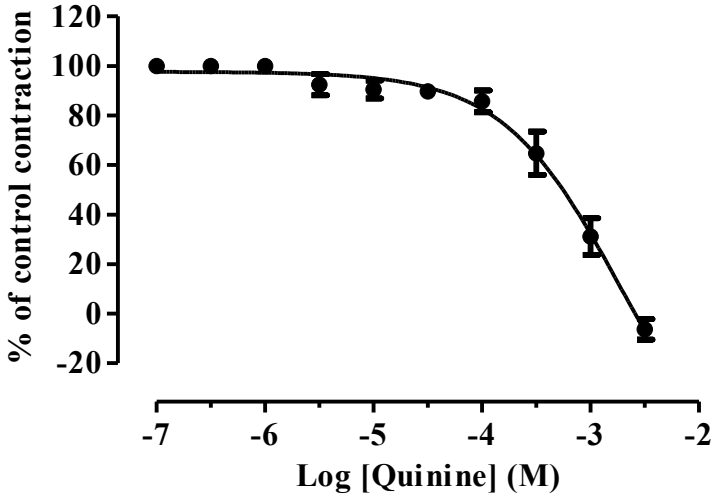

Figure 2.17 Quinine-Induced Relaxation of the U46619 Pre-contracted Rat Pulmonary Artery.

The rat pulmonary artery was pre-contracted with U46619 (1 x 10^{-6} M) and then relaxed with cumulative additions of quinine (1 x 10^{-7} M to 3 x 10^{-3} M). A Concentration-response curve for quinine with a magnitude of the initial contraction equal to 0.35 ± 0.1g (*n* = 4/4). The data is expressed as a percentage of the initial contraction to U46619 and is depicted as the mean ± s.e.m.

2.4 Discussion

2.4.1 Relaxant Effect of Bitter Taste Agonist

There is considerable evidence in the literature that denatonium has an antihypertensive effect in rats (Lund *et al.*, 2013) and mice (Sakai *et al.*, 2016) and this is further supported by a number of *in vitro* studies demonstrating a vasorelaxant effect of the denatonium (Manson *et al.*, 2014; Xin and Chen, 2017). In this study, we have shown that denatonium has vasorelaxant effect on the rat aorta and pulmonary artery. The complimentary finding that quinine and dextromethorphan had a very similar effect provides further support for this notion. The bitter taste agonists used in this study produced a concentration-dependent relaxation of the aorta and pulmonary artery when it was pre-contracted with phenylephrine. Their effects were fully reversed upon their washout indicating that they appear to have had no deleterious effect on the tissue over the concentration range used.

Quinine was able to induce relaxation of the rat aorta and pulmonary artery in a concentration-dependent manner. Thus, suggesting the existence of TAS2Rs in rats. The overall quinine potency and efficacy were not significantly different between the rat aorta and pulmonary artery. Moreover, the potency and efficacy of quinine on rat aorta in this study was seen to be consistent with earlier findings on the quinine-induced relaxation of phenylephrine pre-contracted guinea pig aorta (Manson *et al.*, 2014). Quinine is also inhibited the contraction induced by KCl in the rabbit aorta (Cook, Griffiths and Hoff, 1987). Additionally, quinine produced a concentration-dependent relaxation of KCl-contracted rat aortic rings (del Pozo *et al.*, 1996). These results indicate that quinine-mediated relaxation of aorta may be similar between species. Therefore, these similarities might be useful in translated these works on the human aorta.

Denatonium also induced relaxation of the rat aorta and pulmonary artery in a concentration-dependent manner. These findings were seen to be consistent with Sakai *et al.* (2016) who showed that denatonium caused a concentration-dependent relaxation of the phenylephrine pre-contracted mouse aorta. In this study, the potency of denatonium in the rat pulmonary artery was approximately 2-fold greater than in

the rat aorta, however, this potency was not significantly difference between rat aorta and pulmonary artery ($P > 0.05$). Thus, implying that similar levels of distribution of TAS2R subtypes in those two blood vessels.

The potency and the efficacy of denatonium-mediated relaxation in the rat aorta were similar to what was observed by Manson *et al.* (2014) who found that the denatonium induce relaxation of guinea pig aorta rings pre-contracted with phenylephrine. This indicates that the denatonium potency and efficacy in the aorta, as with quinine, might be the same regardless of species types. Therefore, further research is needed to investigate whether this denatonium effect is similar to human aortic tissue.

Additionally, dextromethorphan also induced relaxation in the rat pulmonary artery in a concentration-dependent manner. In the current study, the magnitude of the relaxation and the potency of dextromethorphan in rat pulmonary artery showed similarity with what was produced by the same agonist in phenylephrine pre-contracted guinea pig aorta (Manson *et al.*, 2014). On the other hand, the findings of Upadhyaya *et al.* (2014) showed a significant contraction that was observed with cumulative additions of dextromethorphan on new-born piglet's pulmonary arterial rings. This discrepancy in results might be due to concentration related changes; in Manson *et al.* (2014) they did not use high concentrations of dextromethorphan (beyond $1x10^{-4}$ M) while in Upadhyaya *et al.* (2014) the dextromethorphan start initial contraction at concentration 3×10^{-4} M and increased slowly until reach maximum contraction at $1x10^{-3}$ M. Moreover, in Manson *et al.* (2014) they used human pulmonary artery to investigate the dextromethorphan response whereas in Upadhyaya *et al.* (2014) they used porcine pulmonary artery. Therefore, this variation might indicate that the effect of dextromethorphan on pulmonary artery is different among species. Hence, these results suggested that unlike quinine and denatonium, the dextromethorphan effect couldn't be translated to the human pulmonary artery and this needed further studies to confirm.

In the absence of the pre-contractile agent, the bitter taste agonists failed to alter the resting tone of the rat pulmonary artery tissues. These findings were consistent with study that evaluated the effect of chloroquine on the resting tone (Sai *et al.*, 2014).

They found that chloroquine did not have an effect on the resting tone of the rat thoracic aortal rings. These results suggesting that bitter taste agonists used in this study had no effect on the normal resting tone.

2.4.2 Influence of Contractile Agent on Quinine-Induced Relaxation

The effect of pre-contracted agents was studied by Manson *et al.* (2014) on guinea pig aorta. They showed quinine, denatonium, and dextromethorphan had different potencies and efficacies in causing relaxations to phenylephrine, U46619, and prostaglandin $F_{2\alpha}$ ($PGF_{2\alpha}$). Manson *et al.* (2014) showed that pre-contracted tissue with phenylephrine having the highest potency and efficacy. In this study, quinine-induced a relaxation of both phenylephrine and U46619 pre-contracted rat pulmonary arteries. There was no statistically significant difference in quinine potency between phenylephrine pre-contracted pulmonary artery and U46619 ($P > 0.05$). However, the overall efficacy was not significantly different between phenylephrine and U46619. The reason behind this difference might be the different species used, different concentrations of bitter taste agonists used as well as different concentrations of pre-contracted agents.

Furthermore, in the current study, the magnitude of the quinine-induced relaxation was similar between phenylephrine and U46619 pre-contractions. On the contrary, the findings of Manson *et al.* (2014) showed the magnitude of quinine relaxation to be markedly smaller (approximately half) with U46619 compared with phenylephrine pre-contracted tissue. This difference in efficacy might be due to the different concentrations used; the highest concentration of quinine used was 1×10^{-3} M with the Manson study whereas the maximum concentration was used in this study was 3×10^{-3} M.

2.4.3 Endothelium Dependency of Bitter Taste Agonist Induced Relaxation of the Rat Pulmonary artery

In this study, removal of the endothelium did not prevent the relaxation of the pulmonary artery to quinine, denatonium, and dextromethorphan in the phenylephrine pre-contracted pulmonary artery. A similar degree of relaxation was

achieved in endothelium-intact and endothelium-denuded tissues, indicating that the relaxation to these bitter taste agonists is endothelium-independent. Moreover, the magnitude of relaxation and potency of the endothelium intact and denuded pulmonary artery for quinine, denatonium, and dextromethorphan were similar. Thus, further confirming that the effect of the bitter taste agonists is not dependent on the presence or absence of the endothelium on the rat pulmonary artery.

These results are in agreement with the observations shown by (Manson *et al.*, 2014). They found that the relaxations to chloroquine, denatonium, dextromethorphan and noscapine were identical in the guinea pig aortal endothelium intact and denuded. Furthermore, a study conducted by (Sai *et al.*, 2014) showed that the IC_{50} for chloroquine in pre-contracted rat thoracic aortic rings was similar between the endothelium intact and denuded.

Additionally, the role of the endothelium was investigated by Upadhyaya *et al.* (2014), who showed that the dextromethorphan-mediated response on the endothelium denuded pulmonary artery did not exhibit a change in the potency of dextromethorphan. Other study supported that and suggested that dextromethorphan endothelium-independent vasorelaxation of aorta (Wu *et al.*, 2012). Thus, the effect of the bitter taste agonists appears to be endothelium-independent. These results indicate that the response mediated by bitter taste agonists could act through the smooth muscle of the pulmonary artery rather than through the release of endothelium-derived mediators, as the relaxatory effect is still present in the absence of endothelium.

2.4.4 Specificity of Bitter Taste Agonist and Their Pharmacological Actions

Extra-oral functions of bitter taste receptors have been reported by several studies based on their interactions with TAS2Rs and their observational effects on different tissues (**Table 1.2**) in the introduction. However, some bitter taste agonists have an ability to both activate TAS2Rs and bind to additional targets including receptors and ion channels (Manson, 2015). For example, quinine activates TAS2R4, TAS2R7,

TAS2R14, TAS2R31, TAS2R39, TAS2R40, TAS2R43, and TAS2R44 (Meyerhof *et al.*, 2010), but also acts as α-adrenoceptor blocker (del Pozo *et al.*, 1996; Mecca *et al.*, 1980) and voltage-gated K^+ channel blocker (Cummings and Kinnamon, 1992; Kinnamon and Roper, 1988). Moreover, denatonium activates TAS2R4, TAS2R8, TAS2R46, and TAS2R47 (Brockhoff *et al.*, 2007) as well as delayed rectifier K^+ channels (Spielman *et al.*, 1989). Dextromethorphan activates TAS2R1 and TAS2R10 (Meyerhof *et al.*, 2010) and will also act as an opioid receptor agonist (Chau, Carter and Harris, 1983; Schneider *et al.*, 1991), N-methyl-D-aspartate (NMDA) receptor antagonist (Church, Lodge and Berry, 1985; Netzer, Pflimlin and Trube, 1993) and VDCC blocker (Larsson *et al.*, 2005). Therefore, the reason behind this might be due to the high concentrations of bitter taste agonists used which increase the possibility to interact with additional targets such as ion channels and receptors, beside TAS2Rs.

Chapter 3

Mechanisms of Bitter Taste Agonist-Mediated Vasorelaxant Effect on the Rat Pulmonary Artery

3.1 Introduction

Once the bitter taste agonist binds to the TAS2Rs, a conformational change occurs to the receptor which is followed by a signalling cascade that in turn relaxes blood vessels (Lund *et al.*, 2013). The data previously reported in Chapter 2 suggests that bitter taste agonists are capable of inducing relaxation of the rat pulmonary artery and aorta, and this relaxation was seen to be fully reversible. However, the mechanism of action of TAS2Rs in blood vessels still remains unclear. This chapter will therefore examine the mechanisms of action of bitter taste receptor agonists which have been proposed in recent years that may help shed light on how bitter taste agonists may work to produce vasorelaxation.

3.1.1 Inhibition of L-type Voltage-Dependent Calcium Channels

Sai *et al.* (2014) and Wu *et al.* (2017) both found that TAS2Rs are capable of inducing a relaxation of the blood vessels by inhibiting L-type voltage-dependent calcium channels. Sai *et al*. (2014) was able to demonstrate that denatonium and chloroquine was inhibited K^+ pre-contracted rat thoracic aortic rings in a concentration- dependent manner. Furthermore, nifedipine, which is a selective blocker of the L-type VDCC, had a similar inhibitory effect on K^+ pre-contracted rat thoracic aortic rings. These results indicate that the L-type VDCC may have a role in the mediated relaxation of the bitter taste agonists (Sai *et al.*, 2014). In order to further investigate the mechanism underlying the chloroquine-induced inhibition of the L-type VDCC, Sai *et al.* (2014) measured the L-type VDCC currents by using the patch clamp technique, with Ba^{2+} as the carrier charge. They found that upon the addition of 1 mM chloroquine to the solution bathing the rat thoracic aortic cells, the L-type VDCC currents were significantly inactivated compared with the same cells at baseline. These results strongly suggested that the L-type VDCC's might involve in the bitter taste agonists induced relaxation.

These findings were further supported by Wu *et al.* (2017) who investigated the direct effect of chloroquine on the L-type VDCC using the patch clamp technique. They used Ba^{2+} as the carrier charge in order to produce an inward current through the L-type

VDCC. Human pulmonary artery cells were superfused with solution containing 0.2 mM chloroquine, which resulted in the cell's inward current through the L-type VDCC to be almost completely abolished. This result further indicates that the chloroquine-mediated relaxation of the pulmonary artery is inhibited through the L-type VDCC.

In order to further clarify at which point L-type VDCCs are inhibited in the canonical bitter taste signalling pathway, rat thoracic aorta rings were incubated with either pertussis toxin (PTX), G_{α} protein inhibitor, or gallein for 6-8 hours. After which, chloroquine's relaxation was determined and compared to the control without these inhibitors. The results indicated that the pre-treatment with PTX and gallein had no effect on the chloroquine induced relaxation on the pre-contracted rings compared with the control. These results indicate that PTX and gallein do not mediate the chloroquine-induced inhibition of Ca^{2+} influx through the L-type VDCC in the rat thoracic aorta (Sai *et al.*, 2014).

Manson *et al.* (2014) questioned the mechanism of action via VDCCs and suggested that the bitter taste agonist-induced vasodilation was mainly through an L-type VDCCs independent pathway. For that study, guinea pig aortic rings were pre-contracted with $1x10^{-6}$ M phenylephrine, and then repeated this similarly with nifedipine on different experiment. The results showed that the bitter taste agonists were able to induce a complete relaxation of the pre-contracted guinea pig aorta. Manson *et al*. (2014) further reported that the involvement of caveolae, is important in the bitter taste agonists signalling transduction. Caveolae, which is a cluster signal transduction molecules, similar to ion channels and GPCRs, together in the plasma membrane (Parton and Del Pozo, 2013). Manson *et al.* (2014) then studied the response of chloroquine and noscapine in mice aortic rings and in the aortic rings from genetically manipulated mice lacking caveolin-1 (an important protein for the formation of caveolae) (Razani *et al.*, 2001). The results showed that the relaxation of the U46619 pre-contracted tissue with noscapine or chloroquine was impaired in the caveolin-1-deficient mice. The results from the Manson study indicate that the relaxation induced by chloroquine or noscapine is at least partially medicated through caveolae.

3.1.2 Contribution of Potassium-Activated Calcium Channels in the Induced Vasorelaxation of Bitter Taste Agonists

Deshpande *et al.* (2010) showed that the bronchodilation is mediated through the TAS2Rs canonical signalling pathway that results in a transient increase in the localized Ca^{2+} which subsequently activates the BK_{ca} channels and enhances K^+ efflux leading to membrane hyperpolarization and then bronchorelaxation. To investigate whether the activation of BK_{ca} channel has a role in the bitter taste agonists mediated vasorelaxation, Manson *et al.* (2014) and Wu *et al.* (2017) studied the involvement of BK_{ca} channel on bitter taste agonists induce vasorelaxation using iberiotoxin.

The involvement of BK_{ca} channel in the bitter taste agonists induced relaxation of guinea pig aortic rings was evaluated using (100 nM) iberiotoxin (Manson *et al.*, 2014). Iberiotoxin was able to decrease the potency of both chloroquine and denatonium without affecting their maximum relaxations, whereas the relaxation to noscapine, a natural bitter compound which can activate TAS2R14, was unchanged. These results indicate that the presence of BK_{ca} channels is not required for the relaxation induced by chloroquine, denatonium and noscapine (Manson *et al.*, 2014).

This was further supported by another group of researchers Wu *et al.* (2017), who showed that the chloroquine-induced pulmonary vasodilation is not inhibited by the blockade of BK_{ca} channels. The rat pulmonary artery rings were pre-treated with (5 μM) paxilline (a BK_{ca} channel blocker), 100 nM charybdotoxin (a BK_{ca} and IK channel blocker) or 10 mM TEA (a non-selective K^+ channel blocker that blocks the voltage-gated K^+ channels and BK_{ca} channels) for 30 minutes and then contracted with 1 μM phenylephrine. Their results showed that all these inhibitors had no effect on the relaxation induced by 0.2 mM chloroquine on the rat pulmonary artery rings.

From these studies, several pathways were supported and showed that bitter taste agonists are able to work through different mechanisms in tissues. Even though the mechanism of action is debated, the general consented is that bitter taste agonists are able to induce vasorelxation. This chapter aims to investigate the signalling

mechanisms behind the bitter taste agonists induced relaxation in the rat pulmonary artery. The involvement of the BK_{ca} channel in the bitter taste agonists mediated relaxation was investigated by using a non-selective K^+ channel blocker (TEA) and a selective BK_{ca} channel blocker (iberiotoxin). Moreover, Zhang *et al.* (2013) showed that the bitter taste agonists inhibit the L-type VDCCs, resulting in the relaxation of the mouse airway, which was pre-contracted with methacholine (Mch). They tested this by using FPL64176, an agonist of the L-type VDCC. They also found at a single cell level, that 10 μM of FPL64176 was able to prevent chloroquine from reducing the $[Ca^{2+}]_i$ increase induced by Mch. At a tissue level, FPL64176 was also able to prevent chloroquine from relaxing the Mch pre-contracted mouse airway smooth muscle in a dose dependent manner (Zhang *et al.*, 2013). Therefore, in order to study this effect on the blood vessels, the effect of the L-type VDCC's on the bitter taste agonist mediated relaxation using the L-type VDCC activator (Bay K8644) and an agonist of the L-type VDCC (FPL64176) were studied. In addition, this chapter further investigated at which point in the canonical bitter taste signalling pathway in the rat pulmonary artery leads to the inhibition of the L-type VDCCs using the Gβγ subunit inhibitor (gallein).

3.2 Methods

3.2.1 Inhibitors

Tetraethylammonium chloride (TEA) (Sigma-Aldrich) was prepared by making 10 mM stock in PSS. Iberiotoxin (Tocris Bioscience, Bristol, UK) was prepared as a 100 μM stock solution dissolved in milli-Q water, aliquoted, and stored at -20°C until required. FPL 64176 (methyl 2,5-dimethyl-4-(2-(phenylmethyl) benzoyl)-1H-pyrrole-3-carboxylate) (Tocris Bioscience, Bristol, UK) was prepared as a 50 mM stock dissolved in DMSO and serially diluted in PSS to a concentration of 5 μM. Bay K 8644 (3-Pyridinecarboxylic acid, 1,4-dihydro-2,6-dimethyl-5-nitro-4-(2-(trifluoromethyl) phenyl)-, Methyl ester) (Tocris Bioscience, Bristol, UK) was prepared as a $1x10^{-5}$ M solution. Gallein (Tocris Bioscience, Bristol, UK) was prepared as a 1 mM stock solution in DMSO (Sigma-Aldrich, Poole, UK), aliquoted, and stored -20 °C until required.

3.2.2 Effect of TEA on Bitter Taste Agonist-Mediated Relaxation

To test whether the potassium channels have a role in the bitter taste agonists mediated relaxation of the rat aorta and pulmonary artery, the effect of TEA was examined. TEA is the mostly common used non-selective K^+ channel blocker (Cook, 1989). Therefore, if the bitter taste agonists induced relaxation is through the activation of potassium channels, the TEA should be able to block this relaxation (Cook, 1989).

The effect of the potassium channel blockage on the bitter taste agonists mediated relaxation was examined on the rat aortic tissue by substituting the normal PSS with PSS containing 1 x 10^{-3} M TEA. Once the tissues responses were stabilised over a 10-minute recovery period, phenylephrine (1 x 10^{-6} M) was added to induce a contraction. After the contractile response was stable, denatonium (1 x 10^{-7} – 3 x 10^{-4} M) was cumulatively added until the magnitude returned to the resting tension or reached a plateau (n = 4/4). The way of applying TEA was done according to the previous study (Wu *et al.*, 2017). The time control was pre-contracted with phenylephrine; however, TEA was not added to the PSS. The same protocol was repeated for quinine (1 x 10^{-7}

– 3 x 10^{-3} M) (*n* = 9/5), denatonium (1 x 10^{-7} – 3 x 10^{-3} M) (*n* = 4/8) and dextromethorphan (1 x 10^{-7} – 3 x 10^{-3} M) (*n* = 4/4) using the rat pulmonary artery rings. U46619 was further used with quinine (1 x 10^{-7} – 3 x 10^{-4} M) as the pre-contractile agent in the pulmonary artery (*n* = 4/4) (Figure 3.1).

3.2.3 Effect of Iberiotoxin on the Bitter Taste Agonists Mediated Relaxation

The involvement of BK_{ca} channels in the bitter taste receptor agonists-mediated relaxation was further evaluated by using a selective and potent BK_{ca} channel blocker, iberiotoxin (100 nM) (Satake, Shibata and Shibata, 1996; Wallner *et al.*, 1995). Iberiotoxin was added for 30 minutes prior to the pre-contraction of the tissue with 1 x 10^{-6} M phenylephrine. This was then followed by cumulative additions of quinine (1 x 10^{-7} – 3 x 10^{-3} M) until the magnitude returned to the resting tension or reached a plateau (*n* = 5/5). The time control was pre-contracted with phenylephrine and followed by cumulative addition of quinine without the addition of iberiotoxin. This protocol was then further repeated for denatonium (1 x 10^{-7} – 3 x 10^{-3} M) (*n* = 5/5) and dextromethorphan (1 x 10^{-7} – 3 x 10^{-3} M) (*n* = 5/4) (Figure 3.5).

3.2.4 Effect of the L-Type Voltage-Dependent Calcium Channels (VDCCs) Agonists on Bitter Taste Mediated Relaxation.

To determine if the bitter taste agonists inhibit the L-type VDCCs and thereby mediating the relaxation, the effect of quinine were tested in the presence and absence of Bay K8644 (L-type VDCC activator) (Bourson *et al.*, 1989). The rat pulmonary arterial rings were pre-contracted by substituting PSS with a mixture of PSS containing 1x10^{-6} M phenylephrine and 1 x 10^{-5} M Bay K8644, followed by the cumulative addition of quinine (1 x 10^{-7} – 3 x 10^{-3} M) (*n* = 6/6). The time control was pre-contracted with phenylephrine and followed by cumulative addition of quinine without the addition of Bay K8644. This protocol was repeated using U46619 as the pre-contractile agent. Furthermore, this entire protocol was repeated with 5 x 10^{-6} M

FPL64176, an agonist of the L-type VDCCs (n = 5/5) (Zheng, Rampe and Triggle, 1991) (Figure 3.8).

3.2.5 Effect of a G- Protein βγ-Subunit Inhibitor on Bitter Taste Agonist-Mediated Relaxation on the Rat Pulmonary Artery Tissue

To further investigate if the bitter taste agonist induced relaxation is dependent on the Gβγ subunit, the effect of the bitter taste agonists were examined in presence of the non-selective blocker of the Gβγ subunit, gallein (Sai *et al*., 2014). The pulmonary arterial rings were pre-treated with 2 x 10^{-5} M gallein for 10 minutes before the pre-contraction with phenylephrine and then followed by the cumulative addition of quinine (1 x 10^{-7} – 3 x 10^{-3} M) (n = 10/9). This protocol was repeated with denatonium (1 x 10^{-7} – 3 x 10^{-3} M) (n = 13/9) and dextromethorphan (1 x 10^{-7} – 3 x 10^{-3} M) (n = 5/4). This protocol was further repeated using U46619 as the pre-contractile agent for quinine.

3.2.6 Statistical Analysis

Calculations and statistical analyses were the same as in Chapter 2. The mean of IC_{50} of agonists in the presence or absence of inhibitors were compared using unpaired Student's t-test where applicable. $P < 0.05$ was considered to be statistically significant.

3.3 Results

3.3.1 The Effect of TEA on the Bitter Taste Agonists-Induced Relaxation of the Rat Aorta and Pulmonary Artery.

The mechanism by which bitter taste agonists are able to produce vasorelaxation remains unclear in the rat pulmonary artery. In 2017, Wu *et al*. showed that the effect of BK_{ca} channel have no role in this mechanism. To establish whether the activation of BK_{ca} channel plays a role in the bitter taste agonists-mediated relaxation on the rat aorta, the effect of denatonium were examined in the presence of TEA, a non-selective K^+ channel blocker. Pre-treatment of the aorta with TEA ($1x10^{-3}$ M) increased the magnitude of phenylephrine-induced contraction by 60% (n = 9/4) when compared to that produced in the absence of TEA. There was a non-significant rightward shift of the denatonium concentration-response curve, and which produced an IC_{50} of 1.0 ± 0.3 x 10^{-4} M and reaching a relaxation of 76 ± 6 % at the concentration of 3 $x10^{-4}$ M (n = 4) (IC_{50} of control 3.0 ± 0.5 x 10^{-5} M and I_{max} of the control 93 ± 3%, $P > 0.05$). Denatonium was able to successfully relax the pre-contracted rat aorta in the presence of TEA. Over the course of the experiment, the vehicle control in the presence of TEA relaxed by 7.7 ± 12.8 % (n = 4/4). These results suggest that the activation of BK_{ca} channels have no role in the denatonium-mediated relaxation of the rat aorta (Figure 3.2).

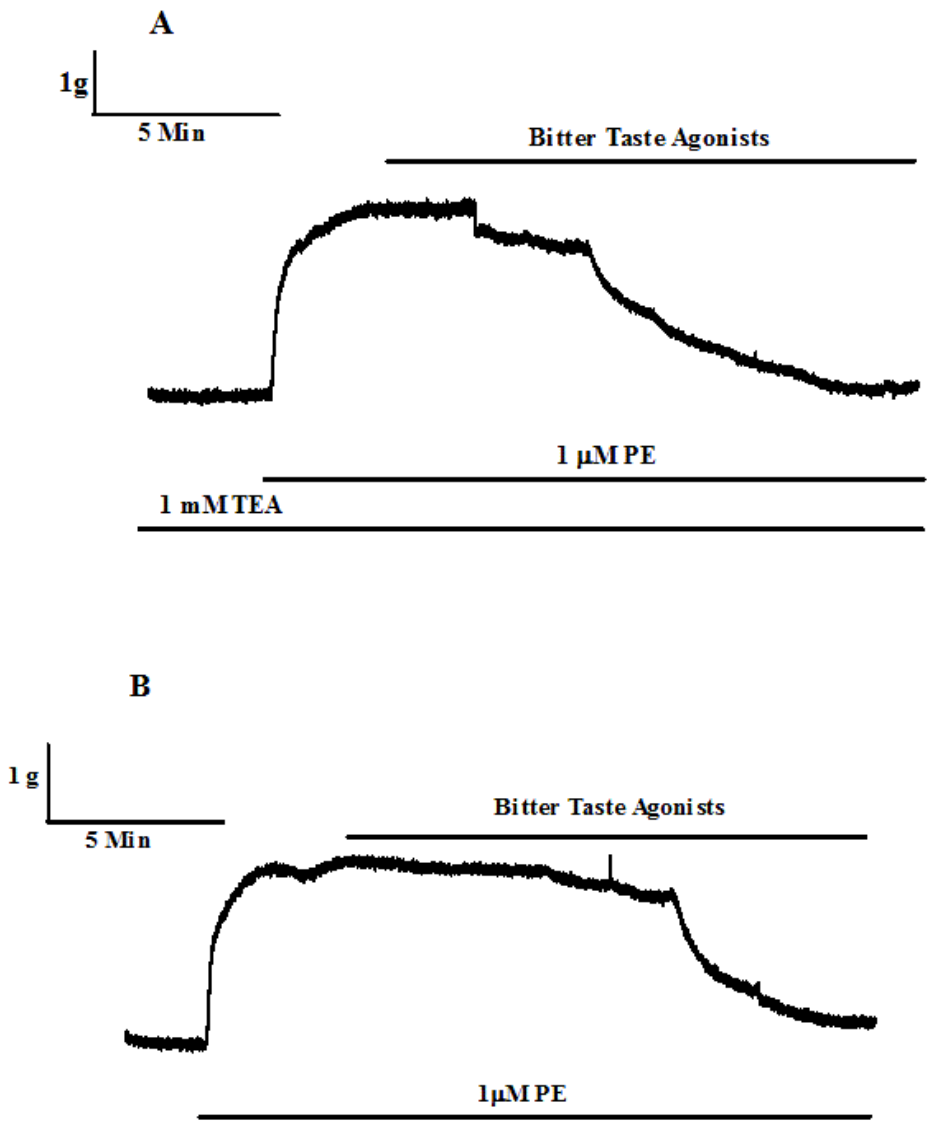

Figure 3.1 Representative Traces of the Effect of TEA on Bitter Taste Agonists - Induced Relaxation of Pre-contracted Rat Aorta / Pulmonary Artery.

(A) Rat aorta/pulmonary artery tissue were treated with TEA (1 x 10^{-3} M) for 10 minutes before the tissue was pre-contracted with phenylephrine (1 x 10^{-6} M). Then, the tissue was relaxed with cumulative additions of bitter taste agonists. For the rat aorta the denatonium (1 x 10^{-7} – 3 x 10^{-4} M), while in the pulmonary artery quinine (1 x 10^{-7} – 3 x 10^{-3} M), denatonium (1 x 10^{-7} – 3 x 10^{-3} M) and dextromethorphan (1 x 10^{-7} – 3 x 10^{-3} M). **(B)** Representative trace in the absence of the TEA.

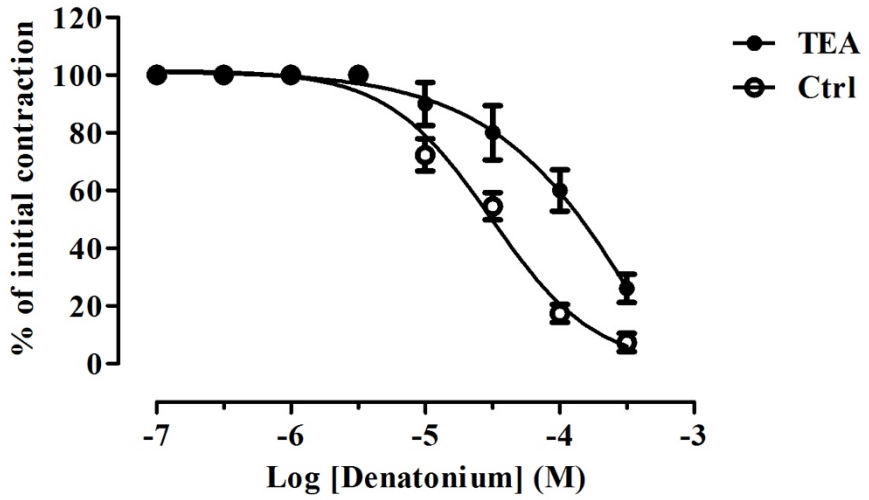

Figure 3.2 The Effect of TEA on the Denatonium-Induced Relaxation of the Pre-Contracted Rat Aorta.

Rat aortic tissue was treated with TEA (1 x 10^{-3} M) for 10 minutes before the tissue was pre-contracted with phenylephrine (1 x 10^{-6} M). The tissue was then relaxed with cumulative additions of denatonium (1 x 10^{-7} M to 3 x 10^{-4} M). Concentration-response curve for denatonium with a magnitude of the initial contraction at 0.60 ± 0.1 g, and 0.64 ± 0.1 g for the studies involving the presence of TEA and absence (Control – Ctrl) respectively. The contractile response is expressed as a percentage of the initial control contraction produced by phenylephrine and is shown as mean ± s.e.m. (n = 4/4) ($P >$ 0.05).

To further investigate the role of BK_{ca} channels on the bitter taste agonist mediated relaxation, the relaxant effect of the bitter taste agonist in the presence of TEA was further repeated on the rat pulmonary artery rings. In the presence of TEA, quinine was able to produce a concentration-dependent full relaxation on the rat pulmonary artery which was pre-contracted with phenylephrine. The IC_{50} was $1.8 \pm 0.3 \times 10^{-4}$ M (n = 9/5), and the relaxation was 106 ± 2 % at the concentration of 3×10^{-3} M quinine (IC_{50} of the control was $1.6 \pm 1.7 \times 10^{-4}$ M and an I_{max} was 111 ± 5.7%, $P > 0.05$) (Figure 3.3 A). The subsequent addition of quinine (1×10^{-7} M - 3×10^{-4} M) in the sustained presence of TEA was also capable of inducing a relaxation of the rat pulmonary artery which was pre-contracted with U46619. There was no significant difference in the quinine-induced relaxation, which produced an IC_{50} of $4.8 \pm 1.4 \times 10^{-5}$ M and reaching a relaxation of 92 ± 7% at the concentration of 3×10^{-4} M quinine (n = 4/4) (IC_{50} of the control was $1.8 \pm 0.2 \times 10^{-3}$ M and the I_{max} 106 ± 4.1%, $P > 0.05$) (Figure 3.3 B). Furthermore, in the presence of TEA, denatonium was able to induce a concentration-dependent relaxation on the rat pulmonary artery which was pre-contracted with phenylephrine, producing an IC_{50} of $1.78 \pm 0.3 \times 10^{-4}$ M (n = 4/8) and a relaxation of 100 ± 8% was observed at a concentration of 3×10^{-3} M denatonium (IC_{50} of the control $6.5 \pm 1.0 \times 10^{-4}$ M, and an I_{max} was 97 ± 4% , $P > 0.05$), (Figure 3.4 A).

Additionally, in the presence of TEA, dextromethorphan also produced a concentration-dependent relaxation of the rat pulmonary artery pre-contracted with phenylephrine. TEA did not affect the dextromethorphan-induced relaxation and the resulting IC_{50} was $6.22 \pm 0.9 \times 10^{-5}$ M (n = 4/4). A relaxation of 111 ± 7 % was induced by 3×10^{-4} M of dextromethorphan (IC_{50} of the control was $2.6 \pm 0.2 \times 10^{-5}$ M and an I_{max} was 109 ± 13%, $P > 0.05$). By the end of the experiments, the vehicle control showed relaxation by 8 ± 5 % (n = 21) (Figure 3.4 B)

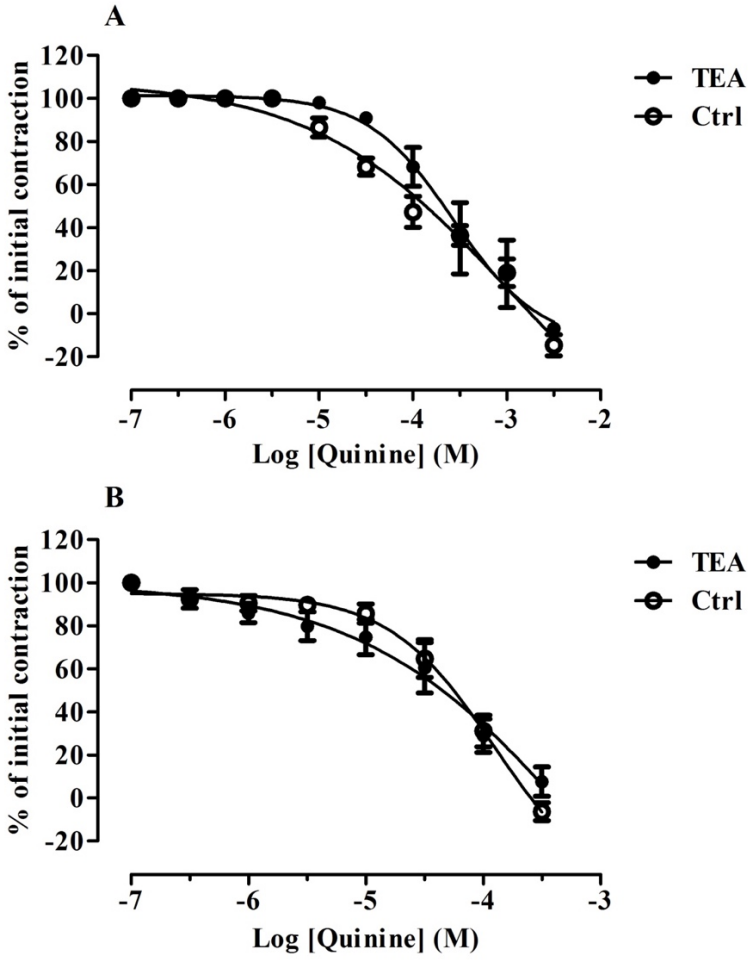

Figure 3.3 The Effect of TEA on the Quinine-Induced Relaxation of the Pre-Contracted Rat Pulmonary Artery.

Rat pulmonary arterial tissue was treated with TEA (1 x 10^{-3} M) for 10 minutes before the tissue was pre-contracted. The tissue was then relaxed with cumulative additions of quinine. (A) Concentration-response curve for quinine (1 x 10^{-7} M to 3 x 10^{-3} M) pre-contracted with phenylephrine (1 x 10^{-6} M) with a magnitude of the initial contraction at 0.32 ± 0.04 g, and 0.2 ± 0.01 g for the studies involving the presence of TEA and absence (Control – Ctrl) respectively (n = 9/5). (B) Concentration-response curve for quinine (1 x 10^{-7} M to 3 x 10^{-4} M) pre-contracted with U46619, with a magnitude of the initial contraction at 0.30 ± 03 g, and 0.35 ± 0.1 g for the studies involving the presence of TEA and absence (Control – Ctrl) respectively (n = 4/4). The contractile response is expressed as a percentage of the initial control contraction produced by phenylephrine/U46619 and is shown as mean ± s.e.m (P > 0.05).

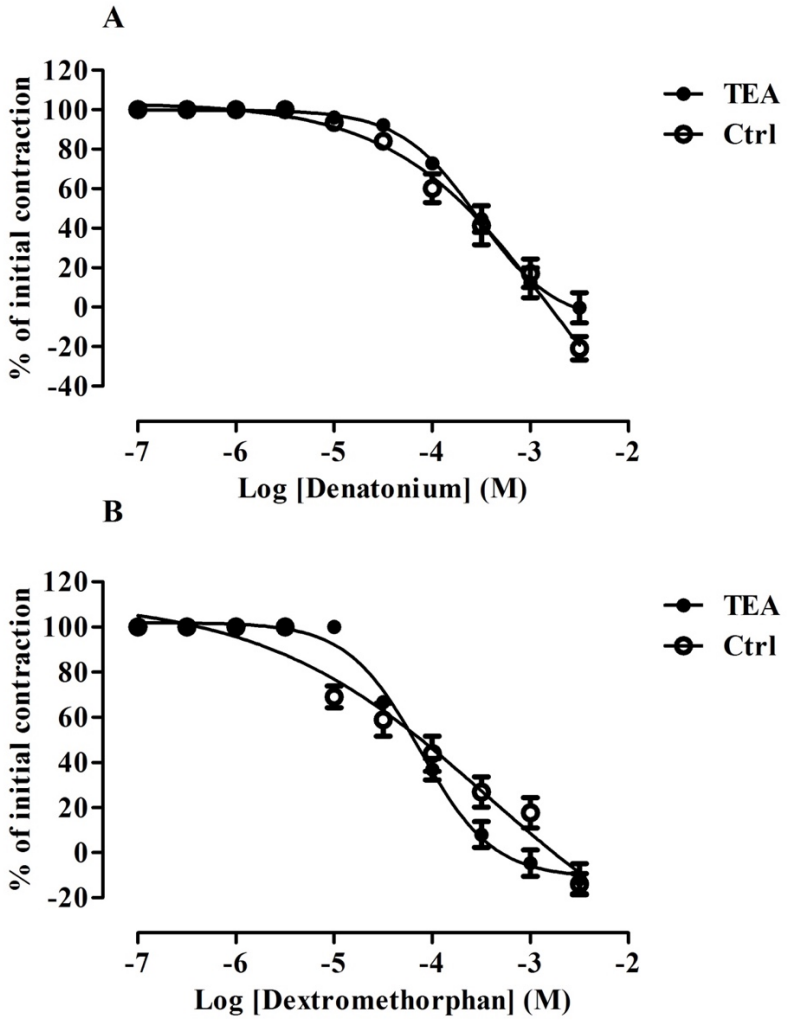

Figure 3.4 The Effect of TEA on the Denatonium and Dextromethorphan Induced Relaxation of the Pre-Contracted Rat Pulmonary Artery.

Rat pulmonary arterial tissue was treated with TEA (1 x 10^{-3} M) for 10 minutes before the tissue was pre-contracted. The tissue was then relaxed with cumulative additions of quinine. A) Concentration-response curve for denatonium (1 x 10^{-7} M to 3 x 10^{-3} M) pre-contracted with phenylephrine (1 x 10^{-6} M) with a magnitude of the initial contraction at 0.36 ± 0.03 g, and 0.25 ± 0.04 g for the studies involving the presence of TEA and absence (Control – Ctrl) respectively (n = 4/8). B) Concentration-response curve for quinine (1 x 10^{-7} M to 3 x 10^{-4} M) pre-contracted with U46619, with a magnitude of the initial contraction at 0.34 ± 0.05 g, and 0.28 ± 0.07 g for the studies involving the presence of TEA and absence (Control – Ctrl) respectively (n = 4/4). The contractile response is expressed as a percentage of the initial control contraction produced by phenylephrine and is shown as mean ± s.e.m ($P > 0.05$).

3.3.2 The Effect of Iberiotoxin on the Bitter Taste Agonist-Induced Relaxation of the Rat Pulmonary Artery

Manson *et al.* (2014) showed that the BK_{ca} channels were not required for bitter taste agonists-induced relaxation. In order to further investigate the role of these channels, the ability of TAS2R agonists (quinine, denatonium, and dextromethorphan) to evoke an inhibition of the rat pulmonary artery in the presence of a BK_{ca} channel blocker, iberiotoxin, was measured. In the presence of iberiotoxin, all of the bitter taste agonists were able to produce a concentration-dependent inhibition of the contraction, reaching a full inhibition. The resulting IC_{50} for quinine was $1.8 \pm 0.9 \times 10^{-4}$ M and reached a relaxation of $106 \pm 4\%$ induced at 3×10^{-3} M quinine ($n = 5/5$) (IC_{50} of the control was $1.6 \pm 1.7 \times 10^{-4}$ M and an I_{max} was $111 \pm 5.7\%$, $P > 0.05$) (Figure 3.6 A). The IC_{50} for denatonium was $5 \pm 0.9 \times 10^{-4}$ M with a maximum relaxation of $105 \pm 5\%$ observed at 3×10^{-3} M denatonium ($n = 5/5$) (IC_{50} of the control $6.5 \pm 1.0 \times 10^{-4}$ M, and an I_{max} was $97 \pm 4\%$, $P > 0.05$) (Figure 3.6 B). These results indicate that the potency and efficacy of the quinine and denatonium were not affected by the BK_{Ca} channel blocker and implies that the BK_{Ca} channels are not involved in the overall inhibitory effect of bitter taste agonists. Additionally, in the presence of iberiotoxin, a non-significant rightward shift of the dextromethorphan concentration-response curve was observed with an IC_{50} of $3.5 \pm 0.1 \times 10^{-4}$ M, and a relaxation of $113 \pm 4\%$ at 3×10^{-3} M dextromethorphan ($n = 5/4$) (IC_{50} of the control $6.5 \pm 1.0 \times 10^{-4}$ M, and an I_{max} was $97 \pm 4\%$, $P > 0.05$). At the end of the experiment, there was a relaxation by $5.0 \pm 6.6\%$ in the vehicle control of the experiment in the presence of the iberiotoxin ($n = 15/14$). These results indicate the overall efficacy of dextromethorphan was not affected by the BK_{Ca} channel blocker and further implies that these BK_{Ca} channels are not involved in the overall inhibitory effect (Figure 3.7).

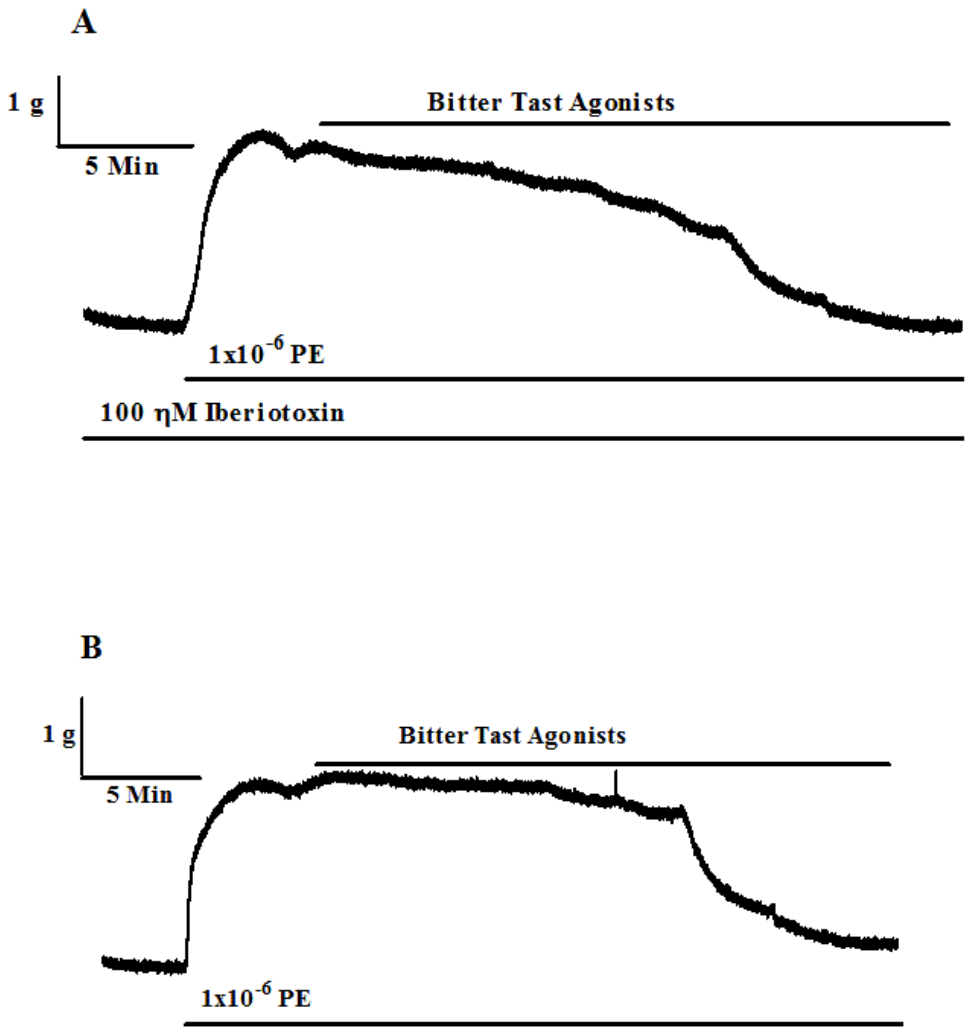

Figure 3.5 Representative Traces of the Effect of Iberiotoxin on the Bitter Taste Agonist-Induced Relaxation of the Rat Pulmonary Artery

(A) Rat pulmonary arterial tissue was treated with iberiotoxin (1 x 10^{-6} M) for 30 minutes before the tissue was pre-contracted with phenylephrine (1 x 10^{-6} M). Then the tissue was relaxed with cumulative additions of bitter taste agonists quinine, denatonium, or dextromethorphan (1 x 10^{-7} – 3 x 10^{-3} M). (**B)** Representative trace in the absence of the iberoitoxin.

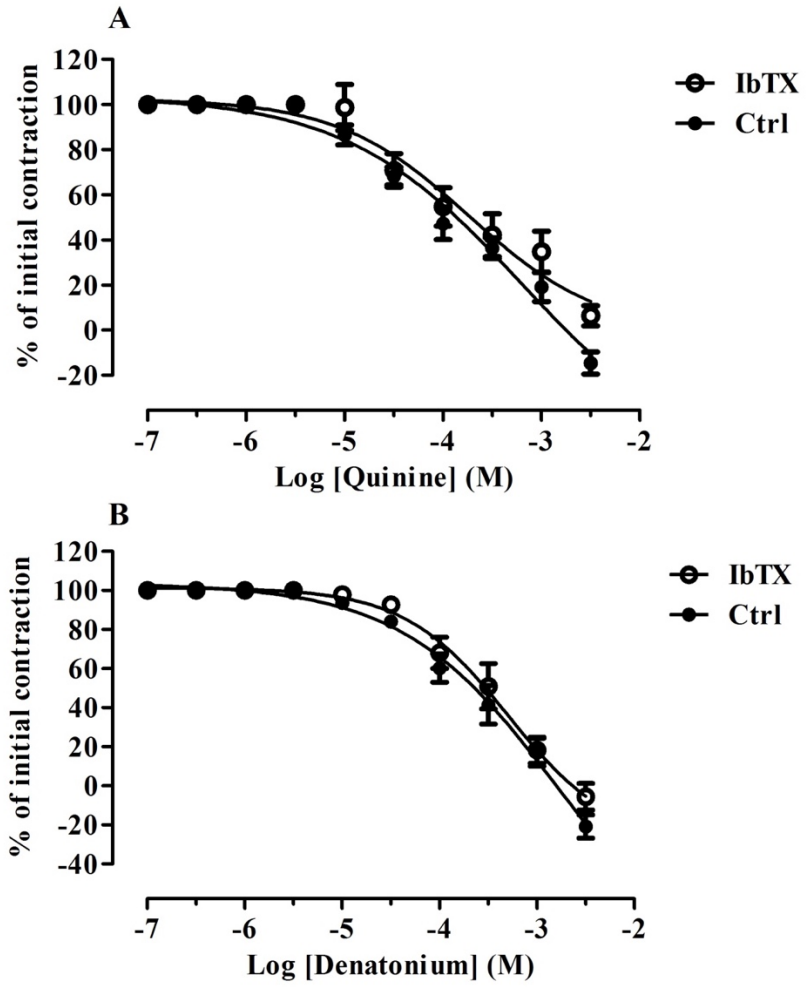

Figure 3.6 The effect of Iberiotoxin on the Quinine and Denatonium Induced Relaxation of the Pre-Contracted Rat Pulmonary Artery.

Rat pulmonary arterial tissue was treated with iberiotoxin (1 x 10^{-6} M) for 30 minutes before the tissue was pre-contracted. The tissue was then relaxed with cumulative additions of quinine. **(A)** Concentration-response curve for quinine (1 x 10^{-7} M to 3 x 10^{-3} M) pre-contracted with phenylephrine (1 x 10^{-6} M) with a magnitude of the initial contraction at 0.37 ± 0.10 g, and 0.2 ± 0.02 g for the studies involving the presence of iberiotoxin (IbTX) and absence (Control – Ctrl) respectively (n = 5/5). **(B)** Concentration-response curve for denatonium (1 x 10^{-7} M to 3 x 10^{-3} M) pre-contracted with phenylephrine, with a magnitude of the initial contraction at 0.39 ± 07 g, and 0.25 ± 0.04 g for the studies involving the presence of (IbTX) and absence (Control – Ctrl) respectively (n = 5/5). The contractile response is expressed as a percentage of the initial control contraction produced by phenylephrine and is shown as mean ± s.e.m (P > 0.05).

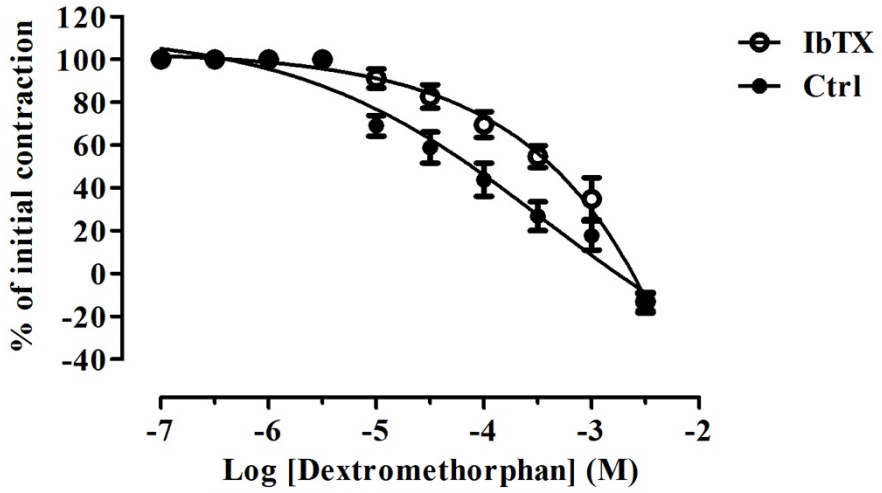

Figure 3.7 The effect of Iberiotoxin on the Dextromethorphan-Induced Relaxation of the Pre-Contracted Rat Pulmonary Artery.

Rat pulmonary arterial tissue was treated with iberiotoxin (1 x 10^{-6} M) for 30 minutes before the tissue was pre-contracted. The tissue was then relaxed with cumulative additions of dextromethrphan. Concentration-response curve for dextromethorphan (1 x 10^{-7} M to 3 x 10^{-3} M) pre-contracted with phenylephrine (1 x 10^{-6} M) with a magnitude of the initial contraction at 0.27 ± 0.04 g, and 0.28 ± 0.07 g for the studies involving the presence of iberiotoxin (IbTX) and absence (Control – Ctrl) respectively (n = 5/4). The contractile response is expressed as a percentage of the initial control contraction produced by phenylephrine and is shown as mean ± s.e.m ($P > 0.05$).

3.3.3 Role of the L-type voltage-dependent calcium channels on the Bitter Taste Agonist-Mediated Relaxation.

Manson *et al.* (2014) showed that the TAS2R agonist induced relaxation was largely independent of the L-type Ca^{2+} channels, as they found that the use of nifedipine, which is an L-type Ca^{2+} channel blocker, was not able to inhibit the TAS2R agonists mediated relaxation on the guinea pig aorta. In order to investigate the possible involvement of the L-type Ca^{2+} channel in the TAS2R–mediated effects, Bay K 8644 and FPL64176 were used on the rat pulmonary artery.

3.3.3.1 Effect of Bay K8644 on Quinine Induced Relaxation of the Rat Pulmonary Artery

Grassin-Delyle *et al.* (2013) showed that the L-type VDCCs might be involved in the mechanism of action of chloroquine, as they found that the use of Bay K8644 on the human bronchi tissues caused a reduction of chloroquine's potency. To study this on the blood vessels, the relaxant activity of quinine was studied in the presence of the L-type VDCC activator, Bay K8644 in the rat pulmonary artery. In the presence of Bay K8644, the IC_{50} of quinine was $1.7 \pm 0.3 \times 10^{-4}$ M and the maximum relaxation induced was $108 \pm 3\%$ by 3×10^{-3} M quinine (IC_{50} of the control was $1.6 \pm 1.7 \times 10^{-4}$ M and an I_{max} was $111 \pm 5.7\%$, $P > 0.05$) ($n = 6/6$) (Figure 3.9A).

Furthermore, the influence of the pre-contractile agent, U46619, was used to evaluate the effect of Bay K8644 on the quinine-induced relaxation of the rat pulmonary artery. In the presence of Bay K8644, the IC_{50} of quinine was $1.9 \pm 0.1 \times 10^{-4}$ M and the maximum relaxation induced was $102 \pm 6\%$ by 3×10^{-3} M quinine ($n = 9/9$) (IC_{50} of the control was $1.8 \pm 0.2 \times 10^{-3}$ M and the I_{max} was $106 \pm 4.1\%$, $P > 0.05$) (Figure 3.9 B). By the end of the experiment, the time control in the presence of Bay K8644 showed a relaxation by 8.0 ± 4.5 % ($n = 15/15$). Together, these results indicate that the quinine-mediated relaxation of the rat pulmonary artery is might dependent on L-type VDCCs.

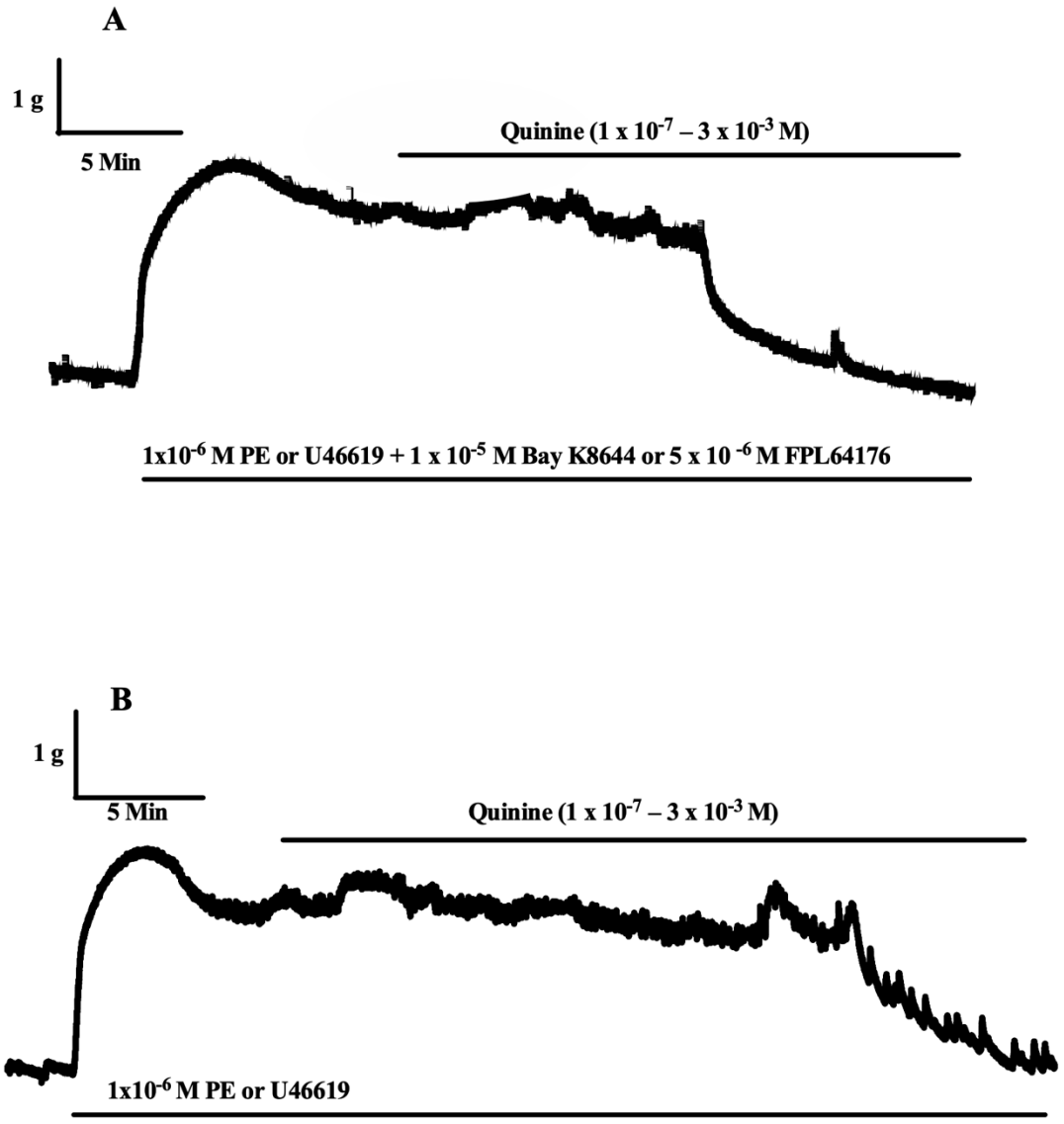

Figure 3.8 Representative traces of the Effect of the Bay K8644 and FPL64176 on Quinine Induced Relaxation of the Rat Pulmonary Artery

A) The rat pulmonary arterial rings were pre-contracted by substituting PSS with a mixture of PSS containing 1x10^{-6} M phenylephrine or U46619 and 1 x 10^{-5} M Bay K8644 or 5 x 10^{-6} M FPL64176, followed by the cumulative addition of quinine (1 x 10^{-7} – 3 x 10^{-3} M). **B)** Representative trace of the time control which was pre-contracted with phenylephrine or U46619 and followed by cumulative addition of quinine without the addition of Bay K8644 or FPL64176.

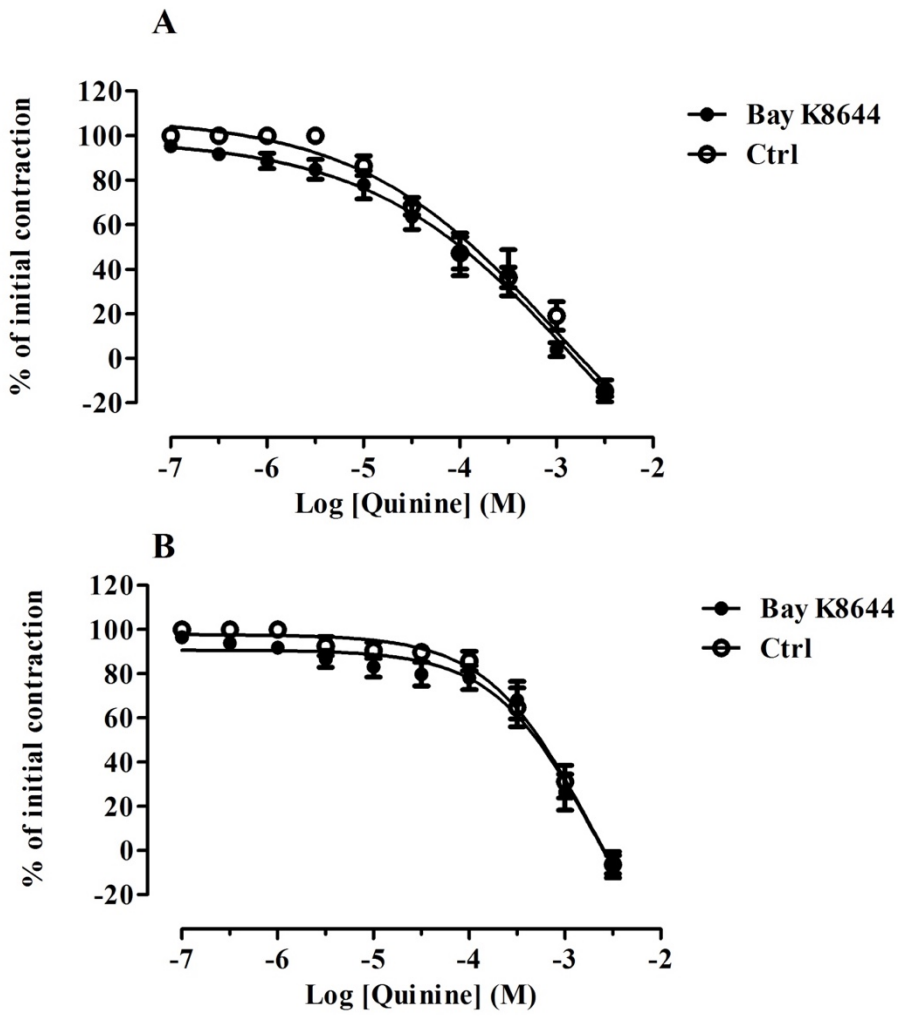

Figure 3.9 The Effect of Bay K8644 on the Quinine-Induced Relaxation of the Pre-Contracted Rat Pulmonary Artery.

Rat pulmonary arterial tissue was treated with a mixture of phenylephrine (1 x 10^{-6} M) and Bay K8644 (1 x 10^{-3} M). The tissue was then relaxed with cumulative additions of quinine. (**A**) Concentration-response curve for quinine (1 x 10^{-7} M to 3 x 10^{-3} M) pre-contracted with phenylephrine (1 x 10^{-6} M) with a magnitude of the initial contraction at 0.28 ± 0.05 g, and 0.28 ± 0.07 g for the studies involving the presence of Bay K8644 and absence (Control – Ctrl) respectively (n = 6/6). (**B**) Concentration-response curve for quinine (1 x 10^{-7} M to 3 x 10^{-4} M) pre-contracted with U46619, with a magnitude of the initial contraction at 0.40 ± 0.06 g, and 0.35 ± 0.08 g for the studies involving the presence of Bay K8644 and absence (Control – Ctrl) respectively (n = 9/9). The contractile response is expressed as a percentage of the initial

control contraction produced by phenylephrine/U46619 and is shown as mean ± s.e.m ($P >$ 0.05).

3.3.3.2 The Effect of FPL64176 on the Quinine-Induced Relaxation of the Rat Pulmonary Artery

FPL64176 was used to investigate whether the L-type VDCCs have a role in the bitter taste agonist induce relaxation of the rat pulmonary artery. In the presence of FPL64176, quinine was able to successfully relax the pulmonary artery with an IC_{50} 1.1 ± 0.3 x10^{-4} M and a maximum relaxation of 130 ± 15% observed at 3 x 10^{-3} M quinine (n = 5/5) (IC_{50} of the control was 1.6 ± 1.7 x 10^{-4} M and an I_{max} was 111 ± 5.7%, $P >$ 0.05) (Figure 3.10 A).

Furthermore, the use of U46619 as a pre-contractile agent was investigated in the presence of FPL64176 on the quinine mediated relaxation of the rat pulmonary artery. In the presence of FPL64176, there was no significant shift of the quinine response curve and IC_{50} was at 8.7 ± x10^{-4} M and a maximum relaxation of 145 ± 12% at 3 x 10^{-3} M quinine (n = 7/7) (IC_{50} of the control was 1.8 ± 0.2 x 10^{-3} M and the I_{max} was 106 ± 4.1%, $P >$ 0.05). By the end of the experiment, the time control in the presence of FPL64176 showed a relaxation by 8.0 ± 1.5 % (n = 12). Taken together these results suggest that the relaxation of the rat pulmonary artery mediated by quinine might be dependent on the inhibition of the L-type VDCCs (Figure 3.10 B).

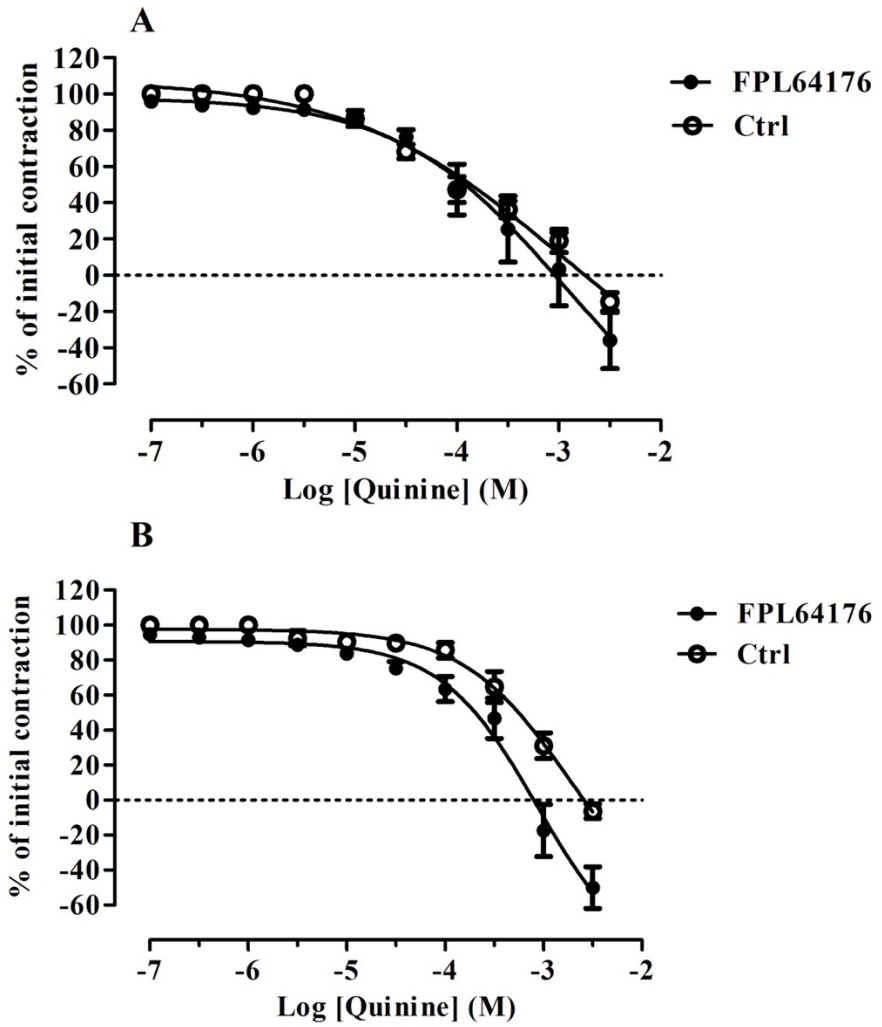

Figure 3.10 The effect of FPL64176 on the Quinine-Induced Relaxation of the Pre-Contracted Rat Pulmonary Artery.

Rat pulmonary arterial tissue was treated with a mixture of phenylephrine (1 x 10^{-6} M) and FPL64176 (5 x 10^{-6} M). The tissue was then relaxed with cumulative additions of quinine. (**A**) Concentration-response curve for quinine (1 x 10^{-7} M to 3 x 10^{-3} M) pre-contracted with phenylephrine (1 x 10^{-6} M) with a magnitude of the initial contraction at 0.12 ± 0.01 g, and 0.28 ± 0.07 g for the studies involving the presence of FPL64176 and absence (Control – Ctrl) respectively (n = 5/5). (**B**) Concentration-response curve for quinine (1 x 10^{-7} M to 3 x 10^{-4} M) pre-contracted with U46619, with a magnitude of the initial contraction at 0.16 ± 0.07 g, and 0.35 ± 0.08 g for the studies involving the presence of FPL64176 and absence (Control – Ctrl) respectively (n = 7/7). The contractile response is expressed as a percentage of the initial

control contraction produced by phenylephrine/U46619 and is shown as mean ± s.e.m (P > 0.05).

3.3.4 The Role of the G-Protein βγ-subunits in the Mechanism of action of Bitter Taste Agonists

Zhang *et al.* (2013) showed that the βγ-subunits of the G-Protein are involved in the mechanism of action of the TAS2R agonists. There results showed that the use of gallein, (a *G*βγ blocker) on the mouse airway smooth muscle cells was able to block the effect of the TAS2R agonists. In order to translate this involvement of the G-Protein βγ-subunit on the vascular vessels, the ability of the TAS2R agonists to evoke an inhibition of the contracted rat pulmonary artery was investigated in the presence of gallein. In the presence of gallein, the IC_{50} produced by quinine was 1.01 ± 0.6 x10^{-4} M and the maximum relaxation induced was 114 ± 0.3% at 3 x 10^{-3} M quinine (n = 10/9). No significant changes were observed with the quinine induced relaxation of the rat pulmonary artery compared with the time control (IC_{50} of the control was 1.6 ± 1.7 x 10^{-4} M and an I_{max} was 111 ± 5.7%, P > 0.05) (Figure 3.8 A).

Furthermore, denatonium also produced a relaxation of the pre-contracted pulmonary artery in the presence of gallein. The IC_{50} for denatonium in the presence of gallien was 5.66 ± 1.5 x 10^{-5} M, which was approximately 3-fold greater than control. However, this was not a statistically significant difference (p > 0.05), and the magnitude of the relaxation was 98 ± 4% at 3 x 10^{-3} M denatonium (n = 13/9) (IC_{50} of the control 6.5 ± 1.0 x 10^{-4} M, and an I_{max} was 97 ± 4% , P > 0.05) (Figure 3.8 B). Dextromethorphan was also found to induce a relaxation of the pre-contracted tissues in the presence of gallein. The resulting IC_{50} in the presence of gallein was 7.8 ± 1.05 x10^{-5} M (n = 5/4) and the magnitude of the relaxation was 115 ± 6 % at 3 x 10^{-3} M dextromethorphan (IC_{50} of the control 6.5 ± 1.0 x 10^{-4} M, and an I_{max} was 97 ± 4%, P > 0.05) (Figure 3.9). Over the duration of the experiment, the vehicle control in the presence of gallein showed a significant relaxation by 9.6 ± 5 % (control p < 0.05) (n = 15). This indicates an overall relaxation of the pulmonary artery tissues. These results further indicate that the G-protein βγ-subunit is not involved in the mechanism of action of TAS2R agonists.

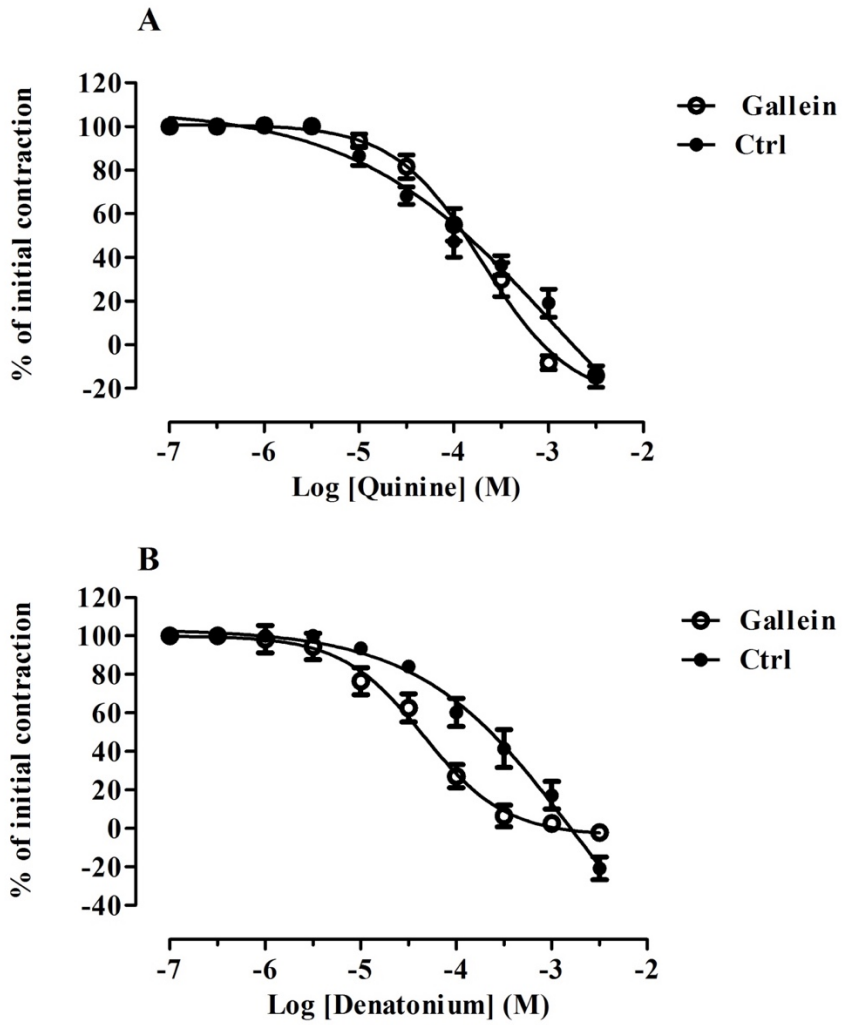

Figure 3.11 The Effect of Gallein on the Quinine and Denatonium-Induced Inhibition of the Pre-Contracted Rat Pulmonary Artery.

Rat pulmonary arterial tissue was treated with gallein (2 x 10^{-5} M) for 10 minutes before the tissue was pre-contracted. The tissue was then relaxed with cumulative additions of quinine. (A) Concentration-response curve for quinine (1 x 10^{-7} M to 3 x 10^{-3} M) pre-contracted with phenylephrine (1 x 10^{-6} M) with a magnitude of the initial contraction at 0.30 ± 0.02 g, and 0.20 ± 0.02 g for the studies involving the presence of gallein and absence (Control – Ctrl) respectively (n = 10/9). (B) Concentration-response curve for denatonium (1 x 10^{-7} M to 3 x 10^{-3} M) pre-contracted with phenylephrine, with a magnitude of the initial contraction at 0.28 ± 02 g, and 0.25 ± 0.04 g for the studies involving the presence of gallein and absence (Control – Ctrl) respectively (n = 13/9). The contractile response is expressed as a percentage of the initial control contraction produced by phenylephrine and is shown as mean ± s.e.m (P > 0.05).

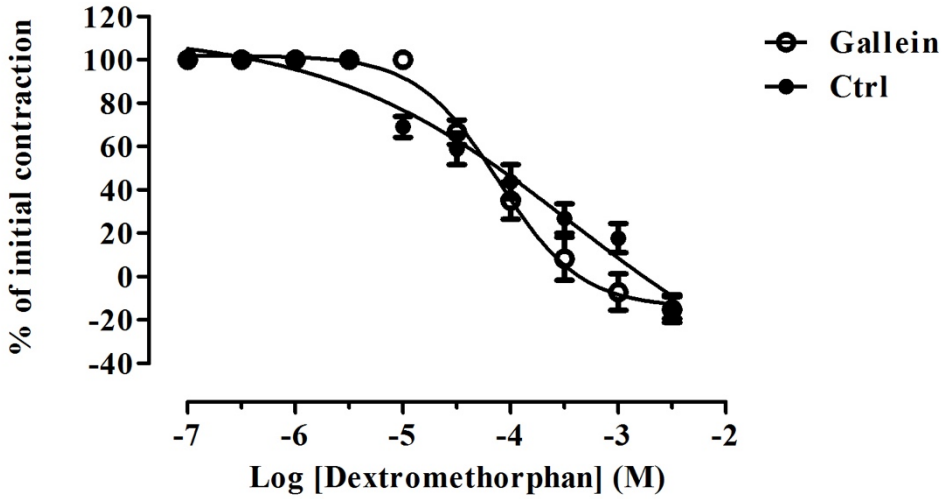

Figure 3.12 The Effect of Gallein on the Dextromethorphan-Induced Relaxation of the Pre-Contracted Rat Pulmonary Artery.

Rat pulmonary arterial tissue was treated with gallein (2 x 10^{-5} M) for 10 minutes before the tissue was pre-contracted. The tissue was then relaxed with cumulative additions of dextromethrphan. Concentration-response curve for dextromethorphan (1 x 10^{-7} M to 3 x 10^{-3} M) pre-contracted with phenylephrine (1 x 10^{-6} M) with a magnitude of the initial contraction at 0.30 ± 0.03 g, and 0.28 ± 0.07 g for the studies involving the presence of gallein and absence (Control – Ctrl) respectively (n = 5/4). The contractile response is expressed as a percentage of the initial control contraction produced by phenylephrine and is shown as mean ± s.e.m (P > 0.05).

3.4 Discussion

This study demonstrates that bitter taste agonists do not induce vasorelaxation via a definite single pathway that only involves BKca channel, Gβγ subunits or L- type VDCCs. Instead, bitter taste agonists may interact individually with different pathways associated with the mobilisation of Ca^{2+} from intracellular and extracellular sources. The pathways underlying denatonium and dextromethorphan, induced responses require further investigations (Figure 3.10).

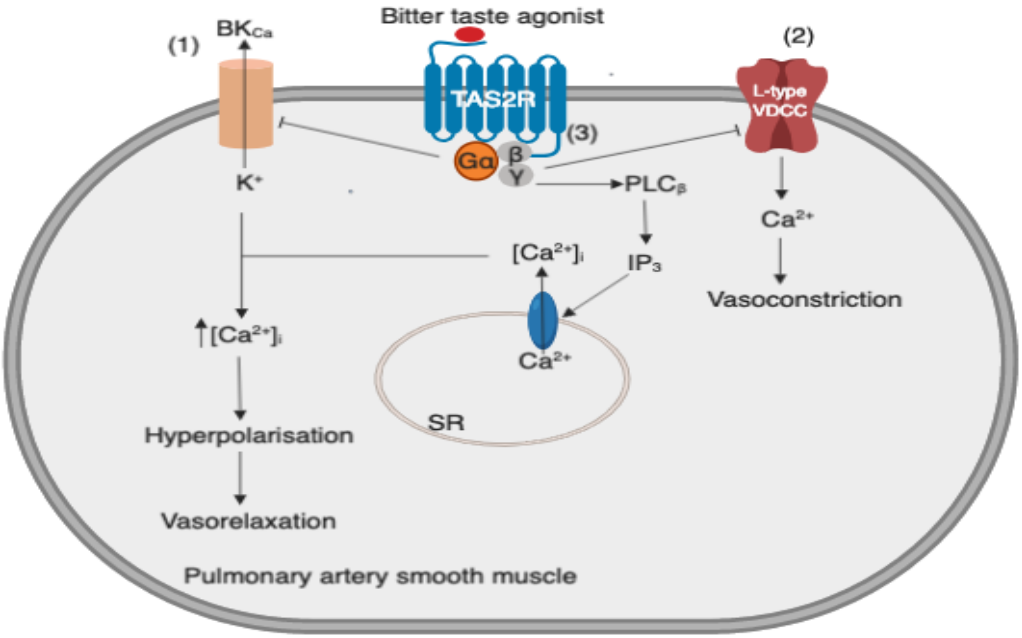

Figure 3.13 Diagrammatic Overview of the Proposed Pathways of Bitter Taste Agonist-Induced Relaxation.

This model proposes a mechanism by which bitter taste agonists elicit pulmonary vasodilation. (1) Hyperpolarization via BKca channel (2) inhibition of L-type voltage dependent Ca^{2+} channel (3) Inhibition of G- protein βγ subunits.

3.4.1 Role of Potassium channels in Bitter Taste Agonists Mediated Relaxation of the Rat Aorta and Pulmonary Artery

This study shows that bitter taste agonists produced a relaxation of the rat aorta and pulmonary artery pre-contracted with phenylephrine, one possible mechanism for their effect is that they are blocking K^+ channels. It was known that the activation of K^+ channels plays a main role in pulmonary artery relaxation (Dong, Bai and Cai, 2016). However, this study did not find that the non-selective K^+ channel blocker TEA, did not prevent the relaxation of pulmonary artery to quinine, denatonium, and dextromethorphan. As such this would argue against them having the main role.

With regard to the rat aorta, there was a slight non-significant rightward shift in the concentration-response curve to denatonium in the presence of TEA. Likewise, in the rat pulmonary artery, the potency and efficacy of quinine, denatonium and dextromethorphan were similar in the presence and absence of TEA. These findings are similar to the observations of Wu *et al.* (2017) on the rat pulmonary artery. They showed that the use of the TEA did not affect the relaxation response induced by chloroquine. When U46619 was responsible for the pre-contraction, there was no noticed changed in the potency and efficacy of the quinine in the presence and absence of TEA.

Hyperpolarization, caused by the opening of large conductance Ca^{2+} activated potassium channels, has been proposed as a mechanism involved in TAS2R agonist-induced relaxation (Deshpande *et al.*, 2010). In this study, both quinine and denatonium were not affected by iberiotoxin in the state tissue/s. Quinine and denatonium still produced a concentration-dependent inhibition of the phenylephrine pre-contraction which were approximately identical to their action in the absence of iberiotoxin. Whereas blockade of BKca channels, using iberiotoxin, decreased the potency to dextromethorphan, these effects are not considered to be actual inhibitions of dextromethorphan-mediated relaxation, but might result from the increased pre-contractions that develop in the presence of iberiotoxin. The decrease in bitter taste agonists potency was also observed in different studies (Manson *et al.*, 2014;

Pulkkinen *et al.*, 2012). Manson *et al.* (2014) found that after using iberiotoxin, the potency of denatonium and chloroquine was decreased in guinea pig aorta without affecting the maximum relaxation. Pulkkinen *et al.* (2012) also reported that in the presence of iberiotoxin, the potency of denatonium was decreased in guinea pig trachea without affecting the maximum relaxation.

Taken together, this study showed that BK_{Ca} and non-selective K^+ channel blockers did not inhibit bitter taste agonist-mediated relaxation of the aorta and rat pulmonary artery. This study, therefore, provides further support to the previous studies conducted on the human and guinea pig aorta demonstrated that the inhibition of K^+ channels are not involved in bitter taste agonist-induced relaxation (Manson *et al.*, 2014; Wu *et al.*, 2017).

3.4.2 Role of L-type Voltage-Dependent Calcium Channel in Bitter Taste Agonists induced Relaxation of the Rat Pulmonary Artery

Intracellular Ca^{2+} is one of the most critical regulators of cell function in pulmonary smooth muscle cells. A rise in the $[Ca^{2+}]_i$ in pulmonary artery smooth muscle is a major stimulant for pulmonary vasoconstriction (Somlyo and Somlyo, 1994). The opening of L-type VDCC is a way for Ca^{2+} influx to increase in the $[Ca^{2+}]_i$ and it cause pulmonary artery contraction.

We hypothesised that quinine might induce pulmonary artery relaxation by inhibiting L-type VDCC. Quinine produces a relaxation of the rat pulmonary artery pre-contracted by phenylephrine. One of the possible explanations for this relaxant effect is that blocking of Ca^{2+} channel. It is known that phenylephrine induces contraction and results in a release of Ca^{2+} from either the intracellular store (SR) or through Ca^{2+} influx from the extracellular store such as L-type VDCC and receptor-operated calcium channel (ROCC) (Lee *et al.*, 2001). L-type VDCC activator FPL 64176 or Bay K8644 have been used to study the mechanism of bitter taste agonist-mediated relaxation in mouse airway smooth muscle (Zhang *et al.*, 2013), human bronchi tissue

(Grassin-Delyle *et al.*, 2013) and in mouse gastrointestinal enteroendocrine cells (Chen *et al.*, 2006). Thus, in this study, FPL 64176 and Bay K8644 were therefore appropriate to use in order to translate the effect of bitter taste agonists on the rat pulmonary artery. The contraction induced by FPL 64176 was completely relaxed by quinine more than what was induced when Bay K8644 was used to pre-contract the pulmonary artery, however, the potency was similar. Likewise, the effect of FPL 64176 and Bay K8644 on the rat pulmonary artery was investigated in the presence of the thromboxane A_2 analogue U46619 which is known to activate contraction via both voltage-independent and voltage-dependent pathways as well as by releasing Ca^{2+} from intracellular Ca^{2+}stores (McKenzie, MacDonald and Shaw, 2009; Wilson *et al.*, 2005). These findings were similar to what has been observed previously with (Zheng, Rampe and Triggle, 1991), when they showed that the efficacy of FPL 64176 in the rat tail artery was higher than that of Bay K8644 (Zheng, Rampe and Triggle, 1991).

3.4.3 Involvement of G-Protein Beta-Gamma ($G_{\beta\gamma}$) Subunits in Bitter Taste Agonists Induced Relaxation of the Rat Pulmonary Artery

As bitter taste receptors belong to a family of GPCRs (Adler *et al.*, 2000; Chandrashekar *et al.*, 2000; Matsunami, Montmayeur and Buck, 2000; Mueller *et al.*, 2005), the Gβγ subunits play an important physiological role in the GPCR signal transduction cascade (Dupré *et al.*, 2009). Three subsequent studies have studied their role in bitter taste agonist- mediated relaxation in the airway tissues (Deshpande *et al.*, 2010; Tan and Sanderson, 2014; Zhang *et al.*, 2013). Deshpande *et al*. (2010) showed that bitter taste agonists increase in $[Ca^{2+}]_i$ response in human cultured airway smooth muscle was inhibited with the treatment to gallein (a $G_{\beta\gamma}$ inhibitor). Moreover, Zhang *et al.* (2013) showed that the βγ subunits are involved in the bronchodilatory effect of bitter taste agonists. They found chloroquine to be able to inhibit the induced Ca^{2+} signals from KCl pre-contracted mouse airway smooth muscle cells, whereas this inhibition was blocked in the presence of gallein. These studies showed that bitter taste agonists induced their relaxation in a Gβγ-dependent manner (Deshpande *et al.*, 2010; Zhang *et al.*, 2013). On the other hand, Tan and Sanderson (2014) studied the

involvement of the βγ-subunits by measuring the changes in Ca^{2+} responses in the presence and absence of gallein. They showed gallein pre-treated mice lung tissues were unable to decrease the effects of chloroquine on the induced Ca^{2+} signals from the methacholine pre-contractions (Tan and Sanderson, 2014).

In this study, the presence of the Gβγ inhibitor gallein, did not affect the relaxant effect produced by quinine, denatonium and dextromethorphan in rat pulmonary artery. These results indicated that the relaxation induced by agonist was not mediated through a Gβγ signalling-dependent pathway. These findings were similar to the findings of Sai *et al.* (2014) who examined the effect of gallein on chloroquine-induced relaxation of K^+ pre-contracted rat aortic rings. They observed that gallein had no effect on the relaxation of K^+ pre-contracted rings induced by chloroquine. Thus, gallein-sensitive G-proteins are not involved in chloroquine-induced relaxation of pre-contracted rat thoracic aortic smooth muscle (Sai *et al.*, 2014). Thus, the effect of quinine, denatonium and dextromethorphan in this study has not been shown to be associated with the Gβγ signalling pathway. The effect of TAS2Rs on taste bud cells is predominantly associated with the Gα subunit (Kinnamon, 2012). Hence, the vasorelaxatory effect of bitter taste agonists could be directly associated with the Gα subunit or other G-proteins linked with TAS2Rs. Future studies would need to further investigate the potential association of other G-proteins with the vasorelaxant effect of TAS2R agonists.

Chapter 4

Influence of Bitter Taste Agonists on Ca^{2+} Signalling on Rat Pulmonary Artery Isolated Smooth Muscle Cells

4.1 Introduction

4.1.1 Vascular Smooth Muscle Cells

Vascular smooth muscle cells (VSMCs) are the main component of blood vessels (Brozovich *et al.*, 2016). These cells are highly specialised cells that are located in the middle layer, tunica media, of the blood vessels. VSMCs play an important role in controlling the physiological functioning and pathological changes in blood vessels (Brozovich *et al.*, 2016). In adult organisms, a healthy VSMCs ensure that the blood vessels contract and relax in appropriate way to make a noticeable contribution to the control of blood circulation (Brozovich *et al.*, 2016; Metz, Patterson and Wilson, 2012; Steucke *et al.*, 2015).

4.1.2 Effect of $[Ca^{2+}]_i$ in the VSMCs

Under physiological conditions, $[Ca^{2+}]_i$ is around 50–150 nM in VSMCs, whereas the extracellular $[Ca^{2+}]_i$ is approximately 2 mM (Remillard and Yuan, 2006). An increase in $[Ca^{2+}]_i$ is essential for VSMC contraction and this can be achieved by either release of Ca^{2+} from intracellular storage sites involving the sarcoplasmic reticulum (SR) and/or Ca^{2+} influx from an extracellular source through L-type voltage-dependent Ca^{2+} channels (VDCC), receptor-operated Ca^{2+} channels (ROCC), and store-operated Ca^{2+} channels (SOCC) (Karaki *et al.*, 1997; Shimoda, Wang and Sylvester, 2006; Wu *et al.*, 2017) (Figure 4.1). VDCCs are the main Ca^{2+} channel in the VSMCs, activated by membrane depolarisation (Karaki *et al.*, 1997). The contraction of VSMCs induced by KCl mainly involves depolarisation of the SMC membrane. This subsequently increases Ca^{2+} influx and raises $[Ca^{2+}]_i$ and leading to pulmonary artery SMCs contraction (Mandegar and Yuan, 2002; Hall *et al.*, 2009). The relaxation of this type of contraction is frequently utilised when studying the effect of VDCC blockers (Godfraind, 1983; Karaki and Weiss, 1984; Morel and Godfraind, 1991; Okumura, Ichihara and Nagasaka, 1997; Roy *et al.*, 1995; van Breemen, Hwang and Meisheri, 1981). Using KCl to investigate the role of VDCC in different tissue types has been commonly used in bitter taste agonists-mediated their effects.

ROCC are exist in many types of SMCs, activated by inositol lipid signaling, one of the most well-known signal transduction cascades, which involves G protein-activated phospholipase C and two second messengers, diacylglycerol (DAG) and inositol 1,4,5-trisphosphate (IP_3) (Hallam and Rink, 1989; McFadzean and Gibson, 2002).

SOCC entry plays a very important role in refilling Ca^{2+} in SR and maintaining Ca^{2+} homeostasis in pulmonary artery SMCs. Thapsigargin, an extract from the plant *Thapsia garganica,* is a sarcoplasmic/endoplasmic reticulum Ca^{2+}- ATPase (SERCA) inhibitor, which interferes with the reloading of Ca^{2+}, resulting in a gradual depletion of Ca^{2+} internal stores (Thastrup *et al.*, 1990). As such, thapsigargin has been used extensively in many studies to investigate various Ca^{2+}-signalling mechanisms in cells and tissues (Michelangeli and East, 2011). In the study of bitter taste agonists, Deshpande *et al.* (2010) showed that pre-incubation of human airway SMCs with thapsigargin blocked chloroquine and other bitter tastant-mediated increase in $[Ca^{2+}]_i$, indicating that chloroquine induced their relaxatory effect via intracellular stores (Deshpande *et al.*, 2010). However, another study found that thapsigargin did not affect phenanthroline or chloroquine-induced relaxation of human bronchi isolated SMCs, suggesting that phenanthroline and chloroquine-induced their relaxation through extracellular Ca^{2+} sources (Grassin-Delyle *et al.*, 2013).

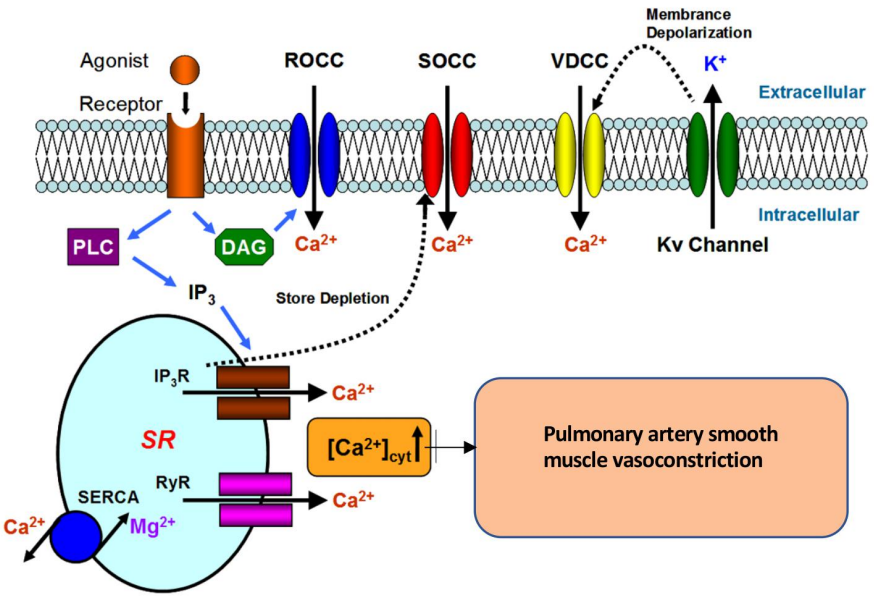

Figure 4.1 Schematic Showing Increased levels of $[Ca^{2+}]_i$ in Pulmonary Artery SMCs Are Required for Pulmonary Vasoconstriction.

L-type voltage-dependent Ca^{2+} channels (VDCC), receptor-operated Ca^{2+} channels (ROCC), and store-operated Ca^{2+} channels (SOCC), diacylglycerol (DAG) and inositol 1,4,5-trisphosphate (IP_3), Ryanodine receptor (RyR), sarcoplasmic reticulium (SR), activated phospholipase C (PLC), sarcoplasmic/endoplasmic reticulum Ca^{2+}-ATPase (SERCA), voltage gated potassium channel (Kv). This figure was partially adapted from (Lai, Lu and Wang, 2015).

Two types of intracellular Ca^{2+} stores have been recognised in many types of cells: one coupled to IP_3 receptors and other coupled to ryanodine receptors (Sharp *et al.*, 1993; Simpson, Challiss and Nahorski, 1995). Studies bitter taste agonists can activate GPCRs. This leads to activation of PLC, which results in an increase in IP_3 that causes the release of Ca^{2+} from the intracellular stores (Akabas, Dodd and Al-Awqati, 1988; Hwang *et al.*, 1990; Ogura, Mackay-Sim and Kinnamon, 1997; Spielman *et al.*, 1994). In recognition of the role this pathway plays in the regulation of $[Ca^{2+}]_i$, the PLC inhibitor, U73122, has been widely used to investigate the signalling mechanism of bitter taste agonists in a number of studies: in human airway SMCs (Deshpande *et al.*, 2010), human bronchi isolated SMCs (Grassin-Delyle *et al.*, 2013), primary cultured human sinonasal epithelial cells (Lee *et al.*, 2014) and in freshly isolated myometrial cells from pregnant mice (Zheng *et al.*, 2017).

ATP is bound to purinergic receptors (P2Y) at the plasma membrane, a family of GPCRs, increasing $[Ca^{2+}]_i$ by causing SOCE (due to IP3-mediated active store depletion and the opening of SOCC) and ROCE (due to the DAG-mediated opening of ROCC) (Chin and Chueh, 2000). ATP also mediates activation of P2X receptors, a family of cation permeable ligand-gated ion channels, increasing $[Ca^{2+}]_i$ by directly inducing Ca^{2+} influx through the channels and/or indirectly inducing Ca^{2+} influx through VDCC via membrane depolarisation (Chin and Chueh, 2000; Gilbert *et al.*, 2016; Wu *et al.*, 2017).

4.1.3 $[Ca^{2+}]_i$ Indicators and Measurements

Intracellular Ca^{2+} is essential in regulating the physiological process in VSMCs such as proper vascular function and regulation of blood flow. Abnormalities in Ca^{2+} signaling have severe pathological consequences. Pulmonary hypertension occurs where changes in $[Ca^{2+}]_i$ have a significant effect in defining the pathogenic mechanisms leading to its development and persistence (Firth, Won and Park, 2013). Fluorescent Ca^{2+} indicators have been frequently used to study the role of $[Ca^{2+}]_i$ in cellular processed and signalling pathways (Paredes *et al.*, 2008). These indicators change their fluorescent properties when bound with Ca^{2+}. There are two main classes of Ca^{2+} indicators, chemical indicators and genetically encoded calcium indicators.

The chemical indicators are the most commonly used as Ca^{2+} indicators (Takahashi *et al.*, 1999). They have advantages over genetically encoded calcium indicators, including a wide range of Ca^{2+} affinities; they are easily available; easy to use and they have well-established cell loading protocols (Takahashi *et al.*, 1999). The main drawback of chemical indicators is during long recording experiments, they are likely to be compartmentalised and ultimately extruded from the cell (Palmer and Tsien, 2006; Rehberg *et al.*, 2008).

4.1.3.1 $[Ca^{2+}]_i$ Indicators Used in Bitter Taste Agonist Research

Detection of $[Ca^{2+}]_i$ is widely used to help characterize GPCRs signalling pathways. As TAS2Rs belong to the GPCRs, the chemical indicators are frequently used to investigate whether the bitter taste agonists induce their effect via an increase $[Ca^{2+}]_i$. The Fura family of acetoxymethyl esters, in particular, Fura-2-acetoxymethyl ester (Fura-2 AM) are amongst the most common Ca^{2+} indicators used in bitter taste agonist studies (Chandrashekar *et al.*, 2000; Chen *et al.*, 2006; Sai *et al.*, 2014; Shah *et al.*, 2009; Tomás *et al.*, 2016; Wu, Chen and Rozengurt, 2005; Wu *et al.*, 2002; Xu *et al.*, 2012).

Although the standard for quantitative $[Ca^{2+}]_i$ measurement Fura-2 AM has several disadvantages such as: it has a low affinity; it tends to be compartmentalised; and it has a wide sensitivity range (Paredes *et al.*, 2008). Fluo-4-acetoxymethyl ester (Fluo-4 AM) has also been used as a Ca^{2+}-sensitive fluorescence dye in bitter taste agonist research (Avau *et al.*, 2015; Deshpande *et al.*, 2010; Lee *et al.*, 2014). The main drawback is that it requires the use of probenecid to improve dye retention, which is known to be toxic to the cells (Li, Llorente and Brasch, 2008). Fluo-4 NW has been used as a Ca^{2+} indicator in bitter taste agonists studies (Clark *et al.*, 2014; Singh *et al.*, 2014; Singh *et al.*, 2011; Upadhyaya *et al.*, 2014). Fluo-4 NW (no wash) is similar to Fluo-4 AM but with the advantage that it provides a simplified method for detecting intracellular Ca^{2+}, without a quencher dye or a wash step.

Oregon green 488 BAPTA-1 indicator has a distinct advantage that it can detect small changes in Ca^{2+} near resting levels. Oregon green 488 BAPTA-1 was used in one study of bitter taste agonists to examine whether quinine-induced increase in $[Ca^{2+}]_i$ on mouse airway SMCs (Tan and Sanderson, 2014). Ca^{2+}orange-acetoxymethyl ester (Ca^{2+} orange-AM) has the main disadvantage that it tends to be compartmentalised rapidly. Ca^{2+}orange-AM has been used with to investigate the effect of denatonium on $[Ca^{2+}]_i$ in mouse urethral brush cells (Deckmann *et al.*, 2014).

Cal-520 AM is a novel next-generation fluorescent Ca^{2+} indicator that has significant advantages over the traditional Ca^{2+} indicators such as Fluo-4 AM. It has distinct chemical properties: it has high Ca^{2+} binding specificity, the fluorescence intensity increases more than 100-fold after binding to Ca^{2+}, it is localised in the cytosol, it has high excitation efficiency which makes it usable at lower concentrations and therefore less toxic to cells, and it has lower background fluorescence which helps raise the signal to noise ratio. The above properties make Cal-520 AM an ideal indicator for measurement of cellular Ca^{2+}, Moreover it is highly sensitive for evaluating GPCR and Ca^{2+} channel targets as well as for screening their agonists and antagonists (Bioquest, 2017; Lock, Parker and Smith, 2015; Tada *et al.*, 2014).

4.1.3.2 Effect of Bitter Taste Agonists on $[Ca^{2+}]_i$

It is known that TAS2Rs belong to a heterotrimeric GPCRs, which mediated their effect through canonical TAS2R signalling that initially results in a transient increase in $[Ca^{2+}]_i$ (Meyerhof *et al.*, 2010). *In vitro* studies have demonstrated the effect of bitter taste agonists on $[Ca^{2+}]_i$,which may provide some insights on their actions in a number of organs and tissues in the body. For the respiratory tract, Shah *et al.* (2009) showed that adding 0.1 mM quinine and denatonium to the human airway epithelial cells caused an increase in $[Ca^{2+}]_i$ and lead to an increased cilia beat frequency. Moreover, the application of 1 mM quinine and denatonium on the cultured human airway SMCs elevated $[Ca^{2+}]_i$, but paradoxically produced airway smooth muscle bronchodilation (Deshpande *et al.*, 2010). Furthermore, denatonium application (0.1-10 mM) to the apical/mucosal surface of primary cultured human sinonasal epithelial cells resulted in a concentration-dependent elevation of $[Ca^{2+}]_i$ (Lee *et al.*, 2014).

Quinine (2.3 - 3.5 μM) and denatonium (0.7- 1.6 mM) induced a concentration-dependent increase in $[Ca^{2+}]_i$ in both rats cultured primary neuronal cells and C6 glial cells which could reveal an impact of bitter taste agonists on the CNS (Singh *et al.*, 2011). In cancer, quinine (2.5 – 3.5 μM) and dextromethorphan (2 - 4.5 μM) induced a concentration–dependent increase in $[Ca^{2+}]_i$ in the human highly metastatic breast cancer cell line MDA-MB-231, poorly metastatic cell line MCF-7, and non-cancerous mammary epithelial cell line MCF-10A (Singh *et al.*, 2014). Denatonium rapidly increases $[Ca^{2+}]_i$ in a concentration-dependent manner in cultured mouse enteroendocrine STC-1 cells (Chen *et al.*, 2006; Wu, Chen and Rozengurt, 2005; Wu *et al.*, 2002). Moreover, denatonium (2.5 -7.5 mM) produced a small contraction mediated via $[Ca^{2+}]_i$ -rises in a concentration-dependent manner in cultured human gastric mouse gut SMCs (Avau *et al.*, 2015). Denatonium-induced increase $[Ca^{2+}]_i$ has been reported in other systems such as in bladder, denatonium caused a dose-dependent (2.5–25 mM) increase in $[Ca^{2+}]_i$ in the mice urethral brush cells (Deckmann *et al.*, 2014). In the male reproductive system, 2 mM denatonium induced an elevation of $[Ca^{2+}]_i$ in mouse male germ cells (Xu *et al.*, 2012). 2 mM quinine, 10 mM denatonium and 2 mM dextromethorphan induced an increase in $[Ca^{2+}]_i$ in the primary cultures of human pulmonary artery SMCs (Upadhyaya *et al.*, 2014).

On the other hand, different studies indicating that bitter taste agonists did not alter the $[Ca^{2+}]_i$; Adding 0.5 mM quinine and on mouse airway SMCs the failed to induced any change in the $[Ca^{2+}]_i$ (Tan and Sanderson, 2014). Moreover, denatonium did not elicit a changed in $[Ca^{2+}]_i$ in the cultured rat choroid plexus epithelial cells (Tomás *et al.*, 2016). Denatonium did not alter the $[Ca^{2+}]_i$ in the human thyrocyte line Nthy Ori 3-1 cells (Clark *et al.*, 2014).

The intracellular signal transduction cascades initiated by bitter taste agonists in pulmonary artery SMCs have not been investigated. The aim of this Chapter was to use pulmonary artery SMCs as a first step to examine the effects of these bitter agonists on calcium signalling. Freshly isolated pulmonary artery SMCs are commonly used to investigate agonist-induced changes in $[Ca^{2+}]_i$ (Hyvelin *et al.*, 1998; Wang *et al.*, 1997; Weir *et al.*, 1994). Moreover, the next aim is to investigate the effect of bitter taste agonists (quinine, denatonium and dextromethorphan) on the

$[Ca^{2+}]_i$ of the isolated pulmonary artery SMCs using the next-generation fluorescent Ca^{2+} indicator, Cal-520 AM. Furthermore, ATP was used to investigate the potential effect of bitter taste agonists (quinine, denatonium and dextromethorphan) on ATP-induce increase in $[Ca^{2+}]_i$. A further aim of this chapter is to elucidate if the increase in $[Ca^{2+}]_i$ is due to extracellular Ca^{2+} influx and/or Ca^{2+} release from intracellular stores using a Ca^{2+}-free solution, Moreover, the involvement of VDCCs in bitter taste agonist-induced increase in $[Ca^{2+}]_i$ of the rat pulmonary artery SMCs will be investigated, as will the intracellular mechanism involved in the bitter taste agonist-induced increase in $[Ca^{2+}]_i$ of the rat pulmonary artery SMCs, such as the activation of phospholipase C.

4.2 Methods

4.2.1 Rat Pulmonary Artery SMC Isolation

Experiments were carried out on SMCs freshly isolated from rat pulmonary arteries. Male Sprague Dawley rats (250–350 g) were killed by cervical dislocation in accordance with UK legislation. The hearts and lungs were removed *en bloc* and placed in a dissecting solution of the following composition (in mM); NaCl 119, KCl 4.7, KH_2PO_4 1.18, $MgSO_4$ 1.17, glucose 5.5, $NaHC0_3$ 25, HEPES 10, pH adjusted to 7.4 with NaOH. Afterwards, the right and left extra-pulmonary arteries were dissected first, followed by the intrapulmonary arteries as described in Chapter 2. The rat pulmonary arteries were then dissected into ~2 mm long ring segments and then were placed in a dissociation solution of the following composition (in mM): NaCl 128, KCl 5.4, KH_2PO_4 0.95, Na_2HPO_4 0.35, $MgSO_4$ 1.17, glucose 10, sucrose 2.9, $NaHCO_3$ 4.16, HEPES 10, pH adjusted to 7.0 with NaOH. Papain (1.5 mg/mL) and DL-dithiothreitol (1.5 mg/mL) both from (Sigma-Aldrich, Poole, UK) were added to the solution and the tissue was maintained at 4˚C for 60 minutes in a refrigerator. The solution containing the tissue was then transferred to a water bath at 37˚C for 6 minutes (Figure 4.2). The arterial rings were then transferred to fresh dissociation solution containing collagenase (Sigma type VIII, 1.5 mg/mL) and incubated in the water bath for a further 5 minutes at 37˚C. Gentle trituration of the tissue (2–3 times) with a fire-polished Pasteur pipette yielded single SMCs, which were observed under microscope. If the rat pulmonary artery cells were not fully dissociated, then this trituration was repeated until they were. These cells remained viable for up to 6 hours and were used on the same day they were isolated.

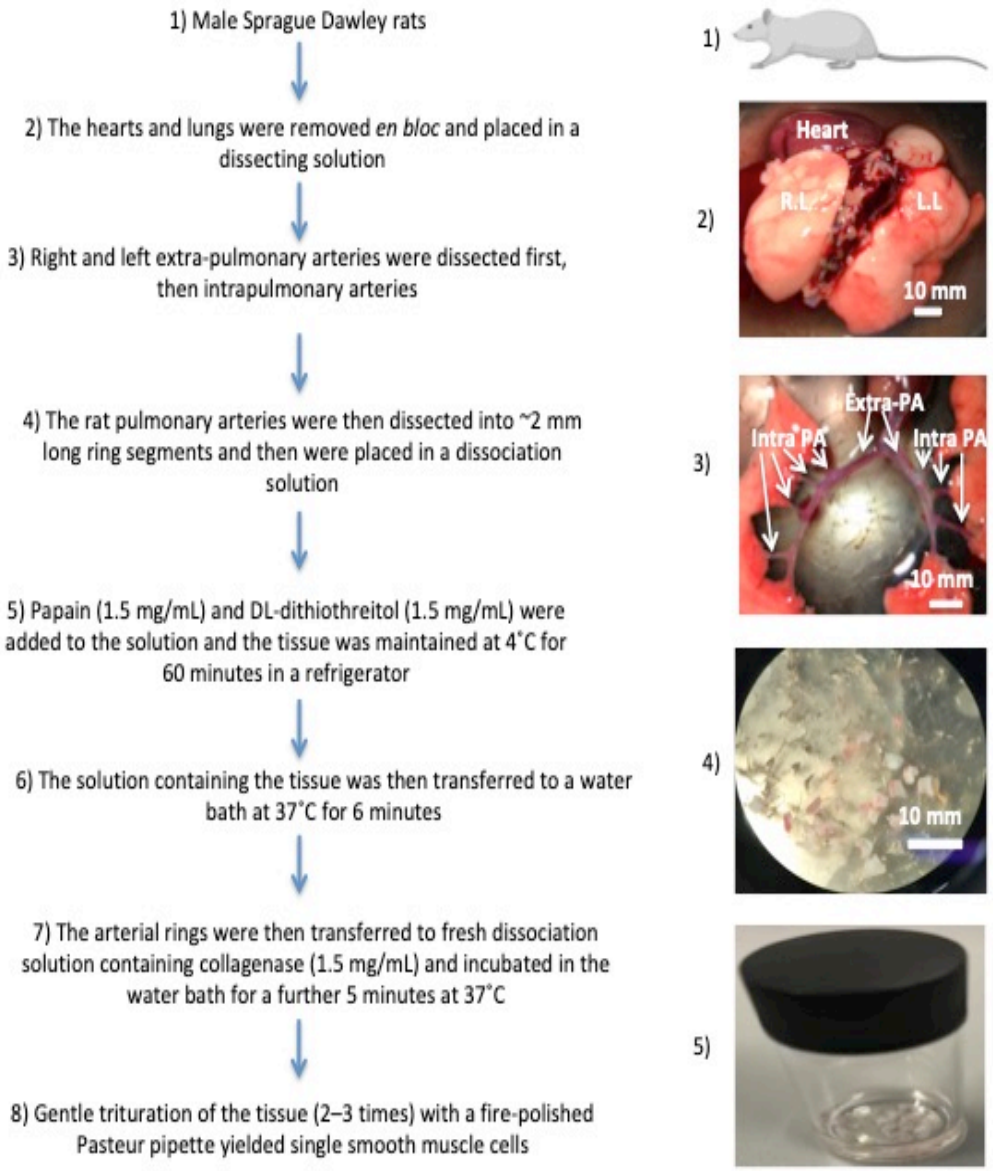

Figure 4.2 Rat Pulmonary Artery SMCs Isolation.

R.L: right lung, L.L: left lung, Extra-PA: extra-pulmonary artery, Intra PA: intrapulmonary artery. Scale bar provides an approximation of the actual size.

4.2.2 Measurement of $[Ca^{2+}]_i$

To measure $[Ca^{2+}]_i$, single rat pulmonary artery SMCs were loaded with 1 mM (10 µl/ml) of the calcium sensitive dye, Cal-520 AM (Abcam, Cambridge, UK) for 60 minutes in a dark place at room temperature. Cal-520 fluorescence was monitored using a PTI DeltaRam microflurimeter (PTI, Lawrenceville, NJ, USA). This PTI DeltaRam microflurimeter have several advantages make it an ideal as fluorescence microscope illuminator including; it is an excellent for quantitative intracellular ion research such as intracellular Ca^{2+} ion (Csordás, Thomas and Hajnóczky, 2001; Szalai *et al.*, 2000). It has been used in the $[Ca^{2+}]_i$ responses to the ATP (Guns *et al.*, 2006). This PTI DeltaRam microflurimeter connected to a Zeiss Axioskop 50 fluorescence microscope (Carl Zeiss, Germany) with an 40x/0.75w objective lens (Achroplan, Carl Zeiss, Germany). Excitation light was provided by a 50 W mercury short arc lamp (Osram, Germany) and filter set 9 (Carl Zeiss, Germany), which consisted of an excitation filter (BP 450–490 nm), beam splitter (FT 510 nm) and emission filter (LP 520 nm).

Fluorescent images were acquired and analysed using fluorescence imaging software, WinFluor v.3.4.9 (University of Strathclyde, Glasgow, UK) running on an IBM-PC, with images obtained at rates of 1-10 frames per second (fps) and exposure times of 400 s (Figure 4.3). 75 µl of the pulmonary artery cell suspension was added to 25 mm glass coverslips housed within custom-built cell observation chamber for 10 minutes until the cells settled and attached, then 2 mL PSS was added to the cells. All experiments were carried out at room temperature (20–25˚C).

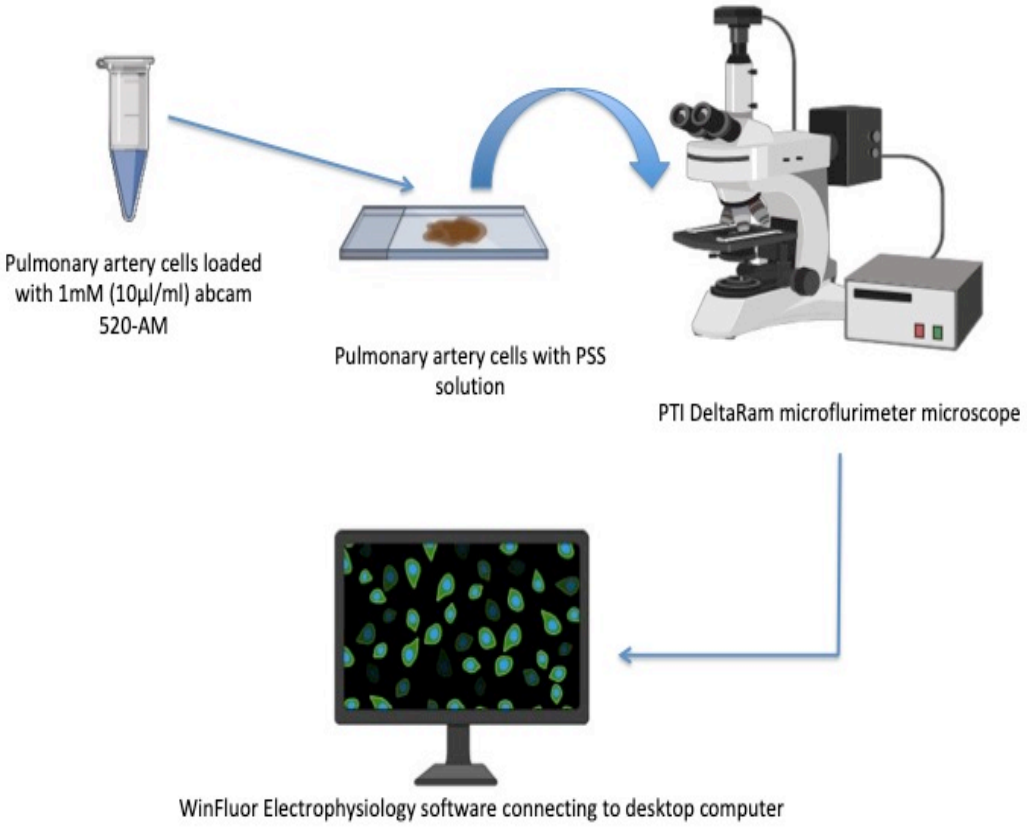

Figure 4.3 Schematic Diagram Representing the Intracellular Calcium Measurement in the Isolated Rat Pulmonary Artery Smooth Muscle Cells.

The pulmonary artery cells were loaded with 1mM (10µl/mL) Cal-520 AM, and then 75 µl of the solution containing isolated pulmonary artery SMCs was placed on the 25 mm glass coverslips in the cell observation chamber under the PTI DeltaRam microflurimeter microscope. The WinFluor Electrophysiology software was used to record the fluorescence image.

4.2.3 Drugs and Inhibitors

The bitter taste agonists used included quinine hydrochloride dihydrate, denatonium benzoate and dextromethorphan hydrobromide (all from Sigma-Aldrich, Poole, UK). Quinine (quinine hydrochloride dihydrate) and denatonium (denatonium benzoate) were prepared as 100 mM stock solutions. Dextromethorphan (dextromethorphan hydrobromide) was prepared as a 50 mM stock solution. All drugs were dissolved in Milli-Q water. Thapsigargin (Tocris Bioscience, Bristol, UK) was prepared as a 0.5 mM stock in DMSO. The phospholipase C inhibitor (U73122) 1-[6-[[17 beta-3-methoxyestra-1, 3, 5(10)-trien-17-yl] amino] hexyl]-1H-pyrrole-2, 5-dione (Tocris Bioscience, Bristol, UK) was prepared as a 2 mM stock and dissolved in DMSO. ATP (Sigma-Aldrich, Poole, UK) was prepared as a 100 mM stock and dissolved in water.

4.2.4 The Effect of Bitter Taste Agonists on the $[Ca^{2+}]_i$ on Isolated Rat Pulmonary Artery SMCs

Cal-520 AM fluorescence imaging was used to examine the effect of bitter taste agonists (quinine, denatonium, and dextromethorphan) on the $[Ca^{2+}]_i$ of rat pulmonary artery SMCs. As described in Section 4.2.2, 75 µl of a solution containing isolated pulmonary artery SMCs was placed within the cell observation chamber under the PTI DeltaRam microflurimeter microscope for 10 minutes until the cells settled and attached, after which 2 ml of PSS was added. After that, 40 µl of 50 mM quinine was added onto the rat pulmonary artery SMCs to give a final concentration 1mM quinine then the reaction was recorded for 400 s (n = 16/3). Treatments of 2 mM and 3 mM quinine were also given to the rat pulmonary artery SMCs and each response was recorded for 400 s (n = 10/3) and (n = 15/3). The same protocol was applied to treatments of the pulmonary SMCs with 1 mM, 2 mM, and 3 mM denatonium (n = 18/3, n = 10/3 and n = 11/3, respectively), and 30 µM, 270 µM, 300 µM and 1 mM dextromethorphan (n = 10/3, n = 11/3, n = 10/3 and n = 15/4, respectively). For each experiment, a time control was obtained which is defined as the Ca^{2+} fluorescence recording of the initial cells suspension.

4.2.5 The Effect of ATP-Induced Changes in $[Ca^{2+}]_i$ of the Rat Pulmonary Artery SMCs.

Cal-520 AM fluorescence imaging was used to investigate the potential effect of ATP, as the extracellular agonist, on the $[Ca^{2+}]_i$ of rat pulmonary artery SMCs. As described in Section 4.2.2, 75 µl of the solution containing isolated pulmonary artery SMCs was placed in the cell observation chamber under the PTI DeltaRam microflurimeter microscope for 10 minutes until the cells settled and attached, after which 2 ml of PSS was addeds. Then, 100 µM ATP was applied onto the rat pulmonary artery SMCs and the reaction recorded for 400 s (*n* = 32/9).

Initial work found that when ATP was applied on to rat pulmonary artery SMCs, some cells responded until the oscillations stopped by themselves, whilst some cells in the recording period finished before the oscillations completed. In order to keep the frequency of oscillations standard for all cells under observation, the frequency was calculated for the first 60 seconds after the ATP was applied.

4.2.6 Effects of Bitter Taste Agonists on ATP-Induced $[Ca^{2+}]_i$ Transients in Rat Pulmonary Artery SMCs

To investigate the potential effect of bitter taste agonists (quinine, denatonium and dextromethorphan) on ROCC, ATP was used as the extracellular agonist to induce ROCE. For control experiments, isolated rat pulmonary artery SMCs were set up for calcium imaging as in Section 4.2.5 with 100 µM ATP as agonist (*n* = 32/9).

To test the effect of quinine on the ATP-induced increase in $[Ca^{2+}]_i$, isolated rat pulmonary artery SMCs were set up for calcium imaging as in Section 4.2.5 but this time 1 mM quinine was added, and after 2 minutes of waiting, 100 µM (final concentration) ATP was applied to these pulmonary artery SMCs (*n* = 17/4) (Figure 4.6 A and B). A similar protocol was applied to experiments with 1 mM denatonium (*n* = 37/5) (Figure 4.7 A and B) and 1 mM dextromethorphan (*n* = 22/4).

4.2.7 Effect of Dextromethorphan on KCl-Induced Increase in $[Ca^{2+}]_i$

Calcium imaging of intracellular stores using Cal-520 AM was conducted as detailed in Section 4.2.2 to examine the involvement of VDCCs in the dextromethorphan-induced increase in $[Ca^{2+}]_i$ of the rat pulmonary artery SMCs. In these experiments, 50 mM KCl was added to freshly isolated rat pulmonary artery SMCs for 120 seconds to induce depolarisation of their membrane, then 1mM dextromethorphan was added (n = 16/4). The time control was applied by adding 1 mM dextromethorphan only (n = 16/5).

4.2.8 Effect of Dextromethorphan on Intracellular Ca^{2+} Stores

To establish whether the increase in $[Ca^{2+}]_i$ was dependent upon Ca^{2+} from the extracellular media, calcium imaging (as detailed in Section 4.2.2) was conducted to observe the effects of 1 mM dextromethorphan applied to rat pulmonary artery SMCs bathed in Ca^{2+}-free extracellular solution. The Ca^{2+}-free extracellular solution had the following composition: 150 mM NaCl, 10 mM HEPES, 5.4 mM KCl, 10 mM glucose, 1.8 mM $CaCl_2$, 3.0 mM $MgCl_2$, 1 mM EGTA. This solution was prepared using Milli-Q water, and NaOH was used to adjust the pH to 7.4. The time control was applied to cells by adding 1 mM dextromethorphan bathed in the PSS containing extracellular Ca^{2+} (n = 11/4).

4.2.9 Role of Ca^{2+} Stores in the Dextromethorphan-Induced increase in $[Ca^{2+}]_i$

Thapsigargin, a sarcoplasmic/endoplasmic reticulum Ca^{2+}-ATPase (SERCA) inhibitors, interferes with the reloading of Ca^{2+} into sarcoplasmic and endoplasmic reticula and has been used extensively in many studies to investigate various Ca^{2+}-signalling mechanisms in cells and tissues (Michelangeli and East, 2011). To further examine the role of Ca^{2+} stores in the dextromethorphan-mediated increase in $[Ca^{2+}]_i$, , 5 μL (1 μM final concentration) thapsigargin was incubated with cells for an hour, which should be sufficient for store depletion, then 1 mM dextromethorphan was added (n = 36/4). Calcium imaging, as detailed in Section 4.2.2, was conducted to

examine the effects of thapsigargin and dextromethorphan on the $[Ca^{2+}]_i$ of the pulmonary artery SMCs Time control was applied to cells by adding 1 mM dextromethorphan (n = 27/4).

4.2.10 Intracellular Signalling Pathway for Dextromethorphan Responses

To determine whether the activation of PLC is involved in the dextromethorphan response, U73122, an inhibitor of PLC was used (Salari *et al.*, 1993). These experiments, as with the others conducted for this Chapter, used Cal-520 AM fluorescence imaging to examine the effects of dextromethorphan and U73122 on the $[Ca^{2+}]_{i.}$ of pulmonary artery SMCs. The procedure followed that covered in Section 4.2.2. Here SMCs were incubated with 10 μM U73122 for 10 minutes, then 1 mM (final concentration) dextromethorphan was added (n = 46 / 5). Time control was applied to cells by adding 1 mM dextromethorphan (n = 17/5).

4.2.11 Data Analysis

Individual rat pulmonary artery SMCs were selected according to their classic spindle shape. Only the relaxed cells at the beginning of each experiment were subsequently analysed. The experiments were repeated several times and the number of observations were expressed in the format of n = number of cells used/number of animals used. $[Ca^{2+}]_i$ was measured as the ratio of fluorescence intensity within an area of a region of interest (ROI) (50 X 50 pixel) in cell recorded every 10 s. The average increase in $[Ca^{2+}]_i$ was measured by $(F_1\text{-}F_0/F_0)$ or $(\Delta F/F_0)$, where F_0 is the fluorescence intensity at the start of the experiment, and F_1 is the fluorescence intensity emission recorded as the experiment runs.

Frequency measures how often the events of a wave occur within a defined time period. The average Ca^{2+} oscillation percentage calculated by the number of cells induced Ca^{2+} oscillations divided by the total number of all cells x100. The average duration displays the average time during Ca^{2+} fluorescence occurs. The number of event means number of Ca^{2+} fluorescence peak. Data were expressed as the mean ±

standard error of the mean (s.e.m). Statistical comparisons between means were made using unpaired Student's *t*-test. Differences between means were considered significant when $P < 0.05$.

4.3 Results

4.3.1 The Effect of Quinine, Denatonium, and Dextromethorphan on Intracellular Ca^{2+} Stores in Rat Pulmonary Artery SMCs.

In the rat pulmonary artery SMCs, imaging of the calcium fluorescent indicator, Cal-520 AM was unchanged following the application of 1 mM quinine (n = 16/3), as shown in Figure 4.4 A. When 2 mM and 3 mM quinine were added to the pulmonary artery SMCs, there were no changes in Ca^{2+} fluorescence observed (n = 10/3, n = 15/3, respectively). Similarly, application of 1 mM, 2 mM, and 3 mM denatonium to the pulmonary artery SMCs had no effect on Ca^{2+} fluorescence, (n = 18/3, n = 10/3 and n = 11/3, respectively) Figure 4.4 B. The lack of change of Cal-520 AM fluorescence with quinine and denatonium under these conditions suggest there were no changes to the $[Ca^{2+}]_i$ of the SMCs by these bitter taste agonists.

However, applying 1 mM dextromethorphan to the rat pulmonary artery SMCs produced a transient increase in $[Ca^{2+}]_i$ as indicated by the increase in Cal-520 AM fluorescence (Figure 4.4 C). The average duration of this elevated fluorescence was 45 ± 9 s (n = 15/4). In order to examine the minimum concentration of dextromethorphan required to induce changes in $[Ca^{2+}]_i$, the fluorescence was examined over 30 μM, 270 μM, and 300 μM concentrations of dextromethorphan (n = 10/3, n = 11/3 and n = 10/3, respectively). None of these concentrations had any effect on the $[Ca^{2+}]_i$ as indicated by the calcium imaging conducted on the SMCs (data not shown).

These Cal-520 AM fluorescence findings indicate that quinine and denatonium did not produce any change in the $[Ca^{2+}]_i$ of pulmonary artery SMCs. However, dextromethorphan showed an increase in $[Ca^{2+}]_i$, suggesting that dextromethorphan could have a distinct mechanism of action in inducing a change in $[Ca^{2+}]_i$ that is different from quinine and denatonium.

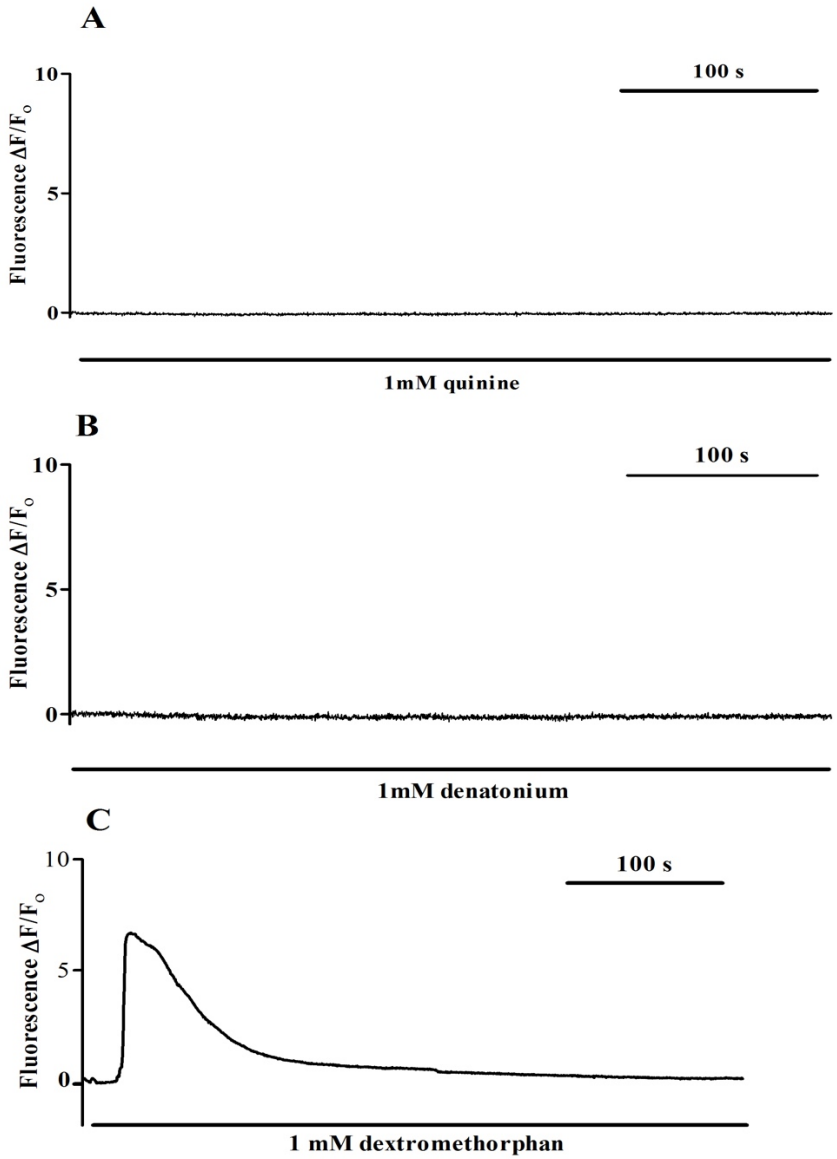

Figure 4.4 Representative Traces of the Effect of Bitter Taste Agonists on Cal-520 AM Fluorescence in the Rat Isolated Pulmonary Artery SMCs.

Microflurimeter microscopy recordings of pulmonary artery SMCs loaded with the calcium-sensitive dye Cal-520 AM which were then subjected to: **A)** addition of 1mM quinine and the reaction recorded for 400 s (n = 16/3). **B)** addition of 1 mM denatonium (n = 18/3) and **C)** addition of 1 mM dextromethorphan (n = 15/4). Data were collected from at least 3 independent experiments for each bitter taste agonist. The average increase in Cal-520 AM fluorescence was measured by ($\Delta F/F_0$).

4.3.2 ATP-Induced Changes in $[Ca^{2+}]_i$ of the Rat Pulmonary Artery Cells

Single rat pulmonary artery cells responded to the application of 100 μM ATP. The ATP-induced Ca^{2+} oscillation percentage was 94% (Figure 4.5A). The magnitude of the ATP-induced increases in $[Ca^{2+}]_i$ in rat pulmonary artery SMCs was ($\Delta F/F_0$ 4.81 ± 0.4). The average duration time was 187 ± 15 s. The average frequency was 0.09 ± 0.01 (Hz).

In the first 60 seconds after the ATP was applied, the magnitude of the ATP-induced increases in Ca^{2+} fluorescence in rat pulmonary artery SMCs was ($\Delta F/F_0$ 4.89 ± 0.3). The average frequency was 0.09 ± 0.008 (Hz) which showed no significant change from the frequency throughout the entire period ($P > 0.05$) ($n = 32/9$) (Figure 4.5 B).

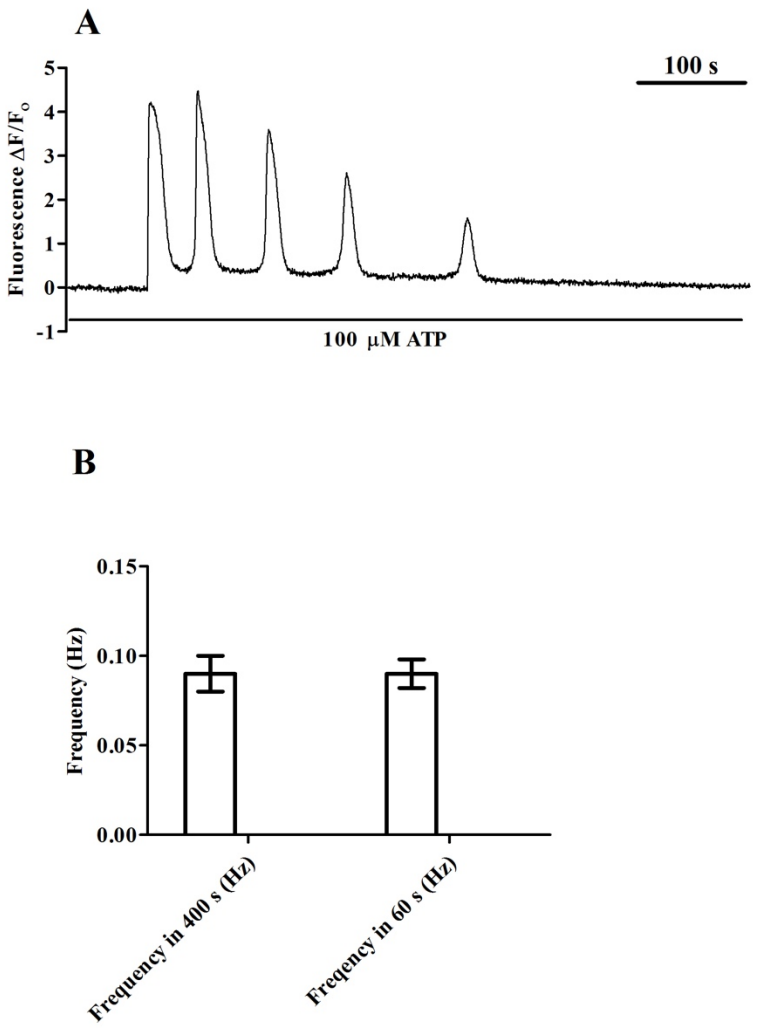

Figure 4.5 A Representative Trace Shows the Effects of ATP on $[Ca^{2+}]_i$ of the Rat Isolated Pulmonary Artery SMCs.

Microflurimeter microscopy recordings of pulmonary artery SMCs loaded with the calcium-sensitive dye Cal-520 AM, which were then given 100 μM ATP (n = 32/9) **A)** $[Ca^{2+}]_i$ oscillation, **B)** The frequency of the isolated rat pulmonary artery cells throughout the entire period (400 s) and in the 60 seconds. The average increase in $[Ca^{2+}]_i$ was measured by ($\Delta F/F_0$). Data are shown as mean ± s.e.m.

4.3.3 Effects of Bitter Taste Agonists on ATP-Induced $[Ca^{2+}]_i$ Transient in Rat Pulmonary Artery SMCs

To examine the potential effect of bitter taste agonists (quinine, denatonium and dextromethorphan) on ROCC, an ATP agonist (100 μM) was used (Chin and Chueh, 2000; Gilbert *et al*., 2016; Wu *et al*., 2017) in SMCs imaged with Cal-520 AM to observe the impact on $[Ca^{2+}]_i$.

In control rat pulmonary artery SMCs, application of ATP caused an increase in $[Ca^{2+}]_i$ mainly due to ROCC (Chin and Chueh, 2000). Treatment with 1 mM quinine inhibited the magnitude of the ATP-induced increases in Cal-520 AM fluorescence in rat pulmonary artery SMCs ($\Delta F/F_0$ 2.59 ± 0.6) compared to control (4.81 ± 0.4) by about 50% ($P < 0.05$, $n = 17/4$) (Figure 4.7 A and B). When quinine was added, there was also a significant decrease in the ATP frequency when (0.03 ± 0.006 Hz) compared to the control (0.09 ± 0.01 Hz, $P < 0.05$) (Figure 4.7 C). Moreover, the duration time of ATP cells that showed Ca^{2+} oscillations was inhibited (65 ± 4.8 s) compared to the control (187 ± 15 s) (Figure 4.7 D). Furthermore, the number of cells demonstrating Ca^{2+} fluorescence oscillations during the recording period was reduced (only 3 cells out of 17 showed Ca^{2+} fluorescence oscillations) compared to the control (30 cells over 35 cells). The number of pulmonary artery smooth muscle cells induced single Ca^{2+} fluorescence was increased (9 cells out of 17) compared to control (1 cell out of 35 cells). The number of pulmonary artery smooth muscle cells induced double Ca^{2+} fluorescence was increased (5 cells out of 17) compared to control (1 cell out of 35 cells) (Figure 4.7 E). The number of events was also reduced with 2.41 ± 0.66 compared to the control (8.77 ± 0.72) (Figure 4.7 F).

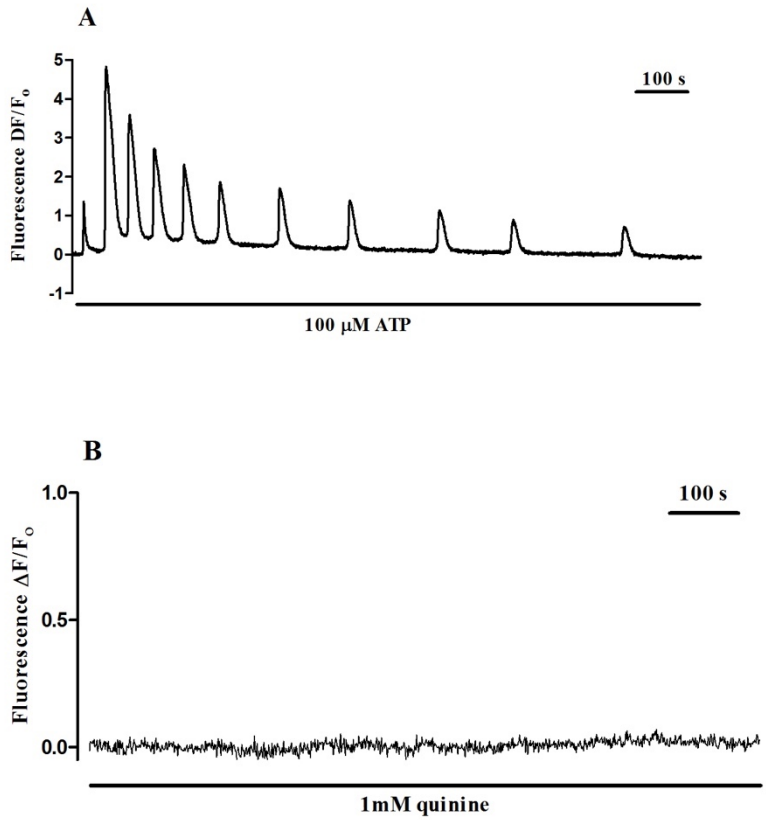

Figure 4.6 Representative Raw Control Traces show the effect of ATP and Quinine of the Rat Isolated Pulmonary Artery SMCs.

Microflurimeter microscopy recordings of pulmonary artery SMCs loaded with the calcium-sensitive dye Cal-520 AM which were then subjected to: **A)** addition of 100 μM ATP then it given $[Ca^{2+}]_i$ oscillation. **(B)** Addition of 1mM quinine and the reaction recorded for 400 s. The average increase in Cal-520 AM fluorescence was measured by ($\Delta F/F_0$).

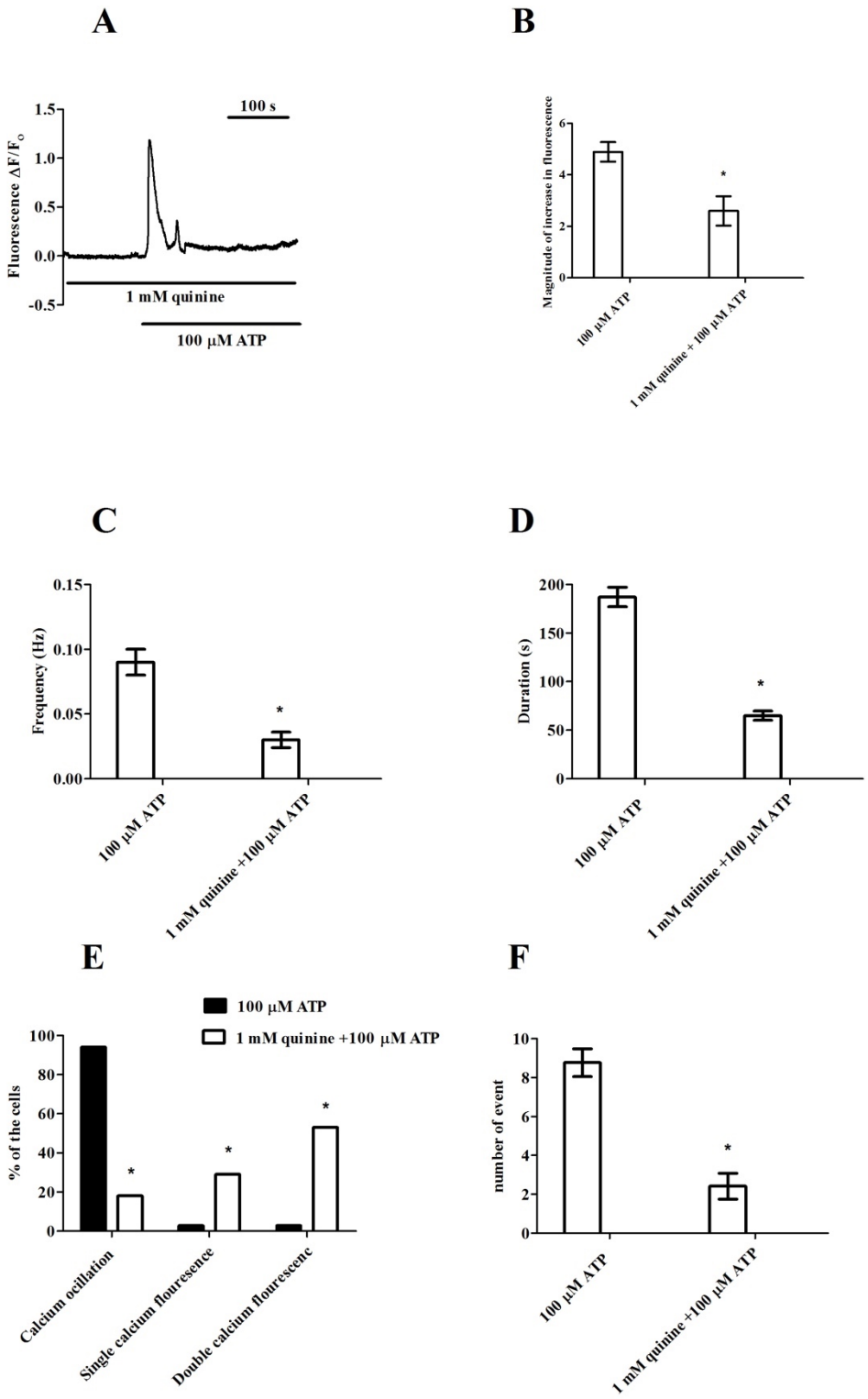

Figure 4.7 Effect of Quinine on the ATP-Induced Increase in Cal-520 AM fluorescence in Rat Isolated Pulmonary Artery SMCs.

Pulmonary artery SMCs were loaded with the calcium-sensitive dye Cal-520 AM, 1 mM (10 µl/ml) for 60 minutes in a dark place at room temperature. 1 mM quinine was added to rat pulmonary artery SMCs, and then 100 µM ATP was added. **A)** Recordings showed changes in Ca^{2+} fluorescence in the rat pulmonary artery after quinine was added. **B)** The magnitude of increase in Ca^{2+} fluorescence in the 100 µM ATP (control) and in 1 mM quinine plus 100 µM ATP (n = 17/4). **C)** The frequency (Hz) in the 100 µM ATP (control) and in 1 mM quinine plus 100 µM ATP. **D)** The duration (s) of Ca^{2+} fluorescence in the 100 µM ATP (control) and in 1 mM quinine plus 100 µM ATP. **E)** The percentage of cells in the 100 µMATP (control) and in 1 mM quinine plus 100 µM ATP. **F)** Number of events in the 100 µM ATP (control) and in 1 mM quinine plus 100 µM ATP. The average increase in $[Ca^{2+}]_i$ was measured by ($\Delta F/F_0$). Data are shown as mean ± s.e.m. * ($P < 0.05$).

Similarly, application of 1 mM denatonium inhibited the magnitude of the ATP-induced increase in $[Ca^{2+}]_i$ in rat pulmonary artery SMCs ($\Delta F/F_0$ 2.62 ± 0.21) compared to control (4.81 ± 0.4) ($P < 0.05$, $n = 37/5$) (Figure 4.9 A and B). There was also a significant decrease in the frequency of Ca^{2+} oscillations when denatonium was added (0.05 ± 0.006 Hz) compared to the control (0.09 ± 0.01 Hz, $P < 0.05$) (Figure 4.9 C).

As with to quinine, when denatonium was added the duration of Ca^{2+} oscillations with cells treated with ATP was reduced (50 ± 8.5 s) compared to the control (187 ± 15 s) (Figure 4.9 D). Furthermore, the number of cells which exhibited Ca^{2+} fluorescence oscillations during the recording period reduced (only 12 cells over 37 induced Ca^{2+} fluorescence oscillations) compared to the control (30 cells over 35 cells). The number of pulmonary artery smooth muscle cells induced single Ca^{2+} fluorescence was increased (17 cells out of 37) compared to control (1 cell out of 35 cells). The number of pulmonary artery smooth muscle cells induced double Ca^{2+} fluorescence was increased (8 cells out of 37) compared to control (1 cell out of 35 cells) (Figure 4.9 E). The number of events was also reduced 2.16 ± 0.22 compared to the control (8.77 ± 0.72) (Figure 4.9 F). Taken together, these data suggested that addition of quinine and denatonium significantly inhibited ATP-induced increase in $[Ca^{2+}]_i$ in the rat pulmonary artery SMCs.

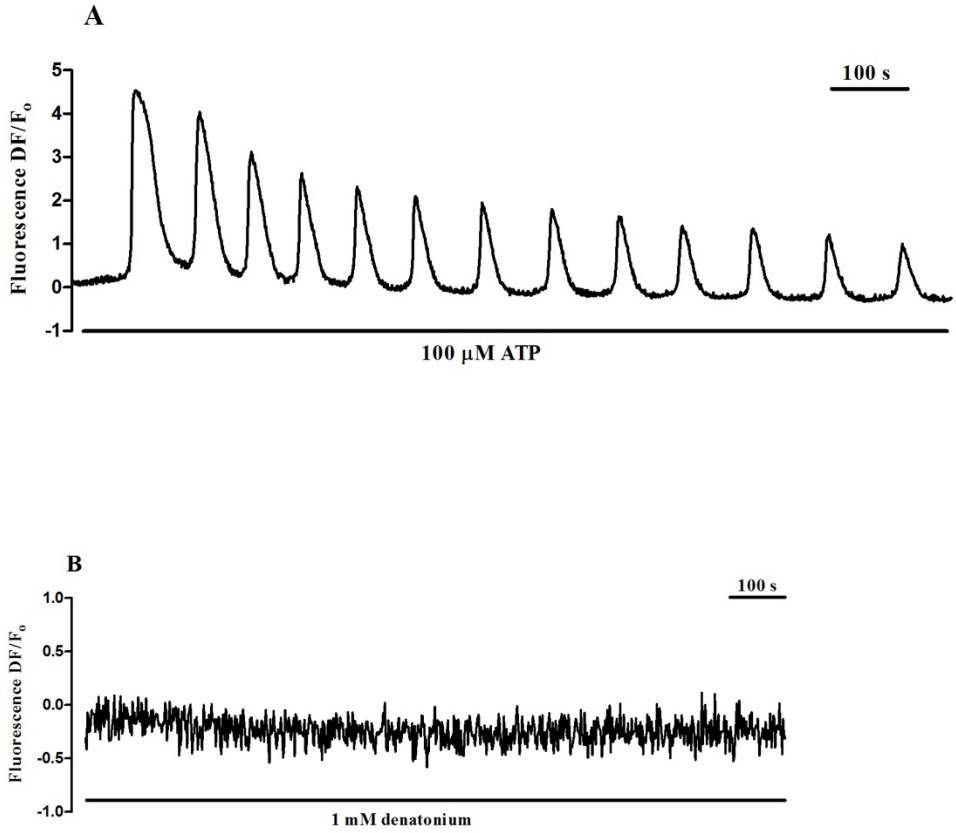

Figure 4.8 Representative Raw Control Traces show the effect of ATP and Denatonium of the Rat Isolated Pulmonary Artery SMCs.

Microflurimeter microscopy recordings of pulmonary artery SMCs loaded with the calcium-sensitive dye Cal-520 AM which were then subjected to: **A)** addition of 100 µM ATP then it given $[Ca^{2+}]_i$ oscillation. **(B)** Addition of 1mM denatonium and the reaction recorded for 400 s. The average increase in Cal-520 AM fluorescence was measured by ($\Delta F/F_0$).

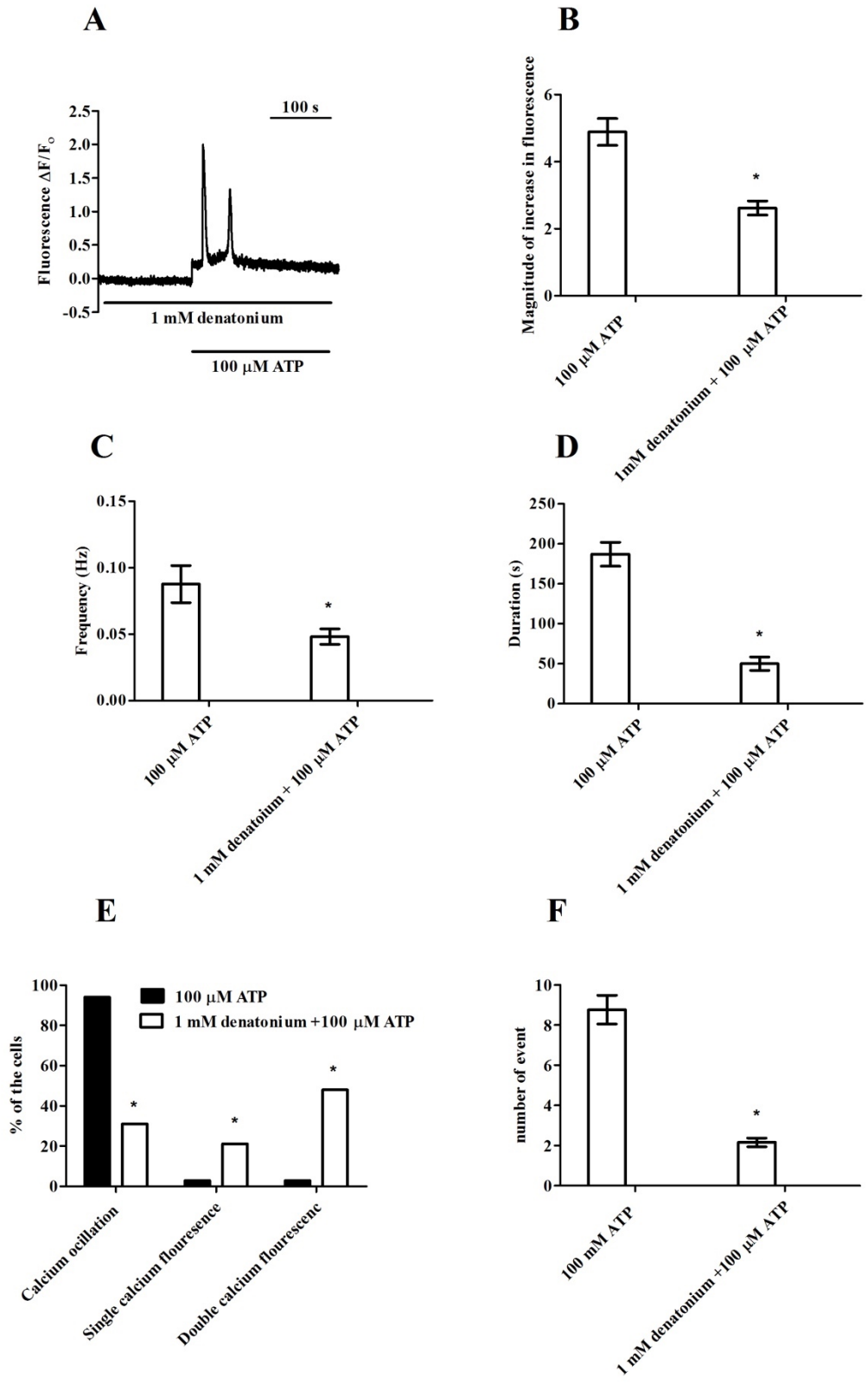

Figure 4.9 Effect of Denatonium on the ATP-Induced Increase in Cal-520 AM fluorescence in Rat Isolated Pulmonary Artery SMCs.

Pulmonary artery SMCs were loaded with the calcium-sensitive dye Cal-520 AM, 1 mM (10 μl/ml) for 60 minutes in a dark place at room temperature. 1 mM denatonium was added to the rat pulmonary SMCs, and then 100 μM ATP was added. **A)** Recordings showed changes in Ca^{2+} fluorescence in the rat pulmonary artery SMCs after denatonium was added. **B)** The magnitude of increase in Ca^{2+} fluorescence in the 100 μM ATP (control) and in 1 mM denatonium plus 100 μM ATP (n = 37/5). **C)** The frequency (Hz) in the 100 μM ATP (control) and in 1 mM denatonium plus 100 μM ATP. **D)** The duration (s) of Ca^{2+} fluorescence in the 100 μM ATP (control) and in 1 mM denatonium plus 100 μM ATP. **E)** The percentage of cells in the 100 μM ATP (control) and in 1 mM denatonium plus 100 μM ATP. **F)** Number of events in the 100 μM ATP (control) and in 1 mM denatonium plus 100 μM ATP. The average increase in $[Ca^{2+}]_i$ was measured by ($\Delta F/F_0$). Data are shown as mean ± s.e.m. * ($P < 0.05$).

4.3.4 Effect of Dextromethorphan on ATP-Induced Ca^{2+} Oscillation

Imaging of the calcium fluorescent indicator, Cal-520 AM was used to examine the effect of dextromethorphan on ATP-induced Ca^{2+} oscillation of the $[Ca^{2+}]_i$ of rat pulmonary artery SMCs. After 1 mM dextromethorphan was applied to the SMCs, the Ca^{2+} fluorescence was allowed to return and stabilise to the baseline level for two minutes before 100 μM ATP was added. Application of ATP caused an increase in Ca^{2+} fluorescence (Figure 4.10 A). Application of dextromethorphan to the SMCs before the addition of ATP, prevented ATP-induced Ca^{2+} fluorescence oscillation ($P < 0.05$, $n = 22/4$) (Figure 4.10 B and C). These results suggested that dextromethorphan significantly inhibited ATP-induced increases in $[Ca^{2+}]_i$ in the rat pulmonary artery SMCs.

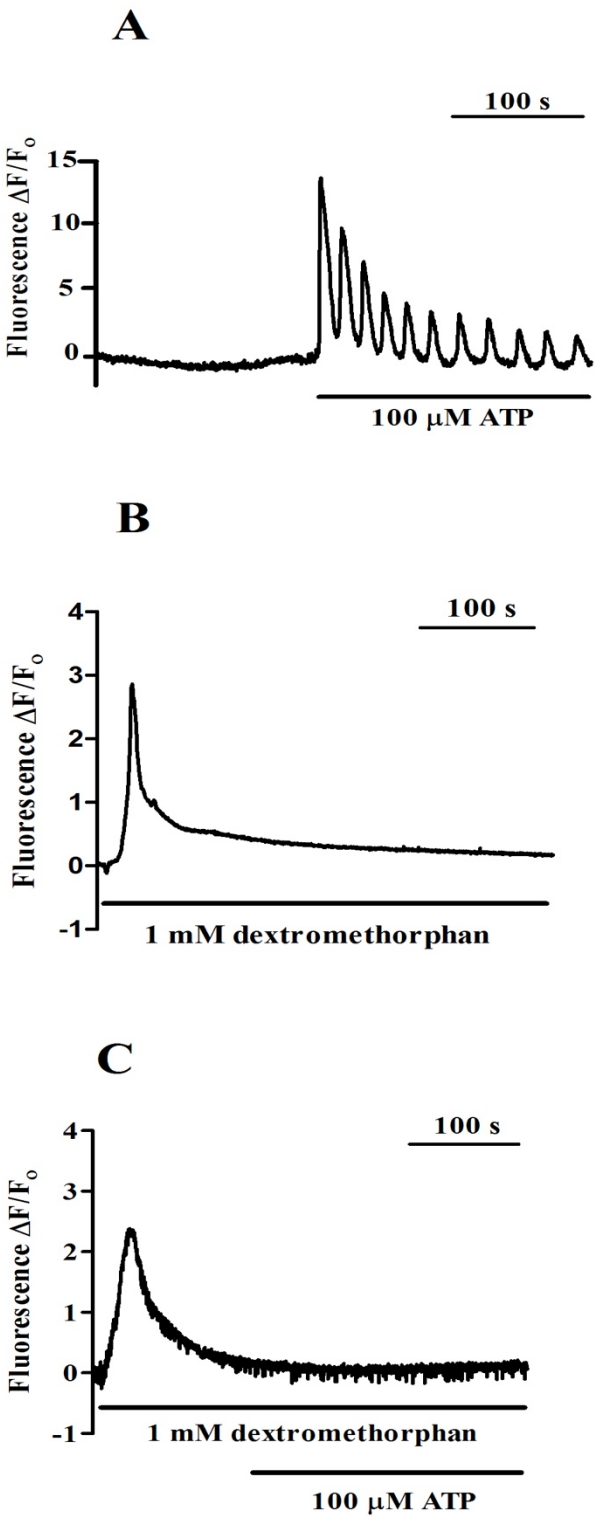

Figure 4.10 The Effects of Dextromethorphan on the ATP-Induced Increase in Ca^{2+} fluorescence in the Rat Isolated Pulmonary Artery SMCs.

A) 100 μM ATP was added to the rat pulmonary artery SMCs. **B)** 1 mM dextromethorphan was added to SMCs. **C)** 1 mM dextromethorphan was added first to SMCs and after 2 minutes passed, 100 μM ATP was added (*n* = 22/4). The average increase in $[Ca^{2+}]_i$ was measured by ($\Delta F/F_0$). Data are shown as mean ± s.e.m.

4.3.5 Effects of Dextromethorphan on the KCl-Induced Increase in $[Ca^{2+}]_i$

To examine the involvement of VDCCs in the dextromethorphan-induced increase in $[Ca^{2+}]_i$ of the rat pulmonary artery SMCs, KCl was used (Figure 4.11 A). It is known that increasing extracellular K^+ results in membrane depolarisation, which subsequently opens VDCC, and allows Ca^{2+} influx. This results in an increase in $[Ca^{2+}]_i$ and ultimately causes pulmonary artery smooth muscle contraction and pulmonary vasoconstriction (Hall *et al.*, 2009; Mandegar and Yuan, 2002)

Calcium imaging with Cal-520 AM found that the dextromethorphan-induced increase in $[Ca^{2+}]_i$ persisted even in the presence of KCl ($\Delta F/F_0$ 2.66 ± 0.31, n = 16/4). The magnitude of the response, although slightly smaller, was not significantly different from that of the control ($\Delta F/F_0$ 4.73 ± 0.54, n = 16/5) (Figure 4.11 B). Moreover, there was no significant difference in the duration of the dextromethorphan response after being treated with KCl compared to the control (Figure 4.11 C). These results suggest that the VDCC might be partially involved in the dextromethorphan-induced increase in $[Ca^{2+}]_i$ of the rat pulmonary artery SMCs.

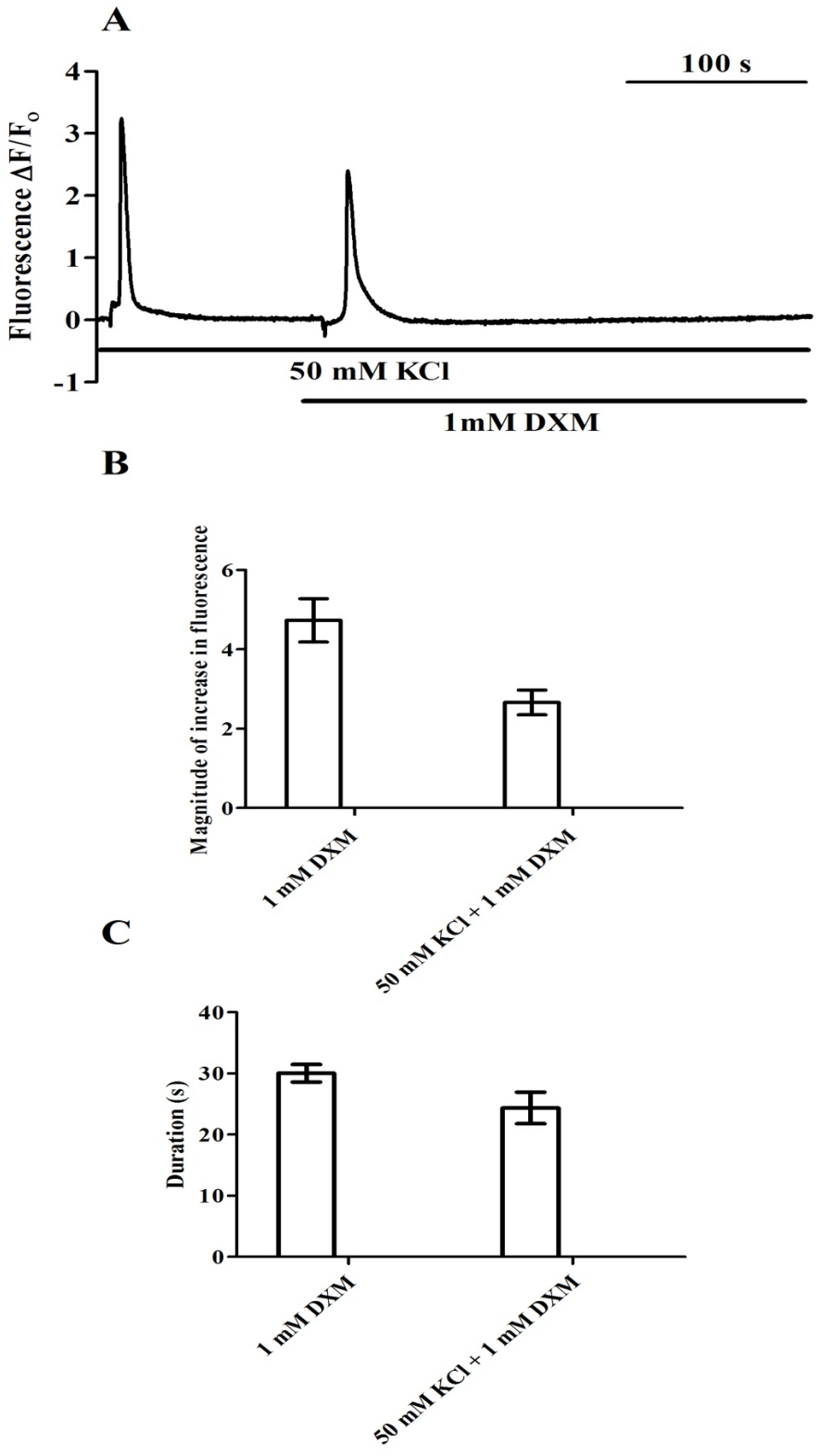

Figure 4.11 The Effects of KCl on the Dextromethorphan-Induced Increase in Ca^{2+} fluorescence of the Rat Isolated Pulmonary Artery SMCs.

50 mM KCl was added to the freshly isolated rat pulmonary artery SMCs for 120 seconds, then 1mM dextromethorphan was added. **A)** Representative trace show the magnitude of $[Ca^{2+}]_i$ response to dextromethorphan after KCl. **B)** Histogram shows the magnitude of $[Ca^{2+}]_i$ response to dextromethorphan after KCl (n = 16/4) and (control, n = 16/5). **C)** The duration in (s) to 1 mM dextromethorphan after KCl and control. Data are shown as mean ± s.e.m. DXM is dextromethorphan.

4.3.6 Effect of Dextromethorphan on Intracellular Ca^{2+} Levels

It is known that the increase in the intracellular Ca^{2+} can occur through two methods: from intracellular stores or through Ca^{2+} influx from extracellular sources. To investigate whether extracellular Ca^{2+} was required, the dextromethorphan-induced increase in $[Ca^{2+}]_i$ in normal cells was compared with the dextromethorphan-induced increase in $[Ca^{2+}]_i$ in cells in a Ca^{2+}-free solution. The dextromethorphan-induced increase in $[Ca^{2+}]_i$ persisted even in Ca^{2+}-free solution ($\Delta F/F_0$ 2.35 ± 0.35, n = 14/4). The magnitude of the response, although slightly smaller, was not significantly different from the control PSS ($\Delta F/F_0$ 3.80 ± 0.76, n = 11/4), indicating that the source for this dextromethorphan response is mainly from internal Ca^{2+} stores (Figure 4.12).

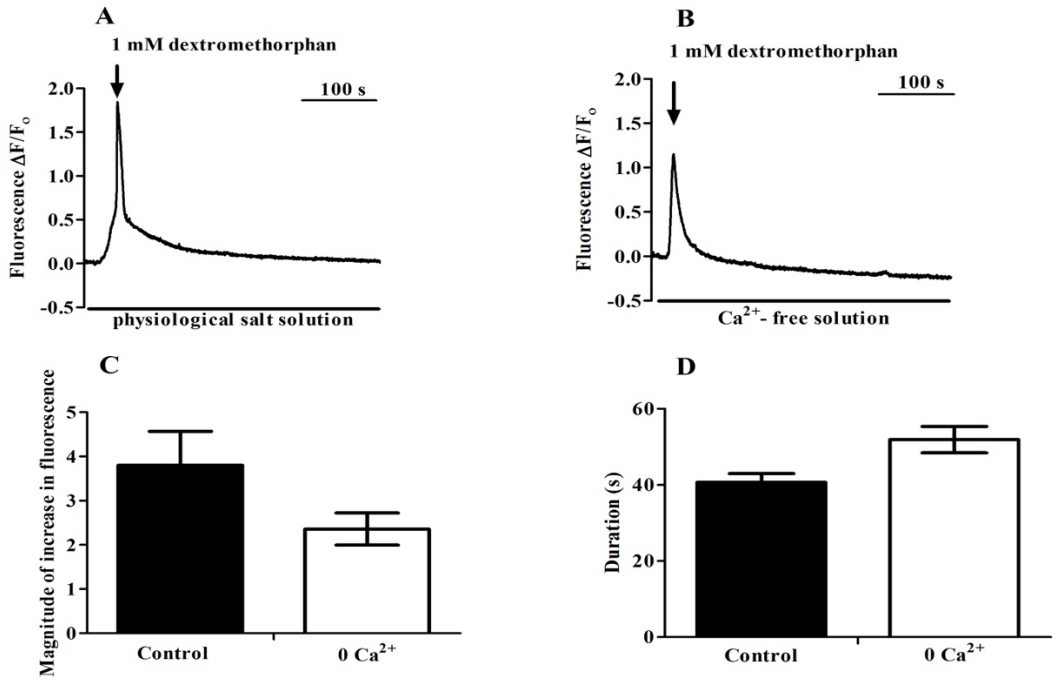

Figure 4.12 The Effects of Ca^{2+}-Free Solution on the Dextromethorphan-Induced Increases in Ca^{2+} fluorescence of the Rat Isolated Pulmonary Artery SMCs.

1 mM dextromethorphan was applied to: **A)** The rat pulmonary artery SMCs in normal physiological solution (control, n = 14/4). **B)** The rat pulmonary artery SMCs in the Ca^{2+}-free extracellular solution (0 Ca^{2+}, n = 11/4). **C)** The magnitude of $[Ca^{2+}]_i$ response. **D)** The

duration in (s) in normal physiological solution and in Ca^{2+}-free extracellular solution. Data are shown as mean ± s.e.m.

4.3.7 Effects of Ca^{2+} Stores on the Dextromethorphan-Induced Increases in Ca^{2+} Fluorescence

To investigate further into the role of Ca^{2+} stores in the dextromethorphan-induced increase in $[Ca^{2+}]_i$ of SMCs, thapsigargin was used as a SERCA inhibitor. After incubation with 1 μM thapsigargin, dextromethorphan failed to induce an increase in Cal-520 AM fluorescence (n = 36/4). The effect of thapsigargin was statistically significant compared to the time control ($P < 0.05$) (n = 27/4). These results strongly suggest that dextromethorphan releases Ca^{2+} from intracellular stores (Figure 4.13).

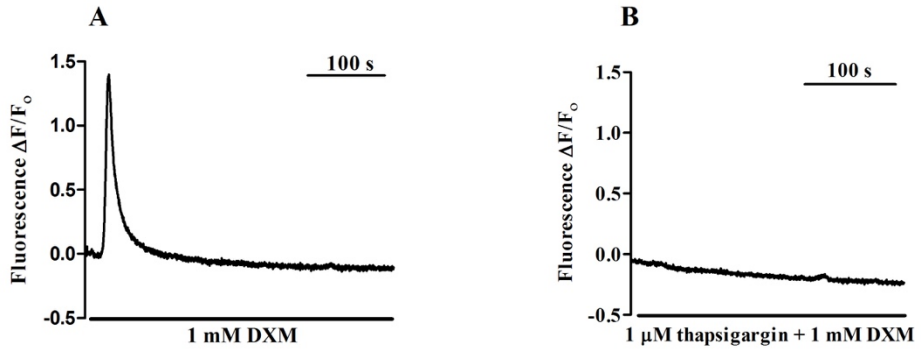

Figure 4.13 The Effect of Thapsigargin on the Response of Rat Isolated Pulmonary Artery SMCs to Dextromethorphan.

A) 1mM dextromethorphan was added to the rat isolated pulmonary artery SMCs as a control (n = 36/4). **B)** Representative traces show that 1 μM thapsigargin abolished the dextromethorphan-induced $[Ca^{2+}]_i$ responses (n = 27/4) ($P < 0.05$). DXM is dextromethorphan.

4.3.8 Intracellular Signalling Pathway for Dextromethorphan Response

Participation of PLC in the dextromethorphan-induced increase in $[Ca^{2+}]_i$ was also examined, using U73122, a PLC inhibitor. In this study, the dextromethorphan–induced increase in $[Ca^{2+}]_i$ was significantly inhibited by incubation with U73122 ($p < 0.05$) (n = 46/5) compared to the control (n =17/5) (Figure 4.14). These results strongly suggest that PLC is involved in the response of rat bitter taste receptors to dextromethorphan.

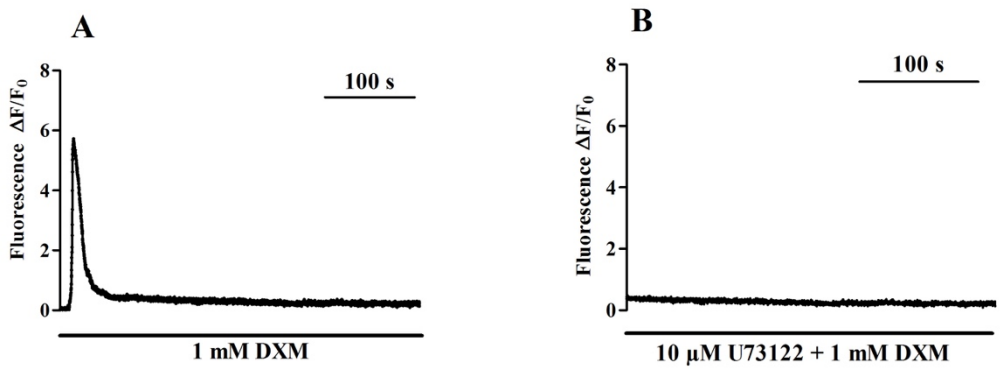

Figure 4.14 The Effect of U73122 on the Response of Isolated Pulmonary Artery SMCs to Dextromethorphan.

A) 1 mM dextromethorphan was added to the isolated rat pulmonary artery SMCs (n = 17/5). **B)** Representative traces show that 10 µM U73122 was added for 10 minutes, then 1 mM dextromethorphan was applied (n = 46/5) ($P < 0.05$). DXM is dextromethorphan.

4.4 Discussion

In this study, Ca^{2+} imaging and PTI DeltaRam microflurimeter recording were used to examine the effect of bitter taste agonists (quinine, denatonium and dextromethorphan) on $[Ca^{2+}]_i$ in rat freshly isolated pulmonary artery SMCs.

4.4.1 Ca^{2+} Responses to Quinine, Denatonium, and Dextromethorphan in the Rat Pulmonary Artery SMCs

The effect of bitter taste agonists on $[Ca^{2+}]_i$ in smooth muscle has been frequently investigated. In this study, 1 mM, 2 mM and 3 mM quinine failed to induce any changes in the $[Ca^{2+}]_i$ in the rat pulmonary artery SMCs. Although at a lower concentration, adding 500 mM quinine to mouse airway SMCs also failed to induced any change in $[Ca^{2+}]_i$ (Tan and Sanderson, 2014). However, quinine was induced increase in $[Ca^{2+}]_i$ in different species; in the human airway SMCs (Shah *et al.*, 2009; Deshpande *et al.*, 2010). The difference responses in $[Ca^{2+}]_i$ between human airway and mouse airway might have different explanations; in Tan and Sanderson (2014) used lower concentrations (micromolar ranges) of bitter taste agonists, whereas in earlier studies (Deshpande *et al.*, 2010; Shah *et al.*, 2009) mainly utilized millimolar concentrations of bitter taste agonists to characterize TAS2R-induce airway smooth muscle Ca^{2+} signalling. Moreover, Tan and Sanderson (2014) used lung slices to study Ca^{2+} responses in airway smooth muscle, while other studies (Deshpande *et al.*, 2010; Shah *et al.*, 2009) used cultured or isolated airway SMCs.

Quinine was observed to induced increase in $[Ca^{2+}]_i$ in the human pulmonary artery SMCs (Upadhyaya *et al.*, 2014). These discrepant effects of quinine on $[Ca^{2+}]_i$ between Upadhyaya *et al.* (2014) and my study are most likely due to differences in species (human vs. rats), concentration used (10 mM vs 3 mM) and cell phenotype (cultured cells vs freshly isolated cells).

In this study, 1 mM, 2 mM, and 3 mM denatonium did not induced any changes in the $[Ca^{2+}]_i$.in the rat pulmonary artery SMCs. Similarly, denatonium did not elicit a change in $[Ca^{2+}]_i$ in the cultured rat choroid plexus epithelial cells (Tomás *et al.*, 2016) and in

the human thyrocyte line Nthy Ori 3-1 cells (Clark *et al.*, 2014). These similarities might be attributed to the concentrations of a similar ranges (between 0.1 to 1 mM).

On the other hand, denatonium was reported to induced increase in $[Ca^{2+}]_i$. in different tissues and different species; In the human airway SMCs (Deshpande *et al.*, 2010; Lee *et al.*, 2014; Shah *et al.*, 2009), in the human pulmonary artery SMCs (Upadhyaya *et al.*, 2014), in the mouse gastrointestinal tract cells (Avau *et al.*, 2015; Chen *et al.*, 2006; Wu, Chen and Rozengurt, 2005; Wu *et al.*, 2002) , in the mouse urethral brush cells (Deckmann *et al.*, 2014). The discrepancy between my study and these studies might be due to the higher concentrations they used (up to 25 mM), whereas in this study the maximum concentration was 3 mM. Taken together, these findings suggesting that quinine and denatonium might be induced increase in $[Ca^{2+}]_i$ in higher concentrations.

Contrarily, in this study, an increase in $[Ca^{2+}]_i$, upon stimulation by dextromethorphan indicated that TAS2Rs in rat pulmonary artery SMCs are functional. This work support the findings of Upadhyaya *et al.* (2014) which showed that adding 2 mM dextromethorphan induced an increase in $[Ca^{2+}]_i$ in the primary cultures of human pulmonary artery SMCs. These results suggest that the bitter taste agonist dextromethorphan might induce an increase in $[Ca^{2+}]_i$, in the pulmonary artery which might be consistence across other species.

4.4.2 Effects of Bitter Taste Agonists on ATP-Induced $[Ca^{2+}]_i$ Transient in Rat Pulmonary Artery SMCs

ATP was used as the extracellular agonist to investigate the potential effect of bitter taste agonists (quinine, denatonium, and dextromethorphan) on ROCC, SOCC, and VDCC. ATP-mediated activation of P2Y receptors, a family of GPCRs, increased $[Ca^{2+}]_i$ by causing SOCE, ROCE. Moreover, ATP-mediated activation of P2X receptors, a family of cation-permeable ligand-gated ion channels, increases $[Ca^{2+}]_i$ by directly inducing Ca^{2+} influx through the channels and/or indirectly inducing Ca^{2+} influx via VDCC through membrane depolarization (Chin and Chueh, 2000; Gilbert *et al*., 2016; Wu *et al*., 2017).

In this study, presence of quinine significantly inhibits the magnitude of ATP-induced $[Ca^{2+}]_i$ increases in rat pulmonary artery SMCs by about 50%. Moreover, denatonium inhibited the magnitude of the ATP-induced increases in $[Ca^{2+}]_i$ in rat pulmonary artery SMCs, by about 60%. Furthermore, dextromethorphan induces a complete inhibition of ATP-induced $[Ca^{2+}]_i$ increases in rat pulmonary artery smooth muscle cells. Wu *et al.* (2017) showed that treatment with chloroquine inhibited the magnitude of the ATP-induced increases in $[Ca^{2+}]_i$ in human pulmonary artery SMCs, by about 25%. Chin and Chueh (2000) reported that ATP-induced $[Ca^{2+}]_i$ increase in VSMCs due to Ca^{2+} influx mainly through ROCC, rather than SOCC or VDCC. Therefore, results from this study indicate that quinine, denatonium, and dextromethorphan attenuate the ATP-mediated increase in $[Ca^{2+}]_i$, suggesting that quinine, denatonium, and dextromethorphan may partially block ROCC. Further studies are needed to specify the types of channels that can be blocked by these agonists and to define the precise mechanisms by which they exert their inhibitory effects on Ca^{2+} channels in pulmonary artery SMCs.

4.4.3 Possible Mechanisms Involved in the Dextromethorphan-Induced Increase in $[Ca^{2+}]_i$

Functional studies of this project on the rat isolated pulmonary artery SMCs indicated that an increase in $[Ca^{2+}]_i$ after the application of dextromethorphan, suggesting that TAS2R in rat pulmonary artery SMCs are functional. Similarly, Upadhyaya *et al.* (2014) observed similar results with dextromethorphan on human pulmonary artery SMCs. Moreover, dextromethorphan (2 - 4.5 μM) induced a concentration–dependent increase in $[Ca^{2+}]_i$ in the human highly metastatic breast cancer cell line MDA-MB-231, poorly metastatic cell line MCF-7, and non-cancerous mammary epithelial cell line MCF-10A (Singh *et al.*, 2014).

4.4.3.1 Role of VDCC in the Dextromethorphan-Induced Increase in $[Ca^{2+}]_i$

VDCCs are expressed in VSMCs and vasoconstrictors one of the major mechanisms underlying VSMCs contraction (Fernandez *et al*., 2012). The contraction induced by KCl mainly involves depolarisation of the SMC membrane and subsequently

increases Ca^{2+} influx, raises $[Ca^{2+}]_i$, and cause pulmonary artery SMCs contraction (Hall *et al.*, 2009; Mandegar and Yuan, 2002). To study whether the bitter taste agonist, dextromethorphan, can induce this increase in $[Ca^{2+}]_i$ by L-type VDCCs, KCl was used to study cellular processes mediated by depolarisation. This study found dextromethorphan was able to induce a $[Ca^{2+}]_i$ increase even in the presence of KCl. This increase was slightly inhibited, however, which might suggest that the VDCC is partially involved in the dextromethorphan-induced $[Ca^{2+}]_i$ increase. This finding is nevertheless consistent with what has been observed previously with dextromethorphan in different studies; Carpenter *et al.* (1988) reported that inhibition of Ca^{2+} influx through VDCC might contribute to the pharmacological action of dextromethorphan. Moreover, dextromethorphan inhibited depolarisation-evoked Ca^{2+} dependent contractions of guinea pig ilium SMCs (Kachur, Morgan and Gaginella, 1986). A relationship between dextromethorphan and its antagonistic effect on VDCC have different explanations; It was reported that variety of Ca^{2+} channel antagonists compete for binding sites called [^{3}H] dextromethorphan in guinea pig brain, and dextromethorphan enhances the binding of [^{3}H] dextromethorphan to Ca^{2+} channel antagonists receptor sites in the rat brain (Bolger, Rafferty and Skolnick, 1986). Moreover, radioligand binding data suggest that dextromethorphan modulate L-type channels by acting at a site that is allosterically coupled to the binding site for classical dihydropyridine Ca^{2+} channel antagonists, and which allows certain similarities to the binding site for diltiazem (Bolger, Rafferty and Skolnick, 1986; Carpenter *et al*., 1988).

4.4.3.2 Role of Intracellular Stores in the Dextromethorphan-Induced Increase in $[Ca^{2+}]_i$

While the above findings suggest that dextromethorphan produces pulmonary artery relaxation through partial inhibition of VDCCs, it is also possible that the intracellular stores may be involved. Release of Ca^{2+} from intracellular stores is involved in the transduction mechanisms of many bitter taste agonists which results in an increase in IP_3 level in the taste tissue of rats (Hwang *et al.*, 1990; Spielman *et al.*, 1994). In this study, incubation of the pulmonary artery SMCs in the Ca^{2+}-free solution was still able to induce an increase in $[Ca^{2+}]_i$. These results indicate that

intracellular stores are the primary source for the $[Ca^{2+}]_i$ increase, which was also confirmed using thapsigargin, a SERCA inhibitor. Thapsigargin is frequently used to investigate the transduction mechanisms of bitter taste agonists (Deshpande *et al.*, 2010; Grassin-Delyle *et al.*, 2013; Ogura, Margolskee and Kinnamon, 2002; Ogura, Mackay-Sim and Kinnamon, 1997; Ogura and Kinnamon, 1999). This study found that treatment of pulmonary artery SMCs with thapsigargin abolished the $[Ca^{2+}]_i$ increase following treatment of dextromethorphan. This result supports a previous study that showed that thapsigargin was also abolished the dextromethorphan-induced $[Ca^{2+}]_i$ response in isolated mudpuppy taste cells (Ogura and Kinnamon, 1999). This further confirms that the bitter agonist dextromethorphan releases Ca^{2+} from intracellular stores.

To investigate which types of intracellular Ca^{2+} stores are involved in a dextromethorphan-induced $[Ca^{2+}]_i$ increase, U73122, a PLC inhibitor was used. U73122 has been used in different studies to investigate the signalling mechanism in bitter taste agonists (Deshpande *et al.*, 2010; Grassin-Delyle *et al.*, 2013; Lee *et al.*, 2014; Ogura, Mackay-Sim and Kinnamon, 1997; Weir *et al.*, 1994; Zheng *et al.*, 2017). In this study, dextromethorphan–induced increase in $[Ca^{2+}]_i$ in the rat isolated SMCs was significantly inhibited by U73122. Thus, dextromethorphan caused Ca^{2+} release from IP_3 intracellular stores via a PLC-dependent mechanism. However, Ogura and Kinnamon (1999) reported that dextromethorphan causes release of Ca^{2+} from intracellular store via PLC- IP_3 independent pathway. These discrepant effects of dextromethorphan on PLC- IP_3 are most likely due to differences in species (rat vs. mudpuppy) and tissue (pulmonary artery SMCs vs. taste receptor cells). The findings of this study study suggests that dextromethorphan-induced increases in $[Ca^{2+}]_i$ in the rat pulmonary artery isolated SMCs utilise two main mechanisms for calcium regulation: one that is extracellular in nature and occurs partially via the VDCC, and a second one that is derived from intracellular Ca^{2+} stores via the PLC–IP_3 pathway.

Chapter 5

Determination of the Types of Bitter Taste Receptors Expressed in the Rat Pulmonary Artery

5.1 Introduction

5.1.1 The Expression of Bitter Taste Receptors in the Vascular System

The taste buds within the oral cavity were the first place the TAS2Rs were discovered (Hoon *et al.*, 1999). Recent studies have indicated that in addition to their expression in the gustatory system, TAS2Rs are also expressed in the extra-oral tissue. Among these extra-oral locations is the expression and the potential functional role of the TAS2Rs in the vascular system, which have attracted a lot of scientific interest. Several studies have reported various types of TAS2Rs that are expressed in different locations in the vascular system, and upon activation they produce various functions. In 2013, Lund *et al*. conducted a proteomics and RT-PCR study on TAS2R46, which is a receptor that is responsive to denatonium and is expressed in the human aorta VSMCs. When the VSMCs were treated with denatonium this induced a Ca^{2+} response, while the administration of denatonium to the rats induced a transient decrease in the blood pressure (Lund *et al.*, 2013).

The heart also appears to sense bitter taste agonists through its expression of TAS2Rs. Multiple TAS2Rs are expressed in the cardiac myocytes and fibroblasts of both rodents and humans (Foster *et al.*, 2013). Furthermore, the developmental regulation of TAS2R expression was examined and showed that the gene expression of Tas2r108, Tas2r126, Tas2r135, Tas2r137, and Tas2r143 decreased with age in the heart tissues. In a follow-up study, they found that sodium thiocyanate, a TAS2R108 agonist; sodium benzoate, a TAS2R137 agonist; and sodium arbutin, a TAS2R143 agonist, were able to decrease the left ventricle pressure and systolic blood pressure as well as increase the aortic pressure in the mouse heart (Foster *et al.*, 2014). Taken together, these results indicate that the TAS2Rs play an important role in the cardiac function.

Another group of researchers examined the mRNA for TAS2R3, TASR4, TAS2R10, and TAS2R14 which were detected in isolated human pulmonary arteries. Upon their activation they caused blood vessel relaxation (Manson *et al.*, 2014). In 2014, Upadhyaya *et al*., reported that dextromethorphan was able to induce a

vasoconstriction through a TAS2R1-medated Ca^{2+} response in the human pulmonary artery smooth muscle. They further reported that the increase in Ca^{2+} directly activates the MLCK and subsequently increases the phosphorylated MLC, which in turn leads to a constriction (Upadhyaya *et al.*, 2014). In 2016, Sakai *et al*., showed using RT-PCR that mRNA expression of the Tas2r108 was detected in mouse thoracic aorta (Sakai *et al.*, 2016). Furthermore, Chen *et al*., in 2017 was able to show that the TAS2R3, TAS2R4, TAS2R7, TAS2R10, TAS2R14, TAS2R39 and TAS2R40 mRNAs were expressed in human omental arteries. The subtypes Tas2r39, Tas2r40, Tas2r108, Tas2r114, Tas2r130, Tas2r137, and Tas2r140 were detected via RT-PCR from the rat mesenteric arteries and cerebral arteries, but the PCR amplicon band for Tas2r114 did not appear in the rat cerebral artery (Chen *et al.*, 2017).

As discussed in the previous chapters, TAS2R agonists were able to mediate a relaxation of the rat pulmonary artery rings. In order to understand the vasorelaxant properties of the rat pulmonary vessels, it is imperative to identify which TAS2R subunits are expressed in the rat pulmonary artery. Therefore, this chapter aims to investigate the mRNA expression of the Tas2r subunits in the rat pulmonary artery using RNA-Seq. RT-qPCR will also be conducted using Tas2r-specific primers to validate the results from the RNA sequencing analysis and to conduct further gene expression analysis.

5.2 Methods

5.2.1 Animals and Tissue Sources

The animals used in the DNA and RNA analysis were male Sprague Dawley rats, weighing 250-350 g and they obtained from the Biological Procedures Unit (BPU) within the University of Strathclyde. The rats were housed in a temperature and humidity-controlled holding room and had unlimited access to food and water. They were killed by cervical dislocation.

5.2.2 DNA Isolation for the Rat Genotyping (DNA Extraction)

The genotyping analysis was carried out to determine whether there are any variations in the *Tas2r* genes in the Sprague Dawley rats used in this study. The DNA isolation from the rat liver was performed on 25 mg of tissue using Qiagen DNeasy blood and tissue kit (Qiagen, Manchester, UK) in line with the manufacturer's instructions as shown in Figure 5.1 and as follows. A small section of the rat liver (25 mg) was cut into small pieces, placed in to a 1.5 ml microcentrifuge tube containing 180 µl of ATL lysis buffer, and then rapidly placed in dry ice and stored at -80 ˚C until further required. For the DNA isolation, 20 µl of the supplied Proteinase K was added to the sample and mixed thoroughly by vortexing. The sample was incubated at 56°C for 15 minutes until the tissue was completely lysed. After which 200 µl of the buffer AL was added to the sample and mixed thoroughly by vortexing, and then 200 µl ethanol (96 - 100%) was added and mixed again. The sample mixture was pipetted into DNeasy Mini spin column, placed in a 2 ml collection tube, spun at 6000 x g (8000 rpm) for 1 minute, and then the flow-through was discarded with a collection tube. The DNeasy Mini spin column was placed in a new 2 ml collection tube, then 500 µl buffer AW1 was added, and it was spun again for 1 minute at 6000 x g (8000 rpm) and the flow-through was discarded. 500 µl buffer AW2 was then added to the DNeasy Mini spin column and was spun for 3 minutes at 20,000 x g (14,000 rpm). The DNA sample was dissociated from the spin column by placing the DNeasy Mini spin column in a clean 2 ml microcentrifuge tube and 200 µl of the buffer AE was pipetted directly onto the DNeasy membrane, and was then incubated at room temperature for 1 min. To

elute the DNA sample, it was centrifuged for 1 minute at 6000 x g (8000 rpm). The DNA fragments were quantified using a NanoDrop 2000c Spectrophotometer (ThermoScientific, Wilmington, USA). The DNA sample was stored at -20°C until further required.

Figure 5.1 Diagram Representing the Basic Protocol of the Total DNA Isolation from the Rat Liver Tissue.

(Adapted from the Qiagen DNeasy Blood and Tissue Handbook).

5.2.3 PCR Primers for the *Tas2r* Genotyping and Gene Expression

The PCR primer sequence sets were designed for each of the rat Tas2r gene and mRNA by using the National Centre for Biotechnology Information (NCBI) RefSeq GenBank records and the NCBI Primer-BLAST, a tool to design target-specific primers for polymerise chain reaction (https://www.ncbi.nlm.nih.gov/tools/primer-blast/index.cgi) (Ye *et al.*, 2012).

5.2.3.1 PCR Primers for Tas2r Genotyping

The Tas2r primers used for the PCR genotyping are shown in Table 5.1. All of the PCR primers were synthesised by Integrated DNA Technologies (Leuven, Belgium). Each of the primers was diluted in the DNase/RNase-Free molecular biology grade water to their appropriate concentrations and stored at -20˚C until required. The designing criteria for the PCR primers was followed:

1. Amplicons size = 960 - 1250 bp
2. The melting temperature (Tm) of primers kept between 56 - 59 °C; the ΔTm between forward and reverse primers was ≤ 1˚C
3. Primer length: 22 - 24 bases
4. Amplicon GC content: 45 - 46%

Table 5.1 PCR Primer Sequences for the Tas2r Genotyping of Rat Pulmonary Artery.

Rat Gene Symbol	Gene symbol Alias	Gene accession ID	Primer sequence (5'-3')	Amplicon length (bp)
Tas2r119	Tas2r1	NM_023993.1	Forward CCTTTGTGTTAGCATCATCTCC Reverse GATGGCATTATACAGGCTTCTG	1132
Tas2r137	Tas2r3	NM_001025149.1	Forward AACAAGAGGAGGTAGATCTCAG Reverse CACTGAAAGTCAGAAAGACTCC	1115
Tas2r108	Tas2r4	NM_001024686.1	Forward CCTGAGCCTGCTTACTTATTTC Reverse AGAGTCAGGATGCCAGATAAAG	1058
Tas2r107	Tas2r10	NM_023995.1	Forward CAACATATGGGACATTCTCCAG Reverse GACGAATCTGCATAGTCAAGTC	1163
Tas2r123	Tas2r14	NM_173336.1	Forward CTTCCTAATCGGGTGTAAATGG Reverse CTTGTCTCAGCTTACTGTTTCC	1042
Tas2r145	Tas2r31	NM_176885.2	Forward CAACTGCTTACTGGATTGGTTC Reverse GAACAAGTTACCAGTGACCTTC	1009
Tas2r134	Tas2r34	NM_199158.1	Forward CATGAATCCAGGAAGAGGTTTC Reverse CGTATTAGATGGAGCGAGAAAG	1215
Tas2r144	Tas2r40	NM_001025150.1	Forward CTCTCAACCAAGAAAGGAAGTG Reverse CTGGGTTTCTCAAGATCAGATG	1002
Tas2r126	Tas2r41	NM_139335.1	Forward ACCGTTTATCTACTGTCTGAGC Reverse GTCAGCCTACAAAGACATTTCC	1192
Tas2r143	Tas2r43	NM_001025061.1	Forward CAAATCCTCCCTCAACAAGATG Reverse GAAAGAAGGGTGTACCCAAATC	1019
Tas2r139	Tas2r39	NM_001080905.1	Forward CAACTTCACAAT GGAACTCTATG Reverse GTCAGCATCACC GTTTCTC	960

5.2.3.2 DNA Agarose Gel Electrophoresis

The DNA fragments were electrophoresed for qualitative analysis, sizing, and gel purification using agarose gel electrophoresis and a horizontal submarine mini-gel apparatus (Bioscience Services, UK) which was connected to an electrophoresis power supply (Kodak, UK).

The percentage of agarose concentration used varied between 1 - 2% (w/v) depending on the DNA fragment/amplicon sizes being assessed. In this study, 1% (w/v) agarose gels were used for the genotyping amplicons which were typically around 1000 bp in length. 1 x Tris-Borat-EDTA buffer (TBE) (Life Technologies, Paisley, UK) was used as the electrophoresis buffer for both the gel and running buffer. The TBE buffering solution had the following compositions: 89 mM Tris-Base (2 - amino- 2 - [hydroxymethyl]-1, 3 - propanediol), 89 mM Boric Acid, and 2 mM ethylenediamine tetraacetic acid (EDTA) and had a pH of 8.4. The appropriate amount of agarose (Bioline, London, UK) was added to 50ml of 1x TBE buffer solution in a glass bottle and then heated in a microwave for 1.3 min before the addition of 2 µl of the ethidium bromide dye (10 mg/ml) (Sigma, UK) to the agarose solution. The ethidium bromide works by intercalating the double-stranded DNA and the fluorescence of the ethidium bromide increases by a 25-fold upon the binding of the double-stranded DNA which further allows the visualisation of the electrophoresed DNA fragments under the ultra-violet (UV) light (El-Hamalawi, Thompson and Barker, 1975; Karsten and Wollenberger, 1977; Moore and Sutherland, 1985). A mixture of 15 µl of the PCR products and 2 µl of the DNA Loading Buffer (Bioline, London, UK) was added to the agarose gel wells. The DNA loading buffer increases the density of the sample to help load the DNA fragments onto the agarose gels and contains bromophenol blue dye which is used to monitor the migration rate during the agarose electrophoresis. 6 µl of the Hyper Ladder II size marker (Bioline, UK) was then loaded on to a separate well to determine the PCR products amplicon size. The gel was then electrophoresed at 50 volts for about 45 - 60 minutes.

After the electrophoresis, the DNA products were visualized on a and then photographed using an InGenius UV gel documentation system (Syngen Bio Imaging, UK).

5.2.3.3 Purification of the PCR Products

To confirm the amplicon identity through sequencing, the PCR amplicons were purified from the agarose gel slices following the gel electrophoresis. The PCR products were excised carefully from the electrophoresis gel placed on a UV Transilluminator 4000 (Stratagene, Germany) using a sharp clean scalpel and were placed in a DNase-free 1.5 microcentrifuge tube. The PCR products were purified using Illustra GFX^{TM} PCR DNA and Gel Band Purification Kit (GE Healthcare, UK) in line with the manufacturer's instructions (Figure 5.2). The concentration of the purified DNA was then measured using a NanoDrop 2000c Spectrophotometer (ThermoScientific, Wilmington, USA).

The purified PCR products were obtained for the 11 *Tas2r* genomic DNA PCRs. Aliquots of the samples were sent to GATC (Cologne, Germany) for Sanger sequencing (see Appendix A). The sequence analysis was carried out not only to confirm the identity of the rat Tas2r but also to investigate any possible gene variations. For genotyping analysis (see Appendixes B-G).

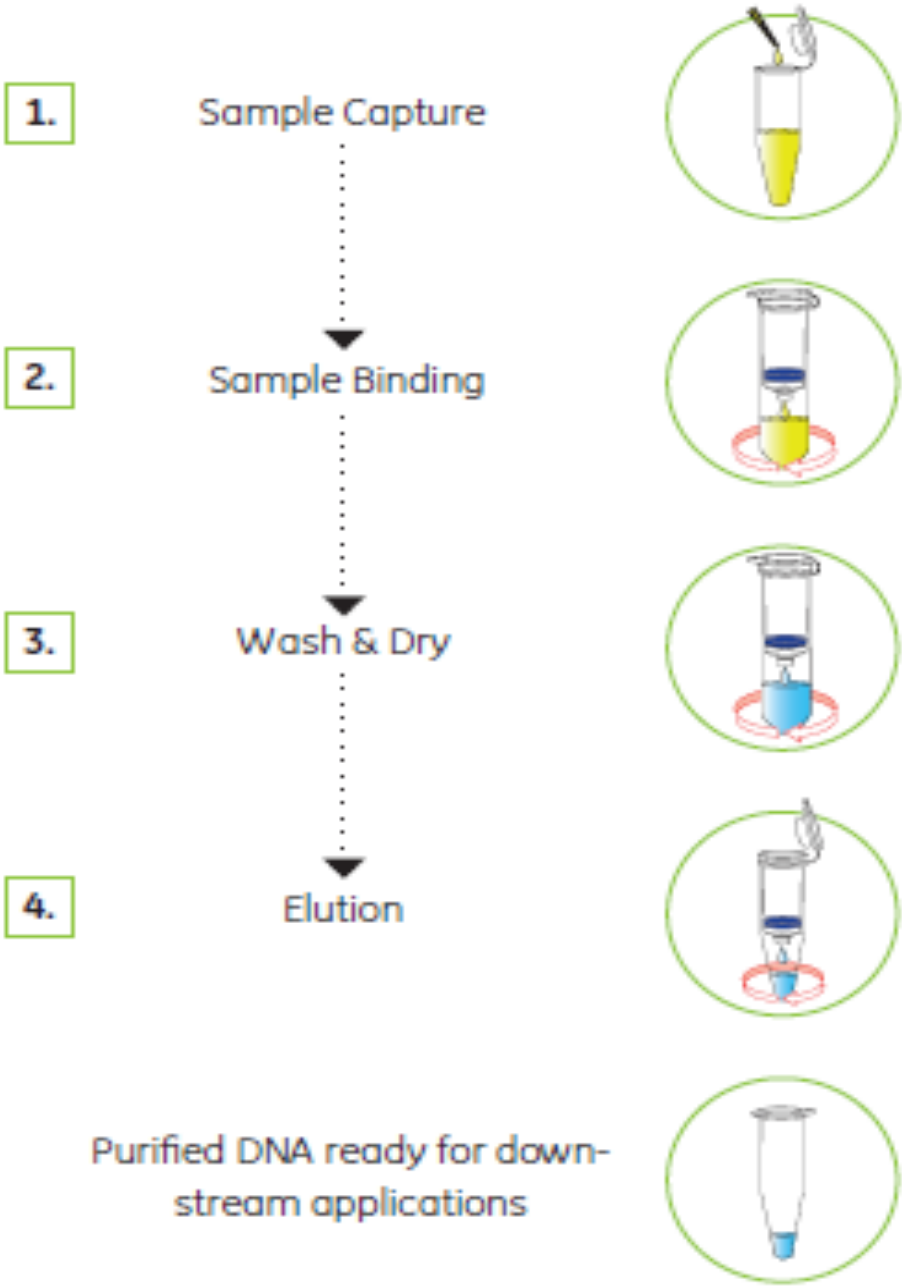

Figure 5.2 Diagram for the Basic Protocol of the DNA Band Gel Purifications.

(adapted from Illustra GFX^{TM} PCR DNA and Gel Band Purification Kit handbook)

5.2.4 Rat Pulmonary Artery Whole Transcriptome RNA Sequencing Analysis

In this study, whole transcriptome RNA sequencing (RNA-Seq) was conducted on RNA isolated rat pulmonary artery. These whole transcriptome expression profiling technologies allow to characterise all the genes expressed in the sample provided (Sukumaran *et al.*, 2017).

5.2.4.1 Tissue Harvest and Total RNA Isolation

The rat pulmonary artery tissues (weight ~ 250 - 350 mg) was collected from male Sprague Dawley rats. To reduce the risk of RNA degradation, the samples were immediately stored in RNA*later* ® solution (Ambion, Austin, TX), an RNA stabilsation solution which inhibits RNases. The tissue was then frozen at -80 ˚C until further required. Total RNA was extracted from the pulmonary artery samples and purified using the Qiazol-based RNeasy Plus Universal Mini Kit (Qiagen, Manchester, UK), Briefly, the tissue was initially disrupted and homogenised using a Mixer Mill MM301 bead mill (Retsch GmbH, Haan, Germany). Each tissue sample was added to a microcentrifuge tube containing a 6mm steel "cone" ball with 500 µl Qiazol lysis reagent. The sample tubes were then placed in the mixer mill which disrupted the samples at a frequency of 30.0 Hz for 1 min. This was repeated up to 3 times until the tissue was completely homogenised. The remainder of the RNA isolation procedure was in line with the RNeasy Plus Universal Mini Kit instructions. An aliquot of the purified RNA was taken for concentration determination and the remainder stored at -80 ˚C until required. An initial procedure assessment examined the impact of RNAlater stabilisation prior to RNA isolation. In addition to rat pulmonary artery tissue, samples of rat bronchi tissue and rat tongue epithelium were also dissected and had their total RNA extracted, to be used as controls for Tas2r gene expression analysis.

5.2.4.2 RNA Concentration

The purity and concentration of the extracted RNA were assessed using a NanoDrop 2000c Spectrophotometer which determined the absorbance of the nucleic acid sample across the 220 – 750 nm range (Thermo Scientific, Wilmington, USA). The NanoDrop

2000c can analyse 2 µl volumes of sample. The system was zeroed using 2 µl of RNase-free water as a blank. The NanoDrop software plots the sample absorption curve along with the calculated RNA concentration and ratios (A_{260} nm/A_{230} nm; A_{260} nm/A_{280} nm) of each RNA sample. DNA and RNA absorb maximally at A_{260} nm, An A_{260} nm/A_{230} nm absorption ratio of around 2.0 indicates low salt contamination or carryover from the isolation method used. The A_{260} nm/A_{280} nm absorption ratio reveals protein carryover and a value of around 2.0 indicates a pure RNA solution.

5.2.4.3 RNA Integrity

RNA is susceptible to degradation before, during, and following their isolation and purification from cells or tissues. The integrity of the RNA cannot be determined by the UV spectroscopy with systems such as the Nanodropspectrophotometer. Electrophoretic methods which can detect and size the fragmentation of RNA as a result of degradation of RNA are typically used. Traditionally, this can be conducted using denaturing agarose gel electrophoresis but more sophisticated and objective methods are available. The Experion Automated Electrophoresis system (Bio-Red, UK) is a lab-on-a-chip microfluidic separation technology using fluorescent sample detection and is suitable for this application. The RNA quality indicator (RQI) feature of the Experion software allows the estimation of the level of degradation in a total RNA sample when RNA samples are run on their RNA chips. The RQI algorithm compares the electropherogram of the RNA samples to data from a series of standardized degraded RNA samples and automatically returns a number between 10 (intact RNA) and 1 (degraded RNA) for each sample (Mueller *et al.*, 2000). RNA integrity assessment on 1 µl aliquotes of the isolated RNA was therefore conducted with the StdSens RNA kit (Bio-Rad, UK) following the manufacturer's instructions.

5.2.4.4 Whole Transcriptome RNA-Seq

20 µl of the total RNA isolated from the rat pulmonary artery was submitted to BGI Tech Solutions (Hong Kong, China) for their PE100 (HiSeq4000) Eukaryotic Transcriptome resequencing RNA-seq Package service using the llumina Hi-Seq 4000

sequencing platform. The remaining 10 µl of this sample was retained and was used in RT-qPCR to validate the RNA-seq results (called representative sample).

5.2.4.5 Gene Expression Analysis

The clean reads were mapped to the reference gene using Bowtie2, version:v2.2.5 (Langmead and Salzberg, 2012), and the gene expression was then calculated using RSEM which is a software package that is used for estimating the gene and isoform expression levels from an RNA-Sequencing data (Li and Dewey, 2011). The read coverage and distribution was calculated on the transcripts, for example, for a sample with high quality and deep enough depth the transcripts would be entirely covered and the mapping reads would be consistently distributed on the transcripts. Unequally mapping: this is referred to when the reads map to only one location of the reference. The transcripts level would be quantified using fragments per kilobase of exon model per million mapped reads (FPKM) (Mortazavi *et al.*, 2008). The rat pulmonary artery expression level of genes was calculated using the formula below.

$$\mathbf{FPKM = 10^9\ C / NL}$$

Where C is the number of mapped reads that fell onto the gene exon, N is the total number of mapped reads in the experiments, and L represent the sum of the exon in bars pairs.

5.2.4.6 Selecting the Reference Gene

An internal control or reference gene was used to normalise the differences in the cDNA concentration added in each PCR reaction (Sharma *et al.*, 2014). Therefore, the mRNA expression of this gene must remain consistent or stable between the samples. In this current project, the reference gene selected was the beta-2 microglobulin (β*2m*). Due to its often ubiquitous expression, β2m is a common candidate reference gene for RT-qPCR gene expression studies (Livak and Schmittgen, 2001; Moine *et al.*, 2018). Moreover, β2m was found to be highly expressed in the rat pulmonary artery.

5.2.4.7 Positive Controls

A positive control is normally used to confirm that the PCR assay process works, and that the reaction has been set up correctly. The positive control is adequate for the RNA quantification method to investigate the changes in the gene expression levels.

The endogenous ATP modulates the arterial blood pressure through the ligand-gated cation channel P2X receptors and the G protein-coupled P2Y receptors (Burnstock and Kennedy, 1985). The P2X receptors are present in the rat pulmonary artery (Liu *et al.*, 1989c) and upon the stimulation of the P2X receptors, this induces vasoconstriction of the rat pulmonary artery. Furthermore, P2X1 being the main P2X subunit which is expressed in the rat pulmonary artery smooth muscle cells, and its stimulation mediates the vasoconstriction of the small and large pulmonary arteries (i-Husain Syed *et al.*, 2010). Therefore, P2X1 was selected as a positive control for this study.

Guanine nucleotide-binding protein G (t) subunit alpha-1 isoform X1 (Gnat1) and guanine nucleotide-binding protein G (t) subunit alpha-2 (Gnat2) were used as a positive control.

5.2.5 Real-Time Polymerase Chain Reaction (RT-PCR)

5.2.5.1 PCR Primers for Tas2r Real-Time Quantitative PCR

A similar approach was carried out for designing the primers for the gene expression analysis by SYBR-green-based real-time quantitative PCR (RT-qPCR) and the following criteria was followed:

1. Amplicons size = 120 - 150 bp
2. The melting temperature (Tm) of primers kept between 58 - 63 °C; the ΔTm between forward and reverse primers was ≤ 1˚C
3. Primer length: 20 - 24 bases
4. Amplicon GC content: 45 - 65%

The details for the RT-qPCR primer sequences are provided in Table 5.2. All of the PCR primers were synthesised by Integrated DNA Technologies (Leuven, Belgium). Each of the primers was diluted in the DNase/RNase-Free molecular biology grade water to their appropriate concentrations and stored at -20˚C until required.

Table 5.2 Real-Time Quantitative PCR Primer Sequences for Rat *Tas2rs* Gene Expression Analysis

Rat Gene Symbol	Gene Symbol Alias	Primer sequence (5'-3')	Amplicon size (bp)
Tas2r119	Tas2r1	Forward CCATTCCTCACCCACTCTTT	126
		Reverse TTGCTGAAGTCTCTCTGCTATG	
Tas2r137	Tas2r3	Forward GGAAGCAGAGACACACAGAATA	144
		Reverse CAGAGAGAGAAGGAGCAGAAAG	
Tas2r108	Tas2r4	Forward GAACTGCTTGTATTGCGTGAAG	130
		Reverse GAGAGTGGTGAAGGCAGAAAT	
Tas2r107	Tas2r10	Forward GCTACCAACCTCAATATCCTCTAC	126
		Reverse CCACGAGGTAAGTAAGCATCC	
Tas2r123	Tas2r14	Forward GGCCCTTACCAGACTCATTTAT	123
		Reverse TCCACTACCCAGATAACACCTA	
Tas2r145	Tas2r31	Forward AGCTCTGTGTTGGTGGTATTT	123
		Reverse CGTTGACAGCTGGTCAGTTA	
Tas2r134	Tas2r34	Forward CTCTTCCTGCTGTCCGTTATC	126
		Reverse CAGCGACTTCAGAGCCATAG	
Tas2r144	Tas2r40	Forward	149

		TCGTGGTCTCGACCATAGAT	
		Reverse CTGTAGCAAGAGCCTGGAAA	
Tas2r126	Tas2r41	Forward CAGCGTCCTGTTCTGTATCAA	122
		Reverse CGATGAAGGACACCAAGATAGAG	
Tas2r143	Tas2r43	Forward CATATCAGCTACCGGGAACATC	124
		Reverse CACTGCGTGAGACAGGTAATAA	
Tas2r139	Tas2r39	Forward GTATCCAGAATAGGCCTCCAAAG	142
		Reverse CAGCAAACCAGAGGCTACAATA	
P2xr1		Forward CTATGTGGTGCGAGAGTCAGG	149
		Reverse TCTCCCCATACAGTCCGTGG	
Gnat1		Forward ACGAAGTGAACCGAATGCAC	150
		Reverse GAAAGCAGATGCTGAGGTGTG	
Gnat2		Forward GGATGTTTGACGTGGGAGGG	150
		Reverse GACTCATGCATGCGATTCACC	

5.2.5.2 cDNA Synthesis

A reverse transcriptase reaction was carried out with the same batch of the RNA samples that were used in RNA-seq. This was to synthesise single-stranded complementary DNA (cDNA) templates for use in the RT-PCR for assessing gene expression levels. The cDNA synthesis was conducted on the extracted rat RNA samples using the Tetro cDNA Synthesis Kit (Bioline, UK) in line with the manufacturer's instructions.

For the cDNA synthesis, up to 5 μg total RNA was added to oligo $(dT)_{18}$ primer (1μl) ,10 mM dNTPs (1μl), 5 x RT buffer (4 μl), RNase Inhibitor (1 μl), 20U/μl Tetro Reverse Transcriptase (1 μl), and DEPC-treated water up to 20 μl was added to a nuclease-free centrifuge tube. The tube was heated in a Model 480 thermal cycler (Applied Biosystems, Warrington, UK). at 45˚C for 60 minutes then 85 ˚C for 15 minutes This cDNA preparation was designed as "RT^{+}". The procedure used to synthesise cDNA from RNA is summarised in (Table 5.4).

A mock cDNA synthesis reaction was also carried out in parallel, in which the reverse transcriptase was replaced with 1 μl DEPC-treated water. This sample was denoted as RT^{-} and ran in PCRs as a control in parallel with the RT^{+} cDNA samples in order to identify any genomic DNA contamination of the RNA sample or polymerase chain reaction. As there would be no synthesis of a cDNA template for PCR, this sample should not produce an amplicon following the PCR. Should the PCR using this RT^{-} sample generate an amplicon, then it is likely that the template DNA could have come from carryover genomic DNA from the RNA extraction or contaminated DNA introduced somewhere in the workflow. The 20 μl cDNA reactions were diluted to 100 μl with 1x RT buffer and stored at -20˚C until required.

Table 5.3 Procedure for Synthesis of cDNA from RNA Samples

Reagents	RT+	RT-
Total RNA	Up to 5 µg	Up to 5 µg
Oligo $(dT)_{18}$ Primer	1 µl	1 µl
10 mM dNTP mix	1 µl	1 µl
5x RT buffer	4 µl	4 µl
RNase Inhibitor	1 µl	1 µl
Tetro Reverse Transcriptase (200u / µl)	1 µl	-
DEPC-treated water	to 20 µl	to 20 µl
Incubate at 45˚C for 60 min		
Terminate reaction at 85˚C for 15 min		
Chill on ice then store reaction at -20˚C		

5.2.5.3 Quantitative Real-Time Polymerase Chain Reaction (RT-qPCR)

RT-qPCR is used to allow the measurement of the expression levels of mRNAs from a tissue by detecting their respective cDNAs using the appropriate PCR primers. During the thermal cycling process, the transcribed target cDNAs are amplified and the fluorescent dye, SYBR-Green, binds to the double-stranded PCR amplicons. This allows the accumulating PCR products to be quantified at every cycle. For each 20 µl RT-qPCR reaction, 10 mM forward primer (1 µl), 10 mM reverse primer (1 µl), *Power* SYBR™ Green PCR 2x Master Mix (10 µl; Applied Biosystems, Paisley, UK), DEPC-treated water (7 µl), and 1µl of cDNA (RT^+ or RT^-) were added to a wells of a MicroAmp fast optical 96-well Reaction Plates (Applied Biosystems, UK). PCR No template controls (NTC) were also included where H_20 was added instead of RT^+ or RT^- cDNA. The thermal cycling of the plates and amplicon detection was conducted on a StepOnePlus Real-Time PCR System (Applied Biosystems, Paisley, UK) under the following cycling conditions: UDG activation for 2 min at 50˚C, followed by activation of the DNA polymerase for 2 min at 95˚C. This was followed by 40 cycles of amplification at 30˚C. 95 ˚C denaturation for 15 seconds and 60 ˚C combined annealing and extension for 60 seconds. At the end of the PCR cycling, a melt curve

analysis was performed in order to conduct a qualitative analysis of the amplification product. The Tas2r mRNA expression levels were presented as their threshold cycle (C_t) value and calculated using the Delta C_t method which is normalised by C_t of the reference gene. Three technical replicates were performed for the RT^+ samples and the biological samples were analysed in duplicates.

5.2.5.4 Delta Ct [ΔCt] Quantification Method

The ΔCt quantification method was selected to assess the expression levels of the Tas2r mRNAs using the Ct values obtained from the Tas2r target genes and the endogenous reference gene. To compare the expression levels in the samples, the following equation was used.

$$\Delta Ct = Ct_{(sample)} - Ct_{(reference\ gene)}$$

The Ct or threshold cycle value is the cycle number at which the fluorescence generated within a reaction crosses the fluorescence threshold, a fluorescent signal significantly above the background fluorescence. At the threshold cycle, a detectable amount of the amplicon product has been generated during the early exponential phase of the reaction. The threshold cycle is inversely proportional to the original relative expression level of the gene of interest.

5.2.6 Data and Statistical Analysis

Calculations and statistical analysis were performed using GraphPad Prism (version 5). The statistical analysis was performed using an unpaired Student's *t*-test where applicable. The data is reported as a mean ± standard error of the mean (s.e.m). The values of $P < 0.05$ were considered to be significant, and the *n* values representing the number of rats used.

5.3 Results

5.3.1 The genotyping analysis of theTas2rs in the Rat Pulmonary Artery Using Endpoint RT-PCR

Several studies have previously conducted endpoint RT-PCR to examine the expression of the TAS2Rs in the vascular systems. Sakai *et al.* (2016) reported the expression of the TAS2R108 in the mice aorta tissues. Another group of researchers conducted a study on the TAS2Rs and found that different TAS2R subtypes were expressed in the rat omental artery and the cerebral arteries (Chen *et al.*, 2017).

To verify the expression of the TAS2R transcripts in the rat pulmonary artery, all 11 of the Tas2rs (Tas2r119, Tas2r137, Tas2r108, Tas2r107, Tas2r123, Tas2r145, Tas2r134, Tas2r139, Tas2r144, Tas2r126, and Tas2r143) underwent endpoint PCRs. The results suggest that the transcripts of most of the TAS2Rs were detected in the rat pulmonary artery except the Tas2r137 and the size of the products corresponded to the predicted amplicon sizes (Figure 5.3). These results showed that the presence of these genes in the rat genomic DNA.

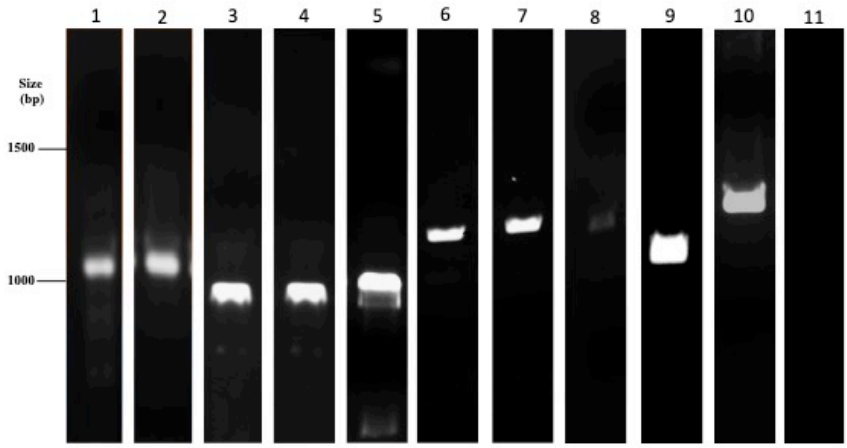

Figure 5.3 . The PCR Screening of the TAS2Rs in the Rat Pulmonary Artery.

Agarose gel electrophoresis of the DNA products from the rat pulmonary artery was conducted using oligonucleotide primers. The PCR products were separated on a 1% agarose gel containing ethidium bromide. All sets of the primers yielded a clear band except for the TAS2R137. Lanes1: M, DNA marker (size marker, measured in base pairs) was 200 bp (Hyperladder 1KB, Bioline.UK), 1, Tas2r119; 2, Tas2r145; 3, Tas2r126; 4, Tas2r123; 5, Tas2r139; 6, Tas2r 107; 7, Tas2r108; 8, Tas2r143; 9, Tas2r144; 10, Tas2r134; 11, Tas2r137. The quality and presence of the PCR products were repeated three times (n = 3).

5.3.2 RNA Concentration

The isolated total RNA quantity was verified by an average of A_{260}/A_{280} ratio of 2.08 ± 0.01 (n = 8). An absorption ratio (A_{260}/A_{280}) greater than 1.8 is usually considered an acceptable indicator for RNA (Sambrook, Fritsch and Maniatis, 1989). All of the extracted RNA samples were of an acceptable purity and yield ratios (Table 5.4).

Table 5.4 RNA Concentrations for the Rat pulmonary Artery Tissues.

	RNA concentration (ng/µl)	260/280	260/230
RNA of pulmonary artery tissue 1	154.5	2.02	1.68
RNA of pulmonary artery tissue 2	91.2	1.99	1.99
RNA of pulmonary artery tissue 3	320.2	2.07	1.51
RNA of pulmonary artery tissue 4	148.9	2.04	1.18
RNA of pulmonary artery tissue 5	433.9	2.09	1.09
RNA of pulmonary artery tissue 6	539	2.04	2.02
RNA of pulmonary artery tissue 7	223.3	2.05	1.73
RNA of pulmonary artery tissue 8	156.3	2.01	1.82

5.3.3 RNA Integrity Concentration

An important requirement for effective quantitative RNA analysis using RT-qPCR is the intact, good quality RNA. The low-quality RNA may affect the RNA expression results, therefore, the verification of the RNA integrity prior to the usage in the downstream RT-qPCR application provides a more precise and reliable results (Fleige *et al.*, 2006).

Following the isolation of the rat pulmonary arterial tissues, the RNA integrity test was conducted (n = 3). The RQI for the two pulmonary arterial tissues that dissolved in the RNA-Later were 8.6 ± 0.5 (n = 2), while the RQI for pulmonary arterial tissue dissolved in Qiazol was 7.1 (n = 1). These results suggested that the RNA-Later may

be better RNA stabilising agent than Qiazol. Furthermore, the RQI for the bronchial tissue dissolved in the RNA-Later was equal to 8.0 ± 0.2 (n = 2), while the RQI for the tongue tissue dissolved in RNA-Later was 9.15 ± 0.05 (n = 2). These findings suggested that the rat tongue has the most intact RNA among all of the tested tissues (Table 5.13).

The RNA integrity reports of a typical sample from this study are shown in the respective figures; the rat pulmonary artery incubated in RNAlater (Figure 5.4), rat pulmonary artery incubated in Qiazol (Figure 5.5), the rat bronchi (Figure 5.6) and the rat tongue (Figure 5.7).

Table 5.5 Different Tissues that were Used for the RNA Integrity Concentrations.

Tissue	Stored Solution	RNA Concentration (ng/µl)	28s/18s Ratio	RQI
Rat PA	RNA-later	178.38	0.94	9.1
Rat PA	RNA-later	147.95	0.90	8.1
Rat PA	Qiazol	162.49	0.86	7.4
Rat Bronchi	RNA-later	296.80	1.00	7.8
Rat Bronchi	RNA-later	76.74	1.06	8.2
Rat Tongue	RNA-later	408.33	1.26	9.1
Rat Tongue	RNA-later	382.33	1.21	9.2

RQI: RNA quality indicator

Well# 3 Rat PA (RNA LATER)

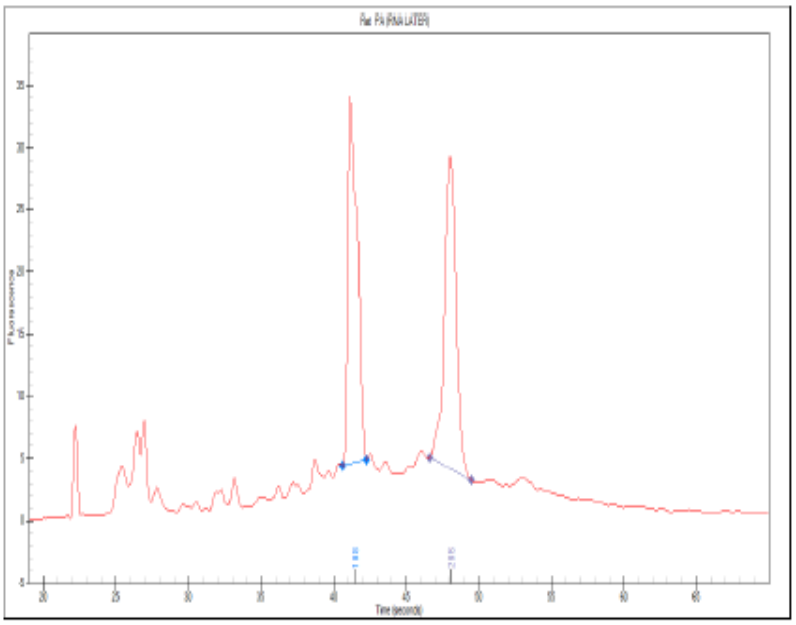

Well# 3 Rat PA (RNA LATER)					
Fragment Number	Fragment Name	Start Time	End Time	Area	% of Total Area
1	18S	40.60	42.30	53.55	16.19
2	28S	46.65	49.45	48.38	14.63

RNA Area: 330.79
RNA Concentration: 147.95 ng/µl
Ratio[28S/18S]: 0.90

RQI: 8.1

Figure 5.4 RNA Integrity Report for the Rat Pulmonary Artery Incubated in RNA-later.

The rat pulmonary artery tissue was stored in the RNA*later* ® solution and then the RNA of the pulmonary artery was extracted and purified using the Qiazol-based RNeasy Plus Universal Mini Kit. The RNA integrity was then confirmed using the Experion Automated Electrophoresis system. The RQI indicates the RNA quality, where 10 represents the intact RNA and 1 represents the degraded RNA sample. The ratio of 28s/18s was used to assess the quality of the total RNA purified from any given

sample and the higher ratio represented a purified RNA which is intact and has not been degraded.

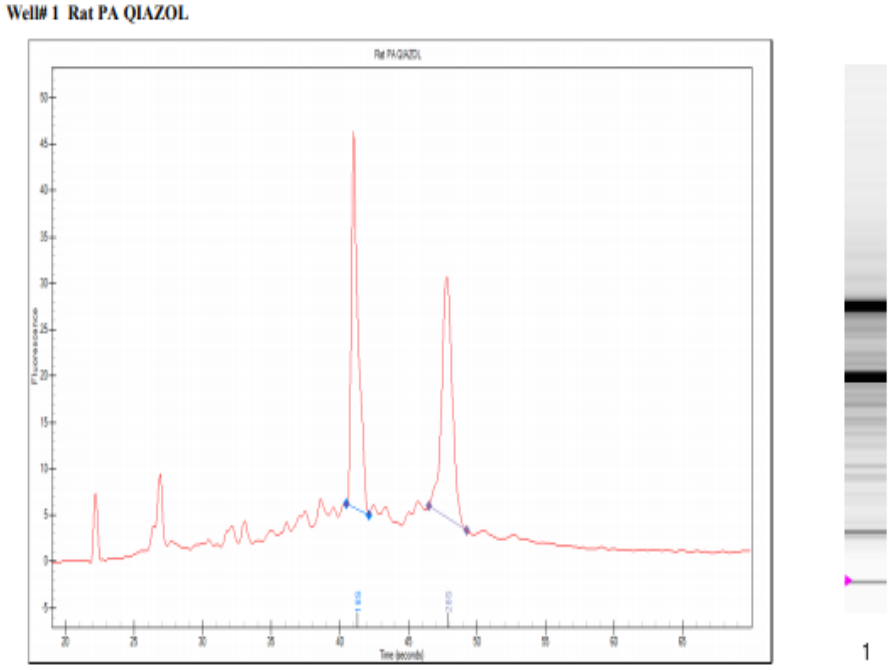

Well# 1 Rat PA QIAZOL

Fragment Number	Fragment Name	Start Time	End Time	Area	% of Total Area
1	18S	40.45	42.10	56.75	15.62
2	28S	46.50	49.25	48.95	13.48

RNA Area: 363.26
RNA Concentration: 162.48 ng/µl
Ratio[28S/18S]: 0.86

RQI: 7.4

Figure 5.5 RNA Integrity Report for the Rat Pulmonary Artery Incubated in Qiazol.

The rat pulmonary artery tissue was stored in the Qiazol® lysis and then the RNA of the pulmonary artery was extracted and purified using the Qiazol-based RNeasy Plus Universal Mini Kit. The RNA integrity was then confirmed using the Experion Automated Electrophoresis system. The RQI indicates RNA quality, where 10 represents the intact RNA and 1 represents the degraded RNA sample. The ratio of 28s/18s was used to assess the quality of the total RNA purified from any given sample

and the higher ratio represented a purified RNA which is intact and has not been degraded.

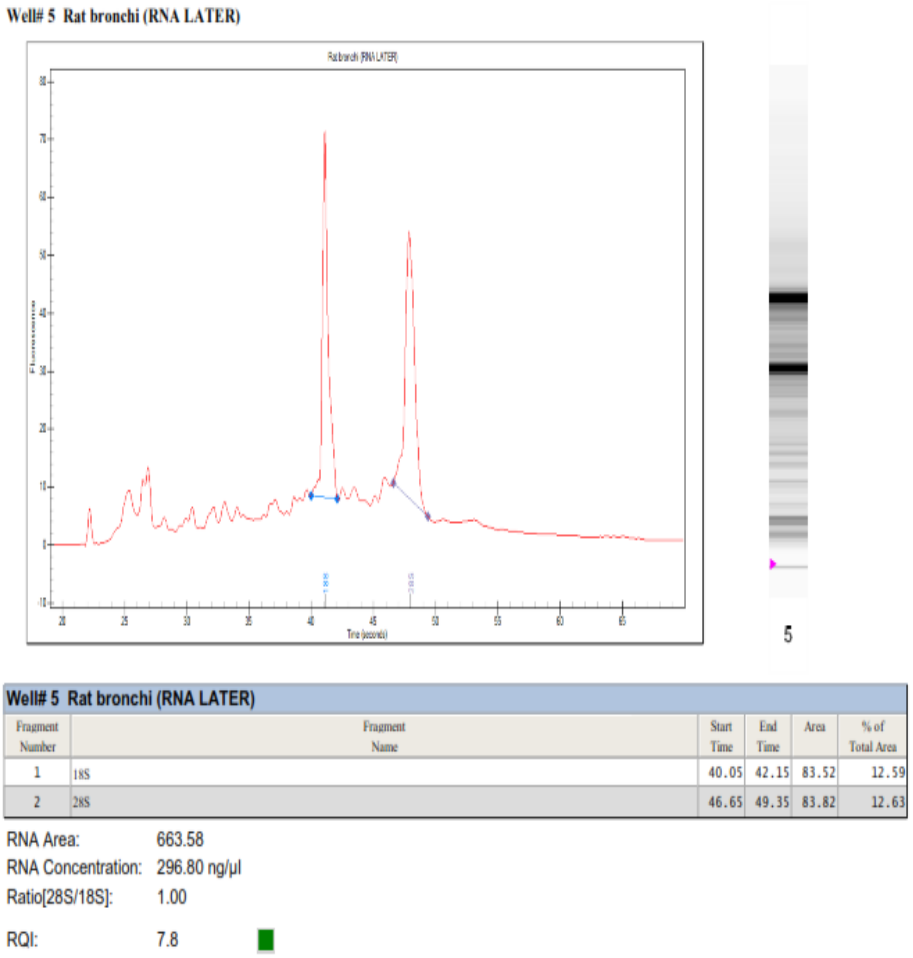

Well# 5 Rat bronchi (RNA LATER)

Fragment Number	Fragment Name	Start Time	End Time	Area	% of Total Area
1	18S	40.05	42.15	83.52	12.59
2	28S	46.65	49.35	83.82	12.63

RNA Area: 663.58
RNA Concentration: 296.80 ng/µl
Ratio[28S/18S]: 1.00
RQI: 7.8

Figure 5.6 RNA Integrity Report for the Rat Bronchi Incubated in the RNA-later.

The rat bronchi tissue was stored in the RNA*later* ® solution and then the RNA of the bronchi was extracted and purified using the Qiazol-based RNeasy Plus Universal Mini Kit. The RNA integrity was then confirmed using the Experion Automated Electrophoresis system. The RQI indicates the RNA quality, where 10 represents the intact RNA and 1 represents the degraded RNA sample. The ratio of 28s/18s was used to assess the quality of the total RNA purified from any given sample and the higher ratio represented a purified RNA which is intact and has not been degraded.

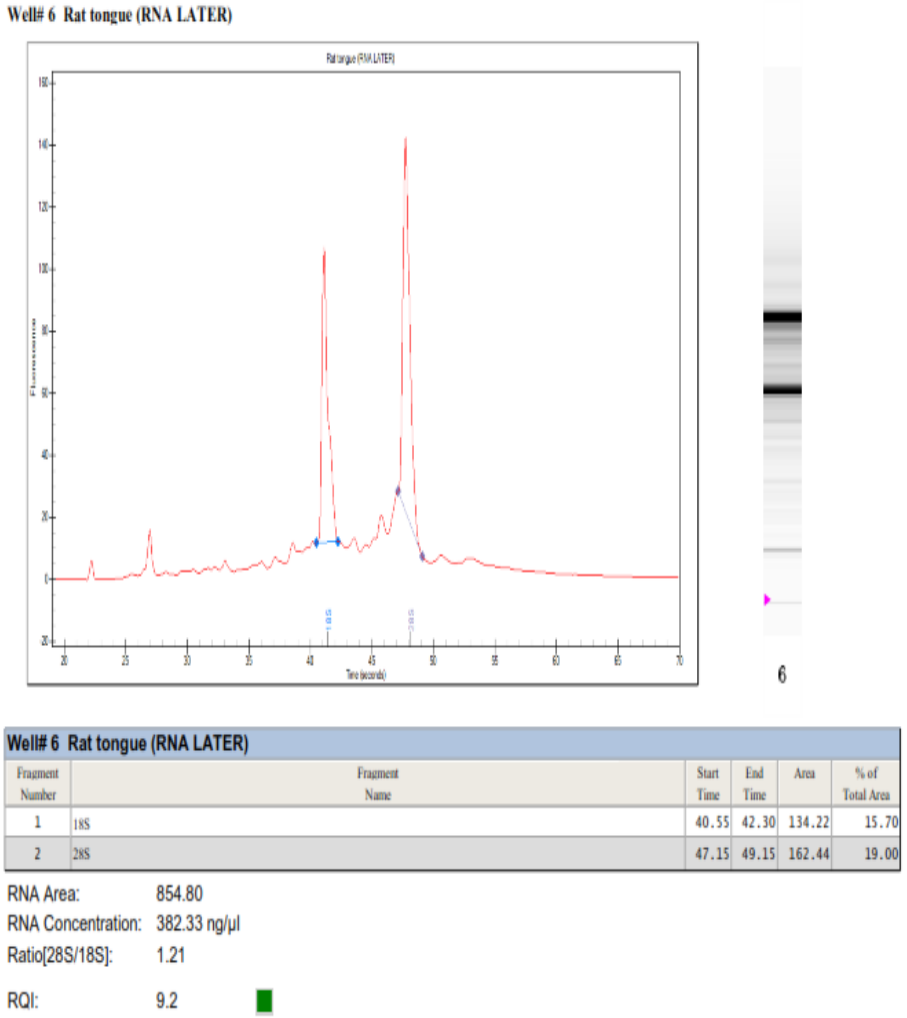

Well# 6 Rat tongue (RNA LATER)					
Fragment Number	Fragment Name	Start Time	End Time	Area	% of Total Area
1	18S	40.55	42.30	134.22	15.70
2	28S	47.15	49.15	162.44	19.00

RNA Area: 854.80
RNA Concentration: 382.33 ng/µl
Ratio[28S/18S]: 1.21
RQI: 9.2

Figure 5.7 RNA Integrity Report for the Rat Tongue Incubated in the RNA- later.

The rat tongue tissue was stored in the RNA*later* ® solution and then the RNA of the tongue was extracted and purified using the Qiazol-based RNeasy Plus Universal Mini Kit. The RNA integrity was then confirmed using the Experion Automated Electrophoresis system. The RQI indicates the RNA quality, where 10 represents the intact RNA and 1 represents the degraded RNA sample. The ratio of 28s/18s was used to assess the quality of the total RNA purified from any given sample and the higher ratio represented a purified RNA which is intact and has not been degraded.

5.3.4 Detecting the Expression of the Tas2rs in the Rat Pulmonary Arteries by Using RNA Sequencing Analysis

5.3.4.1 Gene Expression Analysis

In order to determine the expression of the TAS2Rs in the rat pulmonary artery, 20 µL of the RNA sample was subjected to the RNA sequence analysis. The resulting total gene number was 14,392, which included the 12,616 known gene numbers and the 1,776 novel gene numbers. The summary of gene expression results is shown in Table 5.10.

Table 5.6 Summary of the Gene Expression of the Rat Pulmonary Artery Sample.

Sample	Total Gene Number	Known Gene Number	Novel Gene Number	Total Transcript Number
Rat PA	14,392	12,616	1,776	18,393

Of the 14,392 gene numbers of the rat pulmonary artery sample, the highest level of expression was for the β2m which used as a reference gene. The expression level of the β2m was 640.73 FPKM. Moreover, the P2rx1 (positive control) was expressed in this sample by 136 FPKM and was approximately 4-fold less than the β2m. The expression level of the other two positive controls Gnat 1 and Gnat 2 were 1.34 and 3.57 FPKM respectively. Furthermore, among the different types of the Tas2rs, only the Tas2r108 and Tas2r139 were expressed in the rat pulmonary artery, and the expression levels of the Tas2r108 and Tas2r139 was 0.28 and 0.26 FPKM respectively. Additionally, the expression of TRPM5 was 0.79 (Table 5.11) (Figure 5.13).

Table 5.7 Expressed Gene Lists of Interest in the Rat Pulmonary Artery.

Symbol	Transcript_id(s)	FPKM
Tas2r108	NM_001024686	0.28
Tas2r139	NM_001080905	0.26
P2rx1	NM_001142367, NM_001285415, NM_012997	135.69
Gnat1	NM_001108780	1.34
Gnat2	NM_001108950	3.57
β2m	NM_012512	640.37
TRPM5	NM_001191896	0.79

Transcript_id (s): transcript list of the gene, separated by a comma. FPKM: fragments per kilobase of exon model per million mapped read of this gene.

5.3.5 Validation of the RNA Sequencing Analysis for Expression of the TAS2Rs in the Rat Pulmonary Arteries by Using RT-qPCR

5.3.5.1 Real-Time Polymerase Chain Reaction (RT-PCR)

The RT-qPCR was conducted in this study to validate the RNA-sequence expression results and to allow the conducting expression analysis across a greater number of biological replicates. The expression levels of the 11 Tas2r transcripts (Tas2r119, Tas2r137, Tas2r108, Tas2r107, Tas2r123, Tas2r145, Tas2r134, Tas2r139, Tas2r144, Tas2r126, Tas2r143) in the rat pulmonary artery tissues were assessed using RT-qPCR. The expression levels were then normalised using the β2m as the reference gene (Livak and Schmittgen, 2001) and the gene expression changes were determined using a ΔCt method.

RT-qPCR was conducted firstly on a representative sample (a purified RNA pulmonary artery sample that was used in RNA sequencing analysis and the rest was saved in -80 C˚). The representative sample's Ct values of the TAS2Rs cDNA were undetectable with the exception of the TAS2R108 and TAS2R139, and the mean Ct values for these were 36.1 and 36.6 respectively ($P > 0.05$). To confirm these findings, three different rat pulmonary arterial tissues were tested for each of the Tas2r transcripts and each sample was repeated three times using RT-qPCR. The Ct values of the majority of Tas2r s cDNA were undetectable across all of the samples with exception to the Tas2r108 and Tas2r139. The mean Ct value for the Tas2r 108 was 35.7 ± 0.4, while for the Tas2r139 was equal to 34.45 ± 0.4. Taken together, these results confirm that the expression of the Tas2r108 and Tas2r139 were detected in the different rat pulmonary tissues as well as in their representative samples.

The ΔCt value of the Tas2r108 for the mean of the three pulmonary arterial tissue was 12.5, while the ΔCt value of the Tas2r108 for the representative sample was 13.2. Moreover, the ΔCt value of the Tas2r139 for the mean of the three pulmonary artery tissues and the representative sample were 11.2 and 13.7 respectively (Table 5.8) and (Table 5.9). To compare between the Ct values and FPKM the 1/ΔCt was calculated, and the results are shown in (Figure 5.8).

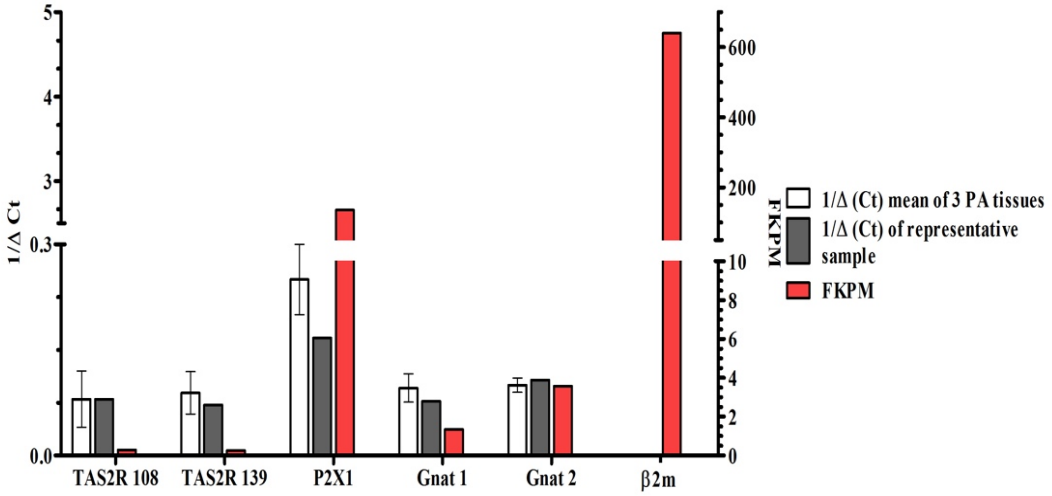

Figure 5.8 Histogram Showing the Expression of the Tas2r108 and Tas2r139, ß2M, P2X1, Gnat1, and Gnat2 in the Rat Pulmonary Artery.

The expression of the TAS2Rs in the rat pulmonary artery using both the RNA sequencing analysis ($n = 1$) and RT-qPCR ($n = 3$). The left Y-axis represents the 1/ΔCt, while the right Y-axis represents the FKPM. The expression levels were normalised using the β2m as the reference gene, and each sample was repeated three times ($P > 0.05$).

Table 5.8 Expression Levels of the Tas2r108, Tas2r139, β2M, P2X1, Gnat1 and Gnat2 in the Rat Pulmonary Artery.

	PA tissues			Representative sample			
	(Ct) Mean ± S.E.M	**ΔCt (Ct (sample) − Ct (reference gene))**	**1/ΔCt**	**Ct**	**ΔCt (Ct (sample) − Ct (reference gene))**	**1/ΔCt**	**FKPM**
Tas2r108	35.747 ± 0.440	12.492	0.08	36.164	13.228	0.08	0.28
Tas2r139	34.45 ± 0.356	11.195	0.089	36.64	13.704	0.072	0.26
P2X1	27.238 ± 0.055	3.983	0.25	28.9	5.964	0.167	135.69
GNAT1	33.577 ± 0.667	10.322	0.096	35.852	12.916	0.077	1.34
GNAT2	33.156 ± 0.112	9.901	0.1	32.254	9.318	0.107	3.57
β2m	23.255 ± 0.129	0		22.936	0		640.37

Table 5.9 Ct values for the Tas2r108, Tas2r139, Reference Gene and Positive Controls for All the Three Samples and Representative Sample.

	PA Tissue 1			PA Tissue 2			PA Tissue 3			Representative sample	
	Ct Mean	Ct Mean – β2M	S.E.M	Ct Mean	Mean – β2M	S.E.M	Ct Mean	Ct Mean – β2M	S.E.M	Ct	FKPM
Tas2r 108	35.7	13.63	0.24	36.46	15.26	0.33	35.07	8.57	0.73	36.16	0.28
Tas2r 139	34.45	12.38	0.17	33.42	12.22	0.63	35.89	9.39	0.25	36.64	0.26
P2X1	25.99	3.92	0.07	29.82	8.62	0.06	25.89	-0.60	0.02	28.9	135.69
GNAT1	33.53	11.46	0.14	34.94	13.74	1.09	32.26	5.76	0.76	35.85	1.34
GNAT2	32.82	10.75	0.07	29.89	8.69	0.03	36.75	10.25	0.23	32.25	3.57
β2M	22.07	0.000	0.02	21.2	0.000	0.04	26.49	0.000	0.31	22.93	640.37

5.4 Discussion

5.4.1 TAS2R Expression in the Rat Pulmonary Arteries

This study reported that TAS2Rs are expressed not only in taste buds but also in the pulmonary artery. Some of the bitter taste agonists in the pulmonary artery may influence the pulmonary function through their TAS2R chemical signalling mechanism. In the previous chapter of this study, the vasorelaxation activity of the bitter compounds was demonstrated on the rat pulmonary artery. This chapter provides evidence of the expression of the TAS2Rs in the rat pulmonary artery using two types of analysis RNA-seq and qRT-PCR. Therefore, these findings strongly supporting the concept that there is more than a ‘‘taste’’ function for TAS2Rs and that they exert non-gustatory functions outside the mouth, which might vary depending on the location of expression.

Some TAS2Rs are promiscuous and bind to a wide variety of bitter substances, whereas others have more specificity and bind to one or a few known bitter substances (Meyerhof *et al.*, 2010). In this study, The RNA sequencing analysis showed that TAS2R transcripts were detected in the rat pulmonary artery, and Tas2r108 Tas2r139 were identified as subtypes that could be involved in the relaxation of the rat pulmonary artery. The level of expression of Tas2r108 and Tas2r139 considers low expression in comparison to the internal control β2m and the RT-PCR analysis confirmed these results.

Tas2r108 and Tas2r139 are both have an intermediated tuned and can bind to 6–16 known bitter compounds including quinine and denatonium. This is supported by Meyerhof et al. (2010) who reported that the majority of TAS2Rs appear to have intermediate promiscuity. Interestingly, TAS2R108 was expressed in the blood vessels in some studies; TAS2R108 was identified in the mouse aorta using RT-PCR and gel electrophoresis, and stimulation of the TAS2R108 using denatonium caused an inhibition of the phenylephrine pre-contracted mice aorta (Sakai et al., 2016). Moreover, the TAS2R108 was investigated in the rat mesenteric arteries and cerebral arteries through agarose gel electrophoresis and RT-PCR (Chen et al., 2017).

The TAS2R108 have been also detected in several tissues (Janssen *et al.*, 2011). In the gastrointestinal tract, the TAS2R108 was identified in the mouse cultured enteroendocrine cell line STC-1 using RT-PCR. Similarly, TAS2R108 was detected in mouse gastrointestinal tissue (fundus, atrium, and duodenum) (Wu, Chen and Rozengurt, 2005). Upon the addition of 10mM of denatonium, (a known ligand for TAS2R108) on the cultured mouse enteroendocrine cell line STC-1 which were loaded with Fura-2 AM (Fluorescence Ca^{2+} indicator) this induced a marked increase in the $[Ca^{2+}]_i$ measured in 97% of the enteroendocrine cell line STC-1 cells examined (Wu *et al.*, 2002). Furthermore, stimulation of the STC-1 cells with denatonium also induced an increase of the $[Ca^{2+}]_i$ which then triggered the release of cholecystokinin (CCK) (Chen *et al.*, 2006). Additionally, the TAS2R108 was detected by another group who conducted RT-PCR. They showed that the mRNA of the TAS2R108 was expressed in the mouse stomach, colon and small intestine (Vegezzi *et al.*, 2014). TAS2R108 was detected in mouse ileum and colon using RT-PCR and gel electrophoresis (Sakai *et al.*, 2016). In the airway, the TAS2R108 was detected in the mouse trachea using RT-PCR (Krasteva *et al.*, 2011). In the male reproductive tissues, TAS2R108 was found in the mouse testis. The bitter taste agonists induced an increase in the $[Ca^{2+}]_i$ in the male germ cells. Each individual male germ cells induced different ligand activation profiles. Indicating a unique expression subset of the TAS2Rs in each of the germ cells. These findings indicate that TAS2Rs play a crucial role in spermatogenesis (Xu *et al.*, 2012). In the heart, Foster *et al.* (2013) showed that the TAS2R108 were detected in the rat and mouse heart using RT-qPCR. Moreover, they studied the developmental regulation of the TAS2Rs expression in the heart throughout the lifespan of the rats. They found the expression of the TAS2R108 in the rat heart tissue to decrease with age. In a follow-up study, stimulation of the TAS2R108 using sodium thiocyanate agonist infusion elicited a 30 to 40% decrease in the left ventricle developed pressure and systolic pressure, as well as a steady increase in the aortic pressure of the mouse heart (Foster *et al.*, 2014).

In this study, RNA-seq data showed that the expression of the taste-related gene TRPM5 suggests that TAS2Rs are functional in the pulmonary artery and that their

signaling mechanisms may be via G protein-dependent pathway. As bitter taste agonists induced their action through different pathways, one possible pathway would involve activation of GPCR through PLCβ and leading to the opening of TRPM channel and the depolarizing the cells and subsequent Na^+ release. Moreover, expression of TRPM5, perhaps suggesting some similarity between the pathway elicited in the pulmonary artery and the final steps of the gustatory pathway. Interestingly, RNA-seq results showed that GNAT3, a gene encoding for the α-subunit of the taste-associated G protein gustducin, did not express in the rat pulmonary artery.

Based on the homology between TAS2R in rats and humans (http://www.ncbi.nlm.nih.gov/homologene/), human TAS2R subtype TAS2R14 and the corresponding homologous rat TAS2R subtype is TAS2R123, which is broadly tuned and can bind to 33 known bitter compounds (Lossow et al., 2016; Meyerhof et al., 2010), did not expressed in the pulmonary artery. human TAS2R subtypes TAS2R1 and TAS2R10, and the corresponding homologous rat TAS2R subtypes Tas2r119 and Tas2r107, which bind to dextromethorphan, did not express in the rat pulmonary artery. The rest of the TAS2Rs transcripts were not detected in the rat pulmonary artery. This could be due to the low copy number or low expression the TAS2R genes in the rat pulmonary artery.

In considering the bitter taste agonists that have been identified; it is important to recognise that they may have other molecular targets in addition to TAS2R. For example, denatonium is an agonist for TAS2R but is also have an α-adrenoreceptor antagonist with an affinity for several other families A GPCRs (Manson *et al.*, 2014). Nevertheless, given the huge number of agonists for these TAS2Rs that have already been characterised, extra-oral TAS2R expressions seem to be promising therapeutic targets for different diseases, the most studied being asthma (Deshpande *et al.*, 2010). Though, it needs to be highlighted that the wide range of expression of TAS2Rs also implicates that many side effects might occur. Extra-oral TAS2Rs might be responsible for many side-effects of drugs in clinical use, given that many drugs have a bitter taste (Ansoleaga *et al.*, 2013; Clark, Liggett and Munger, 2012). Thus, in the drug development, it is important that TAS2Rs have main pharmacological properties including specificity for a receptor with a clear and narrowly tuned expression pattern.

Chapter 6

General Discussion and Conclusion

The results from this research project have improved our understanding of the effect of bitter taste agonists on the rat pulmonary artery. This study has helped examine the mechanisms involved in producing their effect as well as which TAS2Rs transcripts are expressed in the pulmonary artery. The studies have shown that quinine, denatonium and dextromethorphan all produced an endothelium-independent vasorelaxation in a concentration-dependent manner of pre-contracted rat pulmonary artery tissues, and so might contribute, in addition to other factors, to the regulation of the pulmonary circulation. Moreover, these bitter taste agonists reversibly induced vasorelaxation in the rat pulmonary artery rings pre-contracted by phenylephrine, which indicated that they appear to have no detrimental effect on the tissue over the concentration range used. Furthermore, this study suggests that the blocking of BKca channel had no effect on these agonists-mediated relaxations of the rat pulmonary artery tissues. Also, this project has expanded our knowledge of the underlying Ca^{2+} signaling pathways. It revealed that quinine, denatonium, and dextromethorphan attenuated the ATP-mediated increase in $[Ca^{2+}]_i$, suggesting that quinine, denatonium, and dextromethorphan may partially block ROCC in freshly isolated pulmonary artery SMCs. Additionally, dextromethorphan-induced increases in $[Ca^{2+}]_i$ in the rat pulmonary artery isolated SMCs include two mechanisms: one that is extracellular in nature and occurs partially via the VDCC, and a second one that is mainly derived from intracellular Ca^{2+} stores via the PLC–IP_3 pathway. These findings are further supported by molecular studies, which revealed that *Tas2r108* and *Tas2r139* are expressed in the rat pulmonary artery.

6.1 Role of Bitter Taste Agonist in Vasorelaxation

Pulmonary arterial hypertension is a progressive and potentially fatal disease and is a major health care concern due to its poor prognosis, high mortality rate and the absence of therapeutic treatment (Sirnes *et al.*, 2009; Ryerson *et al.*, 2010). Current medications often prescribed for hypertension are calcium channel blockers. Current pulmonary arterial hypertension guidelines suggest that the efficacy of calcium channel blockers is limited to only a small percentage of patients who show a significant acute response to calcium channel blockers or other vasodilators. Administration of prostacyclin

analogues have been central to the main therapeutic approaches for the treatment of pulmonary artery hypertension for approximately two decades (McLaughlin *et al.*, 2015). Epoprostenol was the first prostacyclin treatment approved by the FDA for pulmonary artery hypertension (Barst *et al.*, 1996). However, prostacyclins have low stability, many side effects, and are complex therapies that need to be administered by healthcare professionals who have expertise in complicated delivery systems (Baliga, MacAllister and Hobbs, 2011). Endothelin receptor antagonists act by selectively blocking endothelin-A receptors or by blocking both endothelin-A and -B receptors. Bosentan, a non-selective endothelin-A and -B receptor antagonist has been widely used in patients with pulmonary artery hypertension. Nevertheless, a monthly follow-up monitoring of the liver enzyme functions is highly recommended by the FDA for patients who used bosentan (Lourenço *et al.*, 2012; McLaughlin *et al.*, 2015). As such, there is a constant drive to seek new more effective therapeutics for pulmonary arterial hypertension patients (Badesch *et al.*, 2007; Galiè *et al.*, 2009).

Chloroquine is a synthetic bitter taste agonist and is mainly known for its use in the treatment of malaria (White, 1996). In addition to anti-malarial effect, chloroquine-induced vasodilation and decreased blood pressure in human subjects for treatment of malaria (Anigbogu *et al.*, 1993; Looareesuwan *et al.*, 1986) and also in animals (McCarthy *et al.*, 2016; Musabayane, Ndhlovu and Balment, 1994). In order to clarify the mechanisms behind the effect of chloroquine on vascular systems, a number of *in vitro* studies were conducted. For example, Aziba (2003) found that treatment with chloroquine-induced concentration-dependent relaxation of thoracic aortic tissue pre-contracted with KCl or norepinephrine. In another example, a study conducted by Manson *et al.* (2014) showed that chloroquine-induced relaxation in human pulmonary artery pre-contracted by phenylephrine or U46619. This vasorelaxation followed by chloroquine treatment was believed to be due to the blocking of VDCC (Manson *et al.*, 2014; Sai *et al.*, 2014). Long *et al.* (2013) found that chloroquine treatment prevented pulmonary vascular remodelling and inhibited the development of monocrotaline (MCT)-induced pulmonary hypertension in rats. Furthermore, chloroquine inhibited proliferation in pulmonary artery smooth muscle cells in MCT-pulmonary hypertension rats both *in vitro* and *in vivo* (Long *et al.*, 2013). Wu *et al.*

(2017) reported that intraperitoneal injection of hypoxic rats with chloroquine (50 mg/kg, daily for 3 weeks) significantly reduced the small pulmonary artery wall thickness, in comparison with the hypoxic rats. They also found that the pulmonary artery wall area and the ratio of pulmonary artery wall area to vessel external area were significantly decreased after chloroquine treatment, compared with a vehicle under hypoxic conditions in rats, indicating that chloroquine attenuated pulmonary artery remodelling in hypoxia-induced pulmonary hypertension. Furthermore, they reported that chloroquine can inhibit the progression of established pulmonary hypertension in the Sugen 5416/hypoxia (SuHx) pulmonary hypertension rat model (Wu *et al.*, 2017). Additionally, Wu *et al.* (2017) reported that long term treatment (48 hours) with 20 μM chloroquine inhibited cell proliferation of the human pulmonary artery smooth muscle cells. Therefore, chloroquine could have therapeutic potential in pulmonary hypertension due to a vasodilator effect, anti-remodelling, anti-proliferative effect, as well as an ability to reduce the development and progression of experimental pulmonary hypertension animal models.

The bitter tasting quinine, derived from the cinchona bark, is considered as one of the best-known anti-malarial drugs (White, 1996) and it is one of the bitter taste agonist used in this study. This *in vitro* study, utilizing organ bath experiments provides evidence that quinine-induced a concentration-dependent relaxation of rat aorta and pulmonary artery rings pre-contracted with phenylephrine. The data obtained in this work supports earlier studies; quinine-induced relaxation of phenylephrine pre-contracted guinea pig aorta (Manson *et al.*, 2014). Additionally, a number of *in vivo* studies have reported this vasodilatory effect, quinine-induced vasodilation and a decrease in blood pressure in dogs with experimental hypertension (Hiatt, 1948). Moreover, parenteral administration therapeutic doses of quinine produced forearm vasodilatation and reduced mean arterial blood pressure in humans (Schmid *et al.*, 1974; Mariano, Schomer and Rea, 1992).

Likewise, in this project, denatonium has shown that it had a vasorelaxant effect on the rat aorta and pulmonary artery. This supports a number of studies which have found this effect on tissues from a variety of species; Manson *et al.* (2014) and Xin and Chen (2017) showed that denatonium was able to induce a concentration-dependent

relaxation of guinea pig aorta and. The antihypertensive effect of denatonium has also been shown in rats and mice; An *in vivo* study reported that treating rats with denatonium had a transient and significant drop in blood pressure (Lund *et al.*, 2013). Moreover, another *in vivo* study showed that mice treated with denatonium (30 mg/kg, *i.p.*) had lowered systolic, diastolic, and mean blood pressures (Sakai *et al.*, 2016).

Furthermore, in this project, dextromethorphan also showed that it has a vasorelaxant effect on the rat pulmonary artery. This is supporting the work of Manson *et al.* (2014), which reported that dextromethorphan-induced a relaxation of phenylephrine pre-contracted human pulmonary arteries. *In vivo*, dextromethorphan had an antihypertensive effect on hypertensive rats which led to a significant reduction in their blood pressure (Wu *et al.*, 2012).

Generally, not all patients suffering from pulmonary hypertension respond to conventional therapies such as prostacyclin receptor activators, NO-cyclic GMP enhancement or endothelin receptor antagonism. Currently, there are no bitter taste agonists used to treat pulmonary hypertension. Much more work is required to investigate their potential for such a role. If successful they could be an additional option for treatment of pulmonary hypertension in the future. Realistically, however, these bitter taste agonists could face many obstacles in their use here such as efficacy, adverse drug response, and specificity.

6.2 Mechanisms of Bitter Taste Agonist-Induced Vasorelaxation of Rat Pulmonary Arteries

The mechanism of action of bitter taste agonists in pulmonary artery is still uncertain, in order to build a better understanding, this study investigated the involvement of endothelium layer in bitter taste agonists induced vasorelaxation. It is commonly well-known that the presence of endothelium layer is essential in endothelium-dependent vasorelaxation (Mitchell *et al.*, 2008). Moreover, endothelium-derived mediators are often involved in the mechanism of relaxation of the vascular system (Furchgott, 1983). Several studies have examined the role of endothelium in bitter taste agonists induce vasorelaxation; guinea-pig aorta (Manson *et al.*, 2014), rat thoracic aorta (Sai

et al., 2014) and porcine pulmonary artery (Upadhyaya *et al.*, 2014). In the current study, in order to examine whether the bitter taste agonist effect is dependent on the presence of the endothelium, the relaxant response was measured in the absence of the endothelium. A modified wooden cocktail stick was initially used to remove the endothelium from the rat pulmonary artery. It has been used as a common method to remove endothelium in different studies among different species; in the rabbit aorta (Furchgott, 1981, 1983), rat aorta (Roy *et al.*, 1995), guinea-pig pulmonary artery (Satoh and Inui, 1984) and rat pulmonary artery (Shahbazian *et al.*, 2007).

In this study, carbachol was used as an experimental tool to assess the presence or absence of endothelium in the rat pulmonary artery. Carbachol is a muscarinic receptor agonist, has shown to trigger the release of endothelium-derived relaxing factor (EDRF) such as NO (Bolton, Lang and Takewaki, 1984). The current study showed that quinine, denatonium, and dextromethorphan relaxed the rat pulmonary artery rings despite mechanical removal of the endothelium, suggesting that vasorelaxant activity of these bitter agonists are endothelium-independent. The endothelium-independent vasorelaxation of bitter taste agonists was also reported in some studies; in guinea pig aorta (Manson *et al.*, 2014) and rat thoracic aorta (Sai *et al.*, 2014).

The canonical taste transduction cascade downstream of receptor activation shares common components; involving the heterotrimeric G protein subunits, Gα (also called gustducin or GNAT3), Gβ and Gγ, PLCβ_2, and a transient receptor potential ion channel, TRPM5 (Pérez *et al.*, 2002). There have been a number of studies on the activation of GPCRs that participate in the bitter signal transduction mechanism for bitter taste agonists. One possible mechanism involves G-protein-mediated activation of PLC$_{\beta 2}$ through Gβγ (Akabas, Dodd and Al-Awqati, 1988; Hwang *et al.*, 1990; Spielman *et al.*, 1994; Ogura, Mackay-Sim and Kinnamon, 1997; Nakashima and Ninomiya, 1998; Asano-Miyoshi, Abe and Emori, 2000; Clapp *et al.*, 2001; Ogura, Margolskee and Kinnamon, 2002), PLC$_{\beta 2}$ catalyses an increase in DAG and IP_3, IP_3 then activates IP_3R in the SR, resulted in Ca^{2+} from internal store may lead to the activation of TRPM5 or may cause neurotransmitter release (Sawano *et al.*, 2005; Akiyoshi *et al.*, 2007).

In the present study, Gβγ inhibitor gallein was used to investigate the role of Gβγ subunit in bitter taste agonists-mediated rat pulmonary artery vasorelaxation. The presence of gallein, did not affect the relaxant effect produced by quinine, denatonium or dextromethorphan in rat pulmonary artery. These results suggest that the Gβγ-subunit may not be involved in the mechanism of action of bitter taste agonists in the pulmonary artery. These findings support the work by Sai *et al.* (2014) who reported that Gβγ-subunit is not involved in chloroquine-induced relaxation of pre-contracted rat thoracic aortic smooth muscle.

Activation of the bitter taste agonists conical cascade pathway also involved Gα, gustducin, which activates phosphodiesterase (PDE), causing a decrease in intracellular cAMP (Ruiz-Avila *et al.*, 1995; Wong, Gannon and Margolskee, 1996; Ming, Ruiz-Avila and Margolskee, 1998). The Gα subunit has an important role in taste transduction and is frequently used as a genetic marker to identify taste receptor-like cells and signaling pathways in non-gustatory tissues (Foster *et al.*, 2014). Moreover, quinine has been reported to activate the Gα subunit (Naim *et al.*, 1994; Peri *et al.*, 2000). Furthermore, *in vivo* study demonstrated that Gα subunit knockout mice exhibited significantly reduced behavioral and/or nerve responses to the bitter compounds; including denatonium and quinine (Wong, Gannon and Margolskee, 1996). Thus, the vasorelaxatory effect of bitter taste agonists in the rat pulmonary artery could be related to the Gα subunit.

While both above mechanisms generally depending on signaling cascade initiated by GPCRs, different studies reported that GPCRs are not required for bitter taste agonists signaling transduction. For example, quinine directly blocks voltage-gated K^+ channels in mudpuppy taste cells (Bigiani and Roper, 1991; Kinnamon and Roper, 1988), resulting in membrane depolarization and transmitter release.

Therefore, in this study, we hypothesis that activation of K^+ channels may be involved in the bitter taste agonists-mediated relaxation of rat pulmonary artery. K^+ channels are a group of membrane proteins that selectively allow enter of K^+ across the cell membrane (Brayden, 1996). K^+ channels are an important regulator of arterial SMCs due to their effect on the membrane potential (Nelson and Quayle, 1995). The opening

of these channels in the artery SMCs lead to K^+ efflux and then they cause membrane potential hyperpolarisation and this closes voltage-dependent Ca^{2+} channels and then lead to decrease Ca^{2+} entry and subsequently vasodilation (Nelson and Quayle, 1995). There are four distinct types of K^+ channels that are known to be present in the vascular smooth muscle: these are Ca^{2+}-activated K^+ (BK_{Ca}) channels, voltage-dependent K^+ (K_v) channels, ATP-sensitive K^+ (K_{ATP}) channels, and inward rectifier K^+ (K_{ir}) channels. BK_{Ca} and a range of K_v channel subtypes are expressed in the pulmonary artery smooth muscle, which is the subject of this project (McCulloch, Osipenko and Gurney, 1999). The role of BK_{Ca} channels have been investigated in bitter taste agonist-mediated effects; in the airway smooth muscle, Zhang *et al.* (2012) reported that the BK_{Ca} channels are activated by chloroquine to exert its relaxing effect. However, in the rat pulmonary artery, Wu *et al.* (2017) showed that block of BK_{Ca} and K_V channels had no significant effect on the relaxation induced by chloroquine. TEA, which acts as a non-selective K^+ channel blocker that blocks K_v and BK_{Ca} channels, was used to investigate the role of K^+ channel in bitter taste agonist-mediated vasorelaxation (Cook, 1989; Wu *et al.*, 2017). It was reported that if the concentration of the TEA more than 1 mM is required to block other K^+ vascular channels. Whereas, TEA in concentrations of 1 mM or less is a relatively selective blocker of BK_c (Langton *et al.*, 1991). In this study, the concentration was used 1 mM TEA; therefore, it was a mainly selective blocker of $BK_{ca.}$

Likewise, iberiotoxin, which is a selective and potent BK_{ca} channel blocker (Wallner *et al.*, 1995), has been used in several studies to investigate the role of BK_{ca} in the bitter taste agonists-mediated effects. Grassin-Delyle *et al.* (2013) showed that 100 nM iberiotoxin did not inhibit the relaxation induced by chloroquine in human isolated bronchi. Moreover, in the gastrointestinal tract, iberiotoxin did not have a significant effect on the chloroquine-induced inhibition of the longitudinal muscle strips of rat ileum (Jing *et al.*, 2013). Also, in the aortic blood vessel, iberiotoxin decreased the potency of denatonium and chloroquine without affecting their maximum relaxation (Manson *et al.*, 2014). However, these effects were not considered to be actual inhibition of bitter taste agonist-mediated relaxation, but rather the consequence of the increased pre-contraction that developed in the presence of iberiotoxin (Suarez-Kurtz,

Garcia and Kaczorowski, 1991). In this study, neither TEA nor iberiotoxin had a significant effect on the relaxation response induced by either quinine, denatonium or dextromethorphan in the rat pulmonary artery. Hence, this study, therefore, provides further support to previous observations that the opening of BK_{ca} channels cannot explain the relaxations induced by bitter taste agonists.

In this study, the remaining G-protein-independent signal transduction of bitter taste agonists-induced pulmonary artery vasorelaxation are still uncertain but may be related to Ca^{2+} entry mechanisms from the extracellular space. Therefore, the present work was aimed to further understand the effects of these agonists on the vascular smooth muscle in order to shed more light on the mechanisms of the vasorelaxant action of these compounds on rat pulmonary artery rings.

As quinine relaxed the rat pulmonary artery rings, one possible explanation for it's observed effect is that it is blocking Ca^{2+} channels. Voltage-dependent Ca^{2+} channels have been sub-classified into L, N, and T types (Bean, 1989; Triggle, Langs and Janis, 1989). The L-type VDCC is the major Ca^{2+} channel for Ca^{2+} influx upon depolarization in the VSMCs (Karaki *et al.*, 1997). Bay K 8644, a VDCC activator, was used to examine the role of VDCC in bitter taste agonist-mediated effects on the airway smooth muscle. Grassin-Delyle *et al.* (2013) reported that the involvement in VDCC is not sufficient to fully explain the bitter taste agonists-induced bronchorelaxation of the human bronchi tissue. On the other hand, in the gastrointestinal tract, Chen *et al.* (2006) showed that bitter taste agonists increase $[Ca^{2+}]_i$ and cholecystokinin release through mediated Ca^{2+} influx by the opening of L-type VDCC in enteroendocrine STC-1 cells.

The results from Ca^{2+} signaling studies showed that quinine decreased the ATP-mediated increase in $[Ca^{2+}]_i$, suggesting that quinine may partially block VDCC in freshly isolated rat pulmonary artery SMCs. A number of studies supported that quinine inhibits KCl-induced contractions in the rat and rabbit aorta (Cook, Griffiths and Hoff, 1987) in addition to angiotensin II-stimulated contractions in rabbit aorta (Cook, Griffiths and Hoff, 1987). Moreover, quinine also shifts the $CaCl_2$-force response to the right in depolarised guinea pig taenia coli (Spedding and Berg, 1985).

Additionally, quinine produced concentration-dependent relaxation of KCl-contracted rat aortic rings (del Pozo *et al.*, 1996). Taken together, these findings suggest that quinine might inhibit Ca^{2+} influx through VDCC in smooth muscle.

Pulmonary vasoconstriction is a main factor of pulmonary hypertension (Cogolludo, Moreno and Villamor, 2007). $[Ca^{2+}]_i$ is a major trigger for pulmonary vasoconstriction, whereas reduction in the amount of $[Ca^{2+}]_i$ tends to reduce contraction force. This is the basic mechanism of the clinical anti-hypertension medications being used in various hypertension. Extracellular and intracellular Ca^{2+} are both contribute to the increase in $[Ca^{2+}]_i$ (Gibson *et al.*, 1998). Particularly, in VSMCs, removal of extracellular Ca^{2+}, the use of inhibitors of SR Ca^{2+} uptake and blockade of L-type calcium channels are important tools to distinguish which source is providing Ca^{2+} to the cell for functional responses. This underlines the possibility that bitter ligands might also stimulate other signaling pathways through TAS2R activation. TAS2R studies predominantly depend on Ca^{2+} to determine the activity of bitter taste agonists. Therefore Ca^{2+} studies were conducted in this study to investigate the role of bitter taste agonists on the $[Ca^{2+}]_i$.

In this project, Ca^{2+} studies revealed that quinine, denatonium, and dextromethorphan attenuated the ATP-mediated increase in $[Ca^{2+}]_i$ in freshly isolated pulmonary artery SMCs, suggesting that these bitter taste agonists may partially block ROCC. Involvement of these channels in the rat pulmonary artery was supported by Wu *et al.* (2017) who showed that treatment with chloroquine inhibited the magnitude of the ATP-induced increases in $[Ca^{2+}]_i$ in human pulmonary artery SMCs. Taken together, further studies are needed to specify the types of Ca^{2+} that can be blocked by these agonists and to define the precise mechanisms by which they exert their inhibitory effect on Ca^{2+} channels in pulmonary artery SMCs.

Some of bitter taste agonists have dual mechanisms of actions; GPCR-dependent and GPCR-independent mechanisms. For example, the quinine-induced increase in $[Ca^{2+}]_i$ in PC cultured cells includes two main mechanisms: one that is extracellular in nature and occurs via L-type and/or T-type Ca^{2+}channels, and a second that is due to release of Ca^{2+} from intracellular stores via the PLC–IP_3 pathway (Akiyoshi *et al.*, 2007).

Similarly in this study, dextromethorphan-induced increases in $[Ca^{2+}]_i$ in the pulmonary artery isolated SMCs seems to have two mechanisms of action involving; mainly from intracellular Ca^{2+} stores via the PLC–IP_3 pathway, and the extracellular in nature partially via VDCC.

6.3 Expression of TAS2Rs in the Rat Pulmonary Artery

TAS2Rs are expressed in a wide range of tissues including the gastrointestinal tract, brain, airways, and cardiac muscle (Table 1.2 in Chapter 1). The extra-oral expression of TAS2Rs strongly suggests the existence of endogenous ligands, which remain to be discovered. However, in most tissues, it is still not clear which TAS2R variants mediate their effects. The use of molecular biology techniques, such as RNA-seq and qRT-PCR, helped identify the expression of TAS2R variant expression profile of the rat pulmonary airway.

In this study, RNA-seq analysis on the rat pulmonary artery found that low-level expression of the Tas2r108 and Tas2r139 transcripts. A low expression of these two Tas2r subunits in this study is in agreement with the qRT-PCR analysis that exhibited a low expression level. Similar to many other GPCRs, Tas2rs are usually expressed at low levels. However, because GPCRs utilize a great intracellular amplification cascade for signaling mechanisms, high expression levels are not required for them to exert their physiological effects (Clark, Liggett and Munger, 2012). Previously, Sakai et al. (2016) demonstrated the expression of Tas2r108 mRNA in a number of mouse tissues including the thoracic aorta. Moreover, another study conducted by Chen et al. (2017) showed that the mRNA for Tas2r108 was detected in the rat cerebral and mesenteric arteries. Furthermore, TAS2R4, homologous to rat Tas2r108, and TAS2R39, homologous to rat Tas2r139, were expressed in human pulmonary artery SMCs (Wu et al., 2017).

Human TAS2R4 and TAS2R39, have an intermediate tonicity and can bind to 6–20% of known bitter compounds (Meyerhof et al., 2010). Two of bitter taste agonists used in this study are known to bind to TAS2R108 and TAS2R139; quinine binds to TAS2R108 and TAS2R139, whereas denatonium can bind to TAS2R108 (Table 1.1).

This molecular data along with the pharmacological data obtained from this study could provide us a greater understanding about bitter taste agonists and their potential functions in the rat pulmonary vessels. The effect of TAS2Rs on airway epithelial cells is to increase the cilia beat frequency, which can promote sneezing and regulate the rate of respiration to protect against noxious inhalants (Shah et al., 2009). From above we can propose that the protective role of TAS2Rs in pulmonary arteries is similar to that in the airway, Indeed, we can suggest that the bitter taste agonists-mediated vasorelaxation of arteries may be beneficial to human health. Bitter taste agonists enter the body and activate TAS2R to relax blood vessels, thus accelerating the flow of blood to remove harmful bitter substances. Whether the bitter-tasting harmful substances enter systemic circulation through the diet or into the respiratory tract by inhalation, TAS2R may play its protective role in the corresponding organs to excrete the potentially harmful substances a way of the body.

6.4 Limitations

One limitation of this study is that the pulmonary artery vasodilation via TAS2Rs cannot be confirmed because there is a lack of antagonists that can be used to block the TAS2Rs and prevent their vasorelaxant effect. There are no confirmed antagonists for TAS2Rs (Behrens and Meyerhof, 2013). Number of studies have been investigated some compounds as potential antagonists for TAS2Rs (Brockhoff *et al.*, 2011; Pydi *et al.*, 2014). A study conducted by Chen *et al.* (2017) used γ-aminobutyric acid (GABA), a candidate TAS2R4 antagonist, to investigate the mechanism of vasodilation (Pydi *et al.*, 2014). Unfortunately, GABA did not influence the vasodilation induced by chloroquine or quinine (Chen *et al.*, 2017). Therefore, they cannot assert that the vasodilation of induced by chloroquine or quinine is mediated by only the activation of TAS2R (Chen *et al.*, 2017); Given the lack of selective antagonists for the TAS2Rs, the function of a single TAS2R subtype could not be specifically investigated.

Quinine, denatonium, and dextromethorphan are regarded as being safe and are currently used in the treatment of malaria, as a bronchodilator (not approved yet), and as an antitussive, respectively (Deshpande *et al.*, 2010; Tortella, Pellicano and Bowery, 1989; White, 1996). Nevertheless, the clinical use of these TAS2R agonists may be

limited due to the high concentrations (approximately 30 μM) required to produce a maximum response. Therefore, future studies will require to develop both plant-derived and synthetic bitter-tasting compounds to identify more potent bitter taste agonists. Also, the bitter taste of these agonists will make them unpleasant for the patient to take and thus may introduce a barrier for drug development, which would need future research into a pharmaceutical formulation to mask this bitter taste.

There were technical challenges and limitations in the Ca^{2+} signaling experiments in this study. Ideally, the experiments should use the same pulmonary artery cells throughout the treatments with PSS washes in-between to allow addition of bitter taste agonist with an inhibitor such as U73122 or thapsigargin to the same cells. However, the pulmonary artery cells would shrink and not respond to the next addition. Therefore, in Ca^{2+} signaling studies, the control of pulmonary artery cells was done separately in individual experiments.

Power and sample size calculations would help with the determination of treatment impact and significance. In this study, animal use limitations resulted in some experiments using multiple vessels from one rat. While this may reduce inter-animal variability which might be observed, there could be regional tissue biomolecular differences between pulmonary artery sections from an animal which could result in a differential response to the agonists and other treatments.

The low specificity of bitter taste agonists placed additional technical and analytical challenges on this study. Bitter taste agonists do not only interact with TAS2Rs, but they also interact with other receptors and ion channels when they used at relatively high concentrations. For example, quinine can also acts as an α-adrenoceptor blocker (del Pozo *et al.*, 1996; Mecca *et al.*, 1980) (Mecca *et al.*, 1980; del Pozo *et al.*, 1996) and voltage-gated K^+ channel blocker (Cummings and Kinnamon, 1992; Kinnamon and Roper, 1988).

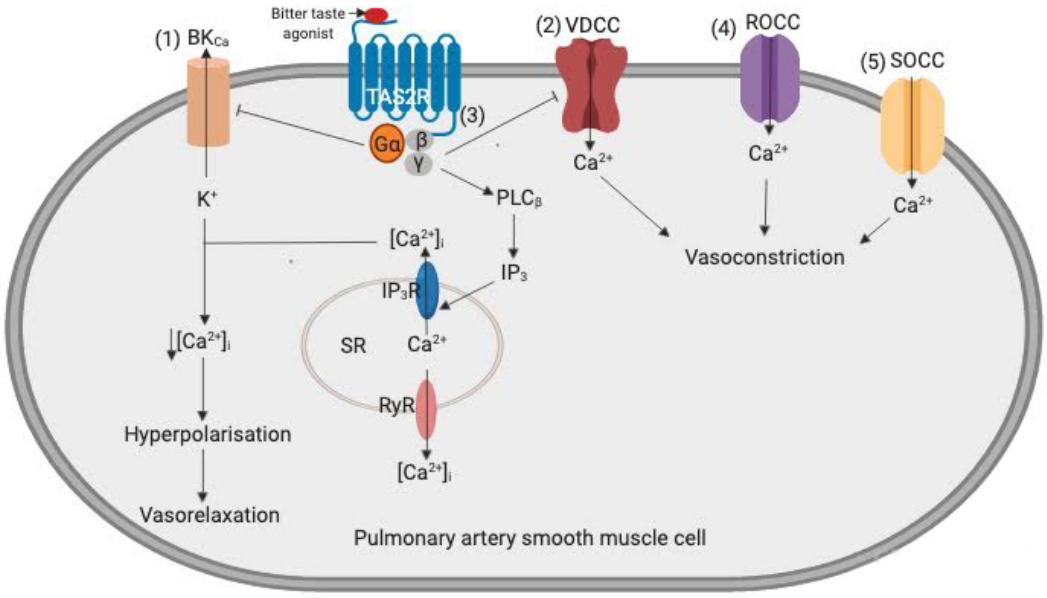

Figure 6.1 Overview of Possible Signalling Mechanisms Involved in Bitter Taste Agonists-Induced Relaxation in The Rat Pulmonary Artery.

This model proposes a mechanism by which bitter taste agonists elicit pulmonary vasodilation. **(1)** Hyperpolarization via BKca channel **(2)** inhibition of L-type voltage dependent Ca^{2+} channel **(3)** Inhibition of G- protein βγ subunits **(4)** inhibition of receptor operated Ca^{2+} channel **(5)** Inhibition of store-operated Ca^{2+} channel.

6.5 Future Directions

Working on this study has demonstrated that these bitter taste agonists can have a vasodilatory effect on the rat pulmonary artery although this work is at an early stage these bitter taste receptor agonists could potentially be developed as therapeutics for pulmonary hypertension in future. Wu *et al.* (2017) have used hypertensive rat model to investigate the effect of chloroquine and they found that it has potent vasodilatory effects. They also conducted histological examinations and revealed that treatment of hypoxic rats with chloroquine (50mg/kg, daily for three weeks) significantly reduced the pulmonary artery wall thickness and thus reduce pulmonary artery vascular remodelling. Therefore, it would be reasonable to consider a case for trialling quinine, denatonium, and dextromethorphan in the same hypoxic rat model to test their effect on pulmonary artery wall thickness and their effect on vascular remodelling. Also, it would be worth considering the use of the Sugen5416/hypoxia rat model (Nicolls *et al.*, 2012) to investigate whether quinine, denatonium, and dextromethorphan would inhibit the progression of established pulmonary hypertension.

The use of the monocrotaline (MCT) animal model could help with our understanding of the effect of bitter taste agonists on vascular remodelling. The monocrotaline (MCT)-induced pulmonary hypertension rat model has been broadly used to study pulmonary hypertension characteristics, particularly to test the effect of agonists on vascular remodelling and inflammation (Stenmark *et al.*, 2009).

Regarding cell proliferation, using cell proliferation assays such as MTT would be helpful to quantify the level of cell proliferation response in pulmonary artery smooth muscle cells. following their incubation with different concentrations of quinine, denatonium, and dextromethorphan.

Since antagonists that are highly selective for the individual TAS2Rs appear to be unavailable, knock-out animals (with Gα subunit, $PLC_{\beta 2}$, and TRPM5) could be used to study the canonical taste transduction pathways involved in the vasorelaxant effect of bitter taste agonists on the pulmonary arteries. The pharmacological studies could be repeated in the pulmonary artery from wild-type rat and the pharmacological effects

compared with that in pulmonary arteries obtained from a rat in which the individual canonical taste transduction elements have been deleted. The genetically modified rat model is recommended nowadays for this type of research (Cozzi, Fraichard and Thiam, 2008).

The RNA sequencing and RT-qPCR data from this study indicate that Tas2r108 and Tas2r139 transcripts are expressed in the rat pulmonary artery tissue. However, an examination of their expression in specific cell types within this tissue was not conducted. A further investigation using in-situ hybridization on ring cross-sections, regional gene expression analysis along the length of the tissue as well as on dissociated cell types from the pulmonary artery would provide a greater depth of insight to the Tas2rs in this tissue. In addition, Western blotting analysis of the Tas2rs in this pulmonary artery would help complete this expression map of this tissue.

Together, the data from these additional experiments, along with the data provided in this thesis, would provide us a comprehensive knowledge of which TAS2R variants are expressed in the rat pulmonary artery, in addition to the signalling mechanisms that link the receptor activation to the vasorelaxation of pulmonary artery.

6.6 Conclusion

In summary, this study showed that the vasorelaxant effect has been observed with quinine, denatonium, and dextromethorphan in the rat pulmonary artery. This study has also shown a reversibility of this effect. Our *in vitro* experiments reported that quinine, denatonium, and dextromethorphan attenuated the ATP- induced increase in $[Ca^{2+}]_i$, suggesting that quinine, denatonium and dextromethorphan may partially block ROCC in freshly isolated pulmonary artery SMCs. Moreover, dextromethorphan–induced increase in $[Ca^{2+}]_i$ was significantly inhibited by incubation with U73122 indicating that the signalling appears to be primarily via intracellular Ca^{2+} stores through the PLC–IP_3 pathway in the rat pulmonary artery SMCs. Additionally, our molecular biology findings reveal that *Tas2r108* and *Tas2r139* are expressed in the rat pulmonary artery. The current observations indicate potential therapeutic applications for bitter taste agonists in different disorders which

affect smooth muscle contractility. The effect of bitter taste agonists on the pulmonary artery may point to a future potential role in the treatment of pulmonary hypertension.

Chapter 7

Appendixes

Appendix A: Sanger Sequencing of TAS2Rs

	TAS2R	Forward	Reverse
1	119	100% identity	No significant similarities found because short nucleotides sequence + low complexity sequence (noise)
2	137	Not expressed by endpoint PCR	Not Expressed by endpoint PCR
3	108	No significant similarities found because short nucleotides sequence + low complexity sequence(noise)	Not present*
4	107	100% identity	Not present
5	123	No significant similarities found because short nucleotides sequence + low complexity sequence(noise)	No significant similarities found because short nucleotides sequence + low complexity sequence(noise)
6	145	100% identity	Not present
7	134	100% identity	Not present
8	144	100% identity	Not present
9	126	No significant similarities found because short nucleotides sequence + low complexity (noise)	Not present
10	143	100% identity	100% identity
11	139	Not present (because Sanger sequence was done before the RNA-seq)	Not present (because Sanger sequence was done before the RNA-seq)

*Not present mean not found by sanger sequencing

Summary statistics

Category	Count
Variants processed	67584
Variants filtered out	0
Novel / existing variants	27997 (41.4) / 39587 (58.6)
Overlapped genes	13226
Overlapped transcripts	18129
Overlapped regulatory features	-

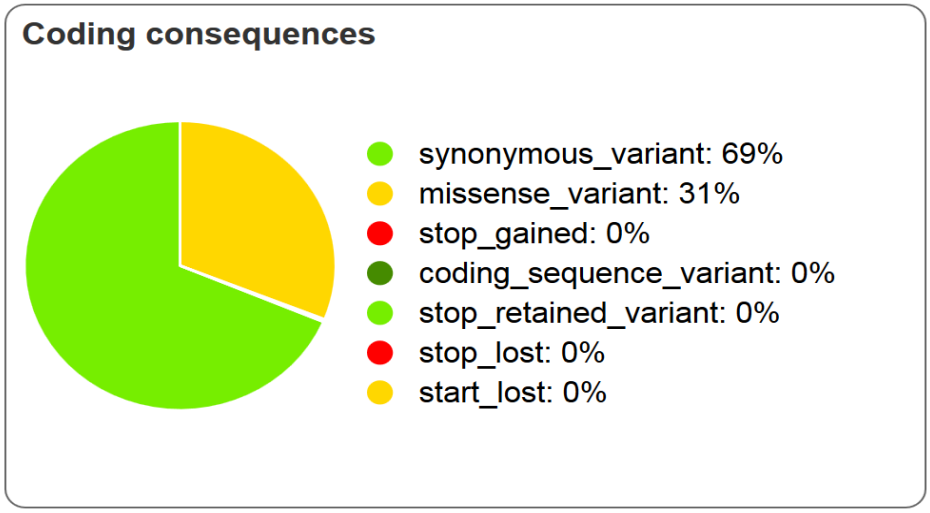

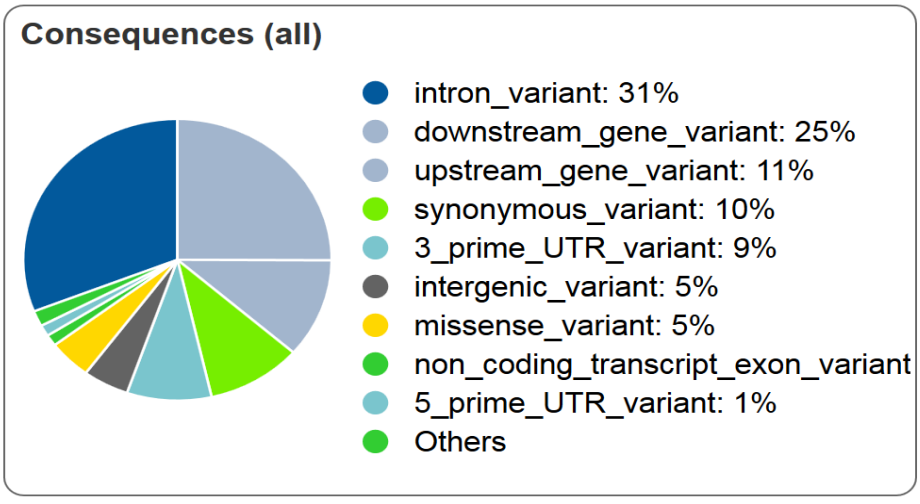

Appendix B: Rat Pulmonary Artery SNPs Results.

Appendix C: Summary of the SNP Variant Types

Sample	A-G	C-T	Transition	A-C	A-T	C-G	G-T	Transversion	Total
Rat PA	25,200	24,996	50,196	4,651	3,933	4,199	4,605	17,388	67584

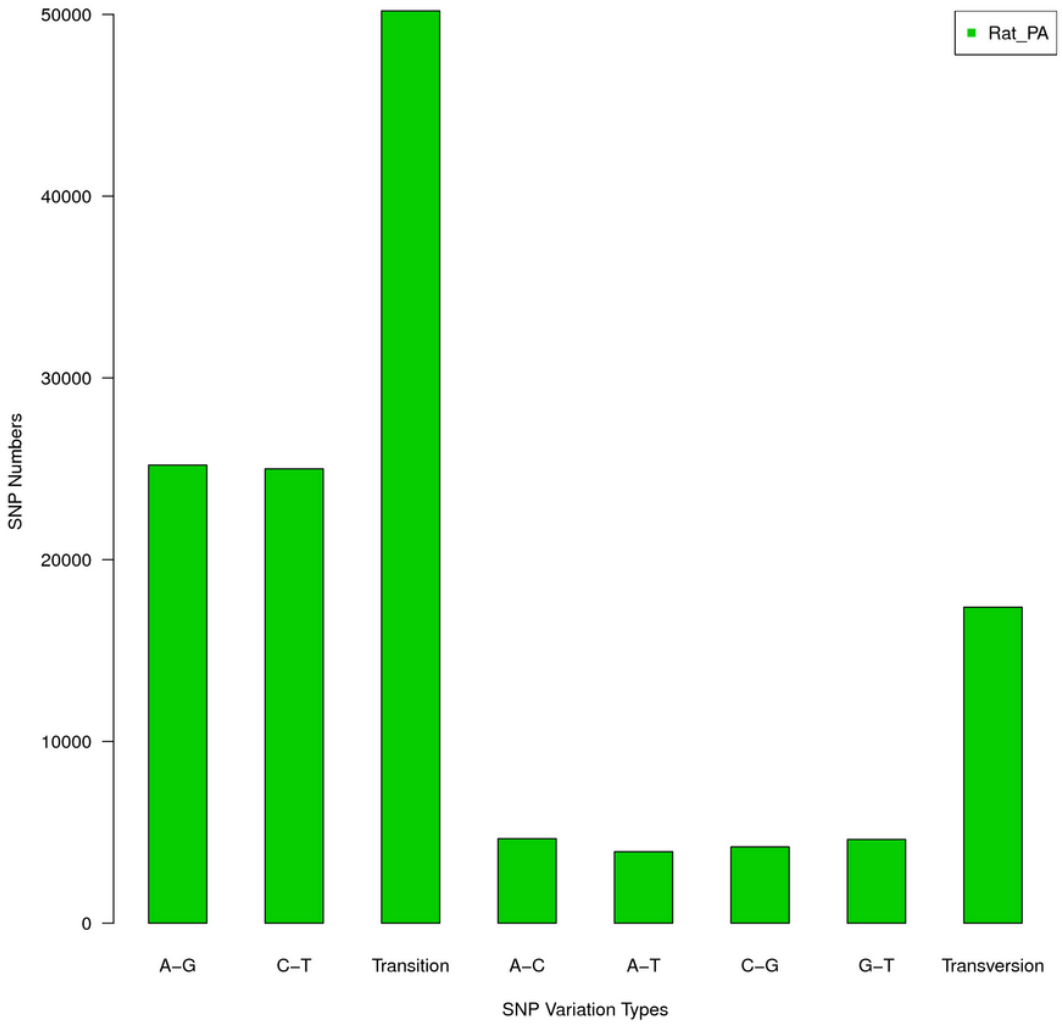

Appendix D: The SNP Variant Type Distribution for the Rat Pulmonary Artery. The X-axis represents the type of SNP, while the Y-axis represents the number of SNP.

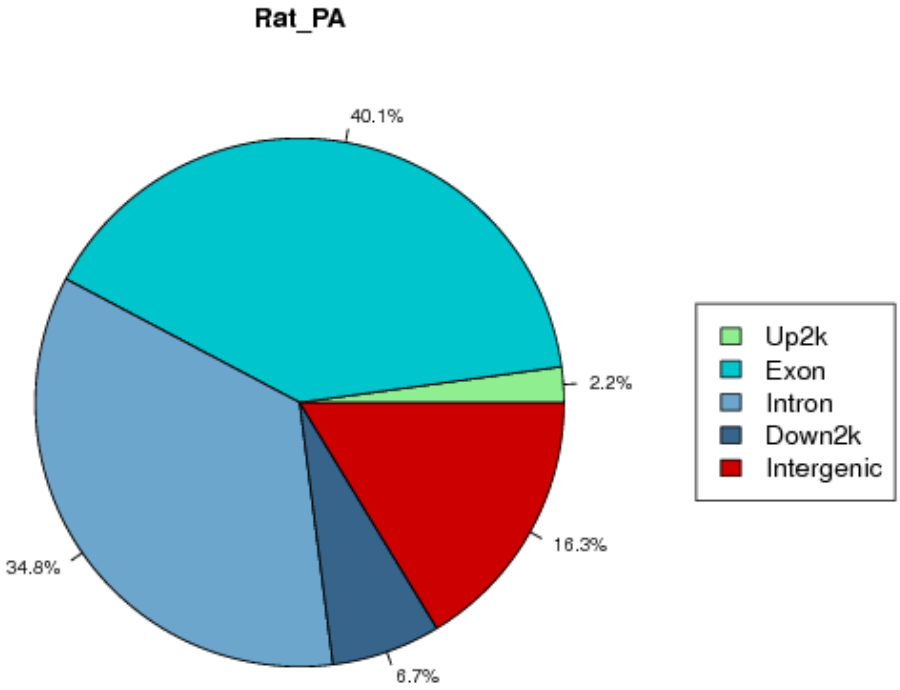

Appendix E: The Distribution of SNP Location of the Rat Pulmonary Artery. This figure shows the distribution of SNP location of the rat pulmonary artery. Up2k means upstream 2000 bp area of gene, while Down2k means downstream 2000 bp area of gene.

Summary statistics

Category	Count
Variants processed	10580
Variants filtered out	0
Novel / existing variants	10577 (100.0) / 3 (0.0)
Overlapped genes	7409
Overlapped transcripts	18850
Overlapped regulatory features	-

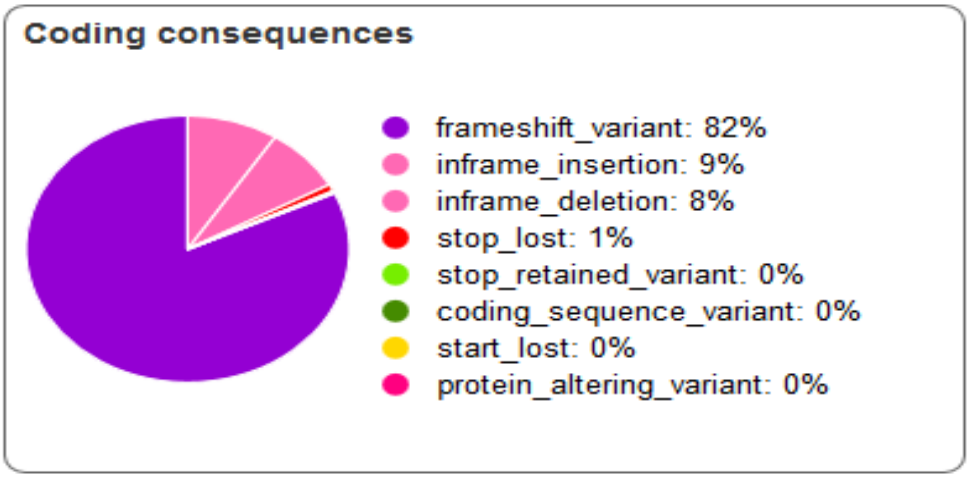

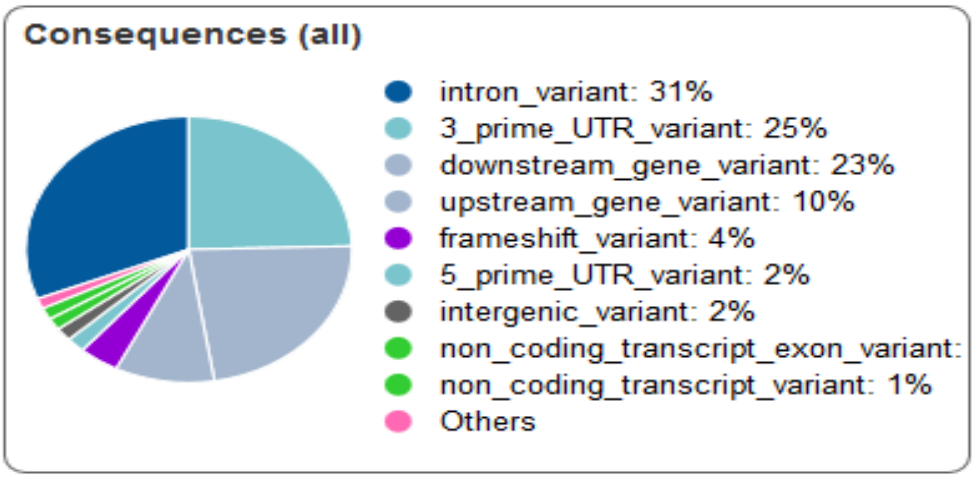

Appendix F: Rat Pulmonary Artery INDEL Results.

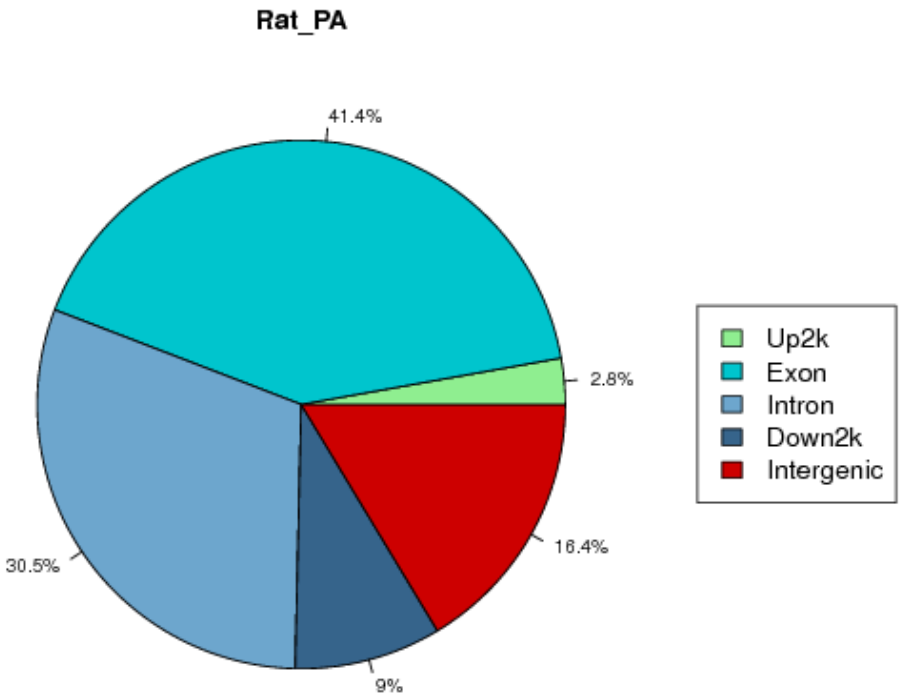

Appendix G: The Distribution of INDEL Location of the Rat Pulmonary Artery. This figure shows the distribution of INDEL location of the rat pulmonary artery. Up2k means upstream 2000 bp area of gene, while Down2k means downstream 2000 bp area of gene.

Chapter 8

List of References

Adachi, T., Weisbrod, R. M., Pimentel, D. R., Ying, J., Sharov, V. S., Schöneich, C. & Cohen, R. A. (2004). S-Glutathiolation by Peroxynitrite Activates Serca During Arterial Relaxation by Nitric Oxide. *Nature Medicine,* 10**,** 1200.

Adler, E., Hoon, M. A., Mueller, K. L., Chandrashekar, J., Ryba, N. J. & Zuker, C. S. (2000). A Novel Family of Mammalian Taste Receptors. *Cell,* 100**,** 693-702.

Akabas, M. H., Dodd, J. & Al-Awqati, Q. (1988). A Bitter Substance Induces a Rise in Intracellular Calcium in a Subpopulation of Rat Taste Cells. *Science,* 242**,** 1047-1050.

Akiyoshi, T., Tanaka, N., Nakamura, T., Matzno, S., Shinozuka, K. & Uchida, T. (2007). Effects of Quinine on the Intracellular Calcium Level and Membrane Potential of Pc 12 Cultures. *Journal of Pharmacy and Pharmacology,* 59**,** 1521-1526.

Andrews, C. N., Verschueren, S., Janssen, P., Maes, A., Deloose, E., Depoortere, I. & Tack, J. F. (2013). Su2072 the Bitter Taste Receptor Agonist Denatonium Benzoate Alters Intragastric Pressure Profiles During Nutrient Drink Test in Healthy Volunteers. *Gastroenterology,* 144**,** S-549.

Anigbogu, C., Adigun, S., Inyang, I. & Adegunloye, B. (1993). Chloroquine Reduces Blood Pressure and Forearm Vascular Resistance and Increases Forearm Blood Flow in Healthy Young Adults. *Clinical Physiology and Functional Imaging,* 13**,** 209-216.

Ansoleaga, B., Garcia-Esparcia, P., Llorens, F., Moreno, J., Aso, E. & Ferrer, I. (2013). Dysregulation of Brain Olfactory and Taste Receptors in Ad, Psp and Cjd, and Ad-Related Model. *Neuroscience,* 248**,** 369-382.

Asano-Miyoshi, M., Abe, K. & Emori, Y. (2000). Co-Expression of Calcium Signaling Components in Vertebrate Taste Bud Cells. *Neuroscience Letters,* 283**,** 61-64.

Avau, B., Rotondo, A., Thijs, T., Andrews, C. N., Janssen, P., Tack, J. & Depoortere, I. (2015). Targeting Extra-Oral Bitter Taste Receptors Modulates Gastrointestinal Motility with Effects on Satiation. *Scientific Reports,* 5**,** 15985.

Aziba, P. I. (2003). Effects of Chloroquine on Smooth Muscle Contracted with Noradrenaline or High-Potassium Solutions in the Rat Thoracic Aorta. *Journal of Smooth Muscle Research,* 39**,** 31-37.

Badesch, D. B., Abman, S. H., Simonneau, G., Rubin, L. J. & Mclaughlin, V. V. (2007). Medical Therapy for Pulmonary Arterial Hypertension: Updated Accp Evidence-Based Clinical Practice Guidelines. *Chest,* 131**,** 1917-1928.

Baggio, L. L. & Drucker, D. J. (2007). Biology of Incretins: Glp-1 and Gip. *Gastroenterology,* 132**,** 2131-2157.

Baliga, R. S., Macallister, R. J. & Hobbs, A. J. (2011). New Perspectives for the Treatment of Pulmonary Hypertension. *British journal of pharmacology,* 163**,** 125-140.

Bárány, M. (1967). Atpase Activity of Myosin Correlated with Speed of Muscle Shortening. *The Journal of General Physiology,* 50**,** 197-218.

Barer, G. R. (1980). Active Control of the Pulmonary Circulation. *Pulmonary Circulation in Health and Disease.* Springer.

Barnes, P. J. (1986). Neural Control of Human Airways in Health and Disease. *American Review of Respiratory Disease,* 134**,** 1289-1314.

Barnes, P. J., Baraniuk, J. N. & Belvisi, M. G. (1991). Neuropeptides in the Respiratory Tract. *American Review of Respiratory Disease,* 144**,** 1187-1198.

Barnes, P. J. & Liu, S. F. (1995). Regulation of Pulmonary Vascular Tone. *Pharmacological Reviews,* 47**,** 87-131.

Barst, R. J., Rubin, L. J., Long, W. A., Mcgoon, M. D., Rich, S., Badesch, D. B., Groves, B. M., Tapson, V. F., Bourge, R. C. & Brundage, B. H. (1996). A Comparison of Continuous Intravenous Epoprostenol (Prostacyclin) with Conventional Therapy for Primary Pulmonary Hypertension. *New England Journal of Medicine,* 334**,** 296-301.

Bean, B. P. (1989). Classes of Calcium Channels in Vertebrate Cells. *Annual Review of Physiology,* 51**,** 367-384.

Behrens, M. & Meyerhof, W. Bitter Taste Receptor Research Comes of Age: From Characterization to Modulation of Tas2rs. (2013). Seminars in Cell and Developmental Biology, 215-221.

Belmonte, K. E. (2005). Cholinergic Pathways in the Lungs and Anticholinergic Therapy for Chronic Obstructive Pulmonary Disease. *Proceedings of the American Thoracic Society,* 2**,** 297-304.

Berkov, S. (1974). Hypoxic Pulmonary Vasoconstriction in the Rat: The Necessary Role of Angiotensin Ii. *Circulation Research,* 35**,** 256-261.

Berridge, M. J. (1984a). Inositol Triphosphate, a Novel Second Messenger in Cellular Signal Transduction. *Nature,* 312**,** 315-321.

Berridge, M. J. (1984b). Inositol Trisphosphate and Diacylglycerol as Second Messengers. *Biochemical Journal,* 220**,** 345.

Bigiani, A. R. & Roper, S. D. (1991). Mediation of Responses to Calcium in Taste Cells by Modulation of a Potassium Conductance. *Science,* 252**,** 126-128.

Bioquest, A. (2017). The Eight Best Green Fluorescent Calcium Indicators. Available from: https://www.aatbio.com/blog/1508861977/the_eight_best_green_fluorescent_calcium_indicators [Accessed 18 Feb 2017].

Boe, J. & Simonsson, B. (1980). Adrenergic Receptors and Sympathetic Agents in Isolated Human Pulmonary Arteries. *European Journal of Respiratory Diseases,* 61**,** 195-202.

Boe, J. & Simonsson, B. (1981). Effects of Angiotensin Ii and Bradykinin on Isolated Human Pulmonary Arteries. *European Journal of Respiratory Diseases,* 62**,** 95-101.

Bolger, G. T., Rafferty, M. F. & Skolnick, P. (1986). Enhancement of Brain Calcium Antagonist Binding by Phencyclidine and Related Compounds. *Pharmacology Biochemistry and Behavior,* 24**,** 417-423.

Bolotina, V. M., Najibi, S., Palacino, J. J., Pagano, P. J. & Cohen, R. A. (1994). Nitric Oxide Directly Activates Calcium-Dependent Potassium Channels in Vascular Smooth Muscle. *Nature,* 368**,** 850.

Bolton, T., Lang, R. & Takewaki, T. (1984). Mechanisms of Action of Noradrenaline and Carbachol on Smooth Muscle of Guinea-Pig Anterior Mesenteric Artery. *The Journal of Physiology,* 351**,** 549-572.

Bourson, A., Moser, P. C., Gower, A. J. & Mir, A. K. (1989). Central and Peripheral Effects of the Dihydropyridine Calcium Channel Activator Bay K 8644 in the Rat. *European Journal of Pharmacology,* 160**,** 339-347.

Brayden, J. E. (1996). Potassium Channels in Vascular Smooth Muscle. *Clinical and Experimental Pharmacology and Physiology,* 23**,** 1069-1076.

Brij, S. O. & Peacock, A. J. (1998). Cellular Responses to Hypoxia in the Pulmonary Circulation. *Thorax,* 53**,** 1075-1079.

Brockhoff, A., Behrens, M., Massarotti, A., Appendino, G. & Meyerhof, W. (2007). Broad Tuning of the Human Bitter Taste Receptor Htas2r46 to Various Sesquiterpene Lactones, Clerodane and Labdane Diterpenoids, Strychnine, and Denatonium. *Journal of Agricultural and Food Chemistry,* 55**,** 6236-6243.

Brockhoff, A., Behrens, M., Roudnitzky, N., Appendino, G., Avonto, C. & Meyerhof, W. (2011). Receptor Agonism and Antagonism of Dietary Bitter Compounds. *Journal of Neuroscience,* 31**,** 14775-14782.

Brozovich, F., Nicholson, C., Degen, C., Gao, Y. Z., Aggarwal, M. & Morgan, K. G. (2016). Mechanisms of Vascular Smooth Muscle Contraction and the Basis for Pharmacologic Treatment of Smooth Muscle Disorders. *Pharmacological Reviews,* 68**,** 476-532.

Bullock, S. & Hales, M. (2012). *Principles of Pathophysiology*, Pearson Higher Education AU.

Burnstock, G. & Kennedy, C. (1985). Is There a Basis for Distinguishing Two Types of P2-Purinoceptor? *General Pharmacology: The Vascular System,* 16**,** 433-440.

Caicedo, A., Pereira, E., Margolskee, R. F. & Roper, S. D. (2003). Role of the G-Protein Subunit A-Gustducin in Taste Cell Responses to Bitter Stimuli. *Journal of Neuroscience,* 23**,** 9947-9952.

Camoretti-Mercado, B., Pauer, S. H., Yong, H. M., Dan'elle, C. S., Deshpande, D. A., An, S. S. & Liggett, S. B. (2015). Pleiotropic Effects of Bitter Taste Receptors on [Ca2+] I Mobilization, Hyperpolarization, and Relaxation of Human Airway Smooth Muscle Cells. *PloS One,* 10**,** e0131582.

Carpenter, C. L., Marks, S. S., Watson, D. L. & Greenberg, D. A. (1988). Dextromethorphan and Dextrorphan as Calcium Channel Antagonists. *Brain Research,* 439**,** 372-375.

Carvajal, J. A., Germain, A. M., Huidobro-Toro, J. P. & Weiner, C. P. (2000). Molecular Mechanism of Cgmp-Mediated Smooth Muscle Relaxation. *Journal of Cellular Physiology,* 184**,** 409-420.

Catravas, J., Buccafusco, J. & El Kashef, H. (1984). Effects of Acetylcholine in the Pulmonary Circulation of Rabbits. *Journal of Pharmacology and Experimental Therapeutics,* 231**,** 236-241.

Chandrashekar, J., Mueller, K. L., Hoon, M. A., Adler, E., Feng, L., Guo, W., Zuker, C. S. & Ryba, N. J. (2000). T2rs Function as Bitter Taste Receptors. *Cell,* 100**,** 703-711.

Chau, T. T., Carter, F. E. & Harris, L. (1983). Antitussive Effect of the Optical Isomers of Mu, Kappa and Sigma Opiate Agonists/Antagonists in the Cat. *Journal of Pharmacology and Experimental Therapeutics,* 226**,** 108-113.

Chaudhari, N. & Roper, S. D. (2010). The Cell Biology of Taste. *The Journal of Cell Biology,* 190**,** 285-296.

Chen, J.-G., Ping, N.-N., Liang, D., Li, M.-Y., Mi, Y.-N., Li, S., Cao, L., Cai, Y. & Cao, Y.-X. (2017). The Expression of Bitter Taste Receptors in Mesenteric, Cerebral and Omental Arteries. *Life Sciences,* 170**,** 16-24.

Chen, M. C., Wu, S. V., Reeve Jr, J. R. & Rozengurt, E. (2006). Bitter Stimuli Induce Ca2+ Signaling and Cck Release in Enteroendocrine Stc-1 Cells: Role of L-Type Voltage-Sensitive Ca2+ Channels. *American Journal of Physiology-Cell Physiology,* 291**,** 726-739.

Cherry, P. D., Furchgott, R. F., Zawadzki, J. V. & Jothianandan, D. (1982). Role of Endothelial Cells in Relaxation of Isolated Arteries by Bradykinin. *Proceedings of the National Academy of Sciences,* 79**,** 2106-2110.

Chin, T. Y. & Chueh, S. H. (2000). Distinct Ca2+ Signalling Mechanisms Induced by Atp and Sphingosylphosphorylcholine in Porcine Aortic Smooth Muscle Cells. *British Journal of Pharmacology,* 129**,** 1365-1374.

Chiva-Blanch, G., Urpi-Sarda, M., Ros, E., Arranz, S., Valderas-Martínez, P., Casas, R., Sacanella, E., Llorach, R., Lamuela-Raventos, R. M. & Andres-Lacueva, C. (2012). Dealcoholized Red Wine Decreases Systolic and Diastolic Blood Pressure and Increases Plasma Nitric Oxide. *Circulation Research,* 111**,** 1065-1068.

Church, J., Lodge, D. & Berry, S. C. (1985). Differential Effects of Dextrorphan and Levorphanol on the Excitation of Rat Spinal Neurons by Amino Acids. *European Journal of Pharmacology,* 111**,** 185-190.

Clapp, T. R., Stone, L. M., Margolskee, R. F. & Kinnamon, S. C. (2001). Immunocytochemical Evidence for Co-Expression of Type Iii Ip 3 Receptor with Signaling Components of Bitter Taste Transduction. *BMC Neuroscience,* 2**,** 6.

Clapp, T. R., Trubey, K. R., Vandenbeuch, A., Stone, L. M., Margolskee, R. F., Chaudhari, N. & Kinnamon, S. C. (2008). Tonic Activity of Gα-Gustducin Regulates Taste Cell Responsivity. *FEBS Letters,* 582**,** 3783-3787.

Clark, A. A., Dotson, C. D., Elson, A. E., Voigt, A., Boehm, U., Meyerhof, W., Steinle, N. I. & Munger, S. D. (2014). Tas2r Bitter Taste Receptors Regulate Thyroid Function. *The FASEB Journal,* 29**,** 164-172.

Clark, A. A., Liggett, S. B. & Munger, S. D. (2012). Extraoral Bitter Taste Receptors as Mediators of Off-Target Drug Effects. *The FASEB Journal,* 26**,** 4827-4831.

Cockcroft, D. W. & Davis, B. E. (2006). Mechanisms of Airway Hyperresponsiveness. *Journal of Allergy and Clinical Immunology,* 118**,** 551-559.

Cogolludo, A., Moreno, L. & Villamor, E. (2007). Mechanisms Controlling Vascular Tone in Pulmonary Arterial Hypertension: Implications for Vasodilator Therapy. *Pharmacology,* 79**,** 65-75.

Cohen, R. A., Weisbrod, R. M., Gericke, M., Yaghoubi, M., Bierl, C. & Bolotina, V. M. (1999). Mechanism of Nitric Oxide–Induced Vasodilatation: Refilling of Intracellular Stores by Sarcoplasmic Reticulum Ca2+ Atpase and Inhibition of Store-Operated Ca2+ Influx. *Circulation Research,* 84**,** 210-219.

Colombo, M., Trevisi, P., Gandolfi, G. & Bosi, P. (2012). Assessment of the Presence of Chemosensing Receptors Based on Bitter and Fat Taste in the Gastrointestinal Tract of Young Pig. *Journal of Animal Science,* 90**,** 128-130.

Comroe, J. H. (1966). The Main Functions of the Pulmonary Circulation. *Circulation,* 33**,** 146-158.

Cook, N. S. (1989). Effect of Some Potassium Channel Blockers on Contractile Responses of the Rabbit Aorta. *Journal of Cardiovascular Pharmacology,* 13**,** 299-306.

Cook, N. S., Griffiths, J. L. & Hoff, R. P. (1987). The Effects of Some K Channel Blockers and the K Channel Activator Brl 34915 Upon the Rabbit Aorta. *British Journal of Pharmacology,* 90**,** 130.

Cozzi, J., Fraichard, A. & Thiam, K. (2008). Use of Genetically Modified Rat Models for Translational Medicine. *Drug Discovery Today,* 13**,** 488-494.

Csordás, G., Thomas, A. P. & Hajnóczky, G. (2001). Calcium Signal Transmission between Ryanodine Receptors and Mitochondria in Cardiac Muscle. *Trends in Cardiovascular Medicine,* 11**,** 269-275.

Cummings, T. A. & Kinnamon, S. C. (1992). Apical K+ Channels in Necturus Taste Cells. Modulation by Intracellular Factors and Taste Stimuli. *The Journal of General Physiology,* 99**,** 591-613.

Daly, I. & Hebb, C. (1966). Innervation of the Lungs. *Pulmonary and Bronchial Vascular Systems***,** 89-117.

Deckmann, K., Filipski, K., Krasteva-Christ, G., Fronius, M., Althaus, M., Rafiq, A., Papadakis, T., Renno, L., Jurastow, I. & Wessels, L. (2014). Bitter Triggers Acetylcholine Release from Polymodal Urethral Chemosensory Cells and Bladder Reflexes. *Proceedings of the National Academy of Sciences***,** 201402436.

Dehkordi, O., Rose, J. E., Fatemi, M., Allard, J. S., Balan, K. V., Young, J. K., Fatima, S., Millis, R. M. & Jayam-Trouth, A. (2012). Neuronal Expression of Bitter Taste Receptors and Downstream Signaling Molecules in the Rat Brainstem. *Brain Research,* 1475**,** 1-10.

Del Pozo, B. F., Pérez-Vizcaíno, F., Villamor, E., Zaragozá, F. & Tamargo, J. (1996). Stereoselective Effects of the Enantiomers, Quinidine and Quinine, on Depolarization-and Agonist-Mediated Responses in Rat Isolated Aorta. *British Journal of Pharmacology,* 117**,** 105-110.

Deshpande, D. A., Wang, W. C., Mcilmoyle, E. L., Robinett, K. S., Schillinger, R. M., An, S. S., Sham, J. S. & Liggett, S. B. (2010). Bitter Taste Receptors on Airway Smooth Muscle Bronchodilate by Localized Calcium Signaling and Reverse Obstruction. *Nature Medicine,* 16**,** 1299.

Dicarlo, V. S., Chen, S., Meng, Q. C., Durand, J., Yano, M., Chen, Y. & Oparil, S. (1995). Eta-Receptor Antagonist Prevents and Reverses Chronic Hypoxia-Induced Pulmonary Hypertension in Rat. *American Journal of Physiology-Lung Cellular and Molecular Physiology,* 269**,** L690-L697.

Dillon, P. F., Aksoy, M. O., Driska, S. P. & Murphy, R. A. (1981). Myosin Phosphorylation and the Cross-Bridge Cycle in Arterial Smooth Muscle. *Science,* 211**,** 495-497.

Dong, D.-L., Bai, Y.-L. & Cai, B.-Z. (2016). Calcium-Activated Potassium Channels: Potential Target for Cardiovascular Diseases. *Advances in Protein Chemistry and Structural Biology.* Elsevier.

Dotson, C. D., Zhang, L., Xu, H., Shin, Y.-K., Vigues, S., Ott, S. H., Elson, A. E., Choi, H. J., Shaw, H. & Egan, J. M. (2008). Bitter Taste Receptors Influence Glucose Homeostasis. *PloS One,* 3**,** e3974.

Dupré, D. J., Robitaille, M., Rebois, R. V., Hébert, T. E. J. a. R. O. P. & Toxicology (2009). The Role of Gβγ Subunits in the Organization, Assembly, and Function of Gpcr Signaling Complexes. *Annual Review of Pharmacology and Toxicology,* 49**,** 31-56.

El-Hamalawi, A.-R. A., Thompson, J. S. & Barker, G. R. (1975). The Fluorometric Determination of Nucleic Acids in Pea Seeds by Use of Ethidium Bromide Complexes. *Analytical Biochemistry,* 67**,** 384-391.

Euler, U. V. & Liljestrand, G. (1946). Observations on the Pulmonary Arterial Blood Pressure in the Cat. *Acta Physiologica Scandinavica,* 12**,** 301-320.

Farhi, L. E. & Sheehan, D. W. (1990). Pulmonary Circulation and Systemic Circulation: Similar Problems, Different Solutions. *Oxygen Transport to Tissue Xii.* Boston, MA: Springer.

Fernandez, R. A., Sundivakkam, P., Smith, K. A., Zeifman, A. S., Drennan, A. R. & Yuan, J. X.-J. (2012). Pathogenic Role of Store-Operated and Receptor-Operated Channels in Pulmonary Arterial Hypertension. *Journal of Signal Transduction,* 2012.

Finger, T. E. & Kinnamon, S. C. (2011). Taste Isn't Just for Taste Buds Anymore. *F1000 Biology Reports,* 3.

Firth, A. L., Won, J. Y. & Park, W. S. (2013). Regulation of Ca2+ Signaling in Pulmonary Hypertension. *The Korean Journal of Physiology & Pharmacology,* 17**,** 1-8.

Fishman, A. P. (1961). Respiratory Gases in the Regulation of the Pulmonary Circulation. *Physiological Reviews,* 41**,** 214-280.

Fleige, S., Walf, V., Huch, S., Prgomet, C., Sehm, J. & Pfaffl, M. W. (2006). Comparison of Relative Mrna Quantification Models and the Impact of Rna Integrity in Quantitative Real-Time Rt-Pcr. *Biotechnology Letters,* 28**,** 1601-1613.

Foster, S. R., Blank, K., See Hoe, L. E., Behrens, M., Meyerhof, W., Peart, J. N. & Thomas, W. G. (2014). Bitter Taste Receptor Agonists Elicit G-Protein-Dependent Negative Inotropy in the Murine Heart. *The FASEB Journal,* 28**,** 4497-4508.

Foster, S. R., Porrello, E. R., Purdue, B., Chan, H.-W., Voigt, A., Frenzel, S., Hannan, R. D., Moritz, K. M., Simmons, D. G. & Molenaar, P. (2013). Expression, Regulation and Putative Nutrient-Sensing Function of Taste Gpcrs in the Heart. *PLoS One,* 8**,** e64579.

Fritts, H., Harris, P., Clauss, R., Odell, J. & Cournand, A. (1958). The Effect of Acetylcholine on the Human Pulmonary Circulation under Normal and Hypoxic Conditions. *The Journal of Clinical Investigation,* 37**,** 99-110.

Fuchgott, R. (1988). Studies on Relaxation of Rabbit Aorta by Sodium Nitrite: The Basis for the Proposal That the Acid-Activatable Inhibitory Factor from Bovine Retractor Penis Is Inorganic Nitrite and the Endothelium-Derived Relaxing Factor Is Nitric Oxide. *Vasodilatation: Vascular Smooth Muscle, Peptides, Autonomic Nerves, and Endothelium***,** 401-414.

Furchgott, R. F. (1981). The Requirement for Endothelial Cells in the Relaxation of Arteries by Acetylcholine and Some Other Vasodilators. *Trends in Pharmacological Sciences,* 2**,** 173-176.

Furchgott, R. F. (1983). Role of Endothelium in Responses of Vascular Smooth Muscle. *Circulation Research,* 53**,** 557-573.

Furchgott, R. F. (1984). The Role of Endothelium in the Responses of Vascular Smooth Muscle to Drugs. *Annual Review of Pharmacology and Toxicology,* 24**,** 175-197.

Furchgott, R. F. & Vanhoutte, P. M. (1989). Endothelium-Derived Relaxing and Contracting Factors. *The FASEB Journal,* 3**,** 2007-2018.

Furchgott, R. F. & Zawadzki, J. V. (1980). The Obligatory Role of Endothelial Cells in the Relaxation of Arterial Smooth Muscle by Acetylcholine. *Nature,* 288**,** 373.

Galiè, N., Hoeper, M. M., Humbert, M., Torbicki, A., Vachiery, J.-L., Barbera, J. A., Beghetti, M., Corris, P., Gaine, S. & Gibbs, J. S. (2009). Guidelines for the Diagnosis and Treatment of Pulmonary Hypertension: The Task Force for the Diagnosis and Treatment of Pulmonary Hypertension of the European Society of Cardiology (Esc) and the European Respiratory Society (Ers),

Endorsed by the International Society of Heart and Lung Transplantation (Ishlt). *European Heart Journal,* 30**,** 2493-2537.

Garcia-Esparcia, P., Schlüter, A., Carmona, M., Moreno, J., Ansoleaga, B., Torrejón-Escribano, B., Gustincich, S., Pujol, A. & Ferrer, I. (2013). Functional Genomics Reveals Dysregulation of Cortical Olfactory Receptors in Parkinson Disease: Novel Putative Chemoreceptors in the Human Brain. *Journal of Neuropathology & Experimental Neurology,* 72**,** 524-539.

Gibson, A., Mcfadzean, I., Wallace, P. & Wayman, C. P. (1998). Capacitative Ca2+ Entry and the Regulation of Smooth Muscle Tone. *Trends in Pharmacological Sciences,* 19**,** 266-269.

Gilbert, D. F., Stebbing, M. J., Kuenzel, K., Murphy, R. M., Zacharewicz, E., Buttgereit, A., Stokes, L., Adams, D. J. & Friedrich, O. (2016). Store-Operated Ca2+ Entry (Soce) and Purinergic Receptor-Mediated Ca2+ Homeostasis in Murine Bv2 Microglia Cells: Early Cellular Responses to Atp-Mediated Microglia Activation. *Frontiers in Molecular Neuroscience,* 9**,** 111.

Glendinning, J. I. (1994). Is the Bitter Rejection Response Always Adaptive? *Physiology and Behavior,* 56**,** 1217-1227.

Glendinning, J. I., Yiin, Y.-M., Ackroff, K. & Sclafani, A. (2008). Intragastric Infusion of Denatonium Conditions Flavor Aversions and Delays Gastric Emptying in Rodents. *Physiology and Behavior,* 93**,** 757-765.

Glusa, E. & Richter, M. (1993). Endothelium-Dependent Relaxation of Porcine Pulmonary Arteries Via 5-Ht 1c-Like Receptors. *Naunyn-Schmiedeberg's Archives of Pharmacology,* 347**,** 471-477.

Godfraind, T. (1983). Actions of Nifedipine on Calcium Fluxes and Contraction in Isolated Rat Arteries. *Journal of Pharmacology and Experimental Therapeutics,* 224**,** 443-450.

Grassin-Delyle, S., Abrial, C., Fayad-Kobeissi, S., Brollo, M., Faisy, C., Alvarez, J.-C., Naline, E. & Devillier, P. (2013). The Expression and Relaxant Effect of Bitter Taste Receptors in Human Bronchi. *Respiratory Research,* 14**,** 134.

Guns, P. J. D., Van Assche, T., Fransen, P., Robaye, B., Boeynaems, J. M. & Bult, H. (2006). Endothelium-Dependent Relaxation Evoked by Atp and Utp in the Aorta of P2y2-Deficient Mice. *British Journal of Pharmacology,* 147**,** 569-574.

Gutierrez, G., Venbrux, A., Ignacio, E., Reiner, J., Chawla, L. & Desai, A. (2007). The Concentration of Oxygen, Lactate and Glucose in the Central Veins, Right Heart, and Pulmonary Artery: A Study in Patients with Pulmonary Hypertension. *Critical Care,* 11**,** R44.

Hai, C. & Murphy, R. A. (1989). Ca2+ Crossbridge Phosphorylation, and Contraction. *Annual Review of Physiology,* 51**,** 285-298.

Hall, J., Jones, T. H., Channer, K. S. & Jones, R. D. (2009). Mechanisms of Agonist-Induced Constriction in Isolated Human Pulmonary Arteries. *Vascular Pharmacology,* 51**,** 8-12.

Hallam, T. J. & Rink, T. J. (1989). Receptor-Mediated Ca2+ Entry: Diversity of Function and Mechanism. *Trends in Pharmacological Sciences,* 10**,** 8-10.

Hartley, T. R., Sung, B. H., Pincomb, G. A., Whitsett, T. L., Wilson, M. F. & Lovallo, W. R. (2000). Hypertension Risk Status and Effect of Caffeine on Blood Pressure. *Hypertension,* 36**,** 137-141.

Hiatt, E. P. (1948). Effects of Repeated Oral Doses of Quinine and Quinidine on the Blood Pressure and Renal Circulation of Dogs with Experimental Neurogenic Hypertension. *American Journal of Physiology-Legacy Content,* 155**,** 114-117.

Hislop, A. & Reid, L. (1978). Normal Structure and Dimensions of the Pulmonary Arteries in the Rat. *Journal of anatomy,* 125**,** 71.

Hoon, M. A., Adler, E., Lindemeier, J., Battey, J. F., Ryba, N. J. & Zuker, C. S. (1999). Putative Mammalian Taste Receptors: A Class of Taste-Specific Gpcrs with Distinct Topographic Selectivity. *Cell,* 96**,** 541-551.

Horowitz, A., Menice, C. B., Laporte, R. & Morgan, K. G. (1996). Mechanisms of Smooth Muscle Contraction. *Physiological Reviews,* 76**,** 967-1003.

Houge, A. (1968). Role of Histamine in Hypoxic Pulmonary Hypertension in the Rat: I. Blockade or Potentiation of Endogenous Amines, Kinins, and Atp. *Circulation Research,* 22**,** 371-383.

Huang, L., Shanker, Y. G., Dubauskaite, J., Zheng, J. Z., Yan, W., Rosenzweig, S., Spielman, A. I., Max, M. & Margolskee, R. F. (1999). Gγ13 Colocalizes with Gustducin in Taste Receptor Cells and Mediates Ip 3 Responses to Bitter Denatonium. *Nature Neuroscience,* 2**,** 1055.

Hughes, J. (2001). *Pulmonary Circulation: From Basic Mechanisms to Clinical Practice*, World Scientific.

Hussain, A., Suleiman, M., George, S., Loubani, M. & Morice, A. (2017). Hypoxic Pulmonary Vasoconstriction in Humans: Tale or Myth. *The Open Cardiovascular Medicine Journal,* 11**,** 1.

Hussain, M. B. & Marshall, I. (1997). Characterization of A1-Adrenoceptor Subtypes Mediating Contractions to Phenylephrine in Rat Thoracic Aorta,

Mesenteric Artery and Pulmonary Artery. *British Journal of Pharmacology,* 122**,** 849-858.

Hwang, P. M., Verma, A., Bredt, D. S. & Snyder, S. H. (1990). Localization of Phosphatidylinositol Signaling Components in Rat Taste Cells: Role in Bitter Taste Transduction. *Proceedings of the National Academy of Sciences,* 87**,** 7395-7399.

Hyman, A. L. & Kadowitz, P. J. (1988). Tone-Dependent Responses to Acetylcholine in the Feline Pulmonary Vascular Bed. *Journal of Applied Physiology,* 64**,** 2002-2009.

Hyman, A. L. & Kadowitz, P. J. (1989). Influence of Tone on Responses to Acetylcholine in the Rabbit Pulmonary Vascular Bed. *Journal of Applied Physiology,* 67**,** 1388-1394.

Hyman, A. L., Nandiwada, P., Knight, D. S. & Kadowitz, P. J. (1981). Pulmonary Vasodilator Responses to Catecholamines and Sympathetic Nerve Stimulation in the Cat. Evidence That Vascular Beta-2 Adrenoreceptors Are Innervated. *Circulation Research,* 48**,** 407-415.

Hyvelin, J.-M., Guibert, C., Marthan, R. & Savineau, J.-P. (1998). Cellular Mechanisms and Role of Endothelin-1-Induced Calcium Oscillations in Pulmonary Arterial Myocytes. *American Journal of Physiology-Lung Cellular and Molecular Physiology,* 275**,** L269-L282.

I-Husain Syed, N., Tengah, A., Paul, A. & Kennedy, C. (2010). Characterisation of P2x Receptors Expressed in Rat Pulmonary Arteries. *European Journal of Pharmacology,* 649**,** 342-348.

Ignarro, L. J., Byrns, R., Buga, G. M. & Wood, K. S. (1987). Mechanisms of Endothelium-Dependent Vascular Smooth Muscle Relaxation Elicited by

Bradykinin and Vip. *American Journal of Physiology-Heart and Circulatory Physiology,* 253**,** H1074-H1082.

Inoue, T. & Kannan, M. (1988). Nonadrenergic and Noncholinergic Excitatory Neurotransmission in Rat Intrapulmonary Artery. *American Journal of Physiology-Heart and Circulatory Physiology,* 254**,** H1142-H1148.

Iyinikkel, J. & Murray, F. (2018). Gpcrs in Pulmonary Arterial Hypertension: Tipping the Balance. *British journal of pharmacology,* 175**,** 3063-3079.

Janssen, S., Laermans, J., Verhulst, P.-J., Thijs, T., Tack, J. & Depoortere, I. (2011). Bitter Taste Receptors and A-Gustducin Regulate the Secretion of Ghrelin with Functional Effects on Food Intake and Gastric Emptying. *Proceedings of the National Academy of Sciences,* 108**,** 2094-2099.

Jeon, T.-I., Zhu, B., Larson, J. L. & Osborne, T. F. (2008). Srebp-2 Regulates Gut Peptide Secretion through Intestinal Bitter Taste Receptor Signaling in Mice. *The Journal of Clinical Investigation,* 118**,** 3693-3700.

Jiang, M. J., Chan, C.-F. & Chang, Y.-L. (1994). Intracellular Calcium and Myosin Light Chain Phosphorylation During U46619-Activated Vascular Contraction. *Life Sciences,* 54**,** 2005-2013.

Jing, F., Liu, M., Yang, N., Liu, Y., Li, X. & Li, J. (2013). Relaxant Effect of Chloroquine in Rat Ileum: Possible Involvement of Nitric Oxide and Bkca. *Journal of Pharmacy and Pharmacology,* 65**,** 847-854.

Kachur, J. F., Morgan, D. W. & Gaginella, T. S. (1986). Effect of Dextromethorphan on Guinea Pig Ileal Contractility in Vitro: Comparison with Levomethorphan, Loperamide and Codeine. *Journal of Pharmacology and Experimental Therapeutics,* 239**,** 661-667.

Kaji, I., Karaki, S.-I., Fukami, Y., Terasaki, M. & Kuwahara, A. (2009). Secretory Effects of a Luminal Bitter Tastant and Expressions of Bitter Taste Receptors, T2rs, in the Human and Rat Large Intestine. *American Journal of Physiology-Gastrointestinal and Liver Physiology,* 296**,** G971-G981.

Karaki, H., Ozaki, H., Hori, M., Mitsui-Saito, M., Amano, K.-I., Harada, K.-I., Miyamoto, S., Nakazawa, H., Won, K.-J. & Sato, K. (1997). Calcium Movements, Distribution, and Functions in Smooth Muscle. *Pharmacological Reviews,* 49**,** 157-230.

Karaki, H. & Weiss, G. B. (1984). Calcium Channels in Smooth Muscle. *Gastroenterology,* 87**,** 960-970.

Karsten, U. & Wollenberger, A. (1977). Improvements in the Ethidium Bromide Method for Direct Fluorometric Estimation of DNA and Rna in Cell and Tissue Homogenates. *Analytical Biochemistry,* 77**,** 464-470.

Kinnamon, S. C. (2012). Taste Receptor Signalling–from Tongues to Lungs. *Acta Physiologica,* 204**,** 158-168.

Kinnamon, S. C. & Roper, S. D. (1988). Membrane Properties of Isolated Mudpuppy Taste Cells. *The Journal of General Physiology,* 91**,** 351-371.

Klein-Schwartz, W. (1991). Denatonium Benzoate: Review of Efficacy and Safety. *Veterinary and human toxicology,* 33**,** 545-547.

Krasteva, G., Canning, B. J., Hartmann, P., Veres, T. Z., Papadakis, T., Mühlfeld, C., Schliecker, K., Tallini, Y. N., Braun, A. & Hackstein, H. (2011). Cholinergic Chemosensory Cells in the Trachea Regulate Breathing. *Proceedings of the National Academy of Sciences,* 108**,** 9478-9483.

Lai, N., Lu, W. & Wang, J. (2015). Ca2+ and Ion Channels in Hypoxia-Mediated Pulmonary Hypertension. *International Journal of Clinical and Experimental Pathology,* 8**,** 1081.

Langmead, B. & Salzberg, S. L. (2012). Fast Gapped-Read Alignment with Bowtie 2. *Nature Methods,* 9**,** 357.

Langton, P., Nelson, M., Huang, Y. & Standen, N. (1991). Block of Calcium-Activated Potassium Channels in Mammalian Arterial Myocytes by Tetraethylammonium Ions. *American Journal of Physiology-Heart and Circulatory Physiology,* 260**,** H927-H934.

Larsson, K. P., Peltonen, H. M., Bart, G., Louhivuori, L. M., Penttonen, A., Antikainen, M., Kukkonen, J. P. & Åkerman, K. E. (2005). Orexin-a-Induced Ca2+ Entry Evidence for Involvement of Trpc Channels and Protein Kinase C Regulation. *Journal of Biological Chemistry,* 280**,** 1771-1781.

Lee, C. H., Poburko, D., Sahota, P., Sandhu, J., Ruehlmann, D. O. & Van Breemen, C. J. T. J. O. P. (2001). The Mechanism of Phenylephrine-Mediated [Ca2+] I Oscillations Underlying Tonic Contraction in the Rabbit Inferior Vena Cava. 534**,** 641-650.

Lee, G. D. J. (1971). Regulation of the Pulmonary Circulation. *Heart,* 33**,** 15-26.

Lee, R. J., Kofonow, J. M., Rosen, P. L., Siebert, A. P., Chen, B., Doghramji, L., Xiong, G., Adappa, N. D., Palmer, J. N. & Kennedy, D. W. (2014). Bitter and Sweet Taste Receptors Regulate Human Upper Respiratory Innate Immunity. *The Journal of Clinical Investigation,* 124**,** 1393-1405.

Lee, R. J., Xiong, G., Kofonow, J. M., Chen, B., Lysenko, A., Jiang, P., Abraham, V., Doghramji, L., Adappa, N. D. & Palmer, J. N. (2012). T2r38 Taste Receptor Polymorphisms Underlie Susceptibility to Upper Respiratory Infection. *The Journal of Clinical Investigation,* 122**,** 4145-4159.

Levick, J. R. (2013). *An Introduction to Cardiovascular Physiology*, Butterworth-Heinemann.

Li, B. & Dewey, C. N. (2011). Rsem: Accurate Transcript Quantification from Rna-Seq Data with or without a Reference Genome. *BMC Bioinformatics,* 12**,** 323.

Li, F. & Zhou, M. (2012). Depletion of Bitter Taste Transduction Leads to Massive Spermatid Loss in Transgenic Mice. *MHR: Basic Science of Reproductive Medicine,* 18**,** 289-297.

Li, X., Llorente, I. & Brasch, M. (2008). Improvements in Live Cell Analysis of G Protein Coupled Receptors Using Second Generation Bd Calcium Assay Kits. *Current Chemical Genomics,* 2**,** 10.

Liu, S., Crawley, D., Evans, T. & Barnes, P. (1991). Endogenous Nitric Oxide Modulates Adrenergic Neural Vasoconstriction in Guinea-Pig Pulmonary Artery. *British Journal of Pharmacology,* 104**,** 565-569.

Liu, S., Crawley, D., Rohde, J., Evans, T. & Barnes, P. (1992). Role of Nitric Oxide and Guanosine 3′, 5′-Cyclic Monophosphate in Mediating Nonadrenergic, Noncholinergic Relaxation in Guinea-Pig Pulmonary Arteries. *British Journal of Pharmacology,* 107**,** 861-866.

Liu, S., Mccormack, D., Evans, T. & Barnes, P. (1989a). Characterization and Distribution of P2-Purinoceptor Subtypes in Rat Pulmonary Vessels. *Journal of Pharmacology and Experimental Therapeutics,* 251**,** 1204-1210.

Liu, S., Mccormack, D., Evans, T. & Barnes, P. (1989b). Evidence for Two P2-Purinoceptor Subtypes in Human Small Pulmonary Arteries. *British journal of pharmacology,* 98**,** 1014.

Liu, S., Mccormack, D., Evans, T. W. & Barnes, P. (1989c). Characterization and Distribution of P2-Purinoceptor Subtypes in Rat Pulmonary Vessels1.

Liu, X., Gu, F., Jiang, L., Chen, F. & Li, F. (2015). Expression of Bitter Taste Receptor Tas2r105 in Mouse Kidney. *Biochemical and Biophysical Research Communications,* 458**,** 733-738.

Livak, K. J. & Schmittgen, T. D. (2001). Analysis of Relative Gene Expression Data Using Real-Time Quantitative Pcr and the 2− Δδct Method. *Methods,* 25**,** 402-408.

Lock, J. T., Parker, I. & Smith, I. F. (2015). A Comparison of Fluorescent Ca2+ Indicators for Imaging Local Ca2+ Signals in Cultured Cells. *Cell Calcium,* 58**,** 638-648.

Long, L., Yang, X., Southwood, M., Lu, J., Marciniak, S. J., Dunmore, B. J. & Morrell, N. W. (2013). Chloroquine Prevents Progression of Experimental Pulmonary Hypertension Via Inhibition of Autophagy and Lysosomal Bone Morphogenetic Protein Type Ii Receptor Degradation. *Circulation research,* 112**,** 1159-1170.

Looareesuwan, S., White, N. J., Chanthavanich, P., Edwards, G., Nicholl, D. D., Bunch, C. & Warrell, D. A. (1986). Cardiovascular Toxicity and Distribution Kinetics of Intravenous Chloroquine. *British Journal of Clinical Pharmacology,* 22**,** 31-36.

Lorenz, M., Wessler, S., Follmann, E., Michaelis, W., Düsterhöft, T., Baumann, G., Stangl, K. & Stangl, V. (2004). A Constituent of Green Tea, Epigallocatechin-3-Gallate, Activates Endothelial Nitric Oxide Synthase by a Phosphatidylinositol-3-Oh-Kinase-, Camp-Dependent Protein Kinase-, and Akt-Dependent Pathway and Leads to Endothelial-Dependent Vasorelaxation. *Journal of Biological Chemistry,* 279**,** 6190-6195.

Lossow, K., Hübner, S., Roudnitzky, N., Slack, J. P., Pollastro, F., Behrens, M. & Meyerhof, W. (2016). Comprehensive Analysis of Mouse Bitter Taste Receptors Reveals Different Molecular Receptive Ranges for Orthologous

Receptors in Mice and Humans. *Journal of Biological Chemistry,* 291**,** 15358-15377.

Lourenço, A. P., Fontoura, D., Henriques-Coelho, T. & Leite-Moreira, A. F. (2012). Current Pathophysiological Concepts and Management of Pulmonary Hypertension. *International journal of cardiology,* 155**,** 350-361.

Lu, P., Zhang, C.-H., Lifshitz, L. M. & Zhuge, R. (2017). Extraoral Bitter Taste Receptors in Health and Disease. *The Journal of General Physiology,* 149**,** 181-197.

Lund, T. C., Kobs, A. J., Kramer, A., Nyquist, M., Kuroki, M. T., Osborn, J., Lidke, D. S., Low-Nam, S. T., Blazar, B. R. & Tolar, J. (2013). Bone Marrow Stromal and Vascular Smooth Muscle Cells Have Chemosensory Capacity Via Bitter Taste Receptor Expression. *PLoS One,* 8**,** 58945.

Maclean, M. R., Herve, P., Eddahibi, S. & Adnot, S. (2000). 5-Hydroxytryptamine and the Pulmonary Circulation: Receptors, Transporters and Relevance to Pulmonary Arterial Hypertension. *British Journal of Pharmacology,* 131**,** 161-168.

Mandegar, M. & Yuan, J. X.-J. (2002). Role of K+ Channels in Pulmonary Hypertension. *Vascular Pharmacology,* 38**,** 25-33.

Manson, M. (2015). *Airway Smooth Muscle as a Target in Asthma: New Insights into Bronchorelaxation and Hyperreactivity*, Institutet för Miljömedicin/Institute of Environmental Medicine.

Manson, M. L., Säfholm, J., Al-Ameri, M., Bergman, P., Orre, A.-C., Swärd, K., James, A., Dahlén, S.-E. & Adner, M. (2014). Bitter Taste Receptor Agonists Mediate Relaxation of Human and Rodent Vascular Smooth Muscle. *European Journal of Pharmacology,* 740**,** 302-311.

Mariano, D. J., Schomer, S. J. & Rea, R. F. (1992). Effects of Quinidine on Vascular Resistance and Sympathetic Nerve Activity in Humans. *Journal of the American College of Cardiology,* 20**,** 1411-1416.

Matsunami, H., Montmayeur, J.-P. & Buck, L. B. (2000). A Family of Candidate Taste Receptors in Human and Mouse. *Nature,* 404**,** 601.

Mccarthy, C. G., Wenceslau, C. F., Goulopoulou, S., Ogbi, S., Matsumoto, T. & Webb, R. C. (2016). Autoimmune Therapeutic Chloroquine Lowers Blood Pressure and Improves Endothelial Function in Spontaneously Hypertensive Rats. *Pharmacological Research,* 113**,** 384-394.

Mccormack, D., Clarke, B. & Barnes, P. (1989). Characterization of Adenosine Receptors in Human Pulmonary Arteries. *American Journal of Physiology-Heart and Circulatory Physiology,* 256**,** H41-H46.

Mcculloch, K. M., Osipenko, O. N. & Gurney, A. M. (1999). Oxygen-Sensing Potassium Currents in Pulmonary Artery. *General Pharmacology: The Vascular System,* 32**,** 403-411.

Mcfadzean, I. & Gibson, A. (2002). The Developing Relationship between Receptor-Operated and Store-Operated Calcium Channels in Smooth Muscle. *British Journal of Pharmacology,* 135**,** 1-13.

Mckenzie, C., Macdonald, A. & Shaw, A. J. B. J. O. P. (2009). Mechanisms of U46619-Induced Contraction of Rat Pulmonary Arteries in the Presence and Absence of the Endothelium. 157**,** 581-596.

Mclaughlin, V. V., Shah, S. J., Souza, R. & Humbert, M. (2015). Management of Pulmonary Arterial Hypertension. *Journal of the American College of Cardiology,* 65**,** 1976-1997.

Mclean, J. (1986). Pulmonary Vascular Innervation. *In:* Bergofsky, E. (ed.) *Abnormal Pulmonary Circulation.* London: Churchill-Livingstone.

Mcmurtry, I. F. (1984). Angiotensin Is Not Required for Hypoxic Constriction in Salt Solution-Perfused Rat Lungs. *Journal of Applied Physiology,* 56**,** 375-380.

Mcmurtry, I. F., Davidson, A. B., Reeves, J. T. & Grover, R. F. (1976). Inhibition of Hypoxic Pulmonary Vasoconstriction by Calcium Antagonists in Isolated Rat Lungs. *Circulation Research,* 38**,** 99-104.

Mecca, T. E., Elam, J. T., Nash, C. B. & Caldwell, R. W. (1980). A-Adrenergic Blocking Properties of Quinine Hcl. *European Journal of Pharmacology,* 63**,** 159-166.

Medina-Remón, A., Tresserra-Rimbau, A., Pons, A., Tur, J. A., Martorell, M., Ros, E., Buil-Cosiales, P., Sacanella, E., Covas, M. I. & Corella, D. (2015). Effects of Total Dietary Polyphenols on Plasma Nitric Oxide and Blood Pressure in a High Cardiovascular Risk Cohort. The Predimed Randomized Trial. *Nutrition, Metabolism and Cardiovascular Diseases,* 25**,** 60-67.

Medina-Remón, A., Zamora-Ros, R., Rotchés-Ribalta, M., Andres-Lacueva, C., Martínez-González, M. A., Covas, M. I., Corella, D., Salas-Salvadó, J., Gómez-Gracia, E. & Ruiz-Gutiérrez, V. (2011). Total Polyphenol Excretion and Blood Pressure in Subjects at High Cardiovascular Risk. *Nutrition, Metabolism and Cardiovascular Diseases,* 21**,** 323-331.

Mescher, A. L. (2018). The Circulatory System. *Junqueira's Basic Histology: Text and Atlas, 15e.* New York, NY: McGraw-Hill Education.

Metz, R. P., Patterson, J. L. & Wilson, E. (2012). Vascular Smooth Muscle Cells: Isolation, Culture, and Characterization. *Cardiovascular Development.* Springer.

Meyerhof, W., Batram, C., Kuhn, C., Brockhoff, A., Chudoba, E., Bufe, B., Appendino, G. & Behrens, M. (2010). The Molecular Receptive Ranges of Human Tas2r Bitter Taste Receptors. *Chemical Senses,* 35**,** 157-170.

Meyerhof, W., Born, S., Brockhoff, A. & Behrens, M. (2011). Molecular Biology of Mammalian Bitter Taste Receptors. A Review. *Flavour and Fragrance Journal,* 26**,** 260-268.

Michelangeli, F. & East, J. M. (2011). A Diversity of Serca Ca2+ Pump Inhibitors. Portland Press Limited.

Ming, D., Ruiz-Avila, L. & Margolskee, R. F. (1998). Characterization and Solubilization of Bitter-Responsive Receptors That Couple to Gustducin. *Proceedings of the National Academy of Sciences,* 95**,** 8933-8938.

Mitchell, J. A., Ali, F., Bailey, L., Moreno, L. & Harrington, L. S. (2008). Role of Nitric Oxide and Prostacyclin as Vasoactive Hormones Released by the Endothelium. *Experimental Physiology,* 93**,** 141-147.

Moine, F., Brechbühl, J., Tosato, M. N., Beaumann, M. & Broillet, M.-C. (2018). Alarm Pheromone and Kairomone Detection Via Bitter Taste Receptors in the Mouse Grueneberg Ganglion. *BMC biology,* 16**,** 12.

Moncada, S., Palmer, R. & Higgs, E. (1991). Nitric Oxide: Physiology, Pharmacology and Pathophysiology. *Pharmacological Reviews,* 43**,** 109-142.

Moncada, S., Palmer, R. M. & Higgs, E. A. (1989). Biosynthesis of Nitric Oxide from L-Arginine: A Pathway for the Regulation of Cell Function and Communication. *Biochemical Pharmacology,* 38**,** 1709-1715.

Moore, S. P. & Sutherland, B. M. (1985). A Densitometric Nondestructive Microassay for DNA Quantitation. *Analytical Biochemistry,* 144**,** 15-19.

Morel, N. & Godfraind, T. (1991). Characterization in Rat Aorta of the Binding Sites Responsible for Blockade of Noradrenaline-Evoked Calcium Entry by Nisoldipine. *British Journal of Pharmacology,* 102**,** 467-477.

Morrell, N. W., Adnot, S., Archer, S. L., Dupuis, J., Jones, P. L., Maclean, M. R., Mcmurtry, I. F., Stenmark, K. R., Thistlethwaite, P. A. & Weissmann, N. (2009). Cellular and Molecular Basis of Pulmonary Arterial Hypertension. *Journal of the American College of Cardiology,* 54**,** S20-S31.

Mortazavi, A., Williams, B. A., Mccue, K., Schaeffer, L. & Wold, B. (2008). Mapping and Quantifying Mammalian Transcriptomes by Rna-Seq. *Nature Methods,* 5**,** 621.

Mueller, K. L., Hoon, M. A., Erlenbach, I., Chandrashekar, J., Zuker, C. S. & Ryba, N. J. (2005). The Receptors and Coding Logic for Bitter Taste. *Nature,* 434**,** 225.

Mueller, O., Hahnenberger, K., Dittmann, M., Yee, H., Dubrow, R., Nagle, R. & Ilsley, D. (2000). A Microfluidic System for High-Speed Reproducible DNA Sizing and Quantitation. *ELECTROPHORESIS: An International Journal,* 21**,** 128-134.

Musabayane, C., Ndhlovu, C. & Balment, R. (1994). The Effects of Oral Chloroquine Administration on Kidney Function. *Renal Failure,* 16**,** 221-228.

Naim, M., Seifert, R., Nürnberg, B., Grünbaum, L. & Schultz, G. (1994). Some Taste Substances Are Direct Activators of G-Proteins. *Biochemical Journal,* 297**,** 451-454.

Nakashima, K. & Ninomiya, Y. (1998). Increase in Inositol 1, 4, 5-Trisphosphate Levels of the Fungiform Papilla in Response to Saccharin and Bitter Substances in Mice. *Cellular Physiology and Biochemistry,* 8**,** 224-230.

Nelson, M. T. & Quayle, J. M. (1995). Physiological Roles and Properties of Potassium Channels in Arterial Smooth Muscle. *American Journal of Physiology-Cell Physiology,* 268**,** C799-C822.

Netzer, R., Pflimlin, P. & Trube, G. (1993). Dextromethorphan Blocks N-Methyl-D-Aspartate-Induced Currents and Voltage-Operated Inward Currents in Cultured Cortical Neurons. *European Journal of Pharmacology,* 238**,** 209-216.

Nicolls, M. R., Mizuno, S., Taraseviciene-Stewart, L., Farkas, L., Drake, J. I., Husseini, A. A., Gomez-Arroyo, J. G., Voelkel, N. F. & Bogaard, H. J. (2012). New Models of Pulmonary Hypertension Based on Vegf Receptor Blockade-Induced Endothelial Cell Apoptosis. *Pulmonary circulation,* 2**,** 434-442.

Ogura, T. & Kinnamon, S. C. (1999). Ip3-Independent Release of Ca2+ from Intracellular Stores: A Novel Mechanism for Transduction of Bitter Stimuli. *Journal of Neurophysiology,* 82**,** 2657-2666.

Ogura, T., Mackay-Sim, A. & Kinnamon, S. C. (1997). Bitter Taste Transduction of Denatonium in the Mudpuppynecturus Maculosus. *Journal of Neuroscience,* 17**,** 3580-3587.

Ogura, T., Margolskee, R. F. & Kinnamon, S. C. (2002). Taste Receptor Cell Responses to the Bitter Stimulus Denatonium Involve Ca2+ Influx Via Store-Operated Channels. *Journal of Neurophysiology,* 87**,** 3152-3155.

Okumura, K., Ichihara, K. & Nagasaka, M. (1997). Effects of Aranidipine, a Novel Calcium Channel Blocker, on Mechanical Responses of the Isolated Rat Portal Vein: Comparison with Typical Calcium Channel Blockers and Potassium Channel Openers. *Journal of Cardiovascular Pharmacology,* 29**,** 209-215.

Olivier, D. & Van Wyk, B.-E. (2013). Bitterness Values for Traditional Tonic Plants of Southern Africa. *Journal of Ethnopharmacology,* 147**,** 676-679.

Orsmark-Pietras, C., James, A., Konradsen, J. R., Nordlund, B., Söderhäll, C., Pulkkinen, V., Pedroletti, C., Daham, K., Kupczyk, M. & Dahlén, B. (2013). Transcriptome Analysis Reveals Upregulation of Bitter Taste Receptors in Severe Asthmatics. *European Respiratory Journal,* 42**,** 65-78.

Palmer, A. E. & Tsien, R. Y. (2006). Measuring Calcium Signaling Using Genetically Targetable Fluorescent Indicators. *Nature Protocols,* 1**,** 1057.

Palmer, R. M. & Moncada, S. (1989). A Novel Citrulline-Forming Enzyme Implicated in the Formation of Nitric Oxide by Vascular Endothelial Cells. *Biochemical and Biophysical Research Communications,* 158**,** 348-352.

Paredes, R. M., Etzler, J. C., Watts, L. T., Zheng, W. & Lechleiter, J. D. (2008). Chemical Calcium Indicators. *Methods,* 46**,** 143-151.

Park, J. I., Shin, C. Y., Lee, Y. W., Huh, I. H. & Sohn, U. D. (2000). Endothelium-Dependent Sensory Non-Adrenergic Non-Cholinergic Vasodilatation in Rat Thoracic Aorta: Involvement of Atp and a Role for No. *Journal of Pharmacy and Pharmacology,* 52**,** 409-416.

Parton, R. G. & Del Pozo, M. A. (2013). Caveolae as Plasma Membrane Sensors, Protectors and Organizers. *Nature Reviews Molecular Cell Biology,* 14**,** 98.

Pelaia, G., Renda, T., Gallelli, L., Vatrella, A., Busceti, M. T., Agati, S., Caputi, M., Cazzola, M., Maselli, R. & Marsico, S. A. (2008). Molecular Mechanisms Underlying Airway Smooth Muscle Contraction and Proliferation: Implications for Asthma. *Respiratory Medicine,* 102**,** 1173-1181.

Pérez, C. A., Huang, L., Rong, M., Kozak, J. A., Preuss, A. K., Zhang, H., Max, M. & Margolskee, R. F. (2002). A Transient Receptor Potential Channel Expressed in Taste Receptor Cells. *Nature Neuroscience,* 5**,** 1169.

Peri, I., Mamrud-Brains, H., Rodin, S., Krizhanovsky, V., Shai, Y., Nir, S. & Naim, M. (2000). Rapid Entry of Bitter and Sweet Tastants into Liposomes and Taste Cells: Implications for Signal Transduction. *American Journal of Physiology-Cell Physiology,* 278**,** C17-C25.

Pollock, J. S., Förstermann, U., Mitchell, J. A., Warner, T. D., Schmidt, H., Nakane, M. & Murad, F. (1991). Purification and Characterization of Particulate Endothelium-Derived Relaxing Factor Synthase from Cultured and Native Bovine Aortic Endothelial Cells. *Proceedings of the National Academy of Sciences,* 88**,** 10480-10484.

Pulkkinen, V., Manson, M. L., Säfholm, J., Adner, M. & Dahlén, S.-E. (2012). The Bitter Taste Receptor (Tas2r) Agonists Denatonium and Chloroquine Display Distinct Patterns of Relaxation of the Guinea Pig Trachea. *American Journal of Physiology-Lung Cellular and Molecular Physiology,* 303**,** 956-966.

Pydi, S. P., Sobotkiewicz, T., Billakanti, R., Bhullar, R. P., Loewen, M. C. & Chelikani, P. (2014). Amino Acid Derivatives as Bitter Taste Receptor (T2r) Blockers. *Journal of Biological Chemistry,* 289**,** 25054-25066.

Qasabian, R., Schyvens, C., Owe-Young, R., Killen, J., Macdonald, P., Conigrave, A. & Williamson, D. (1997). Characterization of the P2 Receptors in Rabbit Pulmonary Artery. *British journal of pharmacology,* 120**,** 553.

Rajkumar, P., Aisenberg, W. H., Acres, O. W., Protzko, R. J. & Pluznick, J. L. (2014). Identification and Characterization of Novel Renal Sensory Receptors. *PLoS One,* 9**,** e111053.

Ratz, P. H., Berg, K. M., Urban, N. H. & Miner, A. S. (2005). Regulation of Smooth Muscle Calcium Sensitivity: Kcl as a Calcium-Sensitizing Stimulus. *American Journal of Physiology-Cell Physiology,* 288**,** 769-783.

Razani, B., Engelman, J. A., Wang, X. B., Schubert, W., Zhang, X. L., Marks, C. B., Macaluso, F., Russell, R. G., Li, M. & Pestell, R. G. (2001). Caveolin-1 Null Mice Are Viable but Show Evidence of Hyperproliferative and Vascular Abnormalities. *Journal of Biological Chemistry,* 276**,** 38121-38138.

Redfield, A. C., Bock, A. V. & Meakins, J. (1922). The Measurement of the Tension of Oxygen and Carbon Dioxide in the Blood of the Pulmonary Artery in Man. *The Journal of Physiology,* 57**,** 76-81.

Reeves, J. T. & Rubin, L. J. (1998). The Pulmonary Circulation: Snapshots of Progress. *American Journal of Respiratory and Critical Care Medicine,* 157**,** S101-S108.

Rehberg, M., Lepier, A., Solchenberger, B., Osten, P. & Blum, R. (2008). A New Non-Disruptive Strategy to Target Calcium Indicator Dyes to the Endoplasmic Reticulum. *Cell Calcium,* 44**,** 386-399.

Reichling, C., Meyerhof, W. & Behrens, M. (2008). Functions of Human Bitter Taste Receptors Depend on N-Glycosylation. *Journal of Neurochemistry,* 106**,** 1138-1148.

Remillard, C. V., Makino, A. & Yuan, J. X. (2011). "Isolation and Culture of Pulmonary Vascular Smooth Muscle and Endothelial Cells". *In:* Yuan, J., Garcia, J., West, J., Hales, C., Rich, S. & Archer, S. (eds.) *Textbook of Pulmonary Vascular Disease.* Boston, MA: Springer.

Remillard, C. V. & Yuan, J. X.-J. (2006). Trp Channels, Cce, and the Pulmonary Vascular Smooth Muscle. *Microcirculation,* 13**,** 671-692.

Revermann, M., Neofitidou, S., Kirschning, T., Schloss, M., Brandes, R. P. & Hofstetter, C. (2014). Inhalation of the Bkca-Opener Ns1619 Attenuates Right Ventricular Pressure and Improves Oxygenation in the Rat Monocrotaline Model of Pulmonary Hypertension. *PLoS One,* 9**,** e86636.

Richardson, J. B. (1979). Nerve Supply to the Lungs. *American Review of Respiratory Disease,* 119**,** 785-802.

Roland, W. S., Van Buren, L., Gruppen, H., Driesse, M., Gouka, R. J., Smit, G. & Vincken, J.-P. (2013). Bitter Taste Receptor Activation by Flavonoids and Isoflavonoids: Modeled Structural Requirements for Activation of Htas2r14 and Htas2r39. *Journal of Agricultural and Food Chemistry,* 61**,** 10454-10466.

Roland, W. S., Vincken, J.-P., Gouka, R. J., Van Buren, L., Gruppen, H. & Smit, G. (2011). Soy Isoflavones and Other Isoflavonoids Activate the Human Bitter Taste Receptors Htas2r14 and Htas2r39. *Journal of Agricultural and Food Chemistry,* 59**,** 11764-11771.

Roura, E., Foster, S., Winklebach, A., Navarro, M., Thomas, W., Campbell, K. & Stowasser, M. (2016). Taste and Hypertension in Humans: Targeting Cardiovascular Disease. *Current Pharmaceutical Design,* 22**,** 2290-2305.

Roy, B., Sicotte, B., Brochu, M. & St-Louis, J. (1995). Effects of Nifedipine and Bay K 8644 on Myotropic Responses in Aortic Rings of Pregnant Rats. *European Journal of Pharmacology,* 280**,** 1-9.

Ruiz-Avila, L., Mclaughlin, S. K., Wildman, D., Mckinnon, P. J., Robichon, A., Spickofsky, N. & Margolskee, R. F. (1995). Coupling of Bitter Receptor to Phosphodiesterase through Transducin in Taste Receptor Cells. *Nature,* 376**,** 80.

Ryerson, C. J., Nayar, S., Swiston, J. R. & Sin, D. D. (2010). Pharmacotherapy in Pulmonary Arterial Hypertension: A Systematic Review and Meta-Analysis. *Respiratory Research,* 11**,** 12.

Sai, W. B., Yu, M. F., Wei, M. Y., Lu, Z., Zheng, Y. M., Wang, Y. X., Qin, G., Guo, D., Ji, G. & Shen, J. (2014). Bitter Tastants Induce Relaxation of Rat Thoracic Aorta Precontracted with High K+. *Clinical and Experimental Pharmacology and Physiology,* 41**,** 301-308.

Sakai, H., Sato, K., Kai, Y., Chiba, Y. & Narita, M. (2016). Denatonium and 6-N-Propyl-2-Thiouracil, Agonists of Bitter Taste Receptor, Inhibit Contraction of Various Types of Smooth Muscles in the Rat and Mouse. *Biological and Pharmaceutical Bulletin,* 39**,** 33-41.

Salari, H., Bramley, A., Langlands, J., Howard, S., Chan-Yeung, M., Chan, H., Schellenberg, R. J. a. J. O. R. C. & Biology, M. (1993). Effect of Phospholipase C Inhibitor U-73122 on Antigen-Induced Airway Smooth Muscle Contraction in Guinea Pigs. 9**,** 405-405.

Sambrook, J., Fritsch, E. F. & Maniatis, T. (1989). *Molecular Cloning: A Laboratory Manual*, Cold spring harbor laboratory press.

Satake, N., Shibata, M. & Shibata, S. (1996). The Inhibitory Effects of Iberiotoxin and 4-Aminopyridine on the Relaxation Induced by B1-and B2-Adrenoceptor Activation in Rat Aortic Rings. *British Journal of Pharmacology,* 119**,** 505-510.

Satoh, H. & Inui, J. (1984). Endothelial Cell-Dependent Relaxation and Contraction Induced by Histamine in the Isolated Guinea-Pig Pulmonary Artery. *European Journal of Pharmacology,* 97**,** 321-324.

Sawano, S., Seto, E., Mori, T. & Hayashi, Y. (2005). G-Protein-Dependent and-Independent Pathways in Denatonium Signal Transduction. *Bioscience, Biotechnology, and Biochemistry,* 69**,** 1643-1651.

Schmid, P. G., Nelson, L. D., Mark, A. L., Heistad, D. D. & Abboud, F. M. (1974). Inhibition of Adrenergic Vasoconstriction by Quinidine. *Journal of Pharmacology and Experimental Therapeutics,* 188**,** 124-134.

Schneider, S. M., Michelson, E. A., Boucek, C. D. & Ilkhanipour, K. (1991). Dextromethorphan Poisoning Reversed by Naloxone. *The American Journal of Emergency Medicine,* 9**,** 237-238.

Schulz, V., Hänsel, R. & Tyler, V. E. (2001). *Rational Phytotherapy: A Physician's Guide to Herbal Medicine*, Psychology Press.

Segarra, G., Medina, P., Revert, F., Masiá, S., Vila, J. M., Such, L. & Aldasoro, M. N. (1999). Modulation of Adrenergic Contraction of Dog Pulmonary Arteries by Nitric Oxide and Prostacyclin. *General Pharmacology: The Vascular System,* 32**,** 583-589.

Sekine, H., Takao, K., Yoshinaga, K., Kokubun, S. & Ikeda, M. (2012). Effects of Zinc Deficiency and Supplementation on Gene Expression of Bitter Taste Receptors (Tas2rs) on the Tongue in Rats. *The Laryngoscope,* 122**,** 2411-2417.

Shah, A. S., Ben-Shahar, Y., Moninger, T. O., Kline, J. N. & Welsh, M. J. (2009). Motile Cilia of Human Airway Epithelia Are Chemosensory. *Science,* 325**,** 1131-1134.

Shahbazian, A., Petkov, V., Baykuscheva-Gentscheva, T., Hoeger, H., Painsipp, E., Holzer, P. & Mosgoeller, W. (2007). Involvement of Endothelial No in the Dilator Effect of Vip on Rat Isolated Pulmonary Artery. *Regulatory Peptides,* 139**,** 102-108.

Sharma, N., Chand, D., Shukla, A., Singh, M., Govil, R. K., Bihari, B., Saxena, A., Bhatia, A. & Singh, R. (2014). Internal Controls for the Quality Assessment of Polymerase Chain Reaction Methods for the Diagnosis of Infectious & Autoimmune Disease. *Scholars Journal of Applied Medical Sciences,* 2**,** 485-8.

Sharp, A., Dawson, T. M., Ross, C. A., Fotuhi, M., Mourey, R. & Snyder, S. H. (1993). Inositol 1, 4, 5-Trisphosphate Receptors: Immunohistochemical Localization to Discrete Areas of Rat Central Nervous System. *Neuroscience,* 53**,** 927-942.

Shimoda, L. A., Wang, J. & Sylvester, J. (2006). Ca 2+ Channels and Chronic Hypoxia. *Microcirculation,* 13**,** 657-670.

Simpson, P. B., Challiss, R. J. & Nahorski, S. R. (1995). Neuronal Ca2+ Stores: Activation and Function. *Trends in Neurosciences,* 18**,** 299-306.

Singh, N., Chakraborty, R., Bhullar, R. P. & Chelikani, P. (2014). Differential Expression of Bitter Taste Receptors in Non-Cancerous Breast Epithelial and Breast Cancer Cells. *Biochemical and Biophysical Research Communications,* 446**,** 499-503.

Singh, N., Vrontakis, M., Parkinson, F. & Chelikani, P. (2011). Functional Bitter Taste Receptors Are Expressed in Brain Cells. *Biochemical and Biophysical Research Communications,* 406**,** 146-151.

Sirnes, P. A., Tendera, M., Vardas, P. & Widimsky, P. (2009). Guidelines for the Diagnosis and Treatment of Pulmonary Hypertension. *European Heart Journal,* 30**,** 2493-2537.

Somlyo, A. P. & Somlyo, A. V. J. N. (1994). Signal Transduction and Regulation in Smooth Muscle. 372**,** 231.

Spedding, M. & Berg, C. (1985). Antagonism of Ca2+-Induced Contractions of K+-Depolarized Smooth Musle by Local Anaesthetics. *European Journal of Pharmacology,* 108**,** 143-150.

Spielman, A. I., Huque, T., Nagai, H., Whitney, G. & Brand, J. G. (1994). Generation of Inositol Phosphates in Bitter Taste Transduction. *Physiology and Behavior,* 56**,** 1149-1155.

Spielman, A. I., Mody, I., Brand, J. G., Whitney, G., Macdonald, J. F. & Salter, M. W. (1989). A Method for Isolating and Patch-Clamping Single Mammalian Taste Receptor Cells. *Brain Research,* 503**,** 326-329.

Stenmark, K. R., Meyrick, B., Galie, N., Mooi, W. J. & Mcmurtry, I. F. (2009). Animal Models of Pulmonary Arterial Hypertension: The Hope for Etiological Discovery and Pharmacological Cure. *American Journal of Physiology-Lung Cellular and Molecular Physiology,* 297**,** L1013-L1032.

Steucke, K. E., Tracy, P. V., Hald, E. S., Hall, J. L. & Alford, P. W. (2015). Vascular Smooth Muscle Cell Functional Contractility Depends on Extracellular Mechanical Properties. *Journal of Biomechanics,* 48**,** 3044-3051.

Suarez-Kurtz, G., Garcia, M. L. & Kaczorowski, G. J. (1991). Effects of Charybdotoxin and Iberiotoxin on the Spontaneous Motility and Tonus of Different Guinea Pig Smooth Muscle Tissues. *Journal of Pharmacology and Experimental Therapeutics,* 259**,** 439-443.

Sukumaran, S. K., Lewandowski, B. C., Qin, Y., Kotha, R., Bachmanov, A. A. & Margolskee, R. F. (2017). Whole Transcriptome Profiling of Taste Bud Cells. *Scientific Reports,* 7**,** 7595.

Sylvester, J., Shimoda, L. A., Aaronson, P. I. & Ward, J. P. (2012). Hypoxic Pulmonary Vasoconstriction. *Physiological Reviews,* 92**,** 367-520.

Szalai, G., Csordás, G., Hantash, B. M., Thomas, A. P. & Hajnóczky, G. (2000). Calcium Signal Transmission between Ryanodine Receptors and Mitochondria. *Journal of Biological Chemistry,* 275**,** 15305-15313.

Tada, M., Takeuchi, A., Hashizume, M., Kitamura, K. & Kano, M. (2014). A Highly Sensitive Fluorescent Indicator Dye for Calcium Imaging of Neural Activity in Vitro and in Vivo. *European Journal of Neuroscience,* 39**,** 1720-1728.

Takahashi, A., Camacho, P., Lechleiter, J. D. & Herman, B. (1999). Measurement of Intracellular Calcium. *Physiological Reviews,* 79**,** 1089-1125.

Tan, X. & Sanderson, M. J. (2014). Bitter Tasting Compounds Dilate Airways by Inhibiting Airway Smooth Muscle Calcium Oscillations and Calcium Sensitivity. *British Journal of Pharmacology,* 171**,** 646-662.

Thastrup, O., Cullen, P. J., Drøbak, B., Hanley, M. R. & Dawson, A. P. J. P. O. T. N. a. O. S. (1990). Thapsigargin, a Tumor Promoter, Discharges Intracellular Ca2+ Stores by Specific Inhibition of the Endoplasmic Reticulum Ca2 (+)-Atpase. 87**,** 2466-2470.

Tizzano, M., Gulbransen, B. D., Vandenbeuch, A., Clapp, T. R., Herman, J. P., Sibhatu, H. M., Churchill, M. E., Silver, W. L., Kinnamon, S. C. & Finger, T. E. (2010). Nasal Chemosensory Cells Use Bitter Taste Signaling to Detect Irritants and Bacterial Signals. *Proceedings of the National Academy of Sciences,* 107**,** 3210-3215.

Tomás, J., Santos, C., Quintela, T. & Gonçalves, I. (2016). "Tasting" the Cerebrospinal Fluid: Another Function of the Choroid Plexus? *Neuroscience,* 320**,** 160-171.

Tortella, F. C., Pellicano, M. & Bowery, N. G. (1989). Dextromethorphan and Neuromodulation: Old Drug Coughs up New Activities. *Trends in Pharmacological Sciences,* 10**,** 501-507.

Townsley, M. I. (2011). Structure and Composition of Pulmonary Arteries, Capillaries, and Veins. *Comprehensive Physiology,* 2**,** 675-709.

Triggle, D. J., Langs, D. A. & Janis, R. A. (1989). Ca2+ Channel Ligands: Structure-Function Relationships of the 1, 4-Dihydropyridines. *Medicinal Research Reviews,* 9**,** 123-180.

Upadhyaya, J. D., Singh, N., Sikarwar, A. S., Chakraborty, R., Pydi, S. P., Bhullar, R. P., Dakshinamurti, S. & Chelikani, P. (2014). Dextromethorphan Mediated Bitter Taste Receptor Activation in the Pulmonary Circuit Causes Vasoconstriction. *PLoS One,* 9**,** 110373.

Vallance, P., Collier, J. & Moncada, S. (1989). Effects of Endothelium-Derived Nitric Oxide on Peripheral Arteriolar Tone in Man. *The Lancet,* 334**,** 997-1000.

Van Breemen, C., Hwang, O. & Meisheri, K. D. (1981). The Mechanism of Inhibitory Action of Diltiazem on Vascular Smooth Muscle Contractility. *Journal of Pharmacology and Experimental Therapeutics,* 218**,** 459-463.

Vegezzi, G., Anselmi, L., Huynh, J., Barocelli, E., Rozengurt, E., Raybould, H. & Sternini, C. (2014). Diet-Induced Regulation of Bitter Taste Receptor Subtypes in the Mouse Gastrointestinal Tract. *PloS One,* 9**,** e107732-e107732.

Voelkel, N. (1986). Mechanisms of Hypoxic Pulmonary Vasoconstriction. *American Review of Respiratory Disease,* 133**,** 1186-1195.

Voigt, A., Hübner, S., Lossow, K., Hermans-Borgmeyer, I., Boehm, U. & Meyerhof, W. (2012). Genetic Labeling of Tas1r1 and Tas2r131 Taste Receptor Cells in Mice. *Chemical Senses,* 37**,** 897-911.

Wallner, M., Meera, P., Ottolia, M., Kaczorowski, G., Latorre, R., Garcia, M., Stefani, E. & Toro, L. (1995). Characterization of and Modulation by a Beta-Subunit of a Human Maxi Kca Channel Cloned from Myometrium. *Receptors and Channels,* 3**,** 185-199.

Wang, Q., Wang, Y.-X., Yu, M. & Kotlikoff, M. I. (1997). Ca (2+)-Activated Cl-Currents Are Activated by Metabolic Inhibition in Rat Pulmonary Artery Smooth Muscle Cells. *American Journal of Physiology-Cell Physiology,* 273**,** C520-C530.

Weir, E. (1978). Does Normoxic Pulmonary Vasodilatation Rather Than Hypoxic Vasoconstriction Account for the Pulmonary Pressor Response to Hypoxia? *The Lancet,* 311**,** 476-477.

Weir, E., Wyatt, C. N., Reeve, H. L., Huang, J., Archer, S. & Peers, C. (1994). Diphenyleneiodonium Inhibits Both Potassium and Calcium Currents in Isolated Pulmonary Artery Smooth Muscle Cells. *Journal of Applied Physiology,* 76**,** 2611-2615.

Welsh, D. J. & Peacock, A. J. (2013). Cellular Responses to Hypoxia in the Pulmonary Circulation. *High Altitude Medicine and Biology,* 14**,** 111-116.

White, N. J. (1996). The Treatment of Malaria. *New England Journal of Medicine,* 335**,** 800-806.

Wiener, A., Shudler, M., Levit, A. & Niv, M. Y. (2011). Bitterdb: A Database of Bitter Compounds. *Nucleic Acids Research,* 40**,** D413-D419.

Wiklund, N. P., Cederqvist, B. & Gustafsson, L. E. (1989). Adenosine Enhancement of Adrenergic Neuroeffector Transmission in Guinea-Pig Pulmonary Artery. *British Journal of Pharmacology,* 96**,** 425.

Wilson, D. P., Susnjar, M., Kiss, E., Sutherland, C. & Walsh, M. P. (2005). Thromboxane A2-Induced Contraction of Rat Caudal Arterial Smooth Muscle Involves Activation of Ca2+ Entry and Ca2+ Sensitization: Rho-Associated Kinase-Mediated Phosphorylation of Mypt1 at Thr-855, but Not Thr-697. *Biochemical Journal,* 389**,** 763-774.

Wölfle, U., Elsholz, F. A., Kersten, A., Haarhaus, B., Schumacher, U. & Schempp, C. M. (2016). Expression and Functional Activity of the Human Bitter Taste Receptor Tas2r38 in Human Placental Tissues and Jeg-3 Cells. *Molecules,* 21**,** 306.

Wolin, M., Davidson, C., Kaminski, P., Fayngersh, R. & Mohazzab-H, K. (1998). Oxidant-Nitric Oxide Signalling Mechanisms in Vascular Tissue. *Biochemistry C/C of Biokhimia,* 63**,** 810-816.

Wong, G. T., Gannon, K. S. & Margolskee, R. F. (1996). Transduction of Bitter and Sweet Taste by Gustducin. *Nature,* 381**,** 796.

Wu, K., Zhang, Q., Wu, X., Lu, W., Tang, H., Liang, Z., Gu, Y., Song, S., Ayon, R. J. & Wang, Z. (2017). Chloroquine Is a Potent Pulmonary Vasodilator That Attenuates Hypoxia-Induced Pulmonary Hypertension. *British Journal of Pharmacology,* 174**,** 4155-4172.

Wu, S. V., Chen, M. C. & Rozengurt, E. (2005). Genomic Organization, Expression, and Function of Bitter Taste Receptors (T2r) in Mouse and Rat. *Physiological Genomics,* 22**,** 139-149.

Wu, S. V., Rozengurt, N., Yang, M., Young, S. H., Sinnett-Smith, J. & Rozengurt, E. (2002). Expression of Bitter Taste Receptors of the T2r Family in the Gastrointestinal Tract and Enteroendocrine Stc-1 Cells. *Proceedings of the National Academy of Sciences,* 99**,** 2392-2397.

Wu, T.-C., Chao, C.-Y., Lin, S.-J. & Chen, J.-W. (2012). Low-Dose Dextromethorphan, a Nadph Oxidase Inhibitor, Reduces Blood Pressure and Enhances Vascular Protection in Experimental Hypertension. *PLoS One,* 7**,** 46067.

Xin, W. & Chen, Q. (2017). The Cellular Mechanism of Bitter Taste Receptor Mediated Relaxation of Rat Aorta. *The FASEB Journal,* 31**,** 672.5-672.5.

Xu, J., Cao, J., Iguchi, N., Riethmacher, D. & Huang, L. (2012). Functional Characterization of Bitter-Taste Receptors Expressed in Mammalian Testis. *MHR: Basic Science of Reproductive Medicine,* 19**,** 17-28.

Ye, J., Coulouris, G., Zaretskaya, I., Cutcutache, I., Rozen, S. & Madden, T. L. (2012). Primer-Blast: A Tool to Design Target-Specific Primers for Polymerase Chain Reaction. *BMC Bioinformatics,* 13**,** 134.

Yuan, X.-J., Tod, M. L., Rubin, L. J. & Blaustein, M. P. (1996). No Hyperpolarizes Pulmonary Artery Smooth Muscle Cells and Decreases the Intracellular Ca2+ Concentration by Activating Voltage-Gated K+ Channels. *Proceedings of the National Academy of Sciences,* 93**,** 10489-10494.

Zhai, K., Yang, Z., Zhu, X., Nyirimigabo, E., Mi, Y., Wang, Y., Liu, Q., Man, L., Wu, S. & Jin, J. (2016). Activation of Bitter Taste Receptors (Tas2rs) Relaxes Detrusor Smooth Muscle and Suppresses Overactive Bladder Symptoms. *Oncotarget,* 7**,** 21156.

Zhang, C.-H., Chen, C., Lifshitz, L. M., Fogarty, K. E., Zhu, M.-S. & Zhuge, R. (2012). Activation of Bk Channels May Not Be Required for Bitter Tastant–Induced Bronchodilation. *Nature Medicine,* 18**,** 648.

Zhang, C.-H., Lifshitz, L. M., Uy, K. F., Ikebe, M., Fogarty, K. E. & Zhuge, R. (2013). The Cellular and Molecular Basis of Bitter Tastant-Induced Bronchodilation. *PLoS Biology,* 11**,** e1001501.

Zhang, Y., Hoon, M. A., Chandrashekar, J., Mueller, K. L., Cook, B., Wu, D., Zuker, C. S. & Ryba, N. J. (2003). Coding of Sweet, Bitter, and Umami Tastes: Different Receptor Cells Sharing Similar Signaling Pathways. *Cell,* 112**,** 293-301.

Zhao, Y. J., Wang, J., Rubin, L. J. & Yuan, X. J. (1997). Inhibition of K (V) and K (Ca) Channels Antagonizes No-Induced Relaxation in Pulmonary Artery. *American Journal of Physiology-Heart and Circulatory Physiology,* 272**,** H904-H912.

Zheng, K., Lu, P., Delpapa, E., Bellve, K., Deng, R., Condon, J. C., Fogarty, K., Lifshitz, L. M., Simas, T. a. M. & Shi, F. (2017). Bitter Taste Receptors as Targets for Tocolytics in Preterm Labor Therapy. *The FASEB Journal,* 31**,** 4037-4052.

Zheng, W., Rampe, D. & Triggle, D. J. (1991). Pharmacological, Radioligand Binding, and Electrophysiological Characteristics of Fpl 64176, a Novel Nondihydropyridine Ca2+ Channel Activator, in Cardiac and Vascular Preparations. *Molecular Pharmacology,* 40**,** 734-741.